Identification and functional characterization of effector proteins from the fungal soil-borne pathogens *Verticillium dahliae* and *Rosellinia necatrix*

Edgar A. Chavarro Carrero

Propositions

1. The *Verticillium dahliae* effector protein Av2 is recognized by tomato plants carrying the *V2* resistance locus.
   (this thesis)

2. Manipulation of the microbiota of its host plants is critical for the infection biology of broad host-range fungal plant pathogens including *Rosellinia necatrix*.
   (this thesis)

3. Artificial Intelligence (AI) will soon surpass academics' abilities in scientific writing and lecturing.

4. Developing high-yield crop varieties for food security undermines the robustness of our agricultural systems when facing climate change.

5. Short-term contracts in academia perpetuate a culture of instability, ultimately hindering the pursuit of knowledge.

6. The prevalent use of visually appealing glass covers on modern buildings increases energy consumption and is therefore unsustainable.

Propositions belonging to the thesis, entitled:
Identification and functional characterization of effector proteins from the fungal soil-borne pathogens *Verticillium dahliae* and *Rosellinia necatrix*

Edgar A. Chavarro Carrero
Wageningen, 17 April 2024

Identification and functional characterization of effector proteins from the fungal soil-borne pathogens *Verticillium dahliae* and *Rosellinia necatrix*

Edgar Andres Chavarro Carrero

Identification and functional characterization of effector proteins from the fungal soil-borne pathogens *Verticillium dahliae* and *Rosellinia necatrix*

Edgar Andres Chavarro Carrero

Thesis
submitted in fulfilment of the requirement for the degree of doctor
at Wageningen University
by the authority of the Rector Magnificus,
Prof. Dr C. Kroeze
in the presence of the
Thesis Committee appointed by the Academic Board
to be defended in public
on Wednesday 17 April 2024
at 4 p.m. in the Omnia Auditorium.

TABLE OF CONTENT

Chapter | **1**

General introduction

Impact of fungal plant pathogens on crop production

Ever since the start of agriculture, crop production has been threatened by plant diseases caused by a wide diversity of pathogens and pests. Various pathogenic microorganisms have caused epidemic outbreaks, from which those that are caused by fungi and oomycetes stand out as most impactful, such as rice blast disease caused by *Magnaporthe oryzae*, rust diseases of wheat and soybean caused by *Puccinia graminis* and *Phakospora pachyrizi*, respectively, and late blight of potato caused by *Phytophthora infestans*, resulting in enormous yield losses and threatening global food security (Fisher et al., 2012). Obviously, besides food crops, also feed, fibre, and ornamental crops are affected by plant pathogens. The Food and Agriculture Organization of the United Nations (FAO) estimates that plant diseases cost the global economy around US$220 billion per year, with 20–40% of crop production lost due to plant pathogens (FAO, 2019). Unsurprisingly, in present times climate change plays a major role in the spread and impact of plant pathogens, and consequently also in their management (Delgado-Baquerizo et al., 2020; Chaloner et al., 2021).

Cultivation of roses, and soil-borne pathogens affecting rose production

Rose (*Rosa* spp.) is an ornamental crop cultivated worldwide with an economic value estimated to exceed over $50 billion per year (Manikas et al., 2020). Comprising around 120 species, the *Rosa* genus belongs to the Rosaceae family. The species are found in northern temperate climate zones and in the subtropical parts of the world. The taxonomic classification of *Rosa* spp. is obscured due to the large number of published names and the generation of hybrids by cross breeding during many centuries, which makes it almost impossible to distinguish naturally evolved species from man-made hybrids (Gahlaut et al., 2021).

Of the many species, only eight have contributed to the development of modern rose varieties. Those species originate from three different geographical regions (Far East, Europe, and the eastern part of the Mediterranean). Usually, rose species flower in spring and in summer, whereas only one type, *Rosa moschata* (R. x noisettiana), flowers in autumn. Interestingly, *R. damascena* (damask rose) displays recurrent flowering, and may be a hybrid with the autumn-flowering R. moschata. Other recurrently flowering roses are the derivates of *R. chinensis* and *R. gigantea* that were introduced from the Far East. Possibly they were the product of many generations of breeding in China, Japan and India (Raymond et al., 2018; Saint-Oyant et al., 2018). Subsequent mutations and cross breeding with roses from Europe and the Middle- East resulted in modern varieties with recurrent flowering that are now used in modern rose cultivation (de Hoog, 2001).

The value of rose crops is derived from its use in the industry for fragrances, as

garden plant and as cut flower (Boskabady et al., 2011; Dobhal et al., 2016; Vazquez-Iglesias et al., 2019). Although the production of cut-roses in the Netherlands is based on soil-free cultivation systems, cut-rose cultivars are commonly grown in soil-based greenhouses systems worldwide using grafts on rootstocks that favour rapid production of shoots from desirable rose cultivars that usually grow weakly on their own roots (Tubbs, 1973). Thus, rootstocks play an important role in rose cultivation as they improve flower production, flower quality, as well as adaptation to different types of soils, and typically display higher disease resistance than the cultivars themselves (Fuchs, 1994). Furthermore, their propagation is typically easier than the propagation of cultivars. Up to the 1980's *R. noisettiana* Manetti and *R. odorata* (Andr.) (syn. *R. indica* L. 'Major', *R. chinensis* 'Major') were the most widely used rootstocks in the greenhouse-based rose cultivation industry in North and South America (de Vries, 2003). During the 1990's, however, the introduction of the rootstock *R. canina* Natal Briar, developed in the Netherlands, has largely replaced *R. noisettiana* Manetti (Cabrera et al., 2009), and has become the most frequently used rootstock worldwide due to his agronomic advantages, including better rooting (Ritter et al., 2018), higher yields (Safi, 2005), and higher resistance to winter conditions (Safi, 2005).

As any other crop, rose is susceptible to a diversity of pathogens, including fungi, bacteria, viruses, nematodes and phytoplasmas (Horst and Cloyd, 2007). These pathogens are all considered economically relevant as they can directly affect ornamental value and crop yield (Debener and Byrne, 2014). While many of these pathogens infect above-ground parts of the rose plants, so-called soil-borne pathogens infect the root system below ground. Although it is generally appreciated that rootstocks can contribute to resistance against these soil-borne pathogens, also the most frequently employed rootstock cultivar Natal Briar is susceptible to soil-borne pathogens (Garcia-Velasco et al. 2012). Consequently, soil-borne fungal pathogens such as *Rosellinia necatrix* and *Rhizoctonia solani*, causal agents of root rots, and *Fusarium oxysporum* and *Verticillium dahliae*, causal agents of wilt diseases, represent a major threat to rose crops in soil-based cultivation systems (Madden, 1931; Bolton, 1982; Barguil et al., 2009; García-Velasco et al., 2012). Arguably, rose cultivation in soil-free systems, such as typically employed for rose cultivation in the Netherlands on artificial substrates, suffers much less from soil-borne pathogens.

Recently, rose cultivation in Mexico has grown due to favourable climate conditions for rose cultivation combined with its proximity to the United States, which is one the biggest importers of cut roses worldwide. Consequently, fields that were used for the cultivation of other crops, such as tomato and avocado were repurposed for rose cultivation. This has made that soil-borne diseases that typically plague tomato and avocado crops, most notably white root rot caused by *R. necatrix* (Garcia-Velasco et

al., 2012) and wilt disease caused by *V. dahliae* (Madden, 1931; Hammett, 1971), have become problematic for rose cultivation too.

Figure 1. Wilt disease symptoms in rose plants caused by soil-borne pathogens. (A) Typical appearance of disease symptoms caused by *Rosellinia necatrix*. (B) Wilting disease symptoms caused by *Verticillium dahliae*.

The soil-borne pathogen *Rosellinia necatrix*

Rosellinia necatrix is a prevalent soil-borne plant-pathogenic fungus that is found in temperate and tropical areas worldwide (Sivanesan and Holliday, 1972). The fungus is the causal agent of white root rot disease that occurs on at least 170 species of dicotyledonous angiosperms that are dispersed over 63 genera and 30 families (Sztejnberg and Madar, 1980). Many of these species are of considerable economic importance, such as *Coffea* spp. (coffee), *Malus* spp. (apple), *Olea europea* L. (olive), *Persea americana* Mill. (avocado), *Prunus* spp. (peaches, almonds, etc.), *Vitis vinifera* L. (grape) and *Rosa* sp. (rose) (Perez-Jimenez, 2006; Eguchi et al., 2009; García-Velasco et al., 2012).

The life cycle of *R. necatrix* is not completely understood. Various studies have shown that the asexual life cycle of *R. necatrix* involves two different spore types: chlamydospores and conidiospores (Perez-Jimnez, 2006). Chlamydospores can be found only under extreme environmental conditions (Pérez-Jiménez et al., 2003), are rather spherical, and originate from condensation of the pyriform swellings in the protoplasm and subsequent formation of a cell wall (Makambila, 1976). Conidia originate at the ends of synnemata of conidiogenous cells, which are produced from either sclerotia (possibly related to pathogen survival in soil) or brown mycelial masses. Conidia are solitary, single-celled, hyaline, elliptical and are borne both apically and laterally to the

conidiogenous cells (Petrini, 1993). *R. necatrix* typically only shows mycelial growth *in vitro* (Perez-Jimnez, 2006).

R. necatrix can also undergo sexual reproduction through the production of ascospores that are formed inside perithecia that, when they reach maturity, are expelled into a mucilaginous mass from the pore of the papilla located at the top of the perithecium (Makambila, 1976; Lin and Duan, 1988; Teixeira de Sousa and Whalley, 1991; Pérez-Jiménez et al., 2003). Fresh perithecia are soft and spherical, with a gelatinous aspect and a honey colour. As they age, they contract and acquire a brown–black colour and a dry aspect as a result of hyphal and cell melanisation. The asci are projected towards the interior of the perithecium (Pérez-Jiménez et al., 2003). Perithecia formation takes a long time under natural conditions and has never been achieved under artificial conditions (Pliego et al., 2011). *R. necatrix* has a heterothallic sexual reproduction cycle, meaning that two individuals of opposite mating type are required to undergo sexual reproduction (Kanda et al., 2003; Ikeda et al., 2011).

Plants infected by *R. necatrix* typically display two types of symptoms. The first type is displayed below-ground on the root system, where white and black colonies of mycelium can occur on the surface of infected roots. As the fungus progresses by penetrating the tissue, leading to root rot, the roots acquire a dark brown colour (Guillaumin et al., 1982). The second type of symptom occurs above-ground. These symptoms can develop rapidly as a consequence of the damaged root system and comprise wilting of leaves, typically after a period of drought or physiological stress, which affects plant vigour and can eventually lead to plant death. Symptoms of *R. necatrix* infection can also appear slowly, leading to a decline in growth, decreasing leaf numbers, along with wilting of leaves, chlorosis, and death of twigs and branches. On perennials these symptoms aggravate over time, and when moisture and temperature are unfavourable, the plant eventually dies (Guillaumin et al., 1982).

The soil-borne pathogen *Verticillium dahliae*

Verticillium dahliae is a soil-borne fungus with a broad host range that comprises hundreds of dicotyledonous plant species, including numerous crops such as tomato, potato, lettuce, olive, cotton, and roses (Fradin and Thomma, 2006, Klosterman et al., 2009). Although *V. dahliae* is considered a broad host-range pathogen and individual strains are typically characterized by their ability to infect a diversity of hosts, host preference exists for particular isolates (Bhat and Subbarao, 1999).

The life cycle of *V. dahliae* can be divided into a dormant, a parasitic and a saprophytic phase (Fradin and Thomma, 2006). In the dormant phase, *V. dahliae* survives in the soil through persistent melanized resting structures, so-called microsclerotia, that offer protection against (a)biotic stresses and survive in the soil for many years.

Microsclerotia, which represent the primary inoculum source in nature, germinate upon stimulation by exudates released by plant roots (Huisman, 1982; Mol et al., 1995; Olsson and Nordbring-Hertz, 1985; Schreiber and Green, 1963) and the hyphae that grow out can traverse only a limited distance, possibly directed by nutrient gradients, to reach potential host plants (Huisman, 1982). The fungus then penetrates the roots, grows through the cortex, and enters the xylem vessels where conidiospores are produced that are transported to distal tissues with the sap stream and germinate once they get trapped, for instance at vessel ends (Huisman,1982). Upon germination, the fungus can penetrate cell walls, enter new xylem vessels, and again sporulates. As a consequence of the systemic colonization of xylem vessels, water transport is disrupted, ultimately leading to the characteristic wilting symptoms. Later during plant senescence, *V. dahliae* initiates a saprophytic stage during which it emerges from the xylem vessels to colonize the decaying tissues where it produces microsclerotia that are released into the soil upon tissue decomposition (Wilhelm, 1955).

V. dahliae has no known sexual stage. For sexual reproduction in fungi two mating-type idiomorphs are required (Debuchy and Turgeon 2006). Nearly all known *V. dahliae* isolates have the same mating type (MAT1-2) (Usami et al., 2009; Heitman et al., 2013; Milgroom et al., 2014) and isolates with mating-type idiomorph MAT1-1 are rare (Inderbitzin et al., 2011; Dung et al., 2012). Moreover, genome sequencing has revealed that the genome of *V. dahliae* strains is typically characterized by large-scale chromosomal rearrangements that are suggested to be involved in host adaptation (de Jonge et al., 2013). The extent of rearrangements likely interferes with pairing of homologous chromosomes during meiosis, and therefore further reduces the probability of sexual reproduction among lineages of the fungus (Seidl and Thomma, 2014).

Verticillium wilt of roses was first observed in a local rose nursery in Ontario in 1928 (Madden, 1931). The main symptoms comprise wilting of leaves at the tips of young canes and a yellowing of the lower leaves. After a few days permanent wilting occurs, and the leaves generally turn yellow and finally brown as they wither and die. Defoliation progresses from the base of canes upward. Canes that show symptoms may continue to grow normally in subsequent seasons, but they may also die back, and progressive dieback can even result in death of entire plants. Vascular discoloration, common on other hosts, is not usually evident in infected roses (Horst, 2007).

The molecular biology of plant-pathogen interactions

The molecular basis of plant–pathogen interactions has been explained throughout time using different conceptual frameworks. Initially, Harold Flor introduced the gene-for-gene model based on his observations for the interaction between *Linum*

usitassimum (flax) and *Melampsora lini* (flax rust) where a single dominant host gene, termed a resistance (*R*) gene, induces resistance in response to a pathogen expressing a single dominant avirulence (*Avr*) gene (Flor, 1942). Isolates of the pathogen that do not express the allele of the *Avr* gene that is recognized escape recognition and are assigned to a resistance-breaking race.

It was not until 1984 that the molecular cloning of the first bacterial *Avr* gene from *Pseudomonas syringae* pv. *glycinea* was reported (Staskawicz et al., 1984), followed by the first fungal *Avr* gene from *Cladosporium fulvum* in 1991 (van Kan et al., 1991), and the first oomycete *Avr* gene from *Phytophthora sojae* in 2004 (Shan et al., 2004). Dozens of additional *Avr* genes have been cloned since then from various pathogens (Parlange et al., 2009; Inami et al., 2012; Lu et al., 2016; Niu et al., 2016; Plissonneau et al., 2016; Praz et al., 2016; Chen et al., 2017; Inoue et al., 2017; Salcedo et al., 2017; Zhong et al., 2017; Anh et al., 2018; Kema et al., 2018; Meile et al., 2018; Bourras et al., 2015, 2019; Petit-Houdenot et al., 2019; Saur et al., 2019).

In parallel to race-specific *Avrs*, non-race-specific elicitors were described as conserved microbial molecules that can be recognized by multiple plant species (Darvill and Albersheim, 1984). The recognition by plants of *Avrs* and of non-race-specific elicitors, presently known as pathogen- or microbe-associated molecular patterns (P/MAMPs), was combined in the 'zig-zag' model (Jones and Dangl, 2006). In this model, P/MAMPs are perceived by cell surface-localized pattern recognition receptors (PRRs) to trigger pattern-triggered immunity (PTI), while pathogen-secreted molecules that promote host invasion, also known as effectors, are recognized by cytoplasmic receptors that are known as resistance (R) proteins to activate effector-triggered immunity (ETI) (Jones and Dangl, 2006). Importantly, the model recognizes that Avrs function to suppress host immune responses in the first place, implying that these molecules, besides being avirulence determinants, act as virulence factors through their function as effector molecules (Jones and Dangl, 2006). A more recent model, termed the invasion model, recognizes that the functional separation of PTI and ETI is problematic and proposes that the corresponding receptors, collectively termed invasion pattern receptors (IPRs), detect either externally encoded or modified-self ligands that indicate invasion, termed invasion patterns (IPs), to mount an effective immune response (Thomma et al., 2011; Cook et al., 2015). Indeed, increasing evidence supports the notion that PTI and ETI are functionally not separated, but rather heavily intertwined (Ngou et al., 2021; Pruitt et al., 2021; Tian et al., 2021; Yuan et al., 2021).

Effectors and their role on plant-pathogen interactions

It is generally accepted that plant pathogens secrete dozens to hundreds of proteins into the apoplast or cytosol of their host plants to mediate host colonization, and that

are typically referred to as effector proteins (Rovenich et al., 2014). These effector proteins are typically ≤300 amino acids, cysteine-rich and have tertiary structures that are stabilized by disulfide bridges (Duplessis et al., 2011; Gan et al., 2013; Stergiopoulos et al., 2013; Lo Presti et al., 2015). However, also larger secreted proteins have been found to act as effectors, such as several LysM effectors (Kombrink and Thomma, 2013). Furthermore, besides proteins also non-proteinaceous effectors have been described, such as fungal secondary metabolites as well as small RNA (sRNA) molecules that are delivered into host cells to suppress host immunity (Collemare and Lebrun, 2011; Weiberg et al., 2014).

A wide range of effectors has been identified in a diversity of pathogens and great efforts have been made to understand their role in disease establishment. Several effectors have been shown to act in the apoplast, such as fungal LysM effectors (de Jonge et al., 2010). Plant chitinases target fungal cell walls to release chitin fragments that activate immune receptors, leading to further chitinase accumulation to induce hyphal lysis (Kombrink et al., 2011). In turn, fungal pathogens secrete chitin-binding LysM effectors to protect their cell walls and to interfere with immune receptor activation (de Jonge et al., 2010; Marshall et al., 2011; Mentlak et al., 2012; Takahara et al., 2016; Kombrink et al., 2017; Chen et al., 2020; Tian et al., 2021). Some other apoplastic effectors target hydrolytic enzymes, such as proteases. For example, effectors of *Cladosporium fulvum* (Avr2), the oomycete *Phytophthora infestans* (EPIC1 and EPIC2B), and the parasitic nematode *Globodera rostochiensis* (Gr-VAP1) inhibit tomato cysteine proteases including Rcr3 (van Esse et al., 2008; Song et al., 2009; Lozano-Torres et al., 2012). In addition to apoplastic effectors, many pathogens deliver effectors that act inside host cells. For example, the rice blast fungus *Magnaporthe oryzae* was shown to secrete various effectors that enter rice cells and that can move to non-infected neighbouring cells (Khang et al., 2010). In the same manner the Cmu1 effector of the maize smut fungus *Ustilago maydis* has been shown to diffuse from infected cells to neighbouring cells to interfere with salicylic acid biosynthesis to reduce plant immune signalling (Djamei et al., 2011). Finally, several effectors target host cell death mechanisms, including the effectors Avr3a and PexRD2 from *P. infestans*, as well as the effector victorin from *Cochliobolus victoriae* (Bos et al., 2010; Lorang et al., 2012; King et al., 2014).

To date, no effectors from *R. necatrix* have been identified and thus their potential role in disease establishment remains unknown. In contrast, various *V. dahliae* effector proteins have been identified and their roles in virulence, but also in avirulence, has been studied on various hosts (de Jonge et al., 2012; 2013; Santhanam et al., 2013; Liu et al., 2014; Santhanam et al., 2017; Qin et al., 2018; Gao et al., 2019). Although intrinsic functions of effectors benefit the pathogen by contributing to host colonization

as virulence factors, some effectors become avirulence factors once they become recognized by plant hosts that carry corresponding resistance (*R*) genes. For *V. dahliae* only a single *Avr* has been identified, namely the effector Ave1 (avirulence on Ve1) that acts as an avirulence factor on tomato genotypes carrying *Ve1* (de Jonge et al., 2012).

Besides the avirulence effector Ave1, several effectors of *V. dahliae* have been characterized that act in virulence, such as members of the well-described family of chitin-binding lysin motif (LysM) effectors, from which one was found to contribute to virulence on tomato (de Jonge et al., 2013; Kombrink et al., 2017). This effector, Vd2LysM, suppresses chitin-triggered immunity and protects fungal hyphae against hydrolysis by plant chitinases (Kombrink et al., 2017; Tian et al., 2021). The secreted protein polysaccharide deacetylase (PDA1) promotes virulence in cotton and tomato through deacetylation of chitin oligomers (Gao et al., 2019). Members of the family of necrosis- and ethylene-inducing-like proteins (NLPs; Gijzen and Nürnberger, 2006; Seidl and Van den Ackerveken, 2019) were identified in *V. dahliae* as well, and two induce plant cell death and promote virulence on tomato and on *Arabidopsis thaliana* plants (Santhanam et al., 2013). Furthermore, the *V. dahliae* isochorismatase (VdIsc1) that converts isochorismate, a precursor of salicylate, to 2,3-dihydro-2,3-dihydroxybenzoate (DDHB) and pyruvate is a virulence factor on cotton (Liu et al., 2014). The effector VdSCP41 has been identified as a virulence factor on *A. thaliana* and cotton plants (Qin et al., 2018).

Effector proteins secreted by plant pathogens have mostly been studied with respect to their activity on plant hosts in a binary fashion. Nevertheless, plant-pathogen interactions typically occur in a microbiota-rich environment, and many infection sites may develop into microbial hot-spots where also opportunists try to gain an advantage. It has been well established that plants shape their rhizosphere microbiota compositions through secretion of exudates (Huang et al., 2019; Koprivova et al., 2019), and therefore they can also recruit beneficial microbes to suppress pathogen invasion (Rudrappa et al., 2008; Berendsen et al., 2012; 2018). Recently, it has been shown that plant pathogens may utilize effector proteins to modulate host microbiota compositions in turn, to facilitate host colonization (Snelders et al., 2018). More specifically, the *V. dahliae* effector protein Ave1 was shown to display antimicrobial activity to facilitate colonization of tomato and cotton plants by suppressing antagonistic bacteria that belong to the *Spingomonadaceae* (Snelders et al., 2020). Moreover, this fungus was shown to secrete the antifungal effector protein AMP3 to ward off fungal antagonists during microsclerotia formation in necrotic plant tissues (Snelders et al., 2021). It is therefore becoming increasingly evident that effectors function beyond the binary interaction between the pathogen and the host and target the host microbiota to stimulate disease development.

1

Outline of this thesis

The aim of my doctoral research was to identify effectors from the soil-borne pathogens *Rosellinia necatrix* and *Verticillium dahliae* and to characterize their roles in the interaction with plant hosts.

In **Chapter 2** we identify the *V. dahliae* avirulence effector Av2 that activates *V2* resistance on tomato. By employing a comparative genomics approach of *V. dahliae* race 2 strains and resistance-breaking race 3 strains, we identify 277 kb of race 2-specific sequences comprising only two genes that encode predicted secreted proteins that are expressed during tomato colonization. Subsequent functional analysis based on introduction into race 3 and targeted deletion from race 2 confirmed that one of the two candidates encodes the avirulence effector Av2 that is recognized by *V2* tomato plants.

Chapter 3 focuses on the characterization and contribution of the effector catalogue of *Verticillium dahliae* to Verticillium wilt disease on rose plants. We investigate whether previously characterized effectors from *V. dahliae* on other plant hosts, most notably tomato, play a role as virulence factor contributing to Verticillium wilt disease on rose as well.

In **Chapter 4** we study the genomic diversity of nine *R. necatrix* strains and establish a near-chromosome genome assembly for one of these strains. For this, we employed Oxford Nanopore sequencing technology to sequence nine strains that were collected from rose and avocado in Mexico and Spain, respectively; and with help of DNA proximity ligation, the genome of one strain was assembled to near-chromosome level. Furthermore, we predict its effector repertoire and tried to predict potential antimicrobial effector proteins that can modulate specific members of a synthetic microbial community.

In **Chapter 5** we developed a Nanopore sequencing pipeline to reveal microbiome modulation by potential antimicrobial effector proteins. To this end, we used *in vitro* conditions where we uncover antimicrobial activities of effector proteins of *R. necatrix* and *V. dahliae* by identifying their ability to modulate synthetic communities using Oxford Nanopore sequencing technology.

Finally, in **Chapter 6** I discuss the results presented in this PhD thesis and present perspectives for future work related to effector identification and functional characterization in the soil-borne rose pathogens *R. necatrix* and *V. dahliae*. Furthermore, I discuss the potential of using Oxford Nanopore sequencing technology to reveal microbiome modulation by these soil-borne rose pathogens, but also by other plant pathogens in general. Finally, I will provide an outlook on how rose cultivation will overcome problems caused by soil-borne pathogens.

Chapter 2

Comparative genomics reveals the *in planta*-secreted *Verticillium dahliae* Av2 effector protein recognized in tomato plants that carry the *V2* resistance locus

Edgar A. Chavarro-Carrero[$], Jasper P. Vermeulen[$], David E. Torres, Toshiyuki Usami, Henk J. Schouten, Yuling Bai, Michael F. Seidl[#] and Bart P. H. J. Thomma[#]

[$,#]These authors contributed equally

2

ABSTRACT

Plant pathogens secrete effector molecules during host invasion to promote colonization. However, some of these effectors become recognized by host receptors to mount a defence response and establish immunity. Recently, a novel resistance was identified in wild tomato, mediated by the single dominant V2 locus, to control strains of the soil-borne vascular wilt fungus *Verticillium dahliae* that belong to race 2. With comparative genomics of race 2 strains and resistance-breaking race 3 strains, we identified the avirulence effector that activates V2 resistance, termed Av2. We identified 277 kb of race 2-specific sequence comprising only two genes encoding predicted secreted proteins that are expressed during tomato colonization. Subsequent functional analysis based on genetic complementation into race 3 isolates and targeted deletion from the race 1 isolate JR2 and race 2 isolate TO22 confirmed that one of the two candidates encodes the avirulence effector Av2 that is recognized in *V2* tomato plants. Two *Av2* allelic variants were identified that encode Av2 variants that differ by a single acid. Thus far, a role in virulence could not be demonstrated for either of the two variants.

INTRODUCTION

In nature, plants are continuously threatened by potential plant pathogens. However, most plants are resistant to most potential plant pathogens due to an efficient immune system that becomes activated by any type of molecular pattern that accurately betrays microbial invasion (Dangl and Jones, 2001; Cook et al., 2015). Throughout time, different conceptual frameworks have been put forward to describe the molecular basis of plant–pathogen interactions and the mechanistic underpinning of plant immunity. Initially, Harold Flor introduced the gene-for-gene model in which a single dominant host gene, termed a resistance (R) gene, induces resistance in response to a pathogen expressing a single dominant avirulence (*Avr*) gene (Flor, 1942). Isolates of the pathogen that do not express the allele of the *Avr* gene that is recognized escape recognition and are assigned to a resistance-breaking race. In parallel to these race-specific Avrs, non-race-specific elicitors were described as conserved microbial molecules that are often recognized by multiple plant species (Darvill and Albersheim, 1984). The recognition by plants of Avrs and of non-race-specific elicitors, presently known as pathogen- or microbe-associated molecular patterns (P/MAMPs), was combined in the 'zig-zag' model (Jones and Dangl, 2006). In this model, P/MAMPs are perceived by cell surfacelocalized pattern recognition receptors (PRRs) to trigger pattern-triggered immunity (PTI), while effectors are recognized by cytoplasmic receptors that are known as resistance (R) proteins to activate effector-triggered immunity (ETI) (Jones and Dangl, 2006). Importantly, the model recognizes that Avrs function to suppress host immune responses in the first place, implying that these molecules, besides being avirulence determinants, act as virulence factors through their function as effector molecules (Jones and Dangl, 2006). A more recent model, termed the invasion model, recognizes that the functional separation of PTI and ETI is problematic and proposes that the corresponding receptors, collectively termed invasion pattern receptors (IPRs), detect either externally encoded or self-modified ligands that indicate invasion, termed invasion patterns (IPs), to mount an effective immune response (Thomma et al., 2011; Cook et al., 2015). However, it is generally appreciated that microbial pathogens secrete dozens to hundreds of effectors to contribute to disease establishment, only some of which are recognized as Avrs (Rovenich et al., 2014).

IPRs encompass typical *R* genes, which have been exploited for almost a century to confer resistance against plant pathogens upon introgression from sexually compatible wild relatives into elite cultivars (Dodds and Rathjen, 2010; Dangl et al., 2013). Most *R* genes encode members of a highly polymorphic superfamily of intracellular nucleotidebinding leucine-rich repeat (NLR) receptors, while others encode cell surface receptors (Dangl et al., 2013). Unfortunately, most *R* genes used in commercial crops are short-lived because the resistance that they provide is rapidly broken by pathogen

populations as their deployment in monoculture-based cropping systems selects for pathogen variants that overcome immunity (Stukenbrock and McDonald, 2008; Dangl et al., 2013). Such breaking of resistance occurs upon purging of the *Avr* gene, sequence diversification, or by employment of novel effectors that subvert the host immune response (Stergiopoulos et al., 2007; Cook et al., 2015).

The molecular cloning of the first bacterial *Avr* gene from *Pseudomonas syringae* pv. *glycinea* was reported in 1984 (Staskawicz et al., 1984), the first fungal *Avr* gene from *Cladosporium fulvum* in 1991 (van Kan et al., 1991) and the first oomycete *Avr* gene from *Phytophthora sojae* in 2004 (Shan et al., 2004). Dozens of additional *Avr* genes have been cloned since then, in various pathogens (Parlange et al., 2009; Inami et al., 2012; Plissonneau et al., 2016; Praz et al., 2016; Lu et al., 2016; Niu et al., 2016; Chen et al., 2017; Inoue et al., 2017; Salcedo et al., 2017; Zhong et al., 2017; Anh et al., 2018; Kema et al., 2018; Meile et al., 2018; Bourras et al., 2015; 2019; Petit-Houdenot et al., 2019; Saur et al., 2019). Most of these *Avr* genes have been identified by map-based cloning and reverse genetics strategies. More recently, advances in (the affordability of) genome sequencing have allowed the cloning of novel *Avrs* by combining comparative genomics or transcriptomics with functional assays, a trend that was spearheaded by the cloning of the first *Avr* gene from *Verticillium dahliae* only in 2012 (de Jonge et al., 2012; Mesarich et al., 2014; Schmidt et al., 2016).

Verticillium dahliae is a soil-borne fungal pathogen and causal agent of Verticillium wilt on a broad range of host plants that comprises hundreds of dicotyledonous plant species, including numerous crops such as tomato, potato, lettuce, olive, and cotton (Fradin and Thomma, 2006; Klosterman et al., 2009). The first source of genetic resistance toward Verticillium wilt was identified in tomato (*Solanum lycopersicum*) in the early 1930s in an accession called Peru Wild (Schaible et al., 1951). The resistance is governed by a single dominant locus, designated Ve (Diwan et al., 1999), comprising two genes that encode cell surface receptors of which one, *Ve1*, acts as a genuine resistance gene (Fradin and Thomma, 2006). Shortly after its deployment in the 1950s, resistance-breaking strains have appeared that were assigned to race 2, whereas strains that are contained by *Ve1* belong to race 1 (Alexander, 1962). Thus, *Ve1* is characterized as a race-specific *R* gene, and resistance-breaking strains have become increasingly problematic over time (Alexander, 1962; Dobinson et al., 1996). With comparative population genomics of race 1 and race 2 strains, the *V. dahliae* avirulence effector that is recognized by tomato Ve1 was identified as VdAve1, an effector that is secreted during host colonization (de Jonge et al., 2012). As anticipated, it was demonstrated that VdAve1 acts as a virulence factor on tomato plants that lack the *Ve1* gene and that, consequently, cannot recognize VdAve1 (de Jonge et al., 2012). Recent evidence demonstrates that VdAve1 exerts selective antimicrobial activity and has the capacity

to manipulate local microbiomes inside host plants as well as in the environment (Snelders et al., 2020). Whereas all race 1 strains carry an identical copy of *VdAve1*, all race 2 strains analysed to date are characterized by complete loss of the *VdAve1* locus (de Jonge et al., 2012; Faino et al., 2016). Intriguingly, phylogenetic analysis has revealed that *VdAve1* was horizontally acquired by *V. dahliae* from plants (de Jonge et al., 2012; Shi-Kunne et al., 2018), after which the effector gene was lost multiple times independently, presumably due to selection pressure exerted by the *Ve1* locus that has been introgressed into most tomato cultivars (Faino et al., 2016).

Despite significant efforts, attempts to identify genetic sources for race 2 resistance in tomato have remained unsuccessful for a long time (Baergen et al., 1993). Recently, however, a source of race 2 resistance was identified in the wild tomato species *Solanum neorickii* (Usami et al., 2017). This genetic material was used to develop the tomato rootstock cultivars Aibou, Ganbarune-Karis and Back Attack by Japanese breeding companies, in which resistance is controlled by a single dominant locus, denoted *V2* (Usami et al., 2017). However, experimental trials using race 2-resistant rootstocks revealed resistance-breaking *V. dahliae* strains that, consequently, are assigned to race 3 (Usami et al., 2017). In this study, we performed comparative genomics combined with functional assays to identify the avirulence effector Av2 that activates race-specific resistance in tomato genotypes that carry *V2*.

2

2

RESULTS

Identification of *Verticillium dahliae* strains that escape V2 resistance

To identify *Av2* as the *V. dahliae* gene that mediates **a**virulence on tomato <u>***V2***</u> plants, we pursued a comparative genomics strategy by searching for genomic regions that are absent from all race 3 strains. To this end, we performed pathogenicity assays with a collection of *V. dahliae* strains on a differential set of tomato genotypes, comprising (I) Moneymaker plants that lack *V. dahliae* resistance genes, (II) *Ve1*-transgenic Moneymaker plants that are resistant against race 1 and not against race 2 strains (Fradin et al., 2009), and (III) Aibou plants that carry *Ve1* and *V2* and are therefore resistant against race 1 as well as race 2 strains (Usami et al., 2017) (Figure 1A). First, we aimed to confirm the race assignment of eight *V. dahliae* strains that were previously tested by Usami et al. (2017) (Table 1). Additionally, three strains that were previously assigned to race 2 were included (de Jonge et al., 2012) as well as *V. dahliae* strain JR2 (race 1) because of its gapless telomere-to-telomere assembly (Faino et al., 2015).

At 3 weeks post inoculation, all strains caused significant stunting on the universally susceptible Moneymaker control (Figure 1A and B), while all strains except for the race 1 strain JR2 caused significant stunting on *Ve1*-transgenic Moneymaker plants (Figure 1A and C), corroborating that, except for strain JR2, none of the strains belongs to race 1 and that a potential containment on Aibou plants cannot be caused by Ve1 recognition of the VdAve1 effector. Importantly, all of the strains that were used by Usami et al. (2017) and that were previously assigned to race 2 did not cause significant stunting on Aibou, whereas all of the strains that were assigned to race 3 caused clear symptoms of Verticillium wilt disease (Figure 1, Table 1; Usami et al., 2017). The previously assigned race 2 strain DVDS26 (de Jonge et al., 2012) caused no significant stunting on Aibou plants, confirming that this remains a race 2 strain, while strains DVD161 and DVD3 caused significant stunting, implying that these strains should actually be assigned to race 3. As expected, the race 1 strain JR2 did not cause stunting on Aibou plants, which can at least partially be attributed to VdAve1 effector recognition by the *Ve1* gene product in these plants. However, the finding that a transgenic *VdAve1* deletion line (JR2ΔAve1; de Jonge et al., 2012) caused significant stunting on *Ve1*-transgenic Moneymaker and not on Aibou plants, indicates that the JR2 strain might also encode Av2. Currently, it is not known whether this is the case, or whether it is simply that basal defence is enhanced in the absence of *Ave1*. After all, we previously showed that the virulence of the *VdAve1* deletion strain on tomato is severely compromised (de Jonge et al., 2012), which can also be observed on Moneymaker plants in our assays (Figure 1B). This observation, combined with the observation that stunting on Aibou plants by any race 3 strain is generally less than stunting on Moneymaker plants (Figure 1B and D),

could indicate that basal defence against Verticillium wilt is enhanced in Aibou plants, and thus that incompatibility of the *VdAve1* deletion strain may be due to enhanced basal defence rather than due to V2-mediated recognition of the JR2 strain.
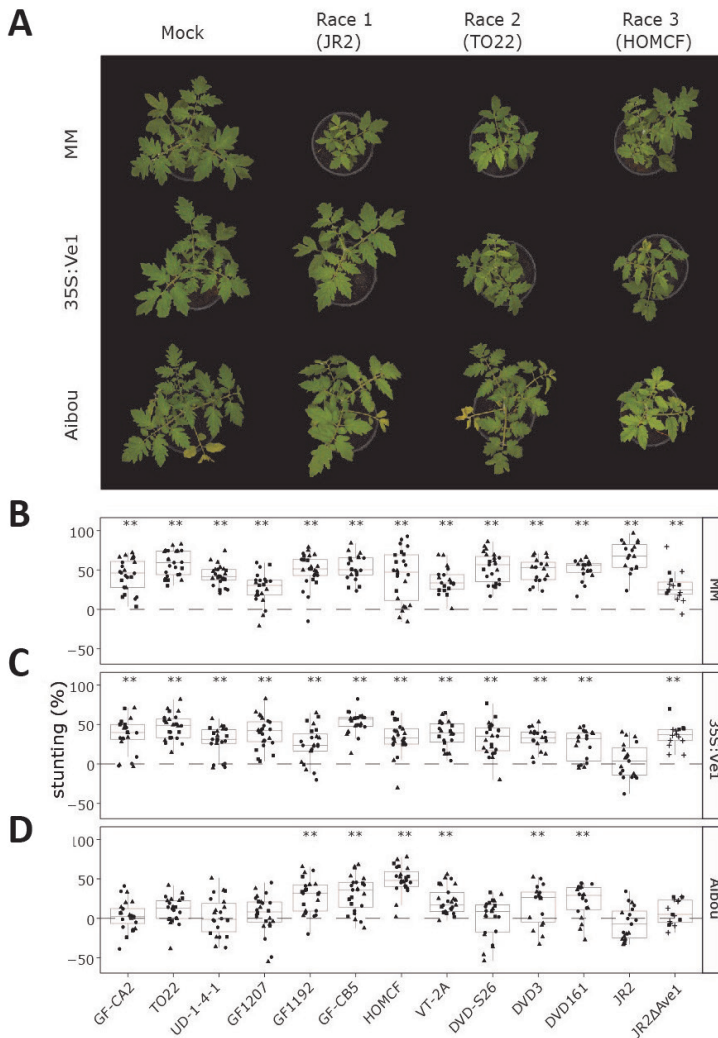
Figure 1. Pathogenicity phenotyping of a collection of *Verticillium dahliae* strains on tomato. (A) Typical appearance of *V. dahliae* infection by strain JR2, TO22 and HOMCF as representatives for race 1, 2 and 3, respectively, on Moneymaker (MM) plants that lack known *V. dahliae* resistance genes, *Ve1*-transgenic Moneymaker plants that are resistant against race 1 and not against race 2 or 3 strains, and Aibou plants that carry *Ve1* and *V2* and are therefore resistant against race 1 as well as race 2 strains, but not against race 3 strains at 21 days post inoculation (dpi). (B–D) Measurement of *V. dahliae*-induced stunting on wild-type Moneymaker plants (B), *Ve1*-transgenic Moneymaker plants (35S:Ve1) (C) and Aibou plants (D) at 21 dpi. The graphs show collective data from four different experiments indicated with different symbols (circles, squares, triangles and plus symbols), and asterisks indicate significant differences between *V. dahliae*- and mock-inoculated plants as determined with an ANOVA followed by a Fisher's LSD test (P < 0.01).

Table 1. *Verticillium dahliae* strains used in this study for comparative genomics and genome assembly statistics.

Strain	Previous race annotation	Ref. isolate[a]	Novel race annotation	Platform[b]	Data (Gb)[c]	Assembly size (Mb)	No. of contigs[d]	Contig N50 (Kb)[d]	Ref. sequencing
JR2	1	A	1	PacBio	8.9	36.1	8	4168	D
DVDS26	2	B	2	Illumina	1	35.3	5361	47.1	B
DVD161	2	B	2, 3	Illumina	1	34.1	4078	42.4	B
DVD3	2	B	2, 3	Illumina	1	34.1	9318	43.9	B
TO22	2	C	2	Nanopore	4	34.9	20	12.4	TS
UD1-4-1	2	C	2	Nanopore	1.9	34.6	18	18.1	TS
GF1207	2	C	2	Nanopore	1.6	34.8	69	8.5	TS
GF-CA2	2	C	2	Nanopore	2	35.0	38	9.1	TS
GF-CB5	3	C	2, 3	Nanopore	4	34.8	19	11.4	TS
VT-2A	3	C	2, 3	Nanopore	1.8	34.8	22	10.2	TS
GF1192	3	C	2, 3	Nanopore	2	34.6	23	14.5	TS
HOMCF	3	C	2, 3	Nanopore	2	36.1	33	10.1	TS

[a]References: A: Fradin et al., 2009; B: de Jonge et al., 2012; C: Usami et al., 2017; D: Faino et al., 2015; TS: this study.
[b]Sequencing platform used.
[c]Amount of sequencing data generated.
[d]For strains DVDS26, DVD161 and DVD3 previously determined scaffold statistics are shown (de Jonge et al., 2012).

Comparative genomics identifies *Verticillium dahliae Av2* candidates

Besides the gapless genome assembly of strain JR2 (Faino et al., 2015), genome assemblies were also available for strains DVDS26, DVD161 and DVD3, albeit that these assemblies were highly fragmented as these were based on Illumina short-read sequencing data (de Jonge et al., 2012) (Table 1). In this study, we determined the genomic sequences of the race 2 strains TO22, UD1-4-1, GF1207 and GFCA2, and the race 3 strains GF-CB5, GF1192, VT2A and HOMCF with Oxford Nanopore sequencing Technology (ONT) using a MinION device (Table 1). For each strain, ~2–4 Gb of sequence data was produced, representing 50–100x genome coverage based on the ~35 Mb gapless reference genome of *V. dahliae* strain JR2 (Faino et al., 2015). Subsequently, we performed self-correction of the reads, read trimming and genome assembly, leading to genome assemblies ranging from 18 contigs for strain UD1-4-1 to 69 for strain GF1207 (Table 1).

Based on the genome sequences, we pursued comparative genomics analyses by exploring two scenarios. The first scenario is that *Av2* is race 2-specific and thus present in race 2 lineage sequences while absent from race 3. The second scenario is that *Av2* is present in isolates that belong to race 1 and race 2, but that the resistance phenotype against race 2 is masked by Ve1 resistance directed against Ave1. In scenario I, comparative genomics was performed making use of race 2 strain TO22 (Usami et al., 2017) as a reference, while in scenario II race 1 strain JR2 (Faino et al., 2015) was used (Table 2). To this end, self-corrected reads from the *V. dahliae* race 3 strains were mapped against the assembly of *V. dahliae* strain TO22 (scenario I) or strain JR2 (scenario II) and regions that were not covered by race 3 reads were retained (Table 2). Next, self-corrected reads from the race 2 strains were mapped against the retained reference genome-specific regions that are absent from the race 3 strains, and sequences that were found in every race 2 strain were retained as candidate regions to encode the Avr molecule. Sequences that are shared by the *V. dahliae* strain TO22 reference assembly and all race 2 strains, and that are absent from all race 3 strains, were mapped against the *V. dahliae* strain JR2 genome assembly, and common genes were extracted. Sequences that did not map to the *V. dahliae* strain JR2 genome assembly were *de novo* annotated and signal peptides for secretion at the N-termini of the encoded proteins were predicted to identify potential effector genes.

Our strategy identified 563 kb of race 2-specific regions, containing 110 genes of which six encode putative secreted proteins, for scenario I (Table 2). For approach II, 222 kb of sequence that lacks in race 3 strains was identified with 40 genes of which only two are predicted to encode secreted proteins; *XLOC_00170* (*VDAG_JR2_Chr4g03680a*) and *evm.model.contig1569.344* (*VDAG_JR2_Chr4g03650a*, further referred to as *Evm_344*). Intriguingly, both these genes were previously recognized as being among the most

highly expressed effector genes during colonization of *Nicotiana benthamiana* plants (de Jonge et al. 2013; Faino et al., 2015).

Table 2. Comparative genomics of race 2 and race 3 strains.

Scenario	I	II
Reference strain	TO22	JR2
Race 2	GF-CA2 TO22 UD-1-4-1 DVDS26 GF1207	GF-CA2 TO22 UD-1-4-1 DVDS26 GF1207
Race 3	GF-1192 GF-CB5 HOMCF DVD161 DVD3 VT-2A	GF-1192 Gf-CB5 HOMCF DVD161 DVD3 VT-2A
Retained (kb)	563	222
Shared with JR2 (kb)	222	222
#JR2 genes	40	40
#Augustus-predicted genes	70	-
#Secreted	6	2
Retained candidates	• XLOC_00170 • evm.model.contig1569.344 • tig00000058:1 027 588–1 028 906 • tig00000058:1 116 044–1 116 494 • tig00000151:403362–404 089 • tig00017428:835657–837 290	• XLOC_00170 • evm.model.contig1569.344

Only two of the *Av2* candidates are expressed *in planta*

We anticipate that the genuine *Av2* gene may not necessarily be expressed in *N. benthamiana* (de Jonge et al. 2013) but should be expressed particularly in tomato. Real-time PCR analysis on a time course of tomato cultivar Moneymaker plants inoculated with the *V. dahliae* JR2 strain revealed that the two candidate genes are expressed during tomato colonization, with a peak in expression around 7 days post inoculation, whereas little to no expression could be recorded upon growth *in vitro* (Figure 2A). Both genes are similarly expressed in *V. dahliae* strain TO22, albeit that the expression peaks slightly later, at 11 dpi (Figure 2B). However, whereas the expression level of both

genes is similar in *V. dahliae* strain JR2, *Evm_344* is higher expressed than *XLOC_00170* in *V. dahliae* strain TO22. Importantly, none of the four additional avirulence effector gene candidates that were identified in comparative genomics scenario I is expressed *in planta* in *V. dahliae* strain TO22 (Figure 2B). Thus, based on the transcriptional profiling, these four avirulence effector genes can be disqualified as *Av2* candidates, and only two genes that display an expression profile that can be expected for a potential avirulence effector gene remain; *XLOC_00170* and *Evm_344*.
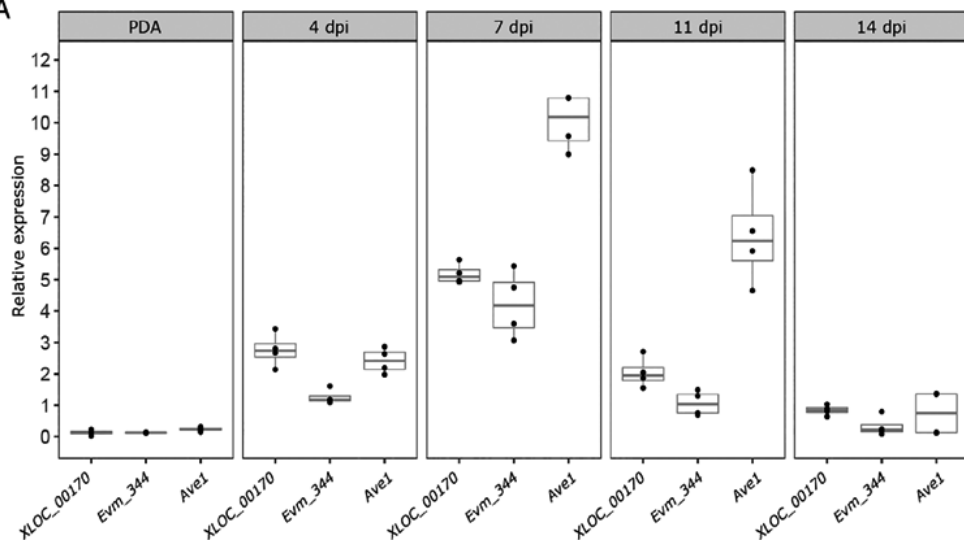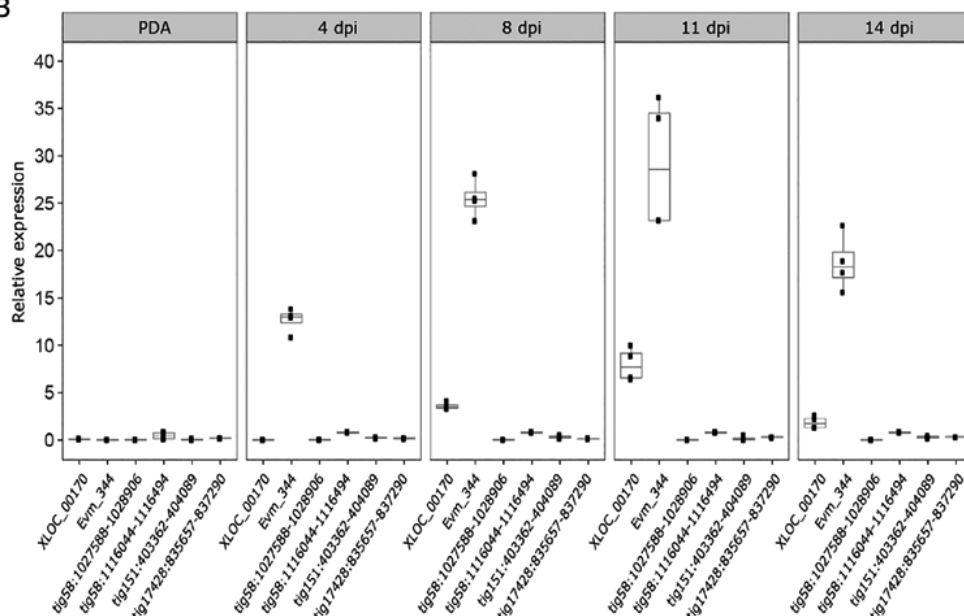
Figure 2. Expression of *V. dahliae* candidate avirulence effector genes *in vitro* and during colonization of tomato plants. To assess in planta expression, 12-day-old tomato cv. Moneymaker seedlings were root-inoculated with *V. dahliae* strain JR2 (A) or strain TO22 (B), and plants were harvested from 4 to 14 days post inoculation (dpi), while conidiospores were harvested from 5-day-old cultures of *V. dahliae* on potato dextrose agar (PDA) to monitor in vitro expression. Real-time PCR was performed to determine the relative expression of *XLOC_00170*, *Evm_344* and the race 1-specific effector gene *VdAve1* as a positive control (de Jonge et al., 2012) for strain JR2, using *V. dahliae* GAPDH as reference (A). Similarly, the relative expression of *XLOC_00170*, *Evm_344* and six additional avirulence effector genes for strain TO22, using *V. dahliae* GAPDH as reference (B).

XLOC_00170 encodes Av2

To identify which of the two candidates encodes Av2, a genetic complementation approach was pursued in which the two candidate genes were introduced individually into the *V. dahliae* race 3 strains GF-CB5 and HOMCF. Subsequently, inoculations were performed on a differential set of tomato genotypes, comprising Moneymaker plants, Ve1-transgenic Moneymaker plants (Fradin et al., 2009), and Aibou plants (Usami et al., 2017). As expected, the non-transformed race 3 strains GF-CB5 and HOMCF as well as the complementation lines containing *XLOC_00170* or *Evm_344* caused clear stunting of the universally susceptible Moneymaker as well as of the *Ve1*-transgenic Moneymaker plants (Figure 3A and B). Interestingly, nontransformed race 3 strains GF-CB5 and HOMCF and the *Evm_344* complementation lines caused clear stunting on Aibou plants, whereas the *XLOC_00170* complementation lines did not induce disease symptoms and stunting on these plants (Figure 3A and B). As such, these complementation transformants of the race 3 strains GF-CB5 and HOMCF behaved essentially as the race 2 strain TO22 (Figure 3A and B). Thus, these findings suggest that *XLOC_00170* encodes Av2. All visual observations of stunting were supported by quantifications of fungal biomass by real-time PCR (Figure 3C). These measurements revealed that fungal biomass levels were only reduced on Aibou plants when inoculated with the race 2 strain TO22, and with the race 3 strains GF-CB5 and HOMCF that were complemented with *XLOC_00170*. Thus, our data confirm that reduced symptomatology is accompanied by significantly reduced fungal colonization and indicate that *XLOC_00170* encodes the race 2-specific avirulence effector Av2.
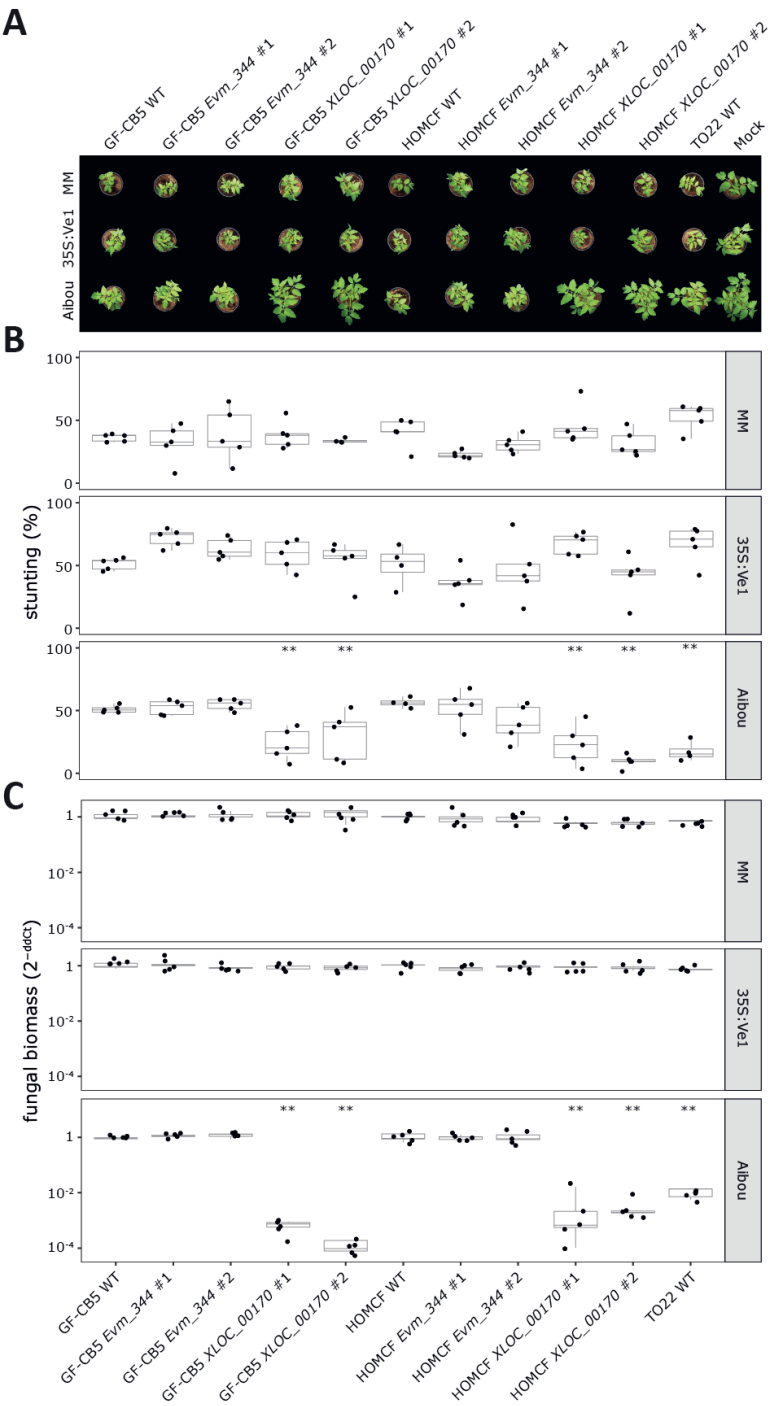
Figure 3. Genetic complementation demonstrates that *XLOC_00170* encodes the avirulence effector Av2 that is recognized in V2 plants. (A) Top pictures of Moneymaker plants that lack known *V. dahliae* resistance genes (MM), *Ve1*-transgenic Moneymaker plants that are resistant against race 1 and not against race 2 strains of *V. dahliae* (MM 35S:Ve1), and Aibou plants that carry *Ve1* and *V2* and are therefore resistant against race 1 as well as race 2 strains of the pathogen (Usami et al., 2017) inoculated with the race 3 WT strains GF-CB5 and HOMCF, and two independent genetic complementation lines that express *XLOC_00170* or *Evm_344*, and the race 2 strain TO22. (B) Quantification of stunting caused by the various *V. dahliae* genotypes on the various tomato genotypes as detailed for panel (A). Each combination is represented by the measurement of five plants. (C) Quantification of fungal biomass with real-time PCR determined for the various *V. dahliae* genotypes on the various tomato genotypes as detailed for panel (A). Each combination is represented by the fungal biomass quantification in five plants. Asterisks indicate significant differences between *V. dahliae*- and mock-inoculated plants as determined with an ANOVA followed by a Fisher's LSD test (P<0.01).

To further confirm that *XLOC_00170* encodes Av2, targeted gene deletions were pursued in race 2 strain TO22 as well as in the JR2Δ*Ave1* strain and inoculations were performed on Moneymaker plants, Ve1-transgenic Moneymaker plants (Fradin et al., 2009), and Aibou plants (Usami et al., 2017). All *V. dahliae* genotypes caused clear stunting on wild-type and *Ve1*-transgenic Moneymaker plants, except for wild-type JR2 on *Ve1*-transgenic Moneymaker (Figure 4A and B). Interestingly, whereas *V. dahliae* strains TO22 and JR2Δ*Ave1* were contained on Aibou plants, the *XLOC_00170* deletion strains caused stunting of these plants in a similar fashion as the race 3 strains GF-CB5 and HOMCF (Figure 4C). All visual observations were supported by quantification of biomass by real-time PCR (Figure 4C). Collectively, our data unambiguously demonstrate that *XLOC_00170* encodes the Av2 effector that is recognized on *V2* tomato plants.
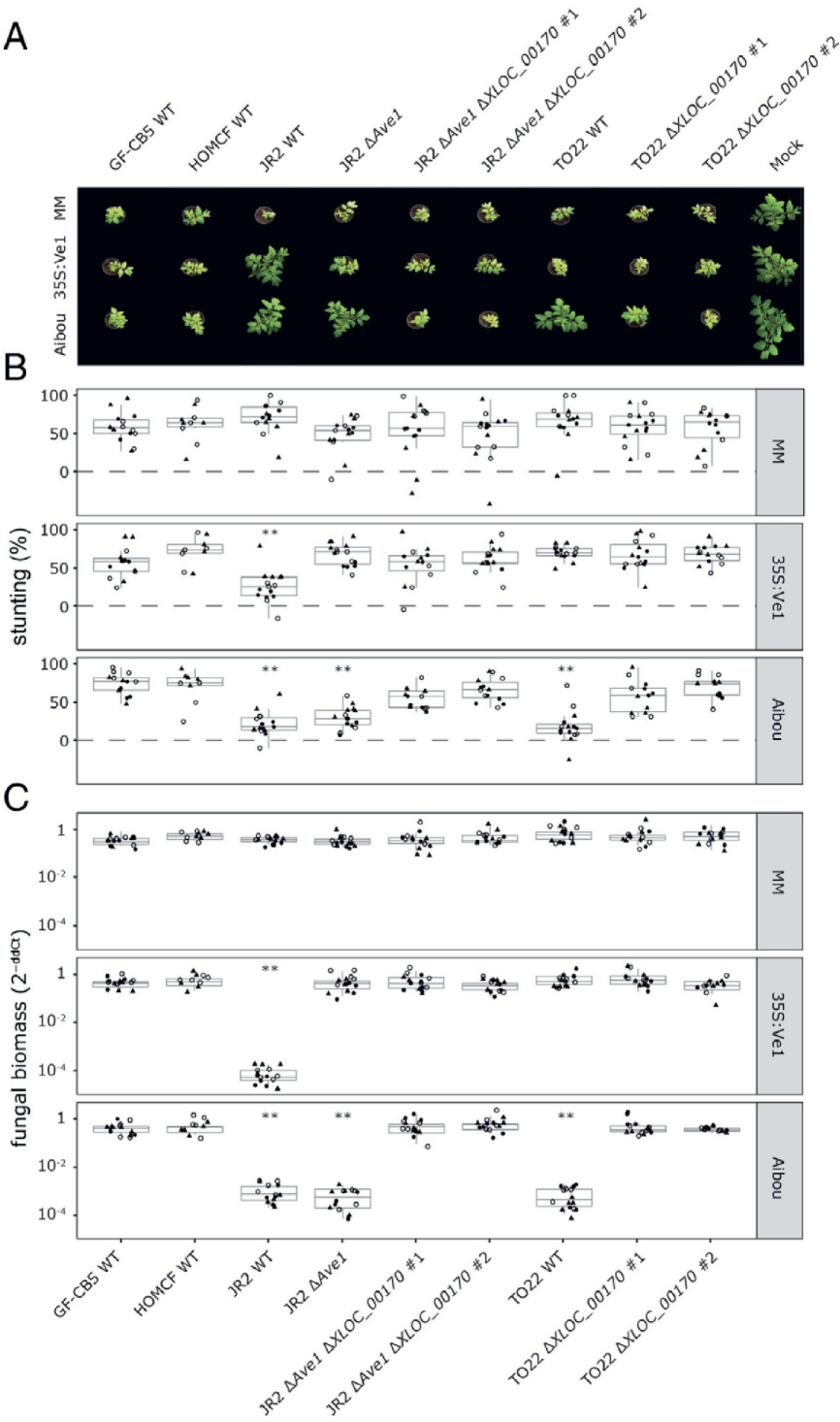
Figure 4. Targeted deletion confirms that *XLOC_00170* encodes the avirulence effector Av2 that is recognized in V2 plants. (A) Top pictures of Moneymaker plants that lack known *V. dahliae* resistance genes (MM), *Ve1*-transgenic Moneymaker plants that are resistant against race 1 and not against race 2 strains of *V. dahliae* (35S:Ve1), and Aibou plants that carry *Ve1* and *V2* and are therefore resistant against race 1 as well as race 2 strains of the pathogen (Usami et al., 2017) inoculated with the race 3 strains GF-CB5 and HOMCF, the race 1 WT strain JR2, the deletion line JR2ΔAve1, two independent knock-out lines of *XLOC_00170* in JR2Δ*Ave1*, the race 2 WT strain TO22 and two independent knock-out lines of *XLOC_00170* in TO22. (B) Quantification of stunting. (C) Quantification of fungal biomass with real-time PCR caused by the various *V. dahliae* genotypes on the various tomato genotypes as detailed for panel (A). Different symbols (empty circles, filled circles and triangles) refer to five plants from three different experiments. Asterisks indicate significant differences between *V. dahliae*- and mock-inoculated plants as determined with an ANOVA followed by a Fisher's LSD test (P<0.01).

Av2 does not seem to contribute to virulence

It has been widely recognized that the intrinsic function of Avrs is to support host colonization by acting as virulence determinants (Jones and Dangl, 2006; Rovenich et al., 2014; Cook et al., 2015). Thus, we assessed the virulence of the complementation lines alongside their wild-type progenitor genotypes on wild-type and *Ve1*-transgenic Moneymaker plants (Figure 3). However, no significant increase in symptomatology nor in fungal colonization could be recorded upon *Av2* introduction. Similarly, no significant decrease in symptomatology, nor a decrease in fungal colonization could be recorded upon *Av2* deletion from *V. dahliae* strain TO22 on these tomato genotypes and upon *Av2* deletion from JR2Δ*Ave1* on wildtype Moneymaker plants (Figure 4), suggesting that Av2 is not a major contributor to virulence on tomato under the conditions of our assays.

Av2 distribution and allelic variation

Av2 encodes a 91 amino acid protein that, after removal of a predicted signal peptide, leaves a mature protein of 73 amino acids that includes four cysteine residues and that lacks known protein domains. Intriguingly, an Av2 homologue is found in *V. nonalfalfae* (78% identity), *V. longisporum* (68% identify) and *V. alfalfae* (49%) that, like *V. dahliae,* belong to the Flavnonexudans clade of *Verticillium* spp. (Figure 5; Shi-Kunne et al., 2018). Furthermore, BLAST searches revealed homologues in *Fusarium phyllophilum* (79% identity), *Fusarium mundagurra* (78%), *F. oxysporum* f. sp. *narcissi* (77%), *Fusarium oxysporum* NRRL32931 (75%), *F. oxysporum* f. sp. *pisi* (73%) and *Fusarium* sp. NRRL66182 (41%) (Figure 5). No homologues are found in any of the other *Fusarium* spp. nor in any other species.
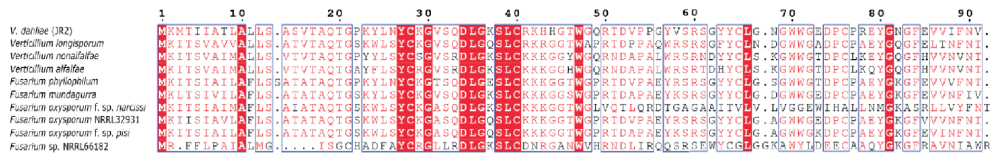
Figure 5. Amino acid alignment of Av2 homologues found in few fungal species. Based on BLAST analyses, homologues of *V. dahliae* Av2 could only be identified in *V. longisporum*, *V. nonalfalfae*, *V. alfalfa* and in *Fusarium phyllophilum*, *F. mundagurra*, three *F. oxysporum* lineages and in *Fusarium* sp. NRRL66182. Global alignments were performed using ClustalW and visualized with Espript3. Conserved amino acids are shown in white font on red background.

To assess *Av2* distribution in *V. dahliae*, presence–absence variations (PAV) were assessed in a collection of 52 previously sequenced *V. dahliae* strains (Figure 6; de Jonge et al., 2012; Faino et al., 2015; Fan et al., 2018; Gibriel et al., 2019), revealing that *Av2* occurred in 17 of the isolates including the four race 2 isolates that were sequenced in this study (Figure 6). To assess the phylogenetic relationships between strains that carry *Av2*, a phylogenetic tree was generated, showing that the strains can be grouped into three major clades, two of which comprising strains that contain *Av2*. However, within these clades closely related strains occur that lost *Av2*, suggesting the occurrence of multiple independent losses (Figure 6). Overall, no obvious phylogenetic structure is apparent with respect to effector presence within the *V. dahliae* population.
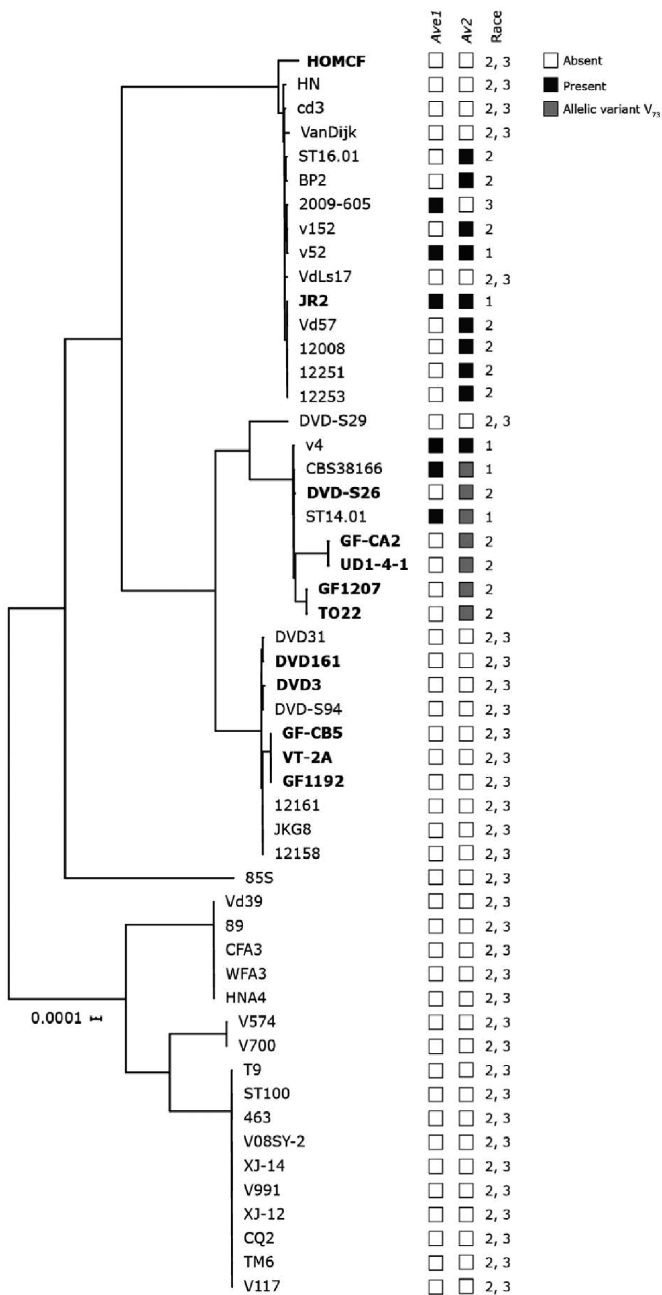
Figure 6. Phylogenetic tree of sequenced *V. dahliae* strains with indication of presence-absence variation for the Ave1 and Av2 effectors. Strains that were phenotyped and included in the comparative genomics (Table 2) are shown in bold. Presence of the avirulence genes *VdAve1* and *Av2*, and the race designation based on the presence or absence of these genes are indicated. Phylogenetic relationships between sequenced *V. dahliae* strains were inferred using Realphy (Langmead and Salzberg, 2012), and branch length represents sequence divergence.

Next, we investigated the genomic organization surrounding *Av2* based on the gapless genome assembly of *V. dahliae* strain JR2 (Faino et al., 2015). Interestingly, *Av2* resides in close proximity to *Evm_344*, separated by only two additional genes, in a lineage-specific (LS) region on chromosome 4 (Figure 7). Furthermore, as typically observed in LS regions that are enriched in repetitive elements (de Jonge et al., 2013; Faino et al., 2016), *Av2* is surrounded by repetitive elements such as transposons that mostly belong to the class II long terminal repeat (LTR) retrotransposons (Figure 7). Typically, LS regions are characterized by the high abundance of PAV. As expected, the flanking genomic regions (100 kb) are highly variable between *V. dahliae* strains (Figure 7).
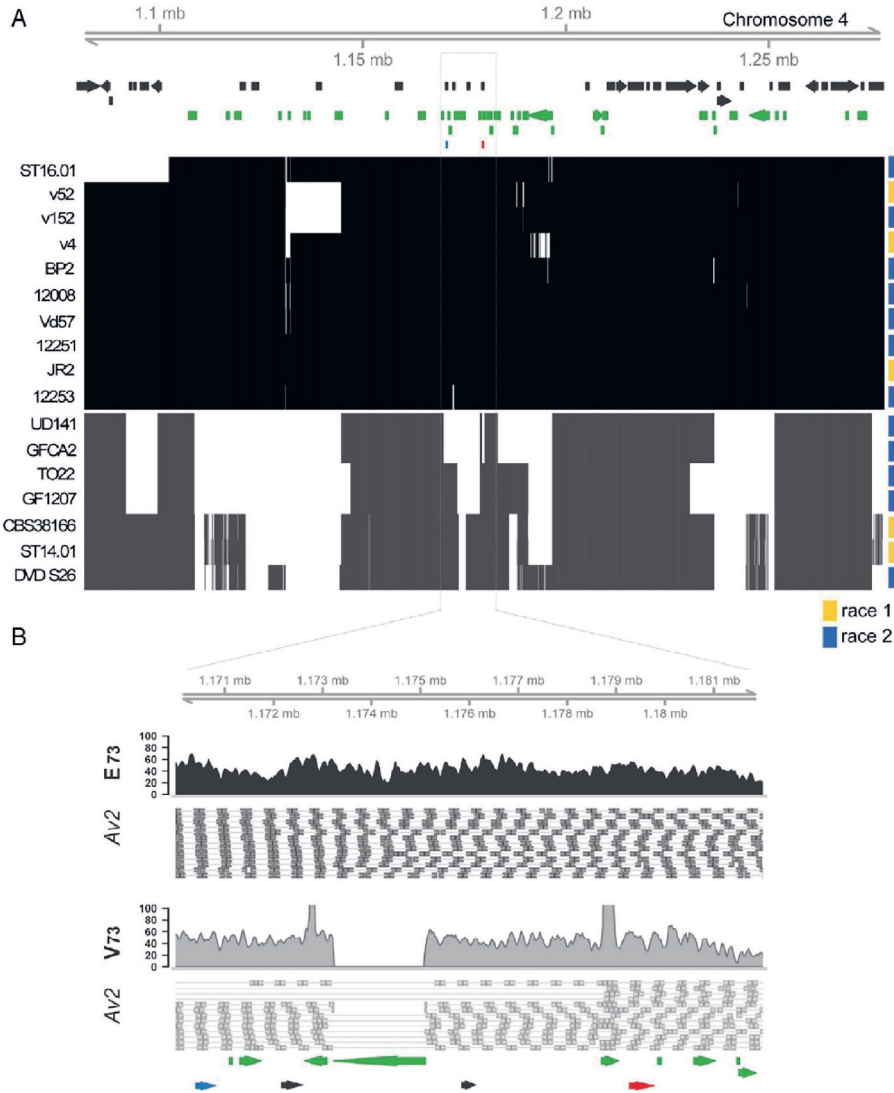
Figure 7. Presence–absence variation in the region surrounding the two candidate *Av2* genes (A) genomic region flanking the *Av2* candidate genes in 17 isolates detailed in Figure 3. The matrix shows the presence (black/grey) and absence (white) in 100 bp non-overlapping windows for *Av2* variant E_{73} (black) and *Av2* variant V_{73} grey. On top, annotated genes are displayed in black and repetitive elements in green, while *Av2* is displayed in red and *Evm_344* in blue. (B) Read coverage for *V. dahliae* strain JR2 that encodes *Av2* variant E_{73} and strain DVD-S26 that encodes *Av2* variant V_{73} depicting a transposable element deletion in isolates that produce the V_{73} variant.

As many Avr effectors are under strong selection pressure and thus often display enhanced allelic variation (Stergiopoulos et al., 2007), we assessed allelic variation among the 17 *Av2* alleles identified in this study. We identified only two allelic variants within the 17 *Av2* alleles that differed by a single nucleotide polymorphism (SNP) in exon 3 leading to a polymorphic amino acid at position 73. Whereas 10 isolates carry a glutamic acid at this position (E73), seven other carry a valine (V_{73}) (Figure 8). Interestingly, strains carrying V_{73} are clustered in the same branch, suggesting that a single event caused this polymorphism (Figure 6). We noticed that all isolates carrying E_{73} carry an extra transposable element of the DNA/Tc-1 Mariner class in the upstream region of the *Av2* gene (Figure 8). Intriguingly, as strains GF-CA2, TO22, UD-1-4-1 DVDS26 and GF1207, that encode the *Av2* variant with V_{73}, as well as JR2ΔAve1, that encodes the variant with E_{73}, are contained on Aibou plants, we conclude that both allelic variants are recognized by V2. Moreover, the *Av2* deletion strain of TO22 (with V_{73}) as well as of JR2ΔAve1 (with E_{73}) is not compromised in aggressiveness on wild-type Moneymaker plants when compared with the TO22 or JR2Δ*Ave1* progenitor strain, indicating that both alleles make no noticeable contribution to *V. dahliae* virulence.
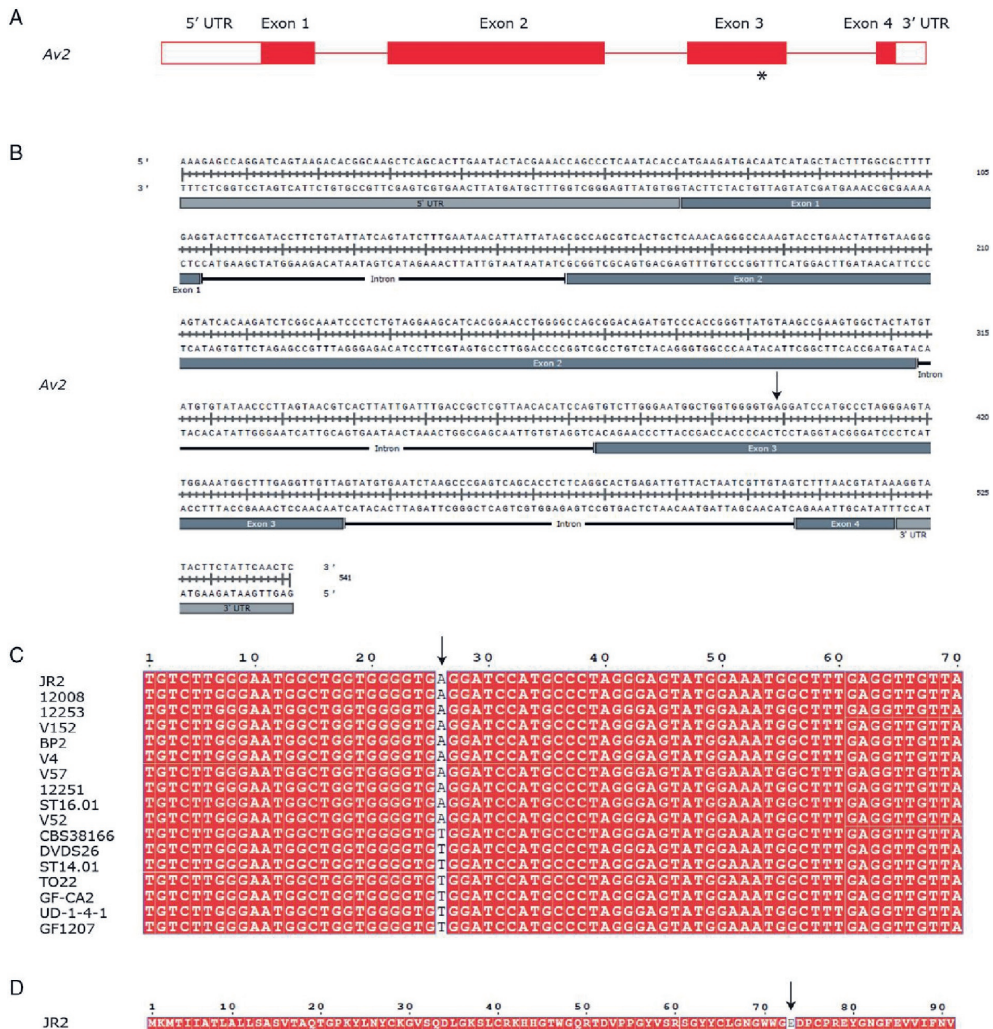
Figure 8. Allelic variation of Av2 in V. dahliae. (A) Gene model for *Av2*. The asterisk indicates the approximate position of the single (A to T) nucleotide substitution in 7 of the 17 isolates that carry the gene, leading to a single amino acid substitution (E$_{73}$V). (B) Genomic sequence of *Av2*. The arrow shows the position of the single nucleotide substitution found in particular strains. (C) Alignment of exon 3 of *Av2* in the 17 strains containing the avirulence effector gene. The arrow shows the single nucleotide substitution that occurs in seven of the strains when compared with strain JR2. (D) Av2 amino acid sequence as encoded by *V. dahliae* strain JR2 with E$_{73}$ that is substituted by V in seven isolates indicated by an arrow.

DISCUSSION

Historically, the identification of avirulence genes has been challenging for fungi that reproduce asexually, as genetic mapping cannot be utilized. However, since the advent of affordable genome sequencing, cumbersome and laborious methods to identify avirulence genes, that include functional screenings of fungal cDNAs or protein fractions for the induction of immune responses in plants (Takken et al., 2000; Luderer et al., 2002), have been supplemented with comparative genomics and transcriptomics strategies (Gibriel et al., 2016). Less than a decade ago, we identified the first avirulence gene of *V. dahliae*, known as VdAve1 for mediating avirulence on ___Ve1___ plants, through a comparative population genomics strategy combined with transcriptomics by utilizing race 1 strains that were contained by the *Ve1* resistance gene of tomato, and resistance-breaking race 2 strains (de Jonge et al., 2013). In this study, we used a similar approach based on comparative population genomics of race 1 and 2 strains with race 3 strains to successfully identify XLOC_00170 as the Av2 effector that mediates avirulence on ___V2___ plants. Intriguingly, besides VdAve1, XLOC_00170 has been identified previously as one of the most highly induced genes of *V. dahliae* during host colonization (de Jonge et al., 2013).

Ve1 and the *V2* locus are Ve1 and the V2 locus are the only two major resistance sources that have been described in tomato against *V. dahliae* thus far (Fradin et al., 2009; Usami et al., 2017). Since its initial introduction from a wild Peruvian tomato accession into cultivars in the 1950s (Deseret News and Telegram, 1955), *Ve1* has been widely exploited as it is incorporated in virtually every tomato cultivar today. Even though soon after the introduction of these cultivars resistance-breaking race 2 strains emerged, first in the United States (Robinson, 1957; Alexander, 1962), and soon thereafter also in Europe (Cirulli, 1969; Pegg and Dixon, 1969), *Ve1* is still considered useful for Verticillium wilt control today. An important factor that contributes to the durability of resistance is the fitness penalty for the pathogen upon losing the corresponding avirulence factor (Brown, 2015). The VdAve1 effector contributes considerably to *V. dahliae* virulence on tomato, which explains why race 2 strains that lack VdAve1 are generally less aggressive (de Jonge et al., 2012). Based on our current observations that differences in aggressiveness between race 2 and race 3 strains on Moneymaker plants are not obvious (Figure 1), that genetic complementation of race 3 strains with *Av2* did not lead to a striking increase in aggressiveness on Moneymaker plants (Figure 3), and that targeted deletion of *Av2* from race 2 strains did not lead to a striking decrease in aggressiveness on Moneymaker plants (Figure 4), we conclude that the contribution of *Av2* to *V. dahliae* virulence under the conditions tested in this study is modest at most.

Thus far, V2 resistance has been exploited scarcely when compared with Ve1, as it has only been introduced in a number of Japanese rootstock cultivars since 2006

(Usami et al., 2017). Previously, *V2* resistance-breaking race 3 strains have been found in several Japanese prefectures on two separate islands (Usami et al., 2017). Intriguingly, our genome analyses demonstrate that race 3 strains that lack *Av2* are ubiquitous and found worldwide, as our collection of sequenced strains comprises specimens that were originally isolated in Europe, China, Canada, and the United States. Arguably, most of these race 3 strains arose in the absence of *V2* selection by tomato cultivation. It is conceivable that, similar to Ve1 homologues that are found in other plant species besides tomato (Song et al., 2017), functional homologues of *V2* occur in other plant species as well, which may have selected against the presence of *Av2* in many *V. dahliae* strains. However, as long as *V2* is not cloned this hypothesis cannot be tested.

Like *VdAve1*, *Av2* also resides in an LS region of the *V. dahliae* genome, albeit in another region on another chromosome. Typically, these LS regions are gene-sparse and enriched in repetitive elements, such as transposons, causing these regions to be highly plastic which is thought to mediate accelerated evolution of effector catalogues (de Jonge et al., 2013; Faino et al., 2016; Cook, et al., 2020). We previously demonstrated that *VdAve1* has been lost from the *V. dahliae* population multiple times, and to date only PAV has been identified as mechanism to escape *Ve1*-mediated immunity (de Jonge et al., 2012; 2013; Faino et al., 2016). Similarly, our phylogenetic analysis reveals that *Av2* has been lost multiple times independently, and although we identified two allelic variants, both variants are recognized by V2. Consequently, PAV remains the only mechanism to overcome *V2*-mediated immunity thus far. Despite the observation that PAV is the only observed mechanism for *V. dahliae* to overcome host immunity, pathogens typically exploit a wide variety of mechanisms, ranging from SNPs (Joosten et al., 1994) to altered expression of the avirulence gene (Na and Gijzen, 2016). Nevertheless, avirulence gene deletion to overcome host immunity is common and has been reported for various fungi, including *C. fulvum* (Stergiopoulos et al., 2007), *Fusarium oxysporum* (Niu et al., 2016; Schmidt et al., 2016), *Leptosphaeria maculans* (Gout et al., 2007; Petit-Houdenot et al., 2019), *Blumeria graminis* (Praz et al., 2016) and *Magnaporthe oryzae* (Pallaghy et al., 1994; Zhou et al., 2007).

It was previously demonstrated that frequencies of SNPs are significantly reduced in the area surrounding the VdAve1 locus when compared with the surrounding genomic regions (Faino et al., 2016), which was thought to point toward recent acquisition through horizontal transfer (de Jonge et al., 2012). However, we recently noted that enhanced sequence conservation through reduced nucleotide substitution is a general feature of LS regions in *V. dahliae* (Depotter et al., 2019). Although a mechanistic underpinning is still lacking, we hypothesized that differences in chromatin organization may perhaps explain this phenomenon. Interestingly, while DNA methylation is generally low and only present at TEs, only TEs in the core genome are methylated while LS TEs are largely

devoid of methylation (Cook et al., 2020). Furthermore, TEs within LS regions are more transcriptionally active and display increased DNA accessibility, representing a unique chromatin profile that could contribute to the plasticity of these regions (Faino et al., 2016; Cook et al., 2020). Possibly, the increased DNA accessibility contributes to the high in planta expression of genes residing in these regions, and *VdAve1* as well as *Av2* belong to the most highly expressed genes during host colonization (de Jonge et al., 2013).

Our identification of *Av2* concerns the cloning of only the second avirulence gene of *V. dahliae*. This identification may permit its use as a functional tool for genetic mapping of the *V2* gene. Typically, *V. dahliae* symptoms on tomato display considerable variability, and disease phenotyping is laborious. Possibly, injections of heterologously produced Av2 protein can be used to screen tomato plants in genetic mapping analyses, provided that such injections result in a visible phenotype such as a hypersensitive response. Similar effector-assisted resistance breeding has previously been used successfully identify resistance sources in tomato against the leaf mould pathogen *C. fulvum* (Lauge et al., 1998; Takken et al., 1999) and potato against the late blight pathogen *Phytophthora infestans* (Vleeshouwers and Oliver, 2014; Du et al., 2015). The identification of *Av2* can furthermore be exploited for race diagnostics of *V. dahliae* to determine whether cultivation of resistant tomato genotypes is useful, but also to monitor *V. dahliae* population dynamics and race structures. Based on the identification of avirulence genes, rapid in-field diagnostics can be developed to aid growers to cultivate disease-free crops.

MATERIALS & METHODS

V. dahliae inoculation and phenotyping

Plants were grown in potting soil (Potgrond 4, Horticoop, Katwijk, the Netherlands) under controlled greenhouse conditions (Unifarm, Wageningen, the Netherlands) with day/night temperature of 24/18ºC for 16-h/8-h periods, respectively, and relativity humidity between 50% and 85%. For *V. dahliae* inoculation, 10-day-old seedlings were root-dipped for 10 min as previously described (Fradin et al., 2009). Disease symptoms were scored at 21 days post inoculation (dpi) by measuring the canopy area to calculate stunting as follows:

$$stunting = \left(1 - \frac{canopy\ area\ V.dahliae - inoculated\ plants}{average\ canopy\ area\ of\ mock - inoculated\ plants}\right) * 100$$

To test for significant stunting, an ANOVA was performed which tests for significant differences in canopy area between mock-inoculated and *V. dahliae* inoculated plants. Outliers were detected based on the studentized residuals from the ANOVA analysis. All datapoints with studentized residuals below −2.5 or above 2.5 were classified as outliers and removed. In total, approximately 1.8% of the datapoints were classified as outlier.

High-molecular weight DNA isolation and nanopore sequencing

Conidiospores were harvested from potato dextrose agar (PDA) plates, transferred to Czapek dox medium and grown for 10 days. Subsequently, fungal material was collected on Miracloth, freeze-dried overnight and ground to powder with mortar and pestle of which 300 mg was incubated for 1 h at 65°C with 350 µL DNA extraction buffer (0.35 M Sorbitol, 0.1 M Tris-base, 5 mM EDTA pH 7.5), 350 µL nucleic lysis buffer (0.2 M Tris, 0.05 M EDTA, 2 M NaCl, 2% CTAB) and 162.5 µL Sarkosyl (10% w/v) with 1% β-mercaptoethanol. Next, 400 µL of phenol/chloroform/isoamyl alcohol (25:24:1) was added, shaken and incubated at room temperature (RT) for 5 min before centrifugation at 16,000 g for 15 min. After transfer of the aqueous phase to a new tube, 10 µL of RNAase (10 mg µL−1) was added and incubated at 37°C for 1 h. Subsequently, half a volume of chloroform was added, shaken and centrifuged at 16,000 g for 5 min at RT, after which the chloroform extraction was repeated. Next, the aqueous phase was mixed with 10 volumes of 100% ice-cold ethanol, incubated for 30 min at RT, and the DNA was fished out using a glass hook, transferred to a new tube, and washed twice with 500 µL 70% ethanol. Finally, the DNA was air-dried, resuspended in nuclease-free water and incubated at 4°C for 2 days. The DNA quality, size and quantity were assessed by Nanodrop, gel electrophoresis and Qubit analyses. Library preparation with the

Rapid Sequencing Kit (SQK-RAD004) was performed according to the manufacturer's instructions (Oxford Nanopore Technologies, Oxford, UK) with 400 ng HMW DNA. An R9.4.1 flow cell (Oxford Nanopore Technologies) was loaded and run for 24 h. Base calling was performed using Guppy (version 3.1.5; Oxford Nanopore Technologies) with the highaccuracy base-calling algorithm. Adapter sequences were removed using Porechop (version 0.2.4 with default settings; Wick, 2018). Finally, the reads were self-corrected, trimmed and assembled using Canu (Version 1.8; Koren et al., 2017). Sequencing data are available at the NCBI SRA database under accession number PRJNA639910.

Comparative genomics and candidate identification

Self-corrected reads from *V. dahliae* race 3 strains were mapped against the reference genome using BWA-MEM (version 0.7.17; default settings; Li, 2013). Reads with low mapping quality (score < 10) were removed using Samtools view (version 1.9; setting: -q 10) (Li et al., 2009), and reads mapping in regions with low coverage (<10x) were discarded using Bedtools coverage (version 2.25.0; setting: -d) (Quinlan and Hall, 2010). Self-corrected race 2 strain reads were mapped against the retained reference genome-specific regions that are absent from the race 3 strains. Retained sequences shared by the reference and every race 2 strain, while absent from every race 3 strain, were retained as *Av2* candidate regions.

The previously determined annotation of *V. dahliae* strain JR2 (Faino et al., 2015) was used to extract genes when JR2 or TO22 were used as alignment references. To this end, retained sequences shared by the TO22 reference assembly and race 2 strains, absent from race 3 strains, were mapped against the JR2 genome assembly, and genes in the shared sequences were extracted. The remaining sequences that did not map to the *V. dahliae* strain JR2 genome assembly were annotated using Augustus (version 2.1.5; default settings; Stanke et al., 2006). SignalP software (version 4.0; Petersen et al., 2011) was used to identify N-terminal signal peptides in predicted proteins.

Real-time PCR

To determine expression profiles of *Av2* candidate genes during *V. dahliae* infection of tomato, 2-week-old tomato (cv. Moneymaker) seedlings were inoculated with *V. dahliae* strain JR2 or TO22, and stems were harvested up to 14 dpi. Furthermore, conidiospores were harvested from 5-day-old PDA plates. Total RNA extraction and cDNA synthesis were performed as previously described (Santhanam et al., 2013). Real time-PCR was performed with primers listed in Table 3, using the *V. dahliae* glyceraldehyde-3-phosphate dehydrogenase gene (*GAPDH*) as endogenous control. The PCR cycling conditions were as follows: an initial 95°C denaturation step for 10 min followed by denaturation for 15 s at 95°C, annealing for 30 s at 60°C, and extension at 72°C for 40 cycles.

Genome mining

In total, 44 previously sequenced *V. dahliae* strains and eight strains sequenced in this study were mined for Av2 gene candidates using BLASTn. Gene sequences were extracted using Bedtools (setting: getfasta) (Quinlan and Hall, 2010) and aligned to determine allelic variation using Espript (version 3.0; default settings) (Robert and Gouet, 2014). Similarly, amino acid sequences were aligned using Espript (Robert and Gouet, 2014). To determine the genomic localization of *XLOC_00170* and *Evm_344*, the *V. dahliae* strain JR2 assembly and annotation were used (Faino et al., 2015) together with coverage plots from reads of race 3 and race 2 strains as described in comparative genomics approach IV (Table 2) using R scripts, with the package karyoploteR for R (version 3.6) using kpPlotBAMCoverage function. The schematic representation of the genomic region on chromosome 4 with *XLOC_00170* and *Evm_344* was generated using Integrative Genomics Viewer (IGV) software v2.6.3 (Robinson et al., 2011) and R package (version 3.6) Gviz (Hahne and Ivanek, 2016).

Phylogenetic tree construction

The phylogenetic tree of 52 *V. dahliae* strains was generated with Realphy (version 1.12) (Bertels et al., 2014) using Bowtie2 (version 2.2.6) (Langmead and Salzberg, 2012) to map genomic reads against the *V. dahliae* strain JR2 assembly. A maximum likelihood phylogenetic tree was inferred using RAxML (version 8.2.8) (Stamatakis, 2014).

Presence–absence variation analysis

Presence–absence variation (PAV) was identified by using whole-genome alignments for 17 *V. dahliae* strains. Paired-end short reads were mapped to *V. dahliae* strain JR2 (Faino et al., 2015) using BWA-mem with default settings (Li and Durbin, 2009). Long-reads were mapped using minimap2 with default settings (Li, 2018). Using the Picard toolkit (http://broadinstitute.github.io/picard/), library artefacts were marked and removed with -*MarkDuplicates* followed by -*SortSam* to sort the reads. Raw read coverage was averaged per 100 bp non-overlapping windows using the BEDtools -*multicov* function (Quinlan and Hall, 2010). Next, we transformed the raw read coverage values to a binary matrix by applying a cut-off of 10 reads for short-read data; > = 10 reads indicate presence (1) and < 10 reads indicate absence (0) of the respective genomic region. For long-read data a cut-off of 1 read was used; > = 1 read indicates presence (1) and < 1 read indicates absence (0). The total number of PAV counts for each of the 100 bp genomic windows within 100 kb upstream and downstream of the candidate effectors was summarized.

Genetic complementation, deletion and functional analysis

For genomic complementation of race 3 strains GF-CB5 and HOMCF, a genomic construct was generated comprising the coding sequence of *XLOC_00170* or *Evm_344* in vector pFBT005 behind the *VdAve1* promoter, using primers CO-XLOC00170-F and CO-XLOC00170-R for *XLOC_00170* or CO-Evm344-F and CO-Evm344-R for *Evm_344* (Table 3).

     For genomic deletion of *XLOC_00170* from JR2Δ*Ave1* and race 2 strain TO22, a genomic construct was generated comprising the flanking regions of *XLOC_00170* in vector pRF-NU2 (for JR2Δ*Ave1*) or pRF-HU2 (for strain TO22), using primers JR2-XLOC170-LB-F, JR2-XLOC170-LB-R, JR2-XLOC170-RB-F and JR2-XLOC170-RB-R for strain JR2, and primers TO22-XLOC170-LB-F, TO22-XLOC170-LB-R, TO22-XLOC170-RB-F and TO22-XLOC170-RB-R for strain TO22 (Table 3).

     Agrobacterium tumefaciens-mediated transformation (ATMT) was performed as described previously (Ökmen et al., 2013) with a few modifications. *A. tumefaciens* was grown in 5 mL minimal medium (MM) supplemented with 50 µg m−1 kanamycin at 28°C for 2 days. After subsequent centrifugation at 3000 g (5 min), cells were resuspended in 5 ml induction medium (IM) supplemented with 50 µg m−1 kanamycin, adjusted to OD_{600} 0.15 and grown at 28°C for minimum 6 h until OD_{600} 0.5. Simultaneously, conidiospores of *V. dahliae* race 3 strains GF-CB5 and HOMCF were harvested after 1 week of cultivation on PDA plates with water, rinsed, and adjusted to a final concentration of 10^6 conidiospores mL−1. The A. tumefaciens suspension was mixed with *V. dahliae* conidiospores in a 1:1 volume ratio and 200 µL of the mixture was spread onto PVDF membranes in the centre of IM agar plates. After 2 days at 22°C, membranes were transferred to fresh PDA plates supplemented with 20 µg m−1 nourseothricin and 200 µM cefotaxime and incubated at 22°C for two weeks until *V. dahliae* colonies emerged. Transformants that appeared were transferred to fresh PDA supplemented with 20 µg ml−1 nourseothricin and 200 µM cefotaxime. Successful transformation was verified by PCR and DNA sequencing. *V. dahliae* inoculations were performed as described previously (Fradin et al., 2009). Disease symptoms were scored 14 days after inoculation by measuring the canopy area to calculate stunting when compared with mock-inoculated plants. Outgrowth of *V. dahliae* from stem slices was assessed as described previously (de Jonge et al., 2012). For biomass quantification, stems were freeze-dried and ground to powder, of which ~100 mg was used for DNA isolation. Real-time PCR was conducted with primers SlRUB-Fw and SlRUB-Rv for tomato RuBisCo and primers ITS1-F and STVe1-R for *V. dahliae* ITS (Table 3). Realtime PCR conditions were as follows: an initial 95°C denaturation step for 10 min followed by denaturation for 15 s at 95°C and annealing for 30 s at 60°C, and extension at 72°C for 40 cycles.

Acknowledgment

2

Chapter 3

The contribution of the effector catalogue of the soil-borne pathogen *Verticillium dahliae* to vascular wilt disease on *Rosa* sp.

Edgar A. Chavarro-Carrero, Michael F. Seidl and Bart P.H.J. Thomma

ABSTRACT

The soil-borne fungus *Verticillium dahliae* is a broad host-range pathogen that infects hundreds of dicotyledonous crops worldwide to cause vascular wilt disease. Soil-borne rose cultivation also suffers from Verticillium wilt. Although individual *V. dahliae* strains generally have a broad host range, particular strains are pathogenic only on a narrow range of hosts. Thus far, it has remained unclear how widespread the ability to infect rose is among *V. dahliae* strains. Here, we show that, besides strains isolated from rose, also a phylogenetically diverse panel of *V. dahliae* strains isolated from other host species is capable to cause disease on rose plants, suggesting that pathogenicity on rose is widely distributed throughout the *V. dahliae* population. Interestingly, while most strains mainly induced stunting of infected rose plants, some strains also induced severe defoliation. Subsequently, we confirmed that various previously described *V. dahliae* effectors contribute to disease development on rose. Furthermore, we demonstrate that defoliation, which is caused by some *V. dahliae* strains that belong to the so-called defoliating pathotype, is caused by a recently identified effector that is responsible for defoliation on cotton and olive. Finally, we show that individual *V. dahliae* strains cause disease on rose based on divergent effector catalogues.

INTRODUCTION

Rose (*Rosa* spp.) is a worldwide cultivated ornamental crop with an economic value estimated to exceed over $50 billion per year (Manikas et al., 2020). As any other crop, rose is susceptible to a diversity of pathogens, including fungi, bacteria, viruses, nematodes and phytoplasmas. These pathogens are all considered economically relevant as they can directly affect ornamental value and crop yield (Debener et al., 2014). Rose is typically a soil-based crop and is therefore also affected by soil-borne pathogens, of which *Verticillium dahliae*, the causal agent of Verticillium wilt, is one of the most important.

Verticillium dahliae is a soil-borne fungus with a broad host range that comprises hundreds of dicotyledonous plant species, including numerous crops such as tomato, potato, lettuce, olive, cotton and roses (Fradin and Thomma, 2006, Klosterman et al., 2009). Although individual *V. dahliae* strains generally have a broad host range, particular strains have been shown to be pathogenic on a few hosts only, while they are non-pathogenic on other hosts. This is the case for strains isolated from peppermint, cocoa, pepper and tobacco, for example (Christie, 1966; Horiuchi et al., 1990; Resende et al., 1994). Isolates from a given host typically cause a range of symptoms in other hosts, but symptoms are generally most severe on the host from which they were originally isolated (Bhat and Subbarao, 1999). Thus far, it remained unknown whether *V. dahliae* strains are generally pathogenic on rose, or whether pathogenicity on rose is confined to particular strains only.

Verticillium wilt of roses was first observed in a local rose nursery in Ontario in 1928 (Madden, 1931). *V. dahliae* invades plants via the root system and subsequently colonizes the water-conducting xylem vessels. The resulting disruption of water transport ultimately leads to the characteristic symptoms of the disease. The main symptoms on rose comprise wilting leaves at the tips of young canes and a yellowing of the lower leaves. After a few days permanent wilting occurs, and the leaves generally turn yellow and finally brown as they wither and die. Defoliation progresses from the base of canes upward. Canes that show symptoms may continue to grow normally in subsequent seasons, but they may also die back, and progressive dieback can even result in death of entire plants. Vascular discoloration, common on other hosts, is not usually evident in infected roses (Horst, 2007).

Molecular mechanisms underlying pathogenicity of *V. dahliae* have been studied extensively, albeit on a limited range of host plants. It is generally accepted that plant pathogens secrete dozens to hundreds of effectors into the apoplast or cytosol of their host plants in order to mediate host colonization (Rovenich et al., 2014). In the narrowest definition, effectors are defined as small, secreted proteins of ≤300 amino acids that are cysteine-rich and have tertiary structures that are stabilized by

3

disulfide bridges and that are secreted by pathogens to promote disease on plant hosts (Duplessis et al., 2011; Gan et al., 2013; Stergiopoulos et al., 2013; Lo Presti et al., 2015). However, also larger secreted proteins have been found to act as effectors, such as several LysM effectors (Djamei et al., 2011; Kombrink and Thomma, 2013). Furthermore, besides proteins also non-proteinaceous effectors have been described, such as fungal secondary metabolites as well as small RNA (sRNA) molecules that are delivered into host cells to suppress host immunity (Weiberg et al., 2014; Mapuranga et al., 2022). Whereas it has been well established that effectors act in the suppression of host immunity and other host-associated physiological processes, recent studies have revealed additional functions of pathogen effector proteins in host colonization. For example, it was recently demonstrated that *V. dahliae* secretes effector proteins to modulate microbiome compositions inside the host plant, as well as outside the host, to support host colonization (Snelders et al., 2020; 2021; 2022; 2023). Importantly, some effectors may become recognized by cell surface- or cytoplasmic-localized host immune receptors, in which case they are termed avirulence (Avr) effectors.

Presently, about a dozen of *V. dahliae* effector proteins have been functionally characterized. The most intensively studied *V. dahliae* effector, Ave1 (avirulence on Ve1), was identified using comparative genomics and was found to act as an avirulence factor on tomato. Ave1 is recognized by tomato plants carrying the resistance (*R*) gene encoding Ve1 (de Jonge et al., 2012). Recently, Ave1 was shown to displays antimicrobial activity and facilitate colonization of the host plants tomato and cotton through host microbiome manipulation by suppressing antagonistic bacteria, such as members of the *Spingomonadaceae* (Snelders et al., 2020). Recently, five alleles with high similarity to *Ave1* have been identified in the *V. dahliae* population that are named *Ave1-like* (*Ave1L1* to *Ave1L5*) (Snelders et al., 2021). While some of the *V. dahliae* strains do not carry any *Ave1L* allele, other strains carry a single *Ave1L* allele in presence or absence of *Ave1*. Three of the five alleles carry premature stop codons and seem to be pseudogenes, suggesting that allelic variation has occurred to evade host recognition. However, none of the Ave1L allelic variants is recognized by Ve1, and no other corresponding immune receptors have been identified (Snelders et al., 2021). Like Ave1, also Ave1L2 acts in host microbiome manipulation albeit likely with different specificity as Ave1L2 was demonstrated to act in the suppression of Actinomycetes (Snelders et al., 2021). Besides *Ave1*, *V. dahliae* was recently shown to carry a second avirulence gene named *avirulence on V2* (*Av2*) that encodes the avirulence effector that is recognized in tomato plants carrying the *V2* resistance locus (Chavarro-Carrero et al., 2021). Thus far, no virulence function has been assigned to Av2.

Besides avirulence effectors, also a number of virulence effectors has been identified. Members of the well-described family of chitin-binding lysin motif (LysM)

effectors are found in *V. dahliae* as well, albeit that only one member in a single *V. dahliae* strain was found to be expressed *in planta* and contribute to virulence on tomato and not on *A. thaliana* or *N. benthamiana* (de Jonge et al., 2013; Kombrink et al., 2017). This effector, Vd2LysM, was shown to suppress chitin-triggered immunity and protect fungal hyphae against hydrolysis by plant chitinases (Kombrink et al., 2017). Members of the family of necrosis- and ethylene-inducing-like proteins (NLPs) were identified in *V. dahliae* as well. Out of seven NLPs, only two were shown to induce plant cell death and promote virulence on tomato and on *A. thaliana* plants (Santhanam et al., 2013).

Recently, in our laboratory, based on comparative genomics several effectors were revealed that are required for pathogenicity or virulence on particular host plants. In this manner, an effector that is required for induction of defoliation on cotton plants was identified, termed the D effector (Li, 2019). In the same fashion, an effector that is required for pathogenicity on tomato was identified, called TOM (Li, 2019), as well as two other effectors that are required for full virulence on tomato (de Jonge et al., 2013). Finally, an effector that is required for virulence on sunflower was identified, named SUN (Li, 2019).

Besides effectors, other virulence factors that include transcriptional regulators such as an ortholog of the *Fusarium oxysporum* transcriptional regulator Sge1 named VdSge1 (Santhanam and Thomma, 2013), and the transcription activator of adhesion Vta2 (Tran et al., 2014) have been identified. Furthermore, the *V. dahliae* isochorismatase (VdIsc1) that converts isochorismate, a precursor of salicylate, to 2,3-dihydro-2,3-dihydroxybenzoate (DDHB) and pyruvate (Liu et al., 2014), and a putative nucleotide-rhamnose synthase/epimerase-reductase (NRS/ER) that is involved in the biosynthesis of the nucleotide sugar deoxy-thymidine diphosphate rhamnose (Santhanam et al., 2017), were identified as virulence factors.

Typically, the role of effectors of *V. dahliae* is described on a single to a few hosts only, but from these studies it has become clear that single effectors may differentially act on diverse plant hosts (de Jonge et al., 2012; 2013; Santhanam et al., 2013; Kombrink et al., 2017; Li, 2019). Thus far, no *V. dahliae* effectors have been characterized with respect to their contribution to virulence on rose plants. In the current study, we tested known *V. dahliae* effectors for involvement in Verticillium wilt disease development on roses.

3

RESULTS

Phylogenetically diverse *Verticillium dahliae* strains cause disease on rose plants

To assess pathogenicity of *V. dahliae* on rose, we assembled a selection of *V. dahliae* strains (Table 1). First, *V. dahliae* strains were selected that were isolated from infected rose plants in Mexico and in the Netherlands. Furthermore, we selected phylogenetically divergent *V. dahliae* strains based on previously performed genome sequencing efforts (Chavarro-Carrero et al., 2021). Subsequently, all selected strains were inoculated on the most commonly use rose rootstock cv. Natal briar.

Table 1. *Verticillium dahliae* strains used in this study.

Strain	Isolated from	Country	Reference
V1	Rose	Mexico	This study
V13	Rose	Mexico	This study
Vmx	Rose	Mexico	This study
I1V	Rose	Mexico	This study
EU7	Rose	the Netherlands	This study
EU35	Rose	the Netherlands	This study
CBS385.49	Rose	the Netherlands	This study
CBS809.97	Rose	the Netherlands	This study
JR2	Tomato	Canada	Fradin et al., 2009
VdLs17	Lettuce	USA	Klosterman et al., 2011
DVDS26	Soil	Canada	de Jonge et al., 2012
85S	Sunflower	France	Depotter et al., 2019
CQ2	Cotton	China	Depotter et al., 2019
ST100	Soil	Belgium	de Jonge et al., 2012

Four weeks after inoculation all *V. dahliae* strains that were originally isolated from rose plants caused significant stunting on the rose rootstock cv. Natal briar (Figure 1a, b). Interestingly, isolate I1V additionally caused defoliation of the plants and appeared considerably more aggressive than the other strains that were isolated from rose (Figure 1a).

The strains that were not originally isolated from roses, but that were chosen based on their phylogenetic diversity (Chavarro-Carrero et al., 2021), also caused significant stunting on the rose rootstock cv. Natal briar, in a similar fashion as the

strains that were originally isolated from rose plants (Figure 1c, d). Like strain I1V, also the strains CQ2 and ST100 induced defoliation of the rose plants. Intriguingly, these latter two strains are known as strains that belong to the "defoliation pathotype" on cotton and on olive plants (Schnathorst and Mathre et al., 1966; Schnathorst, 1969), which suggests that rose isolate I1V belongs to this pathotype as well. Collectively, these findings suggest that pathogenicity of *V. dahliae* on rose is widely distributed throughout the population, and that variation in aggressiveness on rose occurs among *V. dahliae* strains.

A

B

C

D
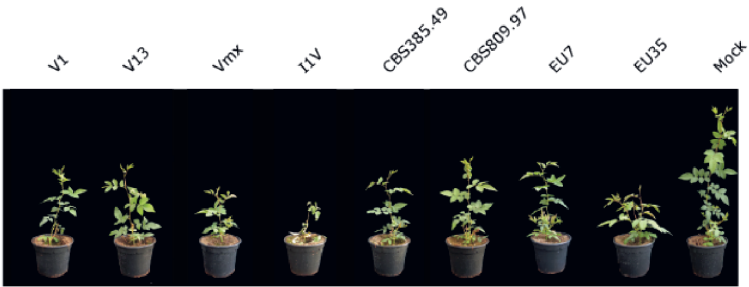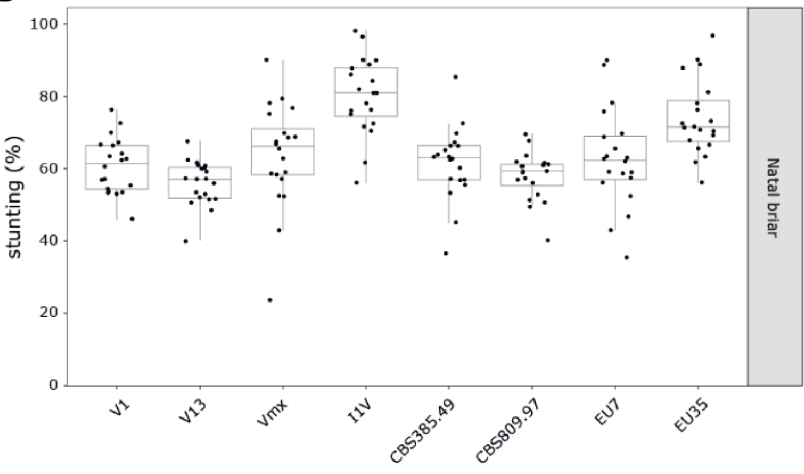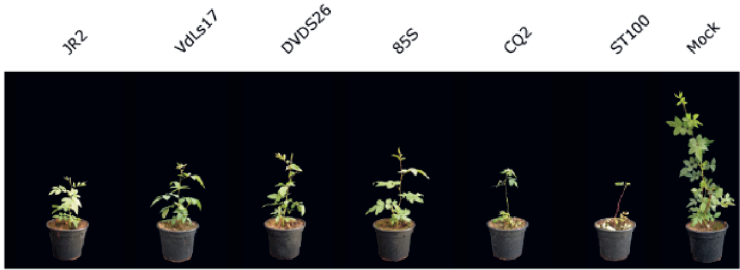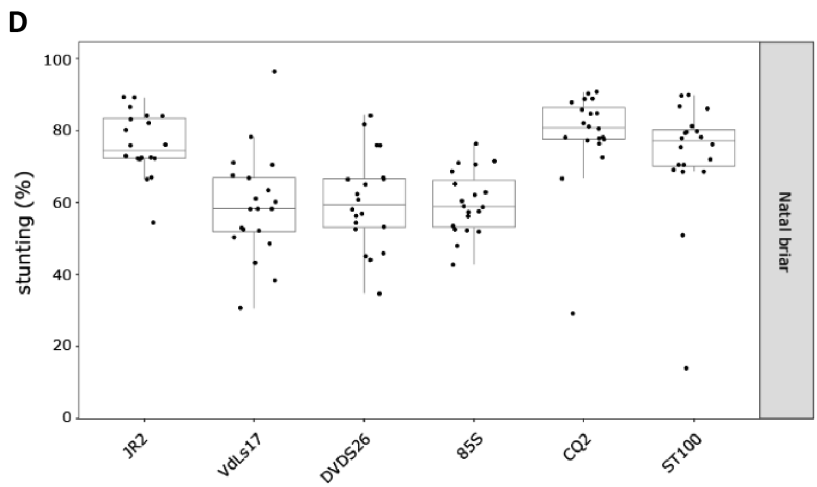
Figure 1. Phylogenetically diverse *Verticillium dahliae* strains cause disease on rose plants. (a) Plants of the rose rootstock cv. Natal briar inoculated with *V. dahliae* strains V1, V13, Vmx and I1V from Mexico, and with strains CBS385.49, CBS809.97, EU7 and EU35 from the Netherlands, which were all originally isolated from roses, at 28 days post inoculation (dpi). (b) Quantification of the degree of stunting of rose rootstock cv. Natal briar plants (n=10) inoculated with *V. dahliae* strains detailed in panel (a) relative to mock-inoculated plants. (c) Plants of the rose rootstock cv. Natal briar inoculated with *V. dahliae* strains JR2, VdLs17, DVDS26, 85S, CQ2 and ST100 at 28 dpi. (d) Quantification of the degree of stunting of rose rootstock cv. Natal briar plants inoculated with *V. dahliae* strains detailed in panel (c) relative to mock-inoculated plants.

Verticillium dahliae strains isolated from roses belong to different *V. dahliae* sub-populations

In this study, we determined the genomic sequences of the strains that were isolated from rose with Oxford Nanopore sequencing Technology (ONT) using a MinION device (Table 2). For each strain, we produced 1–2 Gb of sequence data, corresponding to 25–40x genome coverage based on the ~35 Mb gapless reference genome of *V. dahliae* strain JR2 (Faino et al., 2015). Subsequently, read correction and trimming were performed, followed by genome assembly, leading to assemblies ranging from 21 contigs for strain CBS385.49 to 312 for strain EU7 (Table 2). Subsequently, a phylogenetic tree was constructed that combines the newly sequenced *V. dahliae* strains with 52 strains that were previously sequenced in other studies (de Jonge et al., 2012; Faino et al.,2015; Fan et al., 2018; Gibriel et al., 2019; Chavarro-Carrero et al., 2021). We previously noted that the 52 previously sequenced *V. dahliae* strains grouped in three major clades (Chavarro-Carrero et al., 2021). Interestingly, we found that the eight *V. dahliae* strains that were isolated from rose do not group in a single clade but instead are distributed over these three groups (Figure 2).Notably, the genome of isolate I1V is closely related to that of the strains that belong to the defoliating pathotype, which

Table 2. Sequencing summary and genome assembly statistics of eight *Verticillium dahliae* strains isolated from roses

Strain name	V1	V13	Vmx	I11	CBS385.49	CBS809.97	EU7	EU35
Country of origin	Mexico	Mexico	Mexico	Mexico	The Netherlands	The Netherlands	The Netherlands	The Netherlands
Read N50 (kb)	9	8	8	5	13	9	8	8
Coverage	25X	30X	26X	40X	27X	30X	25X	31X
No. of contigs	156	202	250	124	21	84	312	270
Total length (Mb)	35.2	35.6	34.8	38.7	34.7	35.2	34.9	34.9
Average length (Mb)	0.2	0.1	0.5	0.4	1.6	0.9	0.1	0.3
Maximum length (Mb)	4.7	4	4.4	6.0	4.9	4.4	4.3	3.1
N50 (Mb)	1.2	0.9	1.2	2.4	3.2	1.4	0.6	0.8
N90 (Mb)	0.1	0.1	0.2	0.2	1.3	0.6	0.1	0.1
GC (%)	46.8	47	46.2	45.2	46.5	46.7	46.8	46.5

3

could be expected based on the defoliation phenotype that is displayed by this strain on rose plants (Figure 1), yet the genome sequence also suggests slight divergence from this clade (Figure 2). Collectively, our findings further confirm that pathogenicity on rose is widely distributed throughout the *V. dahliae* population.

Table 3. *Verticillium dahliae* effectors analysed in this study.

Effector	Strain	Gene ID	Reference
Ave1	JR2	VDAG_JR2_Chr5g02170	de Jonge et al., 2012
Av2	JR2	VDAG_JR2_Chr4g03680	Chavarro-Carrero et al., 2021
Vd2LysM	VdLs17	VdLs17_VDAG_05180	de Jonge et al., 2013; Kombrink et al., 2017
NEP1	JR2	VdLs17_VDAG_04701	Santhanam et al., 2013
NEP2	JR2	VdLs17_VDAG_01995	Santhanam et al., 2013
XLOC_009059	JR2	VDAG_JR2_Chr2g09570	de Jonge et al., 2013
XLOC_008951	JR2	VDAG_JR2_Chr4g03660	de Jonge et al., 2013
VdAve1L2	DVDS26		Boshoven, 2017
VdAve1L5	ST100		Boshoven, 2017
TOM	JR2	VDAG_JR2_Chr3g13460	Li, 2019
SUN	85S	85S_MAKER_00010358	Li, 2019
VdNRS/ER	JR2	VDAG_JR2_Chr7g02960	Santhanam et al., 2017
D	CQ2	CQ2_0008g00020a-00002 / CQ2_0028g0007a-00002	Li, 2019
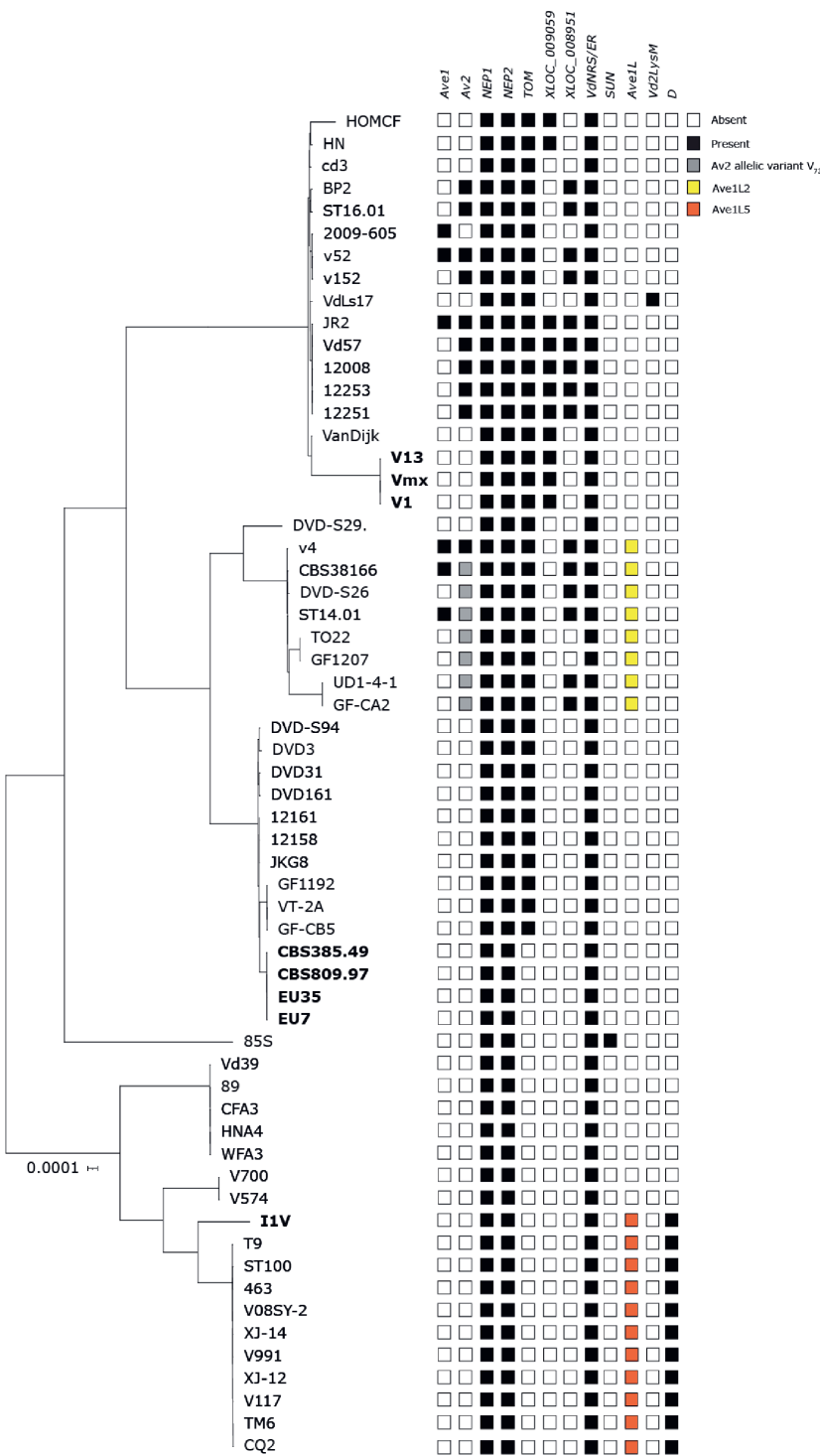
Figure 2. Phylogenetic tree of sequenced *V. dahliae* strains with the presence-absence variation of 13 previously characterized effector genes. Strains sequenced in the present study (Table 3) are shown in bold. Phylogenetic relationships between *V. dahliae* strains were inferred using Realphy (Langmead and Salzberg, 2021), and branch length represents sequence divergence.

Various *V. dahliae* effectors contribute to Verticillium wilt disease on rose

As apparently a wide diversity of *V. dahliae* strains is able to cause disease on rose, we assessed whether a set of previously characterized *V. dahliae* effectors can be implicated in Verticillium wilt disease development. To this end, a panel of 13 previously characterized effectors was selected (Table 2) and pathogenicity assays were performed on the rose rootstock cv. Natal Briar using previously generated targeted deletion lines for each of these effectors (de Jonge et al., 2012, 2013; Santhanam et al., 2013, 2017; Boshoven, 2017; Li, 2019) . The effectors concern the race 1-specific avirulence effector Ave1 (de Jonge et al., 2012) as well as the race 2-specific effector Av2 (Chavarro-Carrero et al., 2021), the LysM effector Vd2LysM (Kombrink et al., 2017), the necrosis- and ethylene-inducing-like protein toxins (NLP) 1 and 2 (Santhanam et al., 2013), the virulence effectors XLOC_009059 and XLOC_008951 (de Jonge et al., 2013), the Ave1 homologues Ave1-like 2 (Ave1L2) and 5 (Snelders et al., 2023) and the TOM and SUN virulence factors that are required for infection on tomato and sunflower, respectively (Li, 2019). Finally, a rhamnose synthase deletion strain was included as well (Santhanam et al., 2017).

Four weeks after inoculation, all wild-type (WT) *V. dahliae* strains caused stunting on the rose rootstock cv. Natal briar (Figure 3a, b). Intriguingly, all effector gene deletion lines caused reduced stunting on the rose rootstock cv. Natal briar when compared with their corresponding WT strain (P<0.01) (Figure 3a, b), except for *ΔNEP2* for which the level of stunting was similar to the wild-type JR2. All phenotypic observations correlated with quantifications of fungal biomass with real-time PCR (Figure 3c), as biomass levels were reduced for the effector deletion lines when compared with their respective wild-type lines, except for the *NEP2* deletion line (P<0.01) (Figure 3c). This finding suggests that all effectors tested, except for NEP2, contribute to disease development on rose plants.

We previously determined that *NEP2* is differentially expressed by *V. dahliae* during colonization on different plant hosts (Santhanam et al., 2013), leading to the hypothesis that this effector gene may not be expressed on rose as well. To test this hypothesis, *NEP2* expression was monitored in *V. dahliae* strain JR2 during colonization of rose in a time course from 0 to 28 dpi. Indeed, we found that *NEP2* was not expressed under these conditions (Figure S1), explaining why no virulence phenotype was observed upon deletion of this effector gene.
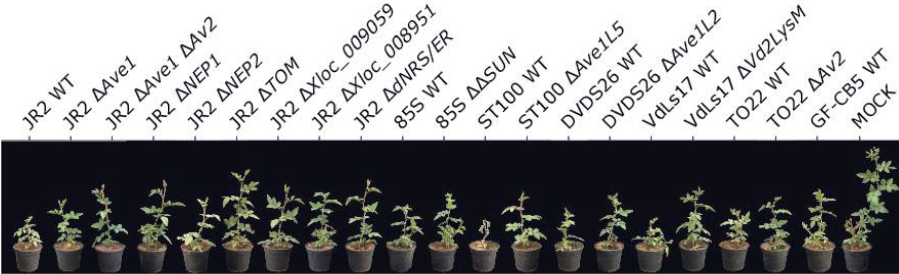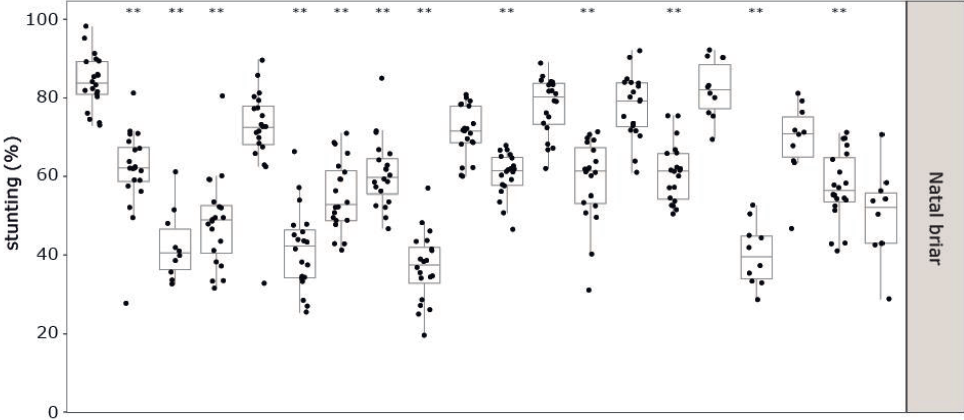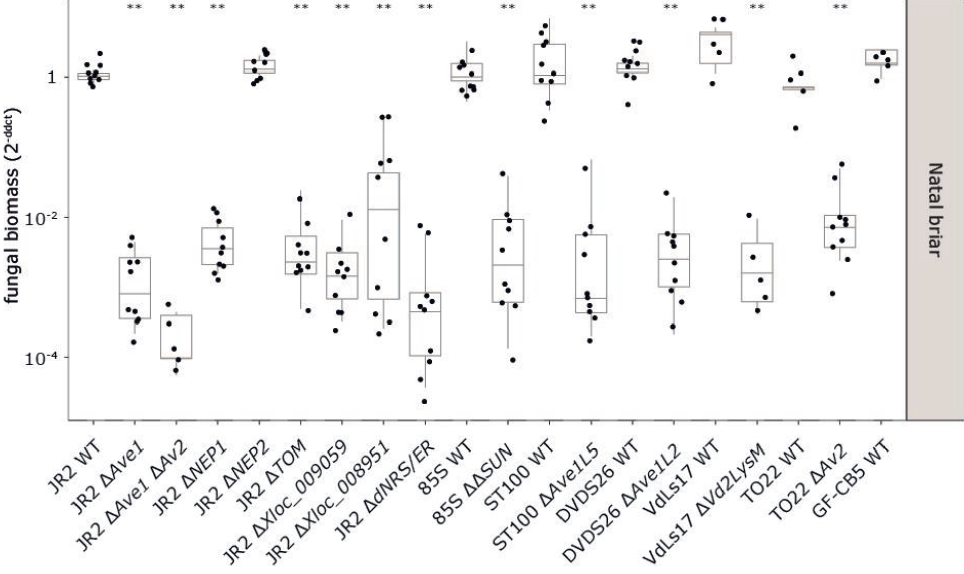
Figure 3. Various effectors from *Verticillium dahliae* contribute to disease development on rose plants. (a) Plants of the rose rootstock cv. Natal briar inoculated with wilt type (WT) *V. dahliae* strains JR2, CQ2, 85S, ST100, DVDS26, VdLs17, TO22 and GFCB5, and deletion lines for 13 previously characterized effector genes at 28 days post inoculation (dpi). (b) Quantification of the degree of stunting of rose rootstock cv. Natal briar plants (n=10) inoculated with *V. dahliae* strains detailed in panel (a) relative to mock-inoculated plants (c) Quantification of fungal biomass with real-time PCR of the various *V. dahliae* genotypes on rose rootstock cv. Natal briar. Asterisks indicate significant differences between *V. dahliae* WT strains and deletion lines as determined with an ANOVA followed by a Fisher's LSD test (P<0.01).

The D effector contributes to defoliation on rose plants

As mentioned above, besides stunting, the Mexican strain I1V induced defoliation of rose plants in a similar fashion as the strains CQ2 or ST100 that belong to the D pathotype (Figure 1). This finding suggests that strain I1V belongs to the defoliating pathotype, which is basically composed of a clonal collection of *V. dahliae* isolates (Li, 2019) (Figure 2). However, the phylogenetic analysis based on whole-genome sequencing revealed that the genome of isolate I1V is closely related to that of the strains that belong to the defoliating pathotype, yet not identical (Figure 2). We recently identified an effector that is responsible for defoliation symptoms caused by strains that belong to the D pathotype (Li, 2019). To test whether this effector is responsible for the defoliation on roses, previously generated *D* effector deletion lines in the CQ2 wild-type strain that belongs to the D pathotype were inoculated on rose rootstock cv. Natal briar. Four weeks after inoculation, plants inoculated with the CQ2 WT strain showed total defoliation of the main stem, while the *D* effector gene deletion lines did not cause defoliation (Figure 4), suggesting that the D effector is responsible for defoliation symptoms on rose. Based on the genome assembly, we determined that the I1V strain, like the CQ2 strain (Li, 2019), contains two copies of the *D* effector gene. Next, *D* effector deletion lines were generated in strain I1V and inoculated on rose. Similar to plants inoculated with *D* gene deletion lines of strain CQ2, *D* gene deletion lines of strain I1V no longer caused defoliation (Figure 4). Moreover, the deletion lines of CQ2 as well as of I1V caused only a mild degree of stunting when compared with mock-inoculated plants, which is also reflected by the amount of fungal biomass that accumulated in the rose plants (Figure 4). These findings suggest that the D effector is not only responsible for causing defoliation symptoms on rose plants, but also suggests that the D effector is a major virulence factor of *V. dahliae* strains of the D pathotype as well as of strain I1V.
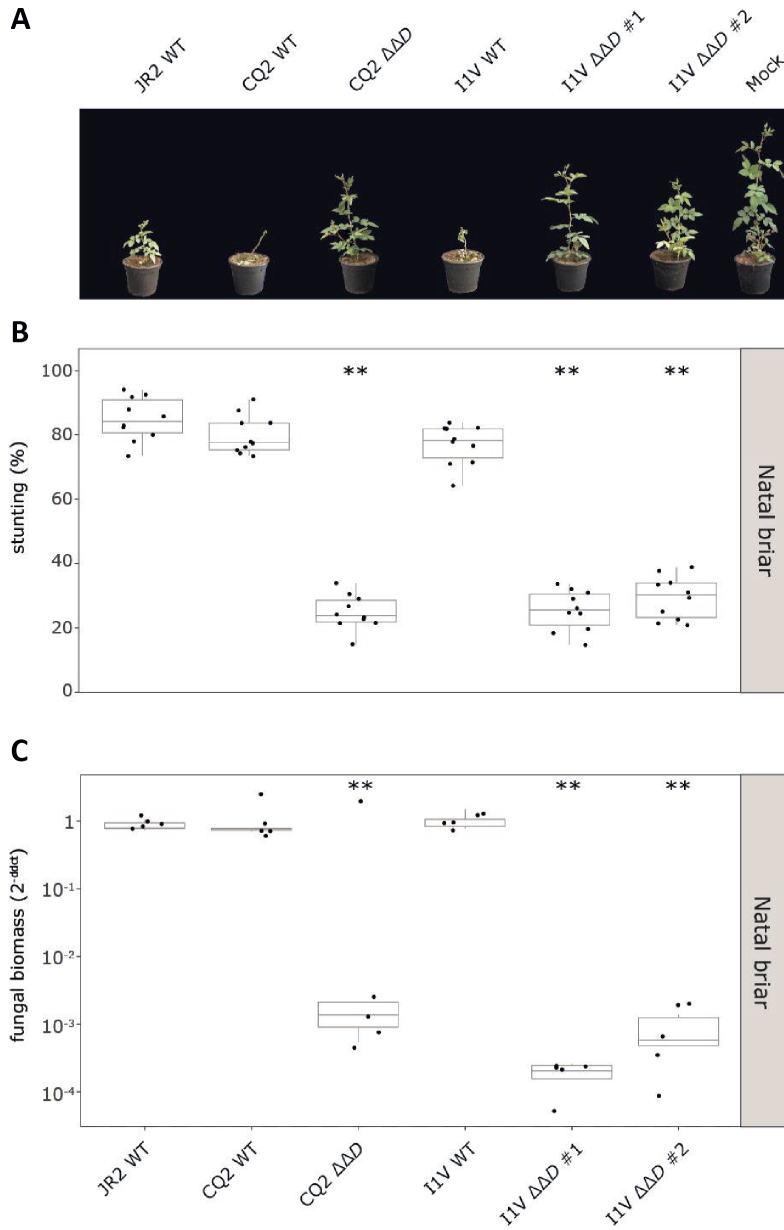
Figure 4. Effector D is involved in defoliation on rose. (a) Plants of the rose rootstock cv. Natal briar inoculated with wild type (WT) strains JR2, CQ2 and I1V, and *D* effector gene deletion lines at 28 days post inoculation (dpi). (b) Quantification of the degree of stunting of rose rootstock cv. Natal briar plants inoculated with *V. dahliae* strains detailed in panel (a) relative to mock-inoculated plants (n=10) (c) Quantification of fungal biomass of the various *V. dahliae* genotypes on rose rootstock cv. Natal briar with real-time PCR. Asterisks indicate significant differences between *V. dahliae* I1V WT strain and the *D* effector gene deletion lines as determined with an ANOVA followed by a Fisher's LSD test (P<0.01).

3

V. dahliae strains isolated from rose display divergent effector catalogues

As a suite of effectors was shown to be able to contribute to disease development on rose plants, we assessed presence-absence variation (PAV) of the 13 effector genes (Table 2) in the eight newly sequenced and the 52 previously sequenced *V. dahliae* strains (Figure 2) (de Jonge et al., 2012; Faino et al., 2015; Fan et al., 2018; Gibriel et al., 2019; Chavarro-Carrero et al., 2021). It is not surprising that the *V. dahliae* isolates that were isolated from rose and that group together carry the same set of effector genes (Figure 2). However, whereas the Dutch strains contain the smallest selection of the 13 effector genes, namely only *NEP1*, *NEP2* and *VdNRS/ER*, the Mexican strains V1, Vmx and V13 additionally carry *TOM* and *XLOC_009059*. Instead of these latter two effector genes, the divergent Mexican strain I1V carries *Ave1L5* and *D* (Figure 2). Thus, we conclude that different *V. dahliae* strains can cause disease on rose plants based on differential effector catalogues.

DISCUSSION

Traditionally, rose cultivation worldwide has been performed based on soil-based cropping systems. However, such soil-based cropping systems are associated with various challenges, including the occurrence of soil-borne diseases. Pathogenic soil-borne fungi such as *Rosellinia necatrix*, *Fusarium oxysporum*, *Rhizoctonia solani* and *Verticillium dahliae* represent a major threat for soil-based rose cultivation (Madden, 1931; Bolton, 1982; Barguil et al., 2009; García-Velasco et al., 2012). In our study, we show that *V. dahliae* strains that were isolated from rose, either in the Netherlands or from Mexico, behave quite similar on rose in controlled greenhouse assays. Moreover, reference strains that were chosen based on their phylogenetic position within a tree of the *V. dahliae* species showed similar symptomatology, demonstrating that rose pathogenicity is widespread within the species.

    V. dahliae is one of the most important soil-borne pathogens worldwide, with a host range that comprises over 400 host species (Farr and Rossman, 2021). Nevertheless, individual *V. dahliae* strains can display divergent host ranges (Green, 1951; Schnathorst and Mathre, 1966; Horiuchi et a., 1990, Bhat and Subbarao, 1999; de Jonge et al., 2012; Song et al., 2017). Previous studies have shown that *V. dahliae* isolates from tomato and radish are not capable to cause disease on peppermint plants (Green, 1951). Similarly, cotton isolates did not produce wilt symptoms in cowpea, muskmelon, and watermelon, while they are differentially pathogenic on cotton, tomato, safflower, and snapdragon (Schnathorst and Mathre, 1966). Furthermore, specificity of *V. dahliae* strains has been shown on tomato, eggplant, bell pepper, as well as on cruciferous plants (Horiuchi et al., 1990). In addition, it has been shown that *V. dahliae* isolated from bell pepper, cabbage, cauliflower, cotton, egg-plant, and mint exhibited host specificity, whereas isolates from artichoke, lettuce, potato, strawberry, tomato, and watermelon are capable to cause disease on different hosts (Bhat and Subbarao, 1999). Recently, *V. dahliae* strain JR2, which was originally isolated from tomato, has been shown to be pathogenic on *Arabidopsis* (de Jonge et al., 2012), but not on *Nicotiana tabacum* (Song et al., 2017). Interestingly, in the present study we showed that the *V. dahliae* strain JR2 isolated from tomato, VdLs17 from lettuce, DVDS26 from soil, 85S from sunflower, CQ2 from cotton, and ST100 from soil are all capable to cause disease on rose plants with differential degrees of aggressiveness. Interestingly, whereas all strains were capable to cause stunting on roses, only few caused defoliation, namely CQ2 isolated from cotton, ST100 from soil, and I1V isolated from rose plants.

    In the 1960s, two pathotypes were described for isolates of *V. dahliae* from cotton based on whether or not they induced severe defoliation; the defoliating (D) and the non-defoliating (ND) pathotype (Schnathorst and Mathre, 1966). Intriguingly, the induction of defoliation by D pathotype strains is only observed on particular plant

species, including cotton, okra, and olive, with isolates from cotton and olive showing cross virulence (Schnathorst and Mathre, 1966; Schnathorst and Sibbett, 1971; Rodriguez-Jurado et al., 1993). Intriguingly, for example, the D pathotype T-1 strain of *V. dahliae* (also known as T9) was reported to cause defoliation on okra and on cotton, while it was highly virulent yet non-defoliating on celery and safflower, mildly virulent on tomato, and non-pathogenic on cowpea, muskmelon, and watermelon (Schnathorst and Mathre, 1966). Similar observations have been made in other studies as well (Jimenez-Diaz et al., 2012). Interestingly, our results suggest that differential symptomatology, involving non-defoliation versus defoliation, occurs on rose as well. Moreover, our findings suggest that that defoliation on rose is caused by strains that belong to the so-called D pathotype on cotton and olive, and thus that cross virulence occurs among all these plant species. This notion is furthermore supported by the observation that the I1V strain that causes defoliation is closely related to other, previously characterized, strains of the D pathotype, and furthermore contains the gene encoding the D effector. This gene was recently shown to be responsible for the defoliation pathotype on cotton (Li, 2019). Interestingly, deletion of the gene encoding the D effector from the I1V strain results in loss of the defoliation phenotype on rose, and a concomitant decline in virulence, suggesting that the gene encoding the D effector is responsible for the defoliation phenotype on rose as well.

V. dahliae is considered a broad host-range pathogen, and thus it is unclear to what extent co-evolution of the pathogen with multiple hosts occurs simultaneously, and what implications this has for the effector repertoires of individual strains. Thus far, multiple *V. dahliae* effectors have been functionally characterized in our laboratory (de Jonge et al., 2012, 2013; Santhanam et al., 2013; 2017; Boshoven, 2017; Li, 2019). These studies have shown that a suite of effectors can contribute to disease development on tomato as well as on other plant species. Moreover, given that many of these studies have revealed virulence phenotypes based on targeted deletion of individual effector genes, it can be concluded that functional redundancy does not play a major role among the characterized effectors. This finding appears to apply to rose infection too, as most of the effectors tested contribute to *V. dahliae* virulence on rose as well. Combined with our finding that different strains that infect rose plants carry divergent effector catalogs, this finding suggests that compatibility on rose can be established in various ways and by targeting divergent molecular processes. Collectively, our findings suggest that pathogenicity of *V. dahliae* on rose depends on the targeting of molecular processes that are relevant for causing disease on other plant species as well, and thus that little host-specific adaptation is required.

MATERIALS AND METHODS

V. dahliae inoculations on rose cuttings

Rose rootstock cv. Natal briar plants were grown in potting soil (Potgrond 4, Horticoop, Katwijk, the Netherlands) under controlled greenhouse conditions (Unifarm, Wageningen, the Netherlands) with day/night temperature of 24/18°C for 16-h/8-h periods, respectively, and relativity humidity between 50 and 85%. Two-month-old plants were pruned and the cuttings were subsequently cut in 4 cm sections containing at least one meristem. Subsequently, the stem cuttings were rooted by dipping in 10% indole-3-butyric acid and placement on soil for one week in the dark. Finally, rooted cuttings were placed under the day/night regime as detailed above.

For *V. dahliae* inoculation, ten 30-day-old cuttings were root-dipped in a conidiospore suspension for 10 min as described previously (Fradin et al., 2009). Disease symptoms were scored at 28 days post inoculation (dpi) by measuring the height of the plant to calculate stunting as follows:

$$stunting = \left(1 - \frac{canopy\ area\ V.dahliae - inoculated\ plants}{average\ canopy\ area\ of\ mock - inoculated\ plants}\right) * 100$$

To test for significant stunting, an ANOVA was performed which tests for significant differences in height between mock-inoculated and *V. dahliae*-inoculated plants.

Testing the contribution of V. dahliae effectors to disease development on rose

V. dahliae inoculations were performed as described above on rose rootstock cv. Natal briar. Thirteen previously described effectors (Table 2) were tested using previously generated targeted deletion lines (de Jonge et al., 2012, 2013; Santhanam et al., 2013, 2017; Boshoven, 2017; Li, 2019). At 28 days post inoculation (dpi) stunting was measured as described above. For biomass quantification, rose stems were freeze-dried and ground to powder of which 100 mg was used for DNA isolation. Real-time PCR was conducted with primers RoRUB-Fw and RoRUB-Rv for rose RuBisCo and primers ITS1-F and STVe1-R for *V. dahliae* ITS (Table 4). Real-time PCR conditions were as follows: an initial 95°C denaturation step for 10 min followed by denaturation for 15 s at 95°C and annealing for 30 s at 60°C, and extension at 72°C for 40 cycles.

Table 3. *Verticillium dahliae* effectors analysed in this study.

Primer name	Oligonucleotide sequence (5'→3')	Usage
RoRUB-Fw	GCTGCGGAATCTTCTACTGG	qPCR
RoRUB-Rv	GGTAGCATCGCCCTTTGTAA	qPCR
ITS1-F	AAAGTTTTAATGGTTCGCTAAGA	qPCR
STVe1-R	CTTGGTCATTTAGAGGAAGTAA	qPCR
VdAve1-F	AGCTTTCTACGCTTGGA	qPCR
VdAve1-R	TTGGCTGGGATTGCT	qPCR
VdGAPDH-F	CGAGTCCACTGGTGTCTTCA	qPCR
VdGAPDH-R	CCCTCAACGATGGTGAACTT	qPCR
qPCR-NLP1-F	CTGCAAGGAAACCAGCAAG	qPCR
qPCR-NLP1-R	GTTTGCGTTGTTCGAGTTGA	qPCR
qPCR-NLP2-F	GCTCAAGTTCAAGCCGTACC	qPCR
qPCR-NLP2-R	GTACAGAAACAAATCGCGGC	qPCR
I1V-D-LB-Fw	GGTCTTAATAATCCCATAAAAGCGCTGAA	Deletion
I1V-D-LB-Rv	GGCATTAAUCTGTCGTTTGCTCAGTTGGA	Deletion
I1V-D-RB-Fw	GGACTTAAUGATGGTAGGGGGAAGGAGAG	Deletion
I1V-D-RB-Rv	GGGTTTAAUGCACCATGCATAAAACGATG	Deletion

Testing the contribution of D effector to defoliation on rose

Targeted deletion of the *D* effector gene was performed by deleting two identical copies of the *D* gene. To this end, a genomic construct was generated comprising the flanking regions of the *D* gene in vector pRF-HU2 for strain I1V, using primers I1V-D-LB-Fw, I1V-D-LB-Rv, I1V-D-RB-Fw and I1V-D-RB-Rv (Table 4). Next, *Agrobacterium tumefaciens*-mediated transformation (ATMT) was performed as described previously (Ökmen et al., 2013) with a few modifications as reported previously (Chavarro-Carrero et al., 2021). Successful deletion was verified by PCR and DNA sequencing. Subsequent *V. dahliae* inoculations using strains JR2, CQ2, and I1V as well as the targeted deletion lines were performed as described above. At 28 days post inoculation (dpi) stunting was measured and biomass was quantified as described above.

Nanopore sequencing

Conidiospores were harvested from potato dextrose agar (PDA) plates, transferred to 1/5 potato dextrose broth (PDB) and grown for ten days. Subsequently, fungal material

was collected on Miracloth, freeze-dried overnight and ground to powder with mortar and pestle. High molecular weight (HMW) DNA extraction was performed as described previously (Chavarro-Carrero et. al., 2021).

Library preparation was performed with the Rapid Sequencing Kit (SQK-RAD004) according to the manufacturer's instructions (Oxford Nanopore Technologies, Oxford, UK) with 400 ng HMW DNA. An R9.4.1 flow cell (Oxford Nanopore Technologies, Oxford, UK) was loaded and run for 24 h. Base calling was performed using Guppy (version 3.1.5; Oxford Nanopore Technologies, Oxford, UK) with the high-accuracy base-calling algorithm. Adapter sequences were removed using Porechop (version 0.2.4 with default settings; Wick, 2018). Finally, the reads were self-corrected, trimmed, and assembled using Canu (Version 1.8; Koren et al., 2017).

Phylogenetic tree construction and presence-absence variation analysis

The phylogenetic tree of the different *V. dahliae* strains was generated as previously described (Chavarro-Carrero et al., 2021). Presence-absence variation (PAV) was assessed by BLAST sequence searches for each effector gene against all *V. dahliae* strains (60) and further confirmation was obtained through whole-genome alignments as described previously (Chavarro-Carrero et al., 2021). Briefly, paired-end short reads or long-reads were mapped to the *V. dahliae* strain for which the effector gene was described (Table 3) using BWA-mem with default settings (Li and Durbin, 2009). Raw read coverage was averaged for 100 bp non-overlapping windows using the BEDtools -multicov function (Quinlan and Hall, 2010). Next, we transformed the raw read coverage values to a binary matrix by applying a cut-off of 10 reads for short-read data; ≥ 10 reads indicate presence (1) and < 10 reads indicate absence (0) of the respective genomic region. For long-read data a cut-off of 1 read was used; ≥ 1 read indicates presence (1) and < 1 read indicates absence (0). The total number of PAV counts for each of the 100 bp genomic windows within 100 kb upstream and downstream of the effector genes was summarized.

Acknowledgements

The soil-borne white root rot pathogen *Rosellinia necatrix* expresses antimicrobial proteins during host colonization

Edgar A. Chavarro-Carrero, Nick C. Snelders[$], David E. Torres[$], Anton Kraege, Ana López-Moral, Gabriella C. Petti, Wilko Punt, Jan Wieneke, Rómulo García-Velasco, Carlos J. López-Herrera, Michael F. Seidl[#] and Bart P.H.J. Thomma[#]

[$,#]These authors contributed equally

ABSTRACT

Rosellinia necatrix is a prevalent soil-borne plant-pathogenic fungus that is the causal agent of white root rot disease in a broad range of host plants. The limited availability of genomic resources for *R. necatrix* has complicated a thorough understanding of its infection biology. Here, we sequenced nine *R. necatrix* strains with Oxford Nanopore sequencing technology, and with DNA proximity ligation we generated a gapless assembly of one of the genomes into ten chromosomes. Whereas many filamentous pathogens display a so-called two-speed genome with more dynamic and more conserved compartments, the *R. necatrix* genome does not display such genome compartmentalization. It has recently been proposed that fungal plant pathogens may employ effectors with antimicrobial activity to manipulate the host microbiota to promote infection. In the predicted secretome of *R. necatrix*, 26 putative antimicrobial effector proteins were identified, nine of which are expressed during plant colonization. Two of the candidates were tested, both of which were found to possess selective antimicrobial activity. Intriguingly, some of the inhibited bacteria are antagonists of *R. necatrix* growth *in vitro* and can alleviate *R. necatrix* infection on cotton plants. Collectively, our data show that *R. necatrix* encodes antimicrobials that are expressed during host colonization and that may contribute to modulation of host-associated microbiota to stimulate disease development.

INTRODUCTION

Rosellinia necatrix is a prevalent soil-borne plant-pathogenic fungus that is found in temperate and tropical areas worldwide (Sivanesan and Holliday, 1972). As causal agent of white root rot disease, *R. necatrix* has a broad host range comprising at least 170 species of dicotyledonous angiosperms that are dispersed over 63 genera and 30 families (Sztejnberg and Madar, 1980). Many of these species are of great economic importance, such as *Coffea* spp. (coffee), *Malus* spp. (apple), *Olea europea* L. (olive), *Persea americana* Mill. (avocado), *Prunus* spp. (peaches, almonds, etc.), *Vitis vinifera* L. (grape) (Eguchi et al., 2009) and *Rosa* sp. (rose) (García-Velasco et al., 2012).

Plants infected by *R. necatrix* usually display two types of symptoms. The first type is displayed below-ground on the root system, where white and black colonies of mycelium can occur on the surface of infected roots. As the fungus penetrates and colonizes the root tissue, the roots acquire a dark brown color (Guillaumin et al., 1982). The second type of symptom occurs above-ground. These symptoms can develop rapidly as a consequence of the damaged root system and comprise wilting of leaves, typically after a period of drought or physiological stress, which affects plant vigor and eventually can lead to plant death. Symptoms of *R. necatrix* infection can also appear slowly, leading to a decline in growth, decreasing leaf numbers, along with wilting of leaves, chlorosis, and death of twigs and branches. On perennials these symptoms aggravate over time, and when moisture and temperature are unfavorable, the plant eventually dies (Guillaumin et al., 1982).

Various studies have addressed the biology of *R. necatrix* (Pérez-Jiménez et al., 2002; Pliego et al., 2009). Nevertheless, the molecular mechanisms underlying pathogenicity of *R. necatrix* remain largely unexplored, mainly because the limited availability of genomic resources to date complicates investigations into the molecular biology of *R. necatrix* infections. Until recently, only a single Illumina technology short-read sequencing-based *R. necatrix* draft genome assembly was generated of strain W97 that was isolated from apple in Japan (Shimizu et al., 2018). This 44 Mb genome assembly is highly fragmented as it comprises 1,209 contigs with 12,444 predicted protein-coding genes (Shimizu et al., 2018). Recently, another assembly was released of a South-African strain (CMW50482) that was isolated from avocado, yet this assembly is even more fragmented with 1,362 contigs (Wingfield et al., 2022).

It is generally accepted that plant pathogens secrete dozens to hundreds of so-called effectors into their host plants to stimulate host colonization (Rovenich et al., 2014; Wilson and McDowell, 2022). Effectors can be defined as small, secreted proteins of ≤300 amino acids that are cysteine-rich and have tertiary structures that are stabilized by disulfide bridges and that are secreted by pathogens to promote disease on plant hosts (Duplessis et al., 2011; Gan et al., 2013; Stergiopoulos et al., 2013; Lo

4

Presti et al., 2015). However, also larger secreted proteins have been found to act as effectors, such as several LysM effectors (Djamei et al., 2011; Kombrink and Thomma, 2013). Furthermore, also non-proteinaceous effectors have been described, such as fungal secondary metabolites as well as small RNA (sRNA) molecules that are delivered into host cells to suppress host immunity (Weiberg et al., 2014). Many effectors have been shown to act in suppression of host immune responses (Rovenich et al., 2014). However, recent studies have uncovered additional functions of pathogen effector proteins in host colonization (Wilson and McDowell, 2022). For example, the soil-borne pathogen *Verticillium dahliae* secretes effector proteins to modulate microbiota compositions inside the host plant as well as outside the host in the soil to support host colonization (Snelders et al., 2020; 2021; 2022; 2023). One of them is the effector protein VdAve1 that was shown to display selective antimicrobial activity and facilitate colonization of tomato and cotton plants through host microbiota manipulation by suppressing antagonistic bacteria, such as members of the *Spingomonadaceae* (Snelders et al., 2020). Besides VdAve1, ten additional potentially antimicrobial effector protein candidates were predicted by mining the *V. dahliae* secretome for structural homologues of known antimicrobial proteins (AMPs) (Snelders et al., 2020). One of these candidates, VdAMP2, was subsequently found to contribute to *V. dahliae* survival in soil through its efficacy in microbial competition (Snelders et al., 2020). Another candidate, VdAMP3, was shown to promote microsclerotia formation in decaying host tissue through its antifungal activity directed against fungal niche competitors (Snelders et al., 2021). Most recently, a multiallelic gene homologous to *VdAve1* was identified as *VdAve1-like* (*VdAve1L*) of which the *VdAve1L2* variant was shown to encode an effector that promotes tomato colonization through suppression of antagonistic Actinobacteria in the host microbiota (Snelders et al., 2023). These findings have led to the hypothesis that microbiota manipulation is a general virulence strategy of plant pathogens to promote host colonization (Snelders et al., 2022). However, thus far evidence for such activity has been lacking for other fungal plant pathogens.

Similar to *V. dahliae*, also *R. necatrix* is a soil-borne pathogen that spends at least part of its life cycle in the soil, known to be an extremely competitive and microbe-rich environment (Smercina et al., 2021). In the present study, we aimed to generate a high-quality genome assembly to mine the *R. necatrix* genome for potential antimicrobial proteins that are exploited during host colonization and test the hypothesis that other pathogenic fungi besides *V. dahliae* exploit effector proteins with antimicrobial activity during host colonization as well.

RESULTS

A chromosome-level assembly of *Rosellinia necatrix* strain R18

Thus far, two fragmented *R. necatrix* draft genome assemblies that comprise over 1,200 contigs are publicly available (Shimizu et al., 2018; Wingfield et al., 2022). To generate additional and more contiguous *R. necatrix* genome assemblies, we sequenced nine strains of *R. necatrix* that were collected from rose and avocado in Mexico and Spain, respectively, with Oxford Nanopore sequencing technology (ONT). This resulted in genome assemblies of 28 (for strain R18) to 399 (for strain CH12) contigs (Table 1). The most contiguous assembly was obtained for strain R18, isolated from infected rose plants in Mexico.

To further improve the genome assembly of strain R18, additional ONT sequencing was performed using ultra HMW (UHMW) DNA as template. Additionally, chromosome conformation capture (Hi-C) followed by high-throughput sequencing was performed (Burton et al., 2013; Varoquaux et al., 2015). Based on these orthogonal sequencing data, we ultimately assembled the R18 genome into 11 contigs (Table 1). Using Tapestry (Davey et al., 2020) twenty telomeric regions ([TTAGGG]n) were identified (Figure 1A), and ten of the 11 contigs were found to contain telomeric regions at both ends, suggesting that these represent completely assembled chromosomes, which could be confirmed by Hi-C analysis (Figure 1B). The 11th, and smallest, contig contained no telomeric regions, displayed a markedly higher coverage (read depth) (Figure 1B), and BLAST analysis revealed hits to fungal mitochondrial genomes, showing that this contig belongs to the mitochondrial genome. Accordingly, no mitochondrial genes could be found on any of the ten chromosomal contigs. Thus, we conclude that our assembly contains ten complete chromosomes that compose the nuclear genome, and an 11th contig that composes the mitochondrial genome, and thus that we generated a gapless, telomere-to-telomere, genome assembly. To measure the completeness of the genome assembly, we used BUSCO v4 with the Ascomycota dataset (Simão et al., 2015), which resulted in a completeness score of 97%.

4

Table 2. Sequencing summary and genome assembly statistics for nine *Rosellinia necatrix* strains.

Strain name	Rn19[a]	CH12[a]	Rn400[a]	R10[a]	R25[a]	R27[a]	R28[a]	R30[a]	R18[a]	R18[b]
Isolated from	Avocado	Avocado	Avocado	Rose	Rose	Rose	Rose	Rose	Rose	
Country of origin	Spain	Granada, Spain	Granada, Spain	State of Mexico, Mexico	State of Mexico, Mexico	State of Mexico, Mexico	State of Mexico, Mexico	State of Mexico, Mexico	State of Mexico, Mexico	
Year	2001	1988	1991	2005	2008	2005	2011	2014	2014	
Read N50 (kb)	23	17	21	18	16	21	21	9	18	30
Coverage	45X	46X	35X	35X	45X	46X	41X	52X	42X	120X
No. of contigs	35	399	37	50	58	31	47	130	28	11
Total length (Mb)	48.2	49.9	48.2	48.9	49.2	49.2	48.7	48.3	49	49.1
Average length (Mb)	1.3	0.1	1.3	1	0.8	1.5	1	0.3	0.8	4
Maximum length (Mb)	6.4	6.3	5.8	4.4	4	6.4	6.4	4.5	4	7.1
N50 (Mb)	3.4	4.6	3.8	1.9	2.5	3.2	3.4	1.6	3.1	5.1
N90 (Mb)	0.8	3.1	1.3	0.4	0.5	1.2	0.8	0.3	0.6	3.3
GC (%)	46.28	46.37	46.37	45.35	45.49	45.43	45.50	45.99	45.35	45.46
BUSCO (%)	76.7	69.9	70.2	68.4	78.9	72.3	68.2	80.7	82.5	97

[a] *de novo* assembly based on Nanopore sequencing of high-molecular weight (HMW) DNA.
[b] *de novo* assembly based on Nanopore sequencing of HMW and UHMW DNA and Hi-C sequencing.

4
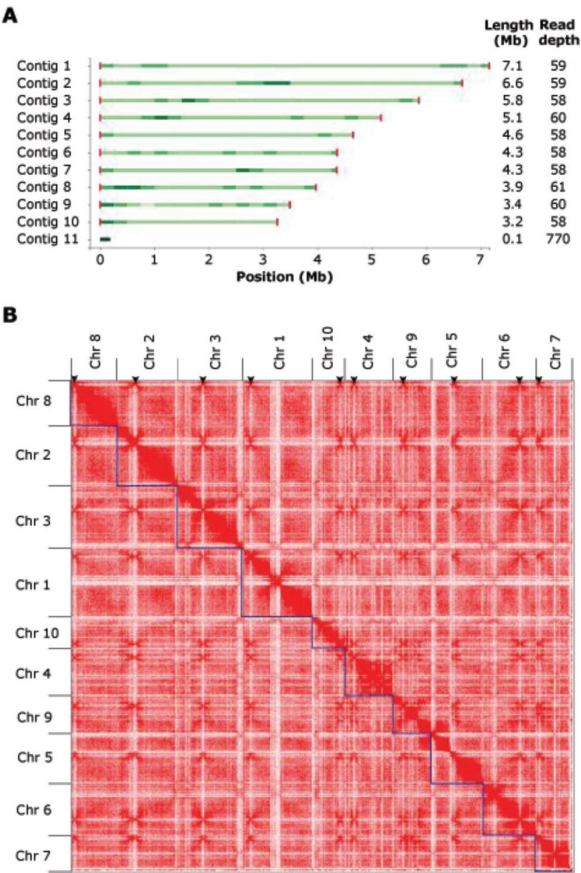
Figure 1. Genome assembly of *Rosellinia necatrix* strain R18. (A) Genome assembly plot generated with Tapestry (Davey et al., 2020). Green bars indicate contig sizes with the color intensity correlating with read coverage, while red bars indicate telomeres with the color intensity correlating with the number of telomeric repeats. Contig 11 lacks telomeres and represents the mitochondrial genome. (B) Hi-C contact matrix showing interaction frequencies between regions in the genome of *Rosellinia necatrix* strain R18. Ten regions with high inter-chromosomal interaction frequencies are indicative of centromeres and are indicated with arrowheads.

To further explore the *R. necatrix* strain R18 assembly, genome annotation was performed using Funannotate (Palmer and Stajich, 2017) guided by publicly available RNAseq data (Shimizu et al., 2018), resulting in 11,760 predicted protein-coding genes (Table 2). Furthermore, effector genes were predicted using EffectorP (Sperschneider et al., 2018). The assembled genome of *R. necatrix* strain R18 was predicted to encode 1,126 secreted proteins, of which 192 were predicted to be effector candidates. BLAST searches revealed that 182 of these have homology to Ascomycete fungal proteins, of which 69 had functional domain annotations, while the remaining 113 were annotated as hypothetical proteins (Supplemental Table 1). The largest group of

annotated effectors were cell wall degrading enzymes, including glycoside hydrolases and carbohydrate esterases that are generally involved in plant cell wall degradation (Underwood, 2012; Malinovsky et al., 2014). Effectors carrying carbohydrate-binding domains while lacking enzymatic domains, specifically a concanavalin A-like lectin and two cell wall integrity and stress response component (WSC) domain-containing proteins, were also found. Concanavalin A-like lectin has been described as a virulence factor, although no molecular mechanism has been presented (Ismail and Able, 2016), while WSC domain-containing proteins can protect fungal cell wall through structural strengthening, but their contribution to plant colonization remains unclear (Wawra et al., 2019). Additionally, two lysin motif (LysM) effectors were found that typically bind chitin and play roles in virulence through suppression of chitin-triggered immunity or shielding hyphae against host-derived chitinases (de Jonge et al., 2010; Kombrink and Thomma, 2013; Tian et al., 2021; 2022). Four genes were found to encode hydrophobins; proteins that have been implicated in virulence through acting as phytotoxin (Takai, 1974), or promoting attachment to plant surfaces and appressoria formation (Talbot et al., 1996), although negative impacts on host colonization have also been reported (Luciano-Rosario et al., 2022). Finally, three potential toxins were found, namely a cerato-platanin domain-containing protein (Carresi et al., 2006) and two necrosis and ethylene-inducing-like (NLP) effectors that are typically thought to be phytotoxic to eudicot plants (Lenarčič et al., 2017; Seidl & van den Ackerveken, 2019) (Supplemental Table 1).

　　　　To investigate the conservation of effector gene catalogues among the *R. necatrix* genomes that we sequenced in our study, we performed BLAST searches to find homologs of each of the predicted effector genes in the genome of strain R18 in each of the other genomes. Intriguingly, we found remarkably little presence-absence variation, with only few effector genes missing in some of the other genomes. While strains R27, R28 and R30 carry all the effector genes that were identified in strain R18, strain R10 and R25 lack two, strains R19 lacks three, and strains CH12 and Rn400 lack four of the 192 predicted effector genes (Supplemental Table 2). Furthermore, we determined the ratio of single nucleotide polymorphisms (SNPs) for each of the predicted effectors. Interestingly, while strains Rn19 and strain Rn400 share no identical effector genes and strain CH12 only a single identical effector gene with strain R18, on the other end of the spectrum strain R10 shares 152 identical effector genes with strain R18. Furthermore, SNP ratios vary from 0% up to 26,12% for effector *FUN_011522* in strain CH12. Generally, we observed higher variability in effectors of the Spanish strains (Rn19, CH12, Rn400) than in the Mexican strains (R10, R25, R27, R28, R30) (Supplemental Table 2).

Table 2. Genome annotation of *Rosellinia necatrix* strain R18.

Genomic trait	Value
Protein-coding genes (Funannotate version 1.8.13, Palmer and Stajich, 2017)	11,760
Mean gene length (bp)	1,689.48
Mean exons per gene	2.92
Mean intergenic length (bp)	1,114
Homologs in InterPro database	8,125
Secreted proteins (SignalP; version 5.0, Almagro et al., 2019)	1,126
Effectors (EffectorP; version 2.0, Sperschneider et al., 2018)	192
CAZymes (Funannotate)	535
CAZymes (secreted) (Funannotate)	300
Small cysteine-rich proteins (Funannotate)	209
LysM (lysin motif) effectors (Funannotate)	2
NLP (necrosis and ethylene-inducing-like) effectors (Funannotate)	2
Secondary metabolite clusters (antiSMASH; version 5.0, Blin et al., 2019)	48

4

Besides proteinaceous effectors, 48 secondary metabolite gene clusters were predicted using antiSMASH fungal version (Blin et al., 2019; Table 2). From these, 13 showed homology to known secondary metabolite clusters, including those for the production of swainsonine, cytochalasin E/K, pyriculol, enniatin, and naphthalene, which have been implicated in pathogenicity through their phytotoxic activity (Thomas, 1978; Sawai et al., 1983; Walton, 1990; Shimizu et al., 2014; Cook et al., 2017; Zhao et al., 2019; Xu et al., 2021), and copalyl diphosphate which has been implicated in elongation disorders in plants (Rademacher and Graebe, 1979; Kawaide, 2006) (Supplemental Table 3).

Absence of distinctive genome compartmentalization

In many filamentous pathogens, effector genes are found in repeat-rich and gene sparse genomic compartments, whereas they are depleted in repeat-poor and gene-dense regions that typically harbor housekeeping genes, a genome organization that is typically referred to as the two-speed genome (Frantzeskakis et al., 2020). Thus, we aimed to explore if effector genes were associated with repetitive regions in *R. necatrix* too. Interestingly, the repeat content in *R. necatrix* strain R18 is low (2.39%) and evenly distributed throughout the genome, with the most abundant families being DNA/Helitron (67%) and long terminal repeats (LTRs; 31%). Accordingly, most repetitive

elements are not preferentially located near effectors (p>0.05 after permutation test for distance). Moreover, effector genes are not preferentially found in regions with large intergenic distances (Figure 2). Thus, our results do not support association of effector genes with repeat-rich regions in *R. necatrix*.
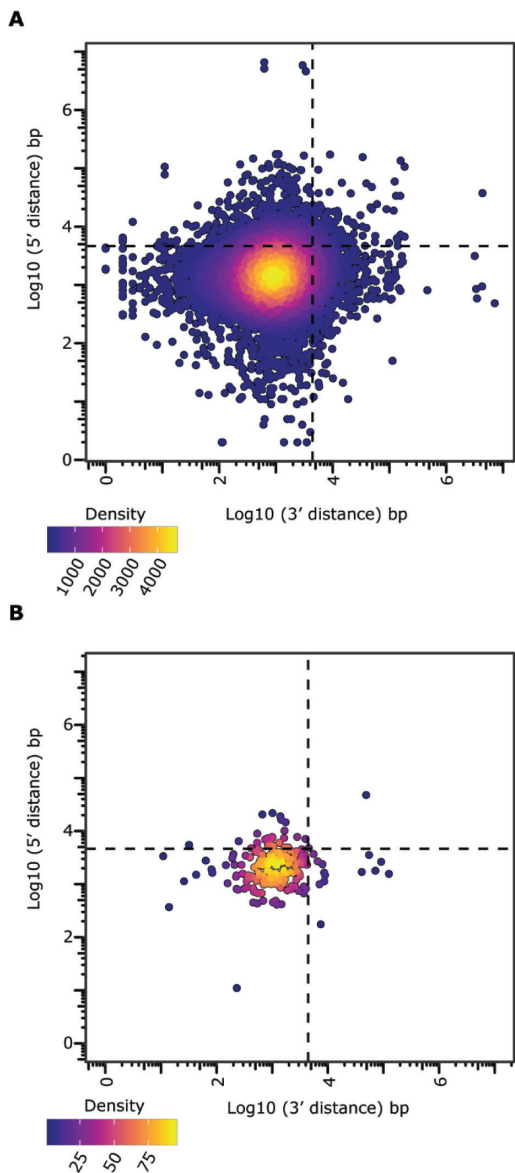
Figure 2. Effector genes do not localize in gene-sparce regions. Gene density plot of '5 and '3 flanking log10 transformed intergenic distance with the dashed lines depicting the mean intergenic distances for all genes (A) and candidate effector genes encoded in the *R. necatrix* genome (B).

Genomic comparisons in various filamentous fungi have revealed extensive chromosomal rearrangements and structural variants (SVs) in close association with effector genes (Torres et al., 2020; Faino et al., 2016; Oggenfuss et al., 2021; Fouché et al., 2020; Shi-Kunne et al., 2018). Thus, we tested whether effector genes are associated with SVs in *R. necatrix*. First, to explore the genomic diversity among *R. necatrix* strains, a phylogenetic tree of all genomes was constructed with Realphy (version 1.12) (Bertels et al., 2014). Two clusters were identified, one with strains from Mexico isolated from roses, and one cluster with the strains from Spain and South Africa, isolated from avocado, as well as Japan, isolated from apple (Figure 3). Then, SVs were predicted for each of the genomes sequenced in this study using NanoSV (version 1.2.4 with default settings; Stancu et al., 2017) by identifying split- and gapped-aligned long reads for the various strains to define breakpoint-junctions of structural variations when using the gapless genome assembly of strain R18 as a reference. We retrieved 2,639 SVs in total, comprising 1,264 insertions, 1,344 deletions, 4 inversions and 27 translocations (Figure 3A). The number of SVs per strain corresponds to their phylogenetic relationships based on whole-genome comparisons. To investigate the occurrence of the SVs in the *R. necatrix* strains, we calculated the frequency of each SV over the strains used in the analysis. Most of the SVs (94.2%) are shared by <50% of the strains, meaning that they occur in less than four strains. This suggests that SV is a common phenomenon in line with the phylogenetic and geographic relationship of *R. necatrix* strains. Interestingly, SVs occur all across the genome (Figure 3B), largely independently of repetitive regions (p>0.05 after permutation test for distance), but are found in close association with effector genes (p<0.05 after permutation test for distance). Collectively, our results for *R. necatrix* substantiate the lack of the typical genome compartmentalization that is associated with the two-speed genome organization that was found in many other filamentous fungi (Raffaele and Kamoun, 2012).

4
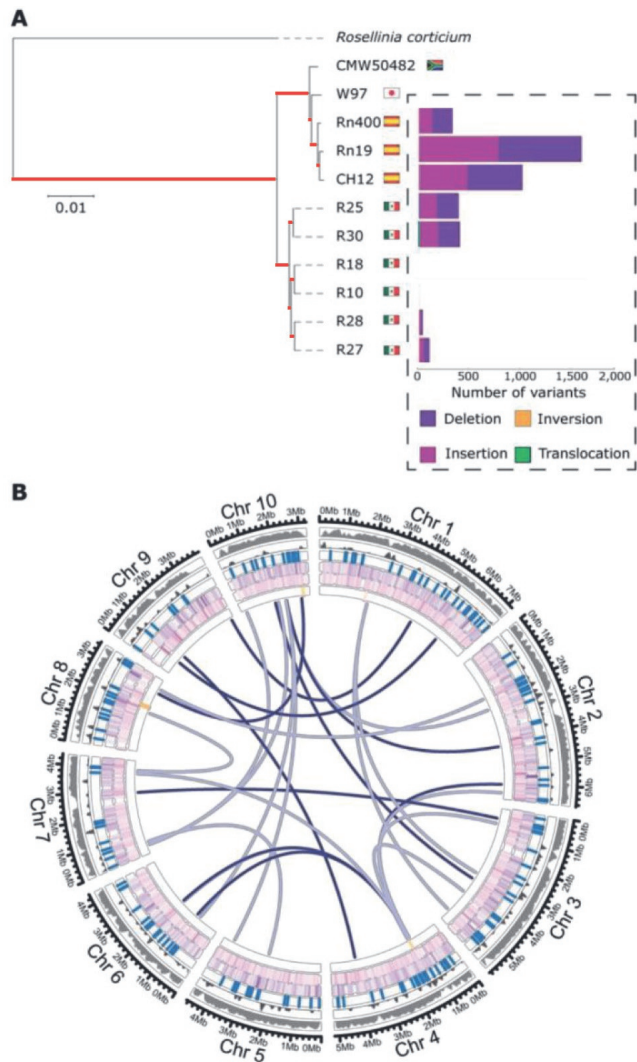
Figure 3. Phylogeny and structural variation of nine *Rosellinia necatrix* strains. (A) Phylogeny of sequenced *R. necatrix* strains was inferred using Realphy (Langmead and Salzberg, 2012). The robustness of the phylogeny was assessed using 1000 bootstrap replicates, and branch lengths represent sequence divergence (branches with maximum bootstrap values are indicated in red). *Rosellinia corticium* was used to root the tree. The amount of structural variants was calculated using NanoSV (Stancu et al., 2017) using strain R18 as a reference. (B) Circular plot displaying the genomic distribution of 2,019 SVs along the 10 chromosomes of *R. necatrix*. The tracks are shown in the following order from outside to inside: Gene density (10 kb), repetitive density (10 kb), effector gene locations, deletions, insertions and inversions and translocations. The color intensity of the lines for each SV track depict frequency in the *R. necatrix* collection.

Weak structural clustering in the effector catalog

Effectors continuously evolve towards optimal functionality while simultaneously evading recognition by plant immune receptors, which is considered one of the reasons for the lack of sequence conservation among effector proteins. Despite this lack of sequence conservation, groups of effector proteins that share their three-dimensional structure have been identified in various filamentous phytopathogens, such as the MAX-effector (*Magnaporthe* Avrs and ToxB like) family of the rice blast fungus *Magnaporthe oryzae* (de Guillen et al., 2015) that, together with some other families, are also found in the scab fungus *Venturia inaequalis* (Rocafort et al., 2022). It has been speculated that MAX effectors exhibit this structural conservation as an adaptation either to the apoplastic environment, or for transport into the plant cytosol (de Guillen et al., 2015). To investigate whether subsets of *R. necatrix* effectors display a similar fold conservation, their structures were predicted with Alphafold2 with an average quality score in a so-called predicted local distance difference test (pLDDT) of 86.1 (SD 11.8) on a scale from 0 to 100, with 100 indicating a perfect prediction. As only 11% of the predicted structures scored lower than 70 and only 2% lower than 50, we conclude that the fold prediction of the *R. necatrix* effector catalogue is generally robust. Next, we performed similarity clustering of the predicted effector folds, revealing that almost 40% of the effector candidates are structurally unique, while the remaining effectors could be assigned to a total of 31 clusters. As these clusters were only small, with on average only four members, we conclude that relatively little clustering occurs among *R. necatrix* effectors.

To examine whether the observed clustering is merely based on structural similarity, or is mainly driven by sequence conservation, the five largest clusters that contain six to 11 members were further analysed (Figure 4B, 4C). Two of the five clusters show high average template modelling (TM) scores, with 0.85 and 0.91, respectively, on a scale from 0-1, while also showing a relatively high degree of sequence conservation of 43 and 47 percent, respectively. The other three clusters exhibit lower sequence conservation, with maximum 21 percent, but also show considerably lower respectively structural conservation, with TM scores between 0.57 and 0.64 only, indicating that structural similarity within the clusters is positively correlating with sequence conservation. Hence, the structural clustering can be explained by the sequence conservation amongst the effector proteins. Taken together, although a considerable number of structural effector clusters can be observed in *R. necatrix*, they contain only few members and structural conservation is mostly based on sequence conservation. Thus, effector family expansion seems to have played only a minor role in *R. necatrix* effector evolution.
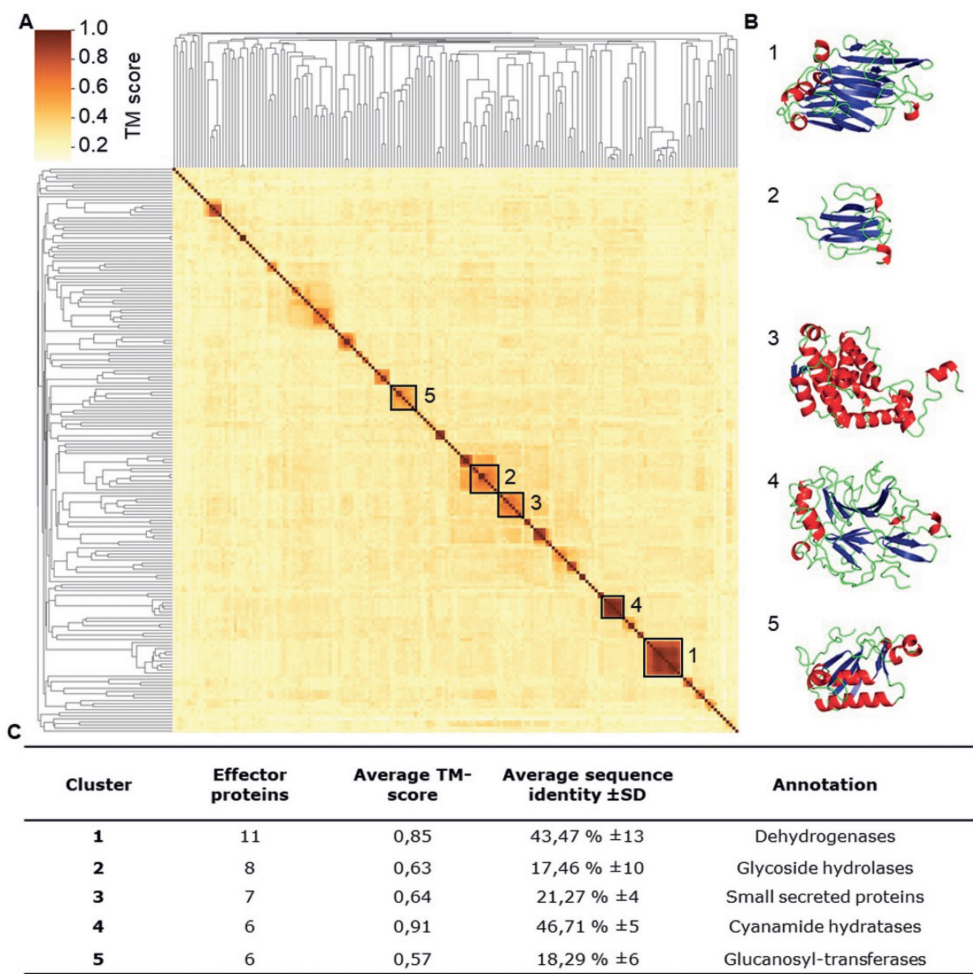
Figure 4. *R. necatrix* effector candidates show weak structural clustering, which is based on sequence conservation. (A) Ordered by hierarchical clustering based on structural similarity, the heatmap displays the structural similarity of each effector pair in an all-vs-all alignment based on template modelling (TM) scores that range from 0 to 1. Effector clusters were identified based on a similarity threshold > 0.5. The five largest clusters are highlighted with a black square and ordered by size. (B) Example structure for each of the five clusters based on the effector with the highest similarity to other effectors in the cluster. (C) Characteristics of the five largest structural effector clusters.

Cluster	Effector proteins	Average TM-score	Average sequence identity ±SD	Annotation
1	11	0,85	43,47 % ±13	Dehydrogenases
2	8	0,63	17,46 % ±10	Glycoside hydrolases
3	7	0,64	21,27 % ±4	Small secreted proteins
4	6	0,91	46,71 % ±5	Cyanamide hydratases
5	6	0,57	18,29 % ±6	Glucanosyl-transferases

Antimicrobial activity in culture filtrates

It has recently been proposed that fungal plant pathogens employ effectors with antimicrobial activity to manipulate the host microbiota to promote infection (Rovenich et al., 2014; Wilson and McDowell, 2022; Snelders et al., 2022). To explore if the soil-borne fungus *R. necatrix* potentially exploits antimicrobials, we first tested whether *R. necatrix culture* filtrates can inhibit the growth of plant-associated bacteria. To this end, we collected *R. necatrix* culture medium after 4, 7 and 9 days of fungal growth by filtration through a 0.45 nm filter, and an aliquot of each of the culture filtrates was heat-inactivated at 95°C for 10 minutes. Finally, the culture filtrates were used as growth medium for individual bacterial species from a diversity panel of 37 plant-associated bacteria (Supplemental Table 4). After overnight incubation, growth of four of the 37 bacteria was inhibited in the 4- and 7-day culture medium filtrates when compared with cultivation in the heat-inactivated culture filtrates, namely *Bacillus drentensis*, *Achromobacter denitrificans*, *Sphingobium mellinum* and *Flavobacterium hauense*. While three of these were not found to be inhibited anymore in the 9-day culture medium filtrate, growth of *B. drentensis* was also still inhibited in this filtrate (Figure 5). Given that the heat-treatment inactivated the antimicrobial activity, suggesting that the activity is of proteinaceous nature, we passed the culture filtrates through a spin column with 3 kDa cut-off and tested the growth of *B. drentensis* and *F. hauense* in these filtrates. Interestingly, none of the filtrates inhibited bacterial growth, suggesting that the activity is mediated by proteins that are retained in the spin column, as metabolites and other small molecules are expected to pass through. Collectively, these findings suggest that the culture medium of *R. necatrix* contains (a) heat-sensitive protein(s) with selective antimicrobial activity.

4
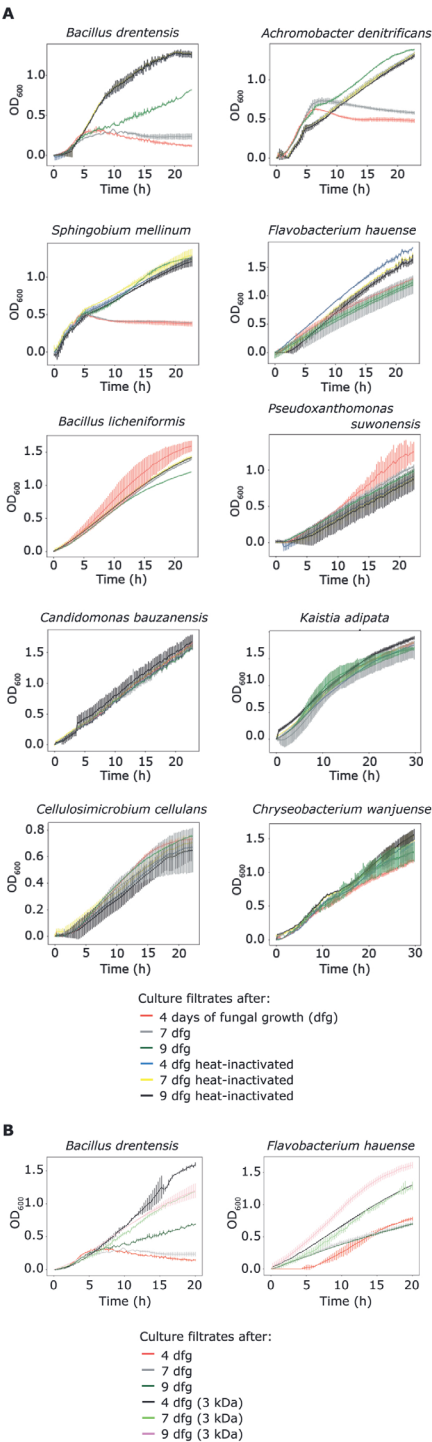
Figure 5. *Rosellinia necatrix* culture filtrates inhibit the growth of particular plant-associated bacterial species. (A) Bacterial growth was measured over time in *R. necatrix* culture filtrates, which were obtained after 4 (red), 7 (grey) and 9 (green) days of fungal growth. Heat-inactivated culture filtrates collected after 4 (blue), 7 (yellow) and 9 (black) days of fungal growth were used as controls. (B) Growth of *Bacillus drentensis* and *Flavobacterium hauense* was measured in culture filtrates collected after 4 (red), 7 (grey) and 9 (green) days of fungal growth, and additionally, in culture filtrates passed through spin-columns with 3 kDa cut-off after 4 (black), 7 (light green) and 9 (pink) days of fungal growth. The experiment was performed twice and error bars display standard deviations (n=3).

Table 3. Predicted secreted proteins of *R. necatrix* strain R18 with structural homology to known antimicrobial proteins.

R. necatrix gene ID	SignalP prediction confidence[a]	Structural homolog[b]	Prediction confidence (%)	Alignment coverage (%)[c]	Homolog protein size (kDa)[d]	Cys (%)[e]	pI[f]
FUN_000307	96.4	Bacterial enterotoxin	38.6	14	22.2	2.8	4.86
FUN_000408	99.3	Toxin	100	64	40.7	3.8	5.68
FUN_000625	99.3	Peptidoglycan-binding	100	98	12.3	4.5	8.79
FUN_000907	98.4	Toxin	40.1	35	28	2.6	5.03
FUN_001825	99.9	Hydrolase	100	95	38.4	1.8	5.11
FUN_001865	98.7	EGF/Laminin	91.4	13	34.6	3.6	7.01
FUN_002055	99.7	Endoglucanase	100	89	28.6	5.9	6.73
FUN_003304	99.3	Hydrolase	100	96	39.2	2.4	5.68
FUN_003451	99.1	Fungal ribonucleases	100	92	14.7	3.6	4.19
FUN_004580	99.8	Antifungal protein AFP1	55.5	6	47	2.5	4.85
FUN_004961	97.4	Toxin	25.2	23	19.7	3.8	7.75
FUN_005431	94.8	Thermolabile hemolysin	100	99	32.4	0.8	4.36
FUN_005483	99.6	NLP	100	87	28.9	3.3	4.87
FUN_005751	98.4	Fungal ribonuclease	100	93	14.4	3.6	6.05
FUN_005940	99.4	Toxin	40.6	17	13.9	5.8	6.63
FUN_006760	86.2	Carboxypeptidase	100	92	60.9	1.5	5.11
FUN_007808	91.5	Toxin	100	55	89	5.8	5.36
FUN_007991	98.2	Toxin	45.1	26	19	2.6	9.00
FUN_008352	99.6	Toxin	100	99	16.9	6.2	6.14
FUN_009115	96.1	Antimicrobial MIAMP1	87.8	33	24	3.2	4.65
FUN_009151	84.6	Phage lysozyme	100	94	20.7	3.6	6.92
FUN_009266	92.6	Neutrophil defensin 4	44.9	10	15.6	3.3	7.59
FUN_010039	97.8	Toxin	100	99	17.0	4.5	6.73
FUN_010165	99.5	Toxin	50.3	11	17.5	5.8	4.83
FUN_011519	98.6	Antimicrobial protein	15.2	57	5.8	5.7	4.78
FUN_011592	92.8	Defensin	49.9	10	18.8	6.7	7.41

[a]Secreted protein prediction confidence based on SignalP Version 5.0 (Almagro et al., 2019).
[b]Structural homology was determined based on Phyre2 prediction (Kelley et al., 2015).
[c]Alignment coverage of the *R. necatrix* gene query to the database homolog (subject).
[d]Protein size expressed in kilodaltons (kDa) of the database homolog.
[e]Amount of cysteines (Cys) present in the database homolog expressed in percentage (%).
[f]Isoelectric point (pI) of the database homolog.

4

Prediction of potential antimicrobial effector candidates

We previously showed that structural prediction successfully identified antimicrobial effector proteins encoded in the genome of *V. dahliae* (Snelders et al., 2020; 2021). Thus, we similarly mined the secretome of the *R. necatrix* strain R18 for structural homologues of known antimicrobial proteins using Phyre2 (Snelders et al., 2020; Kelley et al., 2015), leading to the identification of 26 candidates with potential antimicrobial activity (Table 3). Subsequently, we used publicly available RNAseq data (Shimizu et al., 2018) to assess expression of these candidates and found that nine of the 26 candidates are highly expressed during avocado colonization (Figure 6A). To further assess *in planta* expression of the nine candidates, we measured their expression in *R. necatrix* strain R18 upon cotton inoculation, revealing that five genes are highly expressed during cotton colonization (Figure 6B). To test whether these *in planta*-expressed predicted secreted proteins indeed possess antimicrobial activity, we pursued heterologous protein production in *E. coli*. Unfortunately, we repeatedly failed to produce four of these proteins (FUN_009266, FUN_0100039, FUN_005751 and FUN_006760) which, although it may be interpreted as a sign of potential antimicrobial activity (Ingham and Moore, 2007), obstructs functional analysis. However, one protein could be successfully produced and purified (FUN_004580).

FUN_004580 has predicted structural homology to antifungal protein 1 (AFP1) from the bacterium *Streptomyces tendae* (Campos-Olivas et al., 2001) (Figure 7A). This protein was identified in a screen for antifungal activity as a non-enzymatic chitin-binding antifungal directed against particular Ascomycete fungi (Bormann et al., 1999). Intriguingly, attempts to produce functional AFP1 in the lactic acid bacterium *Lactococcus lactis* failed (Freitas et al., 2005), suggesting that the protein may exert antibacterial activity as well. BLAST searches using the FUN_004580 amino acid sequence revealed ~100 Ascomycete fungal homologs, while HMMER searches revealed homologs in the Streptophyta clade (Viridiplantae) too (Supplemental Table 6). Interestingly, BLAST and HMMER searches using the amino acid sequence of FUN_004580 did not reveal homology to AFP1, underpinning that structural homology, rather than sequence homology, drove the prediction of FUN_004580 as an antimicrobial.
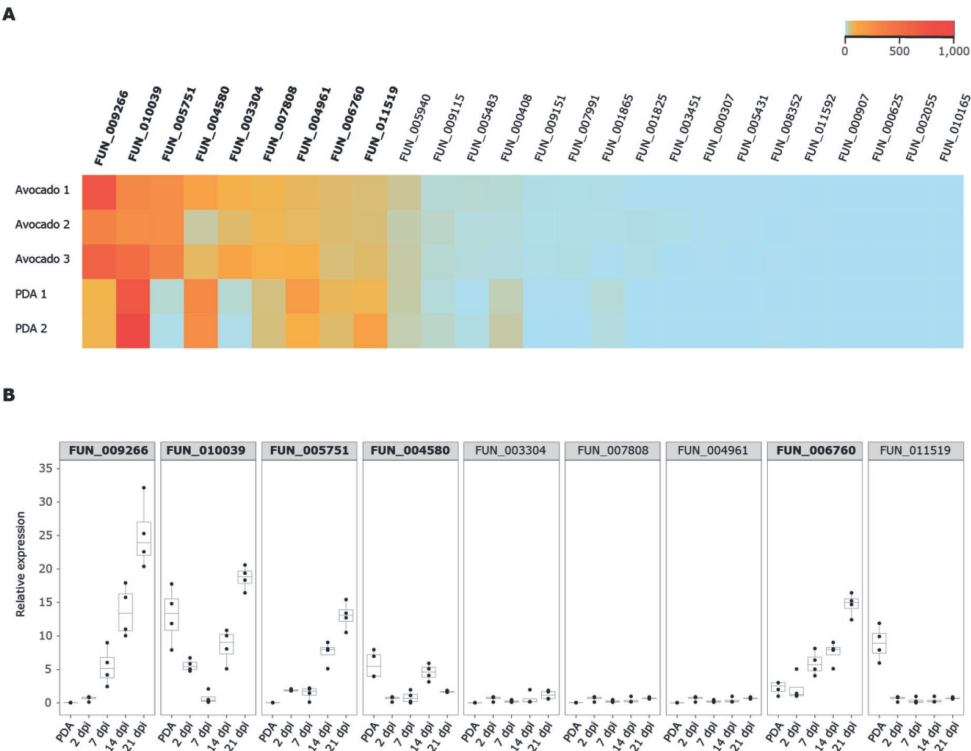
Figure 6. *In planta* expression of *Rosellinia necatrix* genes predicted to encode effector proteins with antimicrobial activity. (A) *In silico* analysis of publicly available RNAseq data of avocado plants infected with *R. necatrix* (n=3) reveals nine genes that are highly induced *in planta* (shown in bold) out of 26 that encode potential antimicrobial proteins (AMPs). Several of these are also expressed upon cultivation of *R. necatrix in vitro* on potato dextrose agar (PDA) (n=2). (B) Real-time PCR of nine *in planta* expressed *R. necatrix* genes identified in (A) reveals that five genes are expressed during cotton colonization at 14 and 21 days post inoculation (shown in bold).

An alternative manner to obtain proteins for functional analysis that does not rely on expression in heterologous microbial expression systems is peptide synthesis, although this is typically limited to sequences shorter than 100 amino acids. Unfortunately, all five effectors that are expressed in cotton are larger than this size. However, among the nine candidates that are highly expressed during avocado colonization, one encodes a protein (FUN_011519) small enough for protein synthesis (Biomatik Corporation, Ontario, Canada).

FUN_011519 has predicted structural homology to the antimicrobial protein AcAMP2 from the plant *Amaranthus caudatus* (Martins et al., 1996) (Figure 7B). This protein was identified based on homology to cysteine/glycine-rich domain of plant chitin-binding proteins and showed antifungal activity, as well as activity against

Gram-positive bacteria (Broekaert et al., 1992). BLAST and HMMER searches revealed only Ascomycete fungal homologs, identifying ~100 fungal proteins (Supplemental Table 7). Interestingly, BLAST and HMMER searches using the amino acid sequence of FUN_011519 did not reveal homology to AcAMP2, underpinning that also in this case structural homology, rather than sequence homology, drove the prediction as antimicrobial.
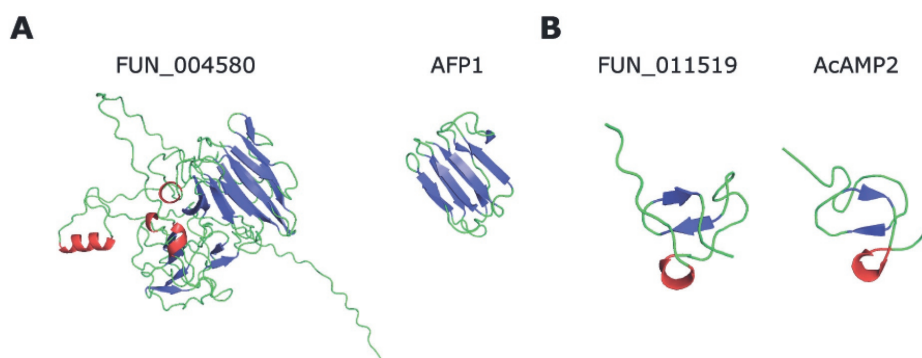
Figure 7. *Rosellinia necatrix* **effector proteins with predicted antimicrobial activity based on structural homology.** (A) Alphafold2 model of *R. necatrix* effector protein FUN_004580 (left) shows structural homology to antifungal protein 1 (AFP1) from the bacterium *Streptomyces tendae* (right). (B) Alphafold2 model of *R. necatrix* effector protein FUN_011519 (left) shows structural homology to antimicrobial protein AcAMP2 from the plant *Amaranthus caudatus* (right).

Candidate antimicrobial effector proteins display selective antimicrobial activity

Given that FUN_004580 and FUN_011519 were identified based on structural homology to proteins with antifungal activity, we tested potential antimicrobial activity on eight fungal species: five filamentous fungi (*V. dahliae*, *Alternaria brassicicola*, *Cladosporium cucumerinum*, *Trichoderma viridae* and *R. necatrix*), and four yeasts (*Pichia pastoris*, *Cyberlindnera jadinii*, *Debaryomyces vanrijiae* and *Rhodorotula bogoriensis*). Interestingly, both proteins displayed selective antifungal activity. Whereas FUN_004580 inhibited the growth of all filamentous fungi tested, except *R. necatrix* (Figure 8A) as well as of all yeasts except *P. pastoris* (Figure 7B), FUN_011519 had a narrower activity spectrum as it only inhibited the growth of *V. dahliae* and *A. brassicicola* (Figure 8C), and the yeasts *C. jadinii* and *R. bogoriensis* (Figure 8D). Thus, we conclude that both proteins possess clear antifungal activity.

To further investigate the antimicrobial activity of the two predicted secreted effector proteins FUN_004580 and FUN_011519, we tested their activity on the diversity panel of 37 bacteria that span a wide range of taxonomic diversity, including

Gram-positive and Gram-negative taxa (Supplemental Table 4). Interestingly, although we found that the growth of most bacteria was not affected by any of the two proteins, growth of some bacteria was clearly hampered. Whereas FUN_004580 strongly impacted growth of *Pseudoxanthomonas suwonensis*, *Flavobacterium hauense*, and *Cellulosimicrobium cellulans*, and inhibited *Chryseobacterium wanjuense* to a lesser extent, FUN_011519 inhibited *Bacillus drentensis* and *Achromobacter denitrificans*, and possibly also *Sphingobium mellinum* and *Candidimonas bauzanensis* (Figure 9). Thus, we conclude that both effectors display antibacterial activity as well. Collectively, our data show that both effector proteins possess selective antimicrobial activity.
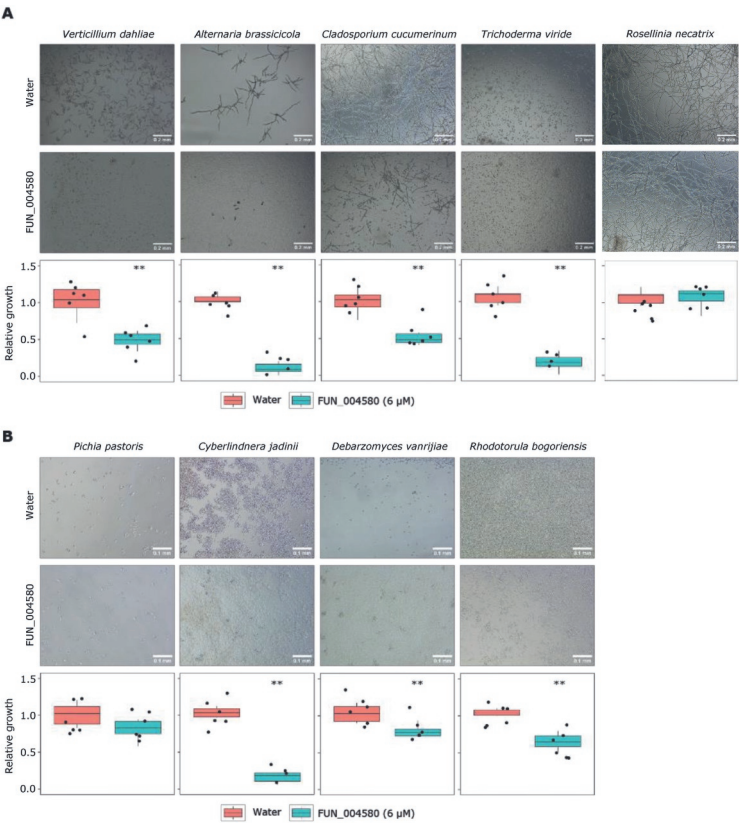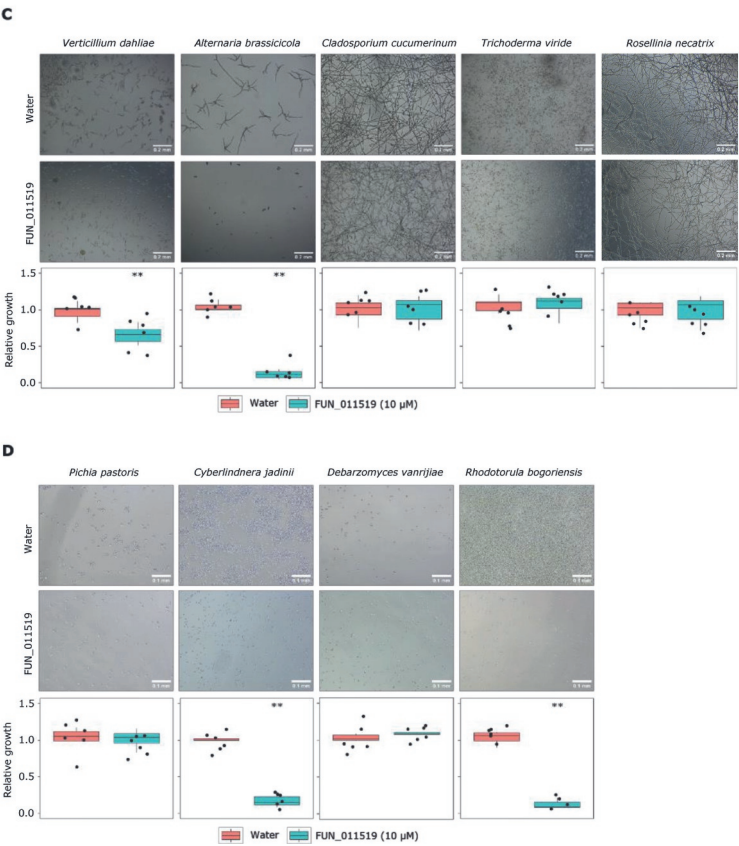
Figure 8. *Rosellinia necatrix* **effector proteins display antifungal activity.** Fungal growth in 5% potato dextrose broth (PDB) in presence of FUN_004580 (6 µM) or water of filamentous fungal species (A) and yeasts (B), or in presence of FUN_011519 (10 µM) or water of filamentous fungal species (C) and yeasts (D). Relative growth as display in microscopic pictures (n=6) was quantified using ImageJ. Asterisks indicate significant differences (unpaired two-sided Student's t test (P<0.01)).
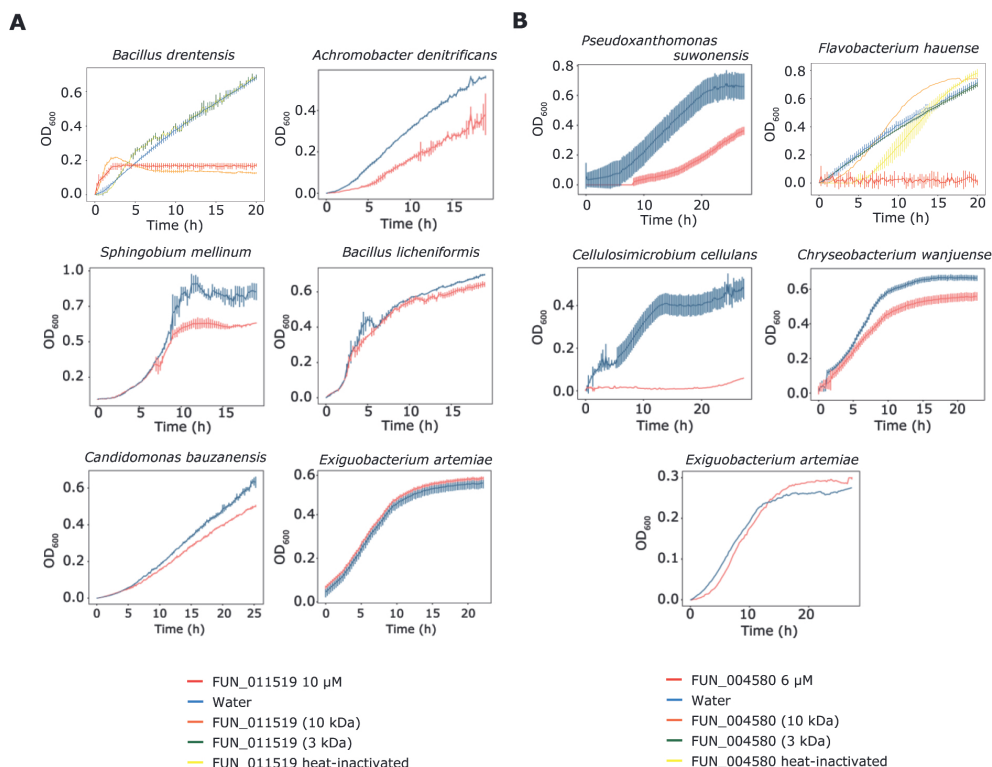
Figure 9. *Rosellinia necatrix* **effector proteins display selective antimicrobial activity against plant-associated bacteria.** (A) Red lines show bacterial growth in presence of FUN_011519 (10 µM) while blue lines show bacterial growth in water. For *Bacillus drentensis* additional orange line shows bacterial growth in protein filtered with spin-column with 10 kDa cut off, green line shows bacterial growth in protein filtered with spin-column with 3 kDa cut off, and yellow line shows growth in heat-inactivated protein. (B) Red lines show bacterial growth in presence of FUN_004580 (6 µM) while blue lines show bacterial growth in water. For *Flavobacterium hauense* additional orange line shows bacterial growth in protein filtered with spin-column with 10 kDa cut off, green line shows bacterial growth in protein filtered with spin-column with 3 kDa cut off, and yellow line shows growth in heat-inactivated protein. Error bars display standard deviations (n=3). Growth of *Exiguobacterium artemiae* is not inhibited by either protein and is shown as a representative of non-inhibited bacterial taxa.

Several plant-associated bacteria display antagonistic activity

One obvious reason for a fungus to target particular microbes with antimicrobials is that these may be detrimental to fungal growth due to the display of antagonistic activities. To test for such activities directed against *R. necatrix*, we conducted confrontation assays *in vitro*, where we grew *R. necatrix* near the individual bacteria species from the diversity panel of 37 bacteria (Supplemental Table 4). In these assays, we observed antagonistic effects of several bacterial species on *R. necatrix* (Figure 10). Interestingly, several of the

bacterial species inhibited by either of the two effector proteins displayed antagonistic activity against *R. necatrix*, including *Bacillus drentensis*, *Bacillus licheniformis*, and *Sphingobium mellinum* (inhibited by FUN_011519), and *Cellulosimicrobium cellulans*, *Chryseobacterium wanjuense* and *Pseudoxanthomonas suwonensis* (inhibited by protein FUN_004580) (Figure 10). However, also some other bacterial species that were not found to be inhibited by either of the two effector proteins displayed antagonistic activity, namely *Kaistia adipata*, *Pedobacter steynii*, *Pedobacter panaciterrae*, *Pseudomonas corrugata*, *Pseudomonas knackmusii*, *Solibacillus isronensis* and *Solibacillus silvestris.* These findings suggest that a diversity of plant-associated bacteria possess inherent antagonistic activity against *R. necatrix* and that some of these bacteria are targeted by effector proteins of *R. necatrix*.

Particular antagonists alleviate Rosellinia disease in cotton

To test whether any of the bacterial species that are inhibited by the *R. necatrix* effector proteins and that display antagonistic activity against the fungus can inhibit disease development, we pursued inoculation assays in the presence and absence of these bacteria. As *R. necatrix* is a broad host range pathogen, we performed infection assays on cotton plants. To this end, 14-day-old cotton cv. XLZ seedlings were inoculated with *R. necatrix* strain R18, leading to clear disease symptoms by two weeks after inoculation (Fig. 11). Next, we pre-treated cotton cv. XLZ seeds with antagonistic bacteria *Bacillus drentensis*, *Sphingobium mellinum*, *Cellulosimicrobium cellulans*, or *Pseudoxanthomonas suwonensis*. To show that the inhibition of disease development by the antagonistic bacteria is not caused by the activation of MAMP-triggered host immunity we included pre-treatment with the non-antagonistic bacteria *Exiguobacterium artemiae*, *Candidomonas bauzanensis*, *Flavobacterium hauense*, *Achromobacter denitrificans*, or soil. Furthermore, a mix of all bacteria including the antagonistic and non-antagonistic bacteria species was included as well as water as a control, followed by *R. necatrix* inoculation. Interestingly, two weeks after inoculation it could be observed that pretreatment with each of the antagonistic bacteria resulted in reduced susceptibility of the cotton plants to *R. necatrix* when compared with the plants that did not receive a bacterial pre-treatment. Because treatment with the non-antagonistic bacterial species or soil suspension did not lead to reduced disease symptoms, we infer that the reduced disease development upon treatment with then antagonistic bacteria is unlikely to be caused by the activation of MAMP-triggered host immunity, but rather likely through direct antagonism towards the fungal pathogen. Finally, none of the bacteria affected growth of the cotton plants in absence of pathogen inoculation (Fig. 11).

Rosellinia necatrix R18

Bacillus drentensis

Bacillus licheniformis

Achromobacter denitrificans

Sphingobium mellinum

Chryseobacterium wanjuense

Flavobacterium hauense

Pseudoxanthomonas suwonensis

Cellulosimicrobium cellulans

Candidimonas bauzanensis

Kaistia adipata

Pedobacter steynii

Pedobacter panaciterrae

Pseudomonas corrugata

Pseudomonas knackmusii

Solibacillus isronensis

Solibacillus silvestris
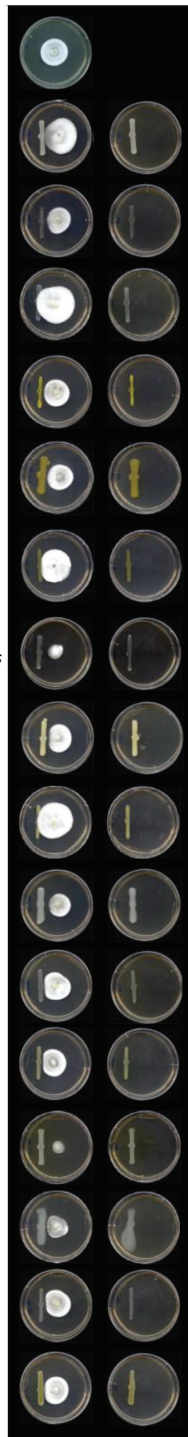
Figure 10. Various plant-associated bacteria display antagonistic activity against *Rosellinia necatrix*. Fungal PDA disks were placed in the center of a petri dish and next to it individual bacteria species were deposited in a straight line with help of a spreader (n=5), bacteria species were placed alone (right column) as controls.

4
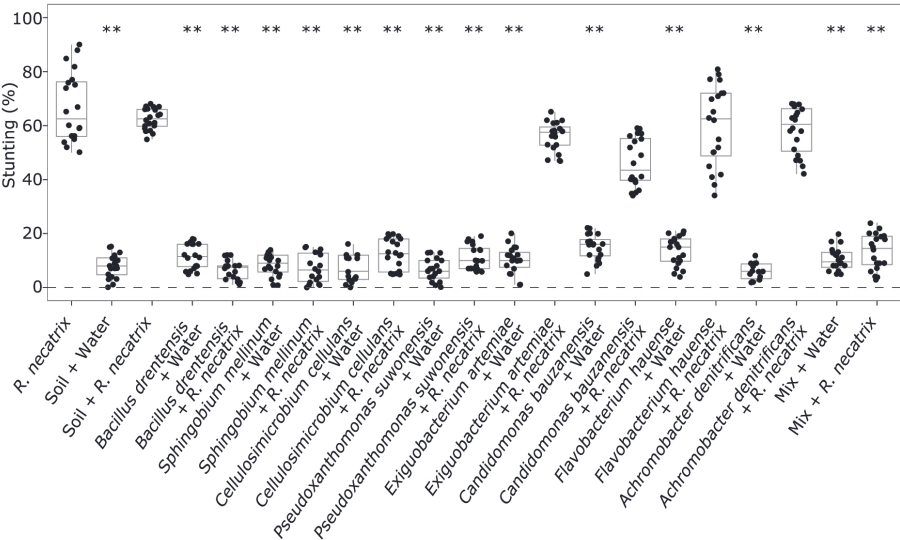
Figure 11. Antagonistic plant-associated bacteria reduce white root rot disease in cotton. (A) Top and side pictures of cotton plants. Cotton seeds were soaked in a suspension of the antagonistic bacteria *Bacillus drentensis*, *Sphingobium mellinum*, *Cellulosimicrobium cellulans*, or *Pseudoxanthomonas suwonensis*, and the non-antagonistic bacteria *Exiguobacterium artemiae*, *Candidomonas bauzanensis*, *Flavobacterium hauense*, or *Achromobacter denitrificans*, a mix of all bacteria, soil suspension, or water as a control. Subsequently, germlings (n=10) were inoculated with *R. necatrix* strain R18 or mock-inoculated. (B) Quantification of stunting. Asterisks indicate significant differences between *R. necatrix*-inoculated plants and plant seeds treated with bacteria (ANOVA followed by Fisher's LSD test (P<0.01)). The experiment was performed twice.

DISCUSSION

Increasing evidence supports the notion that plants can recruit microbes into their microbiota that can help them to withstand pathogen infection (Wang et al., 2012; Pérez-Jaramillo et al., 2016; Zhalnina et al., 2018; Chai and Schachtman, 2022). Based on this notion, it has been hypothesized that pathogens have evolved to counter-act the recruitment of beneficial microbes to promote host colonization (Snelders et al., 2018). In support of this hypothesis, it has been shown that the soil-borne fungal pathogen *Verticillium dahliae* secretes a suite of effector molecules with selective antimicrobial activities to suppress antagonistic microbes in host microbiota to support host ingress (Snelders et al. 2020; 2021; 2022). Although it has been hypothesized that other fungal pathogens are likely to have evolved to modulate host microbiota as well (Snelders et al. 2020; Snelders et al. 2022), evidence for this hypothesis has been lacking thus far. In this study, we show that the soil-borne pathogen *Rosellinia necatrix* similarly expresses predicted secreted effector proteins during host colonization with selective antimicrobial activity. Specifically, we show that two genes encoding the effector proteins, FUN_004580 and FUN_011519, are expressed during host colonization and these predicted secreted effectors display selective antimicrobial activity *in vitro* towards specific plant-associated bacteria and fungi. Intriguingly, some of the bacterial species that are inhibited by the antimicrobial effector proteins display antagonistic activity towards *R. necatrix in vitro*. Moreover, when applied to cotton seeds, several of the antagonistic bacterial species reduce white root rot disease. Collectively, our findings suggest that *R. necatrix* secretes antimicrobial effector proteins during host colonization to modulate host microbiota and support disease development.

The effector proteins FUN_004580 and FUN_011519 were found based on structural homology to AFP1 from the bacterium *Streptomyces tendae* and homology to AcAMP2 from the plant *Amaranthus caudatus*, respectively. AFP1 has been described as a non-enzymatic chitin-binding antifungal directed against particular Ascomycete fungi (Bormann et al., 1999), and recent studies have shown that a homolog of AFP1 isolated from the plant *Carum carvi* (Cc-AFP1) alters fungal cell membrane permeability (Sadat et al., 2021). AcAMP2 was identified based on homology to cysteine/glycine-rich domain of plant chitin-binding proteins and showed antifungal activity, as well as activity against Gram-positive bacteria (Broekaert et al., 1992). The antimicrobial mechanism described for the structural homologs suggest that FUN_004580 and FUN_011519 could potentially be involved in cell membrane disruption, but further functional studies that also include antifungal activity assays are required to investigate this.

The effector proteins FUN_004580 and FUN_011519 showed selective antimicrobial activity against plant-associated bacterial and fungal species *in vitro* and display divergent activity spectra, suggesting that they possess additive activities.

Similar observations have been made for the antimicrobial effector proteins VdAMP2 and VdAve1 of *V. dahliae* that add to each other's activity spectra during soil colonization (Snelders et al., 2020). Divergent activity spectra have been also observed in the *in planta*-expressed effectors VdAve1, VdAve1L2 and VdAMP3 (Snelders et al., 2020; 2022). Furthermore, differential expression of antimicrobial effectors on different plant hosts was observed in *R. necatrix*. Out of the 26 AMP candidates, nine are expressed during avocado colonization, and five of them were also expressed during cotton colonization. From these, *FUN_004580* and *FUN_011519* are expressed during avocado colonization, while only *FUN_004580* is expressed on cotton (Fig. 4). The expression profiles on different host plants suggest differential expression of antimicrobials in *R. necatrix*, potentially due to differential microbiota compositions of these plant hosts. Possibly, FUN_011519 evolved to target microbes that are specifically associated with avocado, or absent from the microbiota of cotton plants.

Various studies have shown that plants shape their microbiota composition (Berendsen et al., 2012). For example, one single gene responsible for the production of glucosinolate significantly altered the microbial community on the roots of transgenic *Arabidopsis* (Bressan, 2009). Moreover, the ATP-binding cassette (ABC) transporter *abcg30* mutant of *Arabidopsis thaliana* secretes root exudates that are enriched in phenolic compounds and contain fewer sugars, resulting in distinct root microbiota compositions (Badri and Vivanco, 2009). Furthermore, *A. thaliana* genes responsible for defense, kinase-related activities, and cell wall integrity impact the microbiota composition (Beilsmith et al., 2019). Besides *A. thaliana*, different potato and tomato plants assemble different microbiota compositions (Weinert et al., 2011; Cordovez et al., 2021).

Like *V. dahliae*, *R. necatrix* is a soil-borne pathogen that resides for part of its life cycle in the microbe-rich soil where inter-microbial competition for limited nutrients is ferocious. Although *R. necatrix* is phylogenetically related to *V. dahliae*, both belonging to the class of Sordariomycetes, our findings suggest that exploitation of antimicrobial effector proteins among soil-borne fungi may be commonplace. However, whether the employment of such effector proteins is relevant for soil-borne pathogens only, or shared by other types of plant pathogens too, presently remains enigmatic (Snelders et al., 2022).

To understand the diversity and functional properties of effectors, we investigated their 3D protein structure. The results of this study demonstrate that there is relatively little structural clustering among *R. necatrix* effectors. The five largest clusters identified were mainly driven by sequence conservation rather than structural similarity, suggesting that effector family expansion based on structural similarity played only a minor role in *R. necatrix* effector evolution. Effector protein structure clustering has revealed that

many plant pathogen effectors fall into distinct structural families. For example, MAX (de Guillen et al., 2015), and RNase-Like proteins associated with haustoria (RALPH) (Spanu, 2017) are effector families with structural similarity. Common themes are emerging like structural homology and in some cases similar modes of action (Lu et al., 2015). While structural conservation has been observed in some pathogenic fungi (de Guillen et al., 2015; Spanu, 2017), sequence conservation is the main driver of structural clustering among *R. necatrix* effectors. Future studies could explore the functional significance of the identified effector clusters in *R. necatrix* and other plant pathogens and investigate the mechanisms underlying the evolution of effector proteins.

4

MATERIALS AND METHODS

Nanopore sequencing and genome assembly

High-molecular weight (HMW) DNA was extracted from nine *R. necatrix* strains (Table 1) as described by Chavarro-Carrero et al. (2021), except that mycelium was grown in 1/5 PDB instead of Czapek Dox medium. DNA quality, size and quantity were assessed with Nanodrop, Qubit analyses, and with gel electrophoresis. Library preparation with the Rapid Sequencing Kit (SQK-RAD004) was performed with ~400 ng HMW DNA according to the manufacturer's instructions (Oxford Nanopore Technologies, Oxford, UK). An R9.4.1 flow cell (Oxford Nanopore Technologies, Oxford, UK) was loaded and ran for 24 h, and subsequent base calling was performed using Guppy (version 3.1.3; Oxford Nanopore Technologies, Oxford, UK). Adapter sequences were removed using Porechop (version 0.2.4 with default settings; Wick, 2018) and the reads were self-corrected, trimmed and assembled using Canu (version 1.8; Koren et al., 2017).

To obtain longer reads ultra-high-molecular weight (UHMW) DNA extraction was performed. To this end, after DNA precipitation, the Nanobind Big DNA Kit (SKU NB-900-801-01, Circulomics, USA) was used following the manufacturer's protocol to select DNA fragments >50 kb. Simultaneously, to allow error correction of the ONT reads, paired-end short read (150 bp) sequencing was performed at the Beijing Genome Institute (BGI) using the DNBseq platform. After error correction using FMLRC (version 1.0.0 with default settings; Wang et al., 2018), ONT reads were trimmed and assembled using Canu.

Hi-C was performed based on the Proximo Hi-C kit (Microbe) (Phase Genomics, Seattle, WA, USA) according to the manufacturer's protocol as previously described (Seidl et al., 2020), and the Hi-C library was paired-end (150 bp) sequenced on the NextSeq500 platform at USEQ (Utrecht, the Netherlands). Subsequently, Hi-C reads were mapped to the Canu assembly using Juicer (version 1.6 with early-stage setting; Durand et al., 2016), and the three-dimensional (3D) *de novo* assembly (3D-DNA) pipeline (version 180922 with contig size threshold 1000; Dudchenko et al., 2017) was used. The genome assembly was further manually improved using Juicebox Assembly Tools (JBAT) (version 1.11.08; Dudchenko et al., 2018) and the 3D-DNA post review asm pipeline (Dudchenko et al., 2017). Tapestry (version 1.0.0 with default settings; (Davey et al., 2020) was used to visualize chromosomes and telomeric regions with telomeric sequence ([TTAGGG]*n*).

Phylogenetic tree construction and structural variant calling

A phylogenetic tree of all sequenced strains was constructed with Realphy (version 1.12) (Bertels et al., 2014). Briefly, genomic reads were mapped against the genome of strain

R18 using Bowtie2 (version 2.2.6) (Langmead and Salzberg, 2012) and a maximum-likelihood phylogenetic tree was inferred using RAxML (version 8.2.8) (Stamatakis, 2014), using the genome sequence of *Rosellinia corticium* to root the tree. Subsequently, to predict SVs, we used NanoSV (version 1.2.4 with default settings; Stancu et al., 2017) for each of the genomes when compared to R18 strain as reference. The output of each strain was initially filtered with bcftools v.1.3.2 using GT=AA, QUAL>50, GQ>10, SUPPORT>20 (Danecek et al., 2021). The results were merged using SURVIVOR v.1.0.6 (Jeffares et al., 2017), allowing 1,000 bp as the maximum distance for breakpoints and considering only same SV types. Only SVs with minimum size >100 bp and maximum size of 100 kb were kept. Permutation tests were computed using R/Bioconductor region v.1.8.1 package (Gel et al., 2016), and 10,000 iterations were performed using the mean distance to evaluate the closest relationship (bp distance) between SV-breakpoints, TEs and effectors, and circular randomization as well to maintain the order and distance of the regions on the chromosomes.

Genome mining

Genome annotation was performed using Funannotate (Version 1.8.13, Palmer and Stajich, 2017) guided by publicly available RNAseq data (Shimizu et al., 2018). Furthermore, secreted genes, effector genes and secondary metabolite gene clusters were predicted using SignalP (Version 5.0, Almagro et al., 2019), EffectorP (Version 2.0, Sperschneider et al., 2018) and antiSMASH (Version 6.0.0, Blin et al., 2019), respectively. The *R. necatrix* R18 genome was mined for gene candidates that encode secreted antimicrobials as described previously (Snelders et al., 2020). Briefly the predicted secretome and effector catalog were mined using Phyre2 (Kelley et al., 2015), followed by manual curation, to search for predicted structural homologues of known antimicrobial proteins. Gene sequences were extracted using Bedtools (setting: getfasta) (Quinlan and Hall, 2010). Subsequently, RNAseq data were used to confirm expression of selected candidates. To this end, RNAseq data was mapped to the R18 assembly and relative expression was calculated using Kallisto (version 0.46.1, default settings, Bray et al., 2016).

Repetitive regions were annotated using EDTA v.1.9.4 (Ou et al., 2019). Briefly, we used the 'sensitive', 'anno' and 'evaluate' options to maximize the transposable element discovery and integrity. Then, the TE library was refined using one code to find them all (Bailly-Bechet et al., 2014), and only full LTRs were kept.

Structural prediction of the *R. necatrix* effector catalog

Structural predictions of effector candidates were done based on mature amino acid sequences, lacking signal peptides, with Alphafold2 (Jumper et al., 2021) using the

4

casp14 preset. Five models were generated for each effector candidate, of which the one with the highest pLDDT score was used for further analysis. To assess structural similarity between effector candidates, an all-vs-all alignment was performed using TM-align (Zhang and Skolnick, 2005). Structures were considered similar when the average TM-score of pairwise reciprocal alignments, calculated on a 0-1 scale, was >0.5. Effector clusters were identified by simple agglomerative hierarchical clustering based on structural similarity using SciPy (Virtanen et al., 2020) and a minimum similarity threshold of 0.5. For the five largest clusters the average sequence identity was calculated from a multiple sequence alignment performed with MAFFT on EMBL-EBI (Katoh and Standley, 2013). Cluster annotation was performed by generating PANNZER (Törönen and Holm, 2022) annotation for each protein followed by manual curation of a consensus annotation for each cluster. Protein structures were generated with PyMOL (The PyMOL Molecular Graphics System, Version 2.0 Schrödinger, LLC, DeLano Scientific, Palo Alto, CA, USA).

Real-time PCR

To determine expression profiles of candidate genes that encode secreted antimicrobials during *R. necatrix* infection of cotton, two-week-old cotton (cv. XLZ) seedlings were inoculated, as previously described (Cazorla et al., 2006), with *R. necatrix* strain R18, and stems were harvested up to 21 dpi. Furthermore, mycelium was harvested from ten-day-old *R. necatrix* strain R18 cultures on potato dextrose agar (PDA) plates. Total RNA extraction and cDNA synthesis were performed as previously described (Santhanam et al., 2013). Real time-PCR was performed with primers listed in Supplemental Table 5, using the *R. necatrix* glyceraldehyde-3-phosphate dehydrogenase gene (GAPDH; FUN_007054) as endogenous control. The PCR cycling conditions consisted of an initial 95°C denaturation step for 10 min followed by denaturation for 15 s at 95°C, annealing for 30 s at 60°C, and extension at 72°C for 40 cycles.

Heterologous protein production

The sequences encoding mature proteins were cloned into vector pET-15b with an N-terminal His6 tag sequence (Novagen, Darmstadt, Germany) (primer sequences, see Supplemental Table 5). The resulting expression vectors were verified by sequencing and used to transform *Escherichia coli* strain BL21. For heterologous protein production, BL21 cells were grown in 2× yeast extract tryptone (YT) medium at 37°C with continuous shaking at 200 rpm until the cultures reached an optical density measurement at 600 nm (OD600) of 2. Protein production was induced with 1 mM isopropyl β-D-1-thiogalactopyranoside (IPTG) at 42°C and shaking at 200 rpm for 2 h. Bacterial cells were pelleted and washed with 50mM Tris HCl and 10% glycerol at pH 8.0. To disrupt

cells, they were sonicated three times according to a cycle composed of one second sonication, followed by 0.5 seconds on ice and a one-minute pause. Next, the samples were centrifuged at 16,000g for 10 min. The insoluble pellets were resuspended in 30 mL of 6 M guanidine hydrochloride (GnHCl), 10 mM Tris at pH 8.0 and 10 mM β-mercaptoethanol and incubated overnight at room temperature. Next, debris was pelleted by centrifuging at 16,000g for 10 min and the resulting protein solution was transferred to a new tube and filtered step-wise from 1.2 to 0.45 μm. Proteins were subsequently purified under denaturing conditions by metal affinity chromatography using a pre-packed HisTrap FF column (Cytiva, Medemblik, The Netherlands) and dialysed (Spectra/Por 3 Dialysis Membrane, molecular weight cut off of 10 kDa; Spectrum Laboratories, Rancho Dominguez, U.S.A) against 20 volumes of 0.01 M BisTris, 10 mM reduced glutathione and 2 mM oxidized glutathione at pH 8.0 with decreasing GnHCl concentrations in five consecutive steps of minimum 24 h from 5 M to 1 M for refolding. Finally, proteins were dialysed against demineralized water for 24 h and final concentrations were determined using Qubit (ThermoFisher Scientific, Waltham, U.S.A).

Culture filtrate production

R. necatrix strain R18 was grown in potato dextrose broth (PDB) at 21°C and 130 rpm. Cultures were collected at 4, 7 and 9 days after the start of incubation and mycelium was separated from the culture medium using a 0.45 nm filter. Half of the culture-filtrate was heat-inactivated at 96°C for 10 minutes. Finally, culture filtrates were stored at -20°C until use.

***In vitro* antimicrobial activity assays**

Growth assays were performed as previously described (Snelders et al., 2020). Briefly, bacterial strains were grown overnight on lysogeny broth agar (LBA), tryptone soya agar (TSA) or R2A agar at 28°C (Supplemental Table 4). Subsequently, single colonies were selected and grown overnight at 28°C while shaking at 130 rpm in low-salt Luria broth (LB) (NaCl, 0.5 g/L; Tryptone, 10 g/L; Yeast Extract, 5 g/L). Overnight cultures were resuspended to OD600=0.05 in low-salt LB and 100 μL were supplemented with 100 μL of purified effector proteins or culture filtrates to a final OD600=0.025 in clear 96 well flat-bottom polystyrene tissue culture plates (Greiner CELLSTAR, Sigma, Burlington, U.S.A). Culture plates were incubated in a CLARIOstar plate reader (BMG LABTECH, Ortenberg, Germany) at 25°C with double orbital shaking every 15 minutes and OD600 was measured every 15 minutes.

Filamentous fungal isolates were grown on PDA at 22°C, while for yeasts, single colonies were selected and grown overnight in 5% PDB at 28°C while shaking at 200 rpm. For yeasts overnight cultures were resuspended to OD600=0.01 in fresh 5% PDB

supplemented with water, 10 µM FUN_011519 or 6 µM FUN_004580. For filamentous fungi, spores were harvested from PDA and suspended in 5% PDB supplemented with 10 µM FUN_011519, 6 µM FUN_004580 or water to a final concentration of 104 spores/mL. Next, 200 µL of the fungal suspensions was aliquoted in clear 96-well flat bottom polystyrene tissue-culture plates (Greiner CELLSTAR, Sigma, Burlington, U.S.A). Plates were incubated at 28°C, and fungal growth was imaged using an SZX10 stereo microscope (Olympus, Tokyo, Japan) with EP50 camera (Olympus, Tokyo, Japan).

Microbial confrontation assays

R. necatrix was grown on PDA for 14 days and mycelium disks of 5 mm diameter were taken using a biopsy puncher (Kai Europe, Solingen, Germany). Single *R. necatrix* disks were placed in the center of a PDA plate and 100 µL (OD600=0.05) of bacterial culture (Supplemental Table 4), grown overnight in LB medium at 28°C at 130 rpm, was added in proximity of the fungal disk with a spreader (n=5). After seven days, pictures were taken. Experiment was repeated three times.

Biocontrol assay

Bacillus drentensis, *Sphingobium mellinum*, *Cellulosimicrobium cellulans* and *Pseudoxanthomonas suwonensis* were grown overnight at 28°C in low-salt LB while shaking at 130 rpm. Subsequently, the bacterial suspension was pelleted, washed, and resuspended to OD600=0.05 in water. Seeds of cotton cv. XLZ were surface-sterilized with 2% sodium hypochlorite for ten minutes, washed three times with sterile water, and then soaked for ten minutes the bacterial suspension. Next, the seeds were transferred to sterile Petri dishes containing filter paper moistened with each of the bacterial suspension and incubated in darkness at room temperature. Once the seeds germinated, germlings were transferred to potting soil in the greenhouse (16 hours light at 24°C and 8 hours darkness at 22°C). Seven days after transfer to potting soil, the seedlings were inoculated with mycelium of a 14-day-old *R. necatrix* culture in PDB. To this end, the mycelium was pelleted, washed, and resuspended in 250 mL water. This mycelial suspension was subsequently used for root-dip inoculation of the cotton seedlings for 10 min, after which they were re-planted and 10 mL of mycelium suspension was poured onto the pot in close proximity to the stem. At 14 days post inoculation (dpi) disease symptoms were recorded. Experiment was repeated three times.

Data availability

Genomes and genome annotation data have been submitted to NCBI under BioProject PRJNA727191.

Acknowledgements

4

4

SUPPLEMENTAL TABLES AND FIGURES

Supplemental Table 1. Annotation of predicted effector proteins of *R. necatrix* strain R18.

Query ID	Accession ID[a]	Annotation[b]	Organism[c]	Query coverage	E value	Identity (%)[d]
Cell wall degrading enzymes						
FUN_005758	XM_047973256.1	1,4-β-xylosidase	*Xylaria bambusicola*	100%	2E-140	77.49%
FUN_004100	XM_047973055.1	1,4-β-xylosidase	*Xylaria bambusicola*	99%	1E-123	85.37%
FUN_007661	XM_047977209.1	1,4-β-xylosidase	*Xylaria bambusicola*	99%	4E-129	85.85%
FUN_007704	XM_047978660.1	Acetylxylan esterase A	*Xylaria bambusicola*	90%	0	91.73%
FUN_003106	XM_047976713.1	Carbohydrate esterase family 4	*Xylaria bambusicola*	100%	0	78.52%
FUN_001755	XM_047979347.1	Carbohydrate esterase family 4	*Xylaria bambusicola*	100%	4E-162	89.27%
FUN_010853	XM_047976371.1	Cellulose monooxygenase	*Xylaria bambusicola*	100%	4E-131	87.32%
FUN_008445	XM_047977156.1	Cellulose monooxygenase	*Xylaria bambusicola*	100%	5E-153	87.39%
FUN_001148	XM_046148909.1	Cutinase	*Microdochium trichocladiopsis*	100%	8E-75	54.39%
FUN_001573	XM_047972062.1	Cutinase-like protein	*Xylaria bambusicola*	91%	2E-97	81.18%
FUN_005500	XM_047972798.1	Glycoside hydrolase family 10	*Xylaria bambusicola*	98%	0	82.68%
FUN_000721	XM_047979386.1	Glycoside hydrolase family 12	*Xylaria bambusicola*	98%	2E-120	73.27%
FUN_002439	XM_047969089.1	Glycoside hydrolase family 16	*Xylaria bambusicola*	100%	1E-150	88.26%
FUN_002410	XM_048004698.1	Glycoside hydrolase family 16	*Daldinia vernicosa*	100%	2E-110	58.33%
FUN_010054	XM_047977697.1	Glycoside hydrolase family 17	*Xylaria bambusicola*	98%	0	85.76%
FUN_008369	XM_047932653.1	Glycoside hydrolase family 43	*Daldinia caldariorum*	100%	0	79.27%
FUN_000284	XM_047979212.1	Glycoside hydrolase family 43	*Xylaria bambusicola*	100%	0	79.88%
FUN_008666	XM_047975058.1	Glycoside hydrolase family 43	*Xylaria bambusicola*	100%	0	82.72%
FUN_010499	XM_047978711.1	Glycoside hydrolase family 45	*Xylaria bambusicola*	99%	2E-133	85.24%
FUN_007581	XM_047971870.1	Glycoside hydrolase family 5	*Xylaria bambusicola*	99%	0	84.94%
FUN_004897	XM_047976082.1	Lytic polysaccharide monooxygenase	*Xylaria bambusicola*	100%	3E-126	84.11%
FUN_007011	XM_022614464.1	Mutanase	*Colletotrichum orchidophilum*	98%	3E-48	70.00%

FUN_008395	XM_047972336.1	O-acetylxylan esterase	*Xylaria bambusicola*	100%	3E-141	89.33%
FUN_007837	XM_040856674.1	Pectate lyase	*Pseudomassariella vexata*	100%	6E-129	84.11%
FUN_004715	XM_047972211.1	Polysaccharide lyase	*Xylaria bambusicola*	100%	4E-154	87.71%
FUN_001279	XM_047975706.1	Polysaccharide lyase family 7 protein	*Xylaria bambusicola*	100%	4E-133	82.38%
FUN_009124	XM_047969579.1	Putative endo-1,3(4)-beta-glucanase	*Xylaria bambusicola*	99%	2E-142	78.03%
FUN_010529	XM_047974852.1	Xylanase	*Xylaria bambusicola*	100%	7E-129	91.41%
FUN_009151	XM_047976406.1	Lysozyme-like domain-containing protein	*Xylaria bambusicola*	99%	1E-95	83.73%
FUN_003275	XM_018318865.1	Muramidase	*Purpureocillium lilacinum*	92%	2E-97	64.29%
FUN_005762	XM_047972660.1	Putative muramidase	*Xylaria bambusicola*	99%	1E-102	71.16%
FUN_001575	XM_047978226.1	Chloroperoxidase	*Xylaria bambusicola*	99%	2E-133	76.17%
Carbohydrate binding						
FUN_003047	XM_047979309.1	Concanavalin A-like lectin	*Xylaria bambusicola*	99%	1E-176	81.06%
FUN_003763	XM_047969123.1	WSC domain-containing protein	*Xylaria bambusicola*	88%	3E-121	77.39%
FUN_000265	XM_047976926.1	WSC domain-containing protein	*Xylaria bambusicola*	100%	0	79.34%
Lysin motif (LysM) effectors						
FUN_000206	XM_001268710.1	LysM domain-containing protein	*Aspergillus clavatus*	83%	4E-08	38.46%
FUN_006904	XM_001268710.1	LysM domain-containing protein	*Aspesgillus clavatus*	98%	8E-25	37.84%
Hydrophobins						
FUN_007007	XM_040863415.1	Cerato-ulmin family protein	*Pseudomassariella vexata*	81%	1E-32	76.71%
FUN_000192	XM_047977015.1	Cerato-ulmin family protein	*Xylaria bambusicola*	95%	5E-40	82.28%
FUN_001605	XM_047978428.1	Hydrophobin	*Xylaria bambusicola*	100%	1E-31	57.55%
FUN_011531	XM_047976151.1	Hydrophobin-like protein	*Xylaria bambusicola*	84%	6E-40	90.14%
Proteases						
FUN_001370	XM_047978948.1	Acid protease	*Xylaria bambusicola*	100%	7E-106	65.82%
FUN_004271	XM_036641540.1	Neutral protease 2-like protein	*Colletotrichum siamense*	99%	1E-114	51.81%
FUN_000625	XM_033580201.1	Papain inhibitor	*Daldinia childiae*	97%	2E-36	65.12%

4

4

	Accession ID[a]	Annotation[b]	Organism[c]		E-value	Identity[d]
Toxins						
FUN_002843	XM_047969234.1	Necrosis inducing protein-domain-containing protein	*Xylaria bambusicola*	100%	6E-147	82.45%
FUN_005483	XM_046238898.1	Necrosis inducing protein-domain-containing protein	*Ilyonectria robusta*	92%	3E-82	54.20%
FUN_010366	XM_047972065.1	Cerato-platanin family protein	*Xylaria bambusicola*	100%	2E-64	80.83%
Others						
FUN_000283	XM_047980145.1	Deoxyribonuclease NucA/NucB	*Xylaria bambusicola*	99%	1E-124	81.73%
FUN_003451	XM_047976696.1	Guanine-specific ribonuclease N1	*Xylaria bambusicola*	100%	3E-61	79.82%
FUN_009264	XM_047973582.1	emp24/gp25L/p24 family/GOLD-domain-containing protein	*Xylaria bambusicola*	100%	9E-108	75.37%
FUN_009552	XM_047973428.1	emp24/gp25L/p24 family/GOLD-domain-containing protein	*Xylaria bambusicola*	100%	4E-127	88.61%
FUN_005699	XM_047975004.1	emp24/gp25L/p24 family/GOLD-domain-containing protein	*Xylaria bambusicola*	100%	4E-123	90.96%
FUN_001432	XM_047970391.1	2OG-Fe(II) oxygenase superfamily protein	*Xylaria bambusicola*	100%	5E-133	75.95%
FUN_011359	XM_048011353.1	FMN-dependent alpha-hydroxy acid dehydrogenase	*Daldinia vernicosa*	95%	2E-69	74.10%
FUN_011399	KY782142.1	Heme-thiolate peroxidase	*Ustulina deusta*	99%	1E-124	73.33%
FUN_001799	XM_047970313.1	Intradiol ring-cleavage dioxygenase	*Xylaria bambusicola*	100%	0	74.93%
FUN_009516	XM_049306200.1	Putative choline dehydrogenase	*Daldinia loculata*	87%	3E-28	63.10%
FUN_004320	XM_047974920.1	ERV/ALR sulfhydryl oxidase	*Xylaria bambusicola*	91%	1E-87	79.49%
FUN_002834	XM_047975475.1	Acyl transferase	*Xylaria bambusicola*	76%	1E-93	78.57%
FUN_006056	XM_047978164.1	Apc13p ubiquitin ligase	*Xylaria bambusicola*	87%	4E-59	65.41%
FUN_005907	XM_047975260.1	Cyanovirin-N	*Xylaria bambusicola*	93%	1E-57	66.94%
FUN_006163	XM_046160209.1	Cyclophilin-like protein	*Microdochium trichocladiopsis*	100%	1E-102	81.67%
Unknown						
FUN_010039	XM_033580564.1	Bys1 domain-containing protein	*Daldinia childiae*	100%	5E-79	82.09%
FUN_005325	XM_047969535.1	Met-10+ like-protein-domain-containing protein	*Xylaria bambusicola*	100%	1E-95	70.79%

[a]Database accession ID where subject was deposited.
[b]Annotation of the best hit using BLAST (tblastn).
[c]Organism where the homolog was annotated.
[d]Percentage of identity of the query.

Supplemental Table 2. Single nucleotide polymorphism ratios (SNPs in %) and presence-absence variation for predicted effector genes in the *R. necatrix* strains sequenced in this study using *R. necatrix* strain R18 as a reference.

Effector in *R. necatrix* strain R18 (gene ID)	Homologs in other *R. necatrix* strains*							
	Rn19	CH12	Rn400	R10	R25	R27	R28	R30
FUN_000053	3.29	3.29	4.15	0.00	0.17	0.00	0.00	0.17
FUN_000192	3.63	3.29	3.29	0.00	0.17	0.00	0.00	0.17
FUN_000206	3.98	3.81	3.81	0.17	0.17	0.17	0.00	0.17
FUN_000251	3.98	3.98	3.98	0.00	0.35	0.87	0.87	0.35
FUN_000265	8.82	8.65	8.82	0.00	1.04	1.21	1.21	1.04
FUN_000283	6.06	6.06	5.36	A	1.56	1.56	1.38	1.56
FUN_000284	7.61	7.61	8.13	0.35	1.04	1.56	1.56	1.04
FUN_000359	3.46	4.50	3.11	0.00	1.90	1.56	1.56	1.56
FUN_000367	2.25	2.25	2.25	0.00	0.17	0.00	0.00	0.17
FUN_000625	2.60	2.60	2.60	0.00	0.69	0.00	0.00	0.69
FUN_000721	3.81	3.81	1.21	0.00	1.04	0.00	0.17	1.04
FUN_000856	2.42	2.60	2.60	0.17	0.87	0.35	0.35	1.04
FUN_000873	2.77	2.77	2.77	0.00	0.87	0.87	0.87	0.87
FUN_000886	4.33	7.09	4.33	0.00	1.38	1.21	1.21	1.56
FUN_000960	7.61	7.61	8.65	0.52	2.08	1.73	1.38	1.90
FUN_001031	2.42	3.29	2.42	0.17	0.69	2.94	3.29	0.69
FUN_001148	3.29	3.29	3.29	0.00	1.21	0.52	0.52	1.04
FUN_001231	2.25	2.25	2.42	0.00	0.17	0.00	0.00	0.17
FUN_001279	6.75	6.75	6.75	0.00	1.73	1.73	0.87	1.73
FUN_001370	8.13	7.61	7.96	0.00	2.08	2.08	0.87	2.08
FUN_001432	5.54	5.19	5.19	0.00	1.38	1.90	0.87	1.38
FUN_001497	2.42	2.60	2.77	0.00	0.00	0.35	0.69	0.00
FUN_001504	3.29	3.11	3.29	0.00	0.00	0.00	0.00	0.00
FUN_001515	2.08	2.08	2.08	0.00	0.69	0.00	0.00	0.87
FUN_001527	5.88	6.23	5.88	3.98	1.38	6.06	0.00	6.23
FUN_001573	4.50	4.50	4.50	0.00	A	0.00	0.00	0.69
FUN_001575	6.06	5.88	5.88	0.00	1.38	0.00	0.00	1.38
FUN_001585	4.67	4.84	3.98	0.00	0.87	0.17	0.00	0.69
FUN_001595	2.08	2.25	2.25	0.52	0.52	0.00	0.00	0.52
FUN_001605	9.86	9.86	9.86	0.00	3.11	0.00	0.00	2.94
FUN_001636	2.94	2.94	2.77	0.00	0.00	0.00	0.00	0.00
FUN_001689	6.57	6.57	6.92	0.17	2.60	0.00	0.00	2.60

4

FUN_001755	9.17	3.46	3.29	0.00	1.04	0.69	0.00	0.87
FUN_001798	9.69	9.52	9.17	0.00	0.00	0.00	0.00	0.00
FUN_001799	1.56	0.52	0.87	0.17	0.17	0.00	0.00	0.00
FUN_001917	2.42	2.42	1.90	0.00	0.52	0.00	0.00	0.52
FUN_002005	4.84	4.67	4.15	0.17	0.35	2.08	2.08	0.35
FUN_002053	1.04	1.04	1.04	0.00	0.17	0.35	0.17	0.35
FUN_002114	3.46	3.29	3.29	0.00	0.87	0.35	0.35	0.87
FUN_002120	4.50	4.50	3.46	0.00	0.87	1.21	1.21	0.87
FUN_002121	4.50	4.50	3.46	0.00	0.00	0.00	1.21	0.00
FUN_002234	3.11	2.60	2.77	0.00	0.35	0.52	0.52	0.35
FUN_002337	8.13	8.13	8.13	8.30	0.52	0.00	0.00	0.52
FUN_002389	0.69	0.69	0.87	0.35	0.52	0.69	0.52	0.52
FUN_002410	5.88	5.88	5.88	0.00	2.08	1.90	1.90	2.08
FUN_002439	11.76	11.76	11.76	0.00	2.77	2.60	0.00	2.77
FUN_002458	2.42	2.42	2.42	0.17	0.35	1.56	0.35	0.35
FUN_002489	4.33	5.02	5.02	0.17	1.56	0.87	1.04	1.56
FUN_002758	1.21	1.38	1.38	0.00	0.17	1.04	1.04	0.17
FUN_002834	3.11	2.94	3.29	0.00	0.69	0.69	0.69	0.69
FUN_002843	5.71	5.71	5.71	0.00	0.52	1.04	1.04	0.52
FUN_003003	1.38	1.38	1.38	0.00	0.17	0.00	0.00	0.17
FUN_003018	1.38	0.69	0.69	0.00	0.00	0.00	0.00	0.00
FUN_003047	4.50	A	4.33	0.00	0.00	0.00	0.00	0.00
FUN_003077	2.77	2.77	3.29	0.00	0.17	0.35	0.35	0.17
FUN_003106	9.52	9.69	9.52	0.00	0.00	0.87	0.87	0.00
FUN_003133	2.77	2.25	1.90	0.52	1.90	0.00	0.52	1.90
FUN_003175	3.81	3.63	3.81	0.35	0.17	0.17	0.17	0.17
FUN_003209	3.63	3.46	3.29	0.00	0.00	0.00	0.00	1.21
FUN_003212	4.67	4.67	4.67	0.00	0.35	0.35	0.35	3.46
FUN_003275	2.94	2.77	2.77	0.00	0.00	0.00	0.00	0.00
FUN_003286	3.46	3.46	3.46	0.00	0.00	0.00	0.00	0.00
FUN_003451	3.63	3.63	3.63	0.00	0.35	0.52	0.52	0.35
FUN_003513	1.38	1.38	1.38	0.00	0.00	0.35	0.35	0.00
FUN_003763	4.67	4.67	4.67	0.35	0.17	0.17	0.00	0.17
FUN_003889	8.13	8.30	8.13	0.00	2.94	0.00	0.00	2.94
FUN_003947	9.17	8.82	8.82	0.00	0.69	0.00	0.00	0.87
FUN_004082	4.15	4.15	4.15	0.17	0.00	0.00	0.00	0.00
FUN_004100	5.54	5.54	5.88	0.00	0.35	0.52	0.52	0.35
FUN_004157	4.67	1.21	6.40	0.52	7.96	7.96	0.00	4.84

FUN_004244	5.36	7.44	4.50	0.00	1.38	0.00	0.00	1.38
FUN_004254	1.73	1.90	1.73	0.35	0.00	0.35	0.00	0.17
FUN_004271	3.63	3.63	3.46	0.00	0.17	0.00	0.00	0.17
FUN_004305	5.71	5.88	5.54	0.17	0.00	0.87	0.69	0.00
FUN_004320	3.46	3.46	3.46	0.00	1.04	1.38	1.38	1.04
FUN_004483	4.15	4.15	4.15	0.00	0.00	1.04	1.04	0.00
FUN_004569	2.42	2.77	2.77	0.00	2.60	2.08	1.90	2.60
FUN_004715	1.90	1.73	1.90	0.00	0.35	0.35	0.35	0.35
FUN_004770	4.15	4.15	4.15	0.00	0.00	0.00	0.00	0.00
FUN_004897	4.67	4.33	4.50	0.17	0.00	0.00	0.00	0.00
FUN_004961	4.15	4.15	4.33	0.00	0.35	0.17	0.00	0.35
FUN_005189	5.36	1.38	5.19	0.00	0.00	0.69	0.87	0.00
FUN_005222	4.84	4.67	4.67	0.00	0.00	0.00	0.00	0.00
FUN_005300	4.67	1.90	5.36	0.00	1.21	1.21	1.21	1.21
FUN_005325	0.87	1.38	1.38	0.00	0.35	1.04	1.04	0.35
FUN_005445	1.56	1.90	1.73	0.00	0.17	0.00	0.00	0.17
FUN_005483	2.77	4.84	5.02	0.69	2.94	2.94	2.08	2.60
FUN_005500	4.67	3.46	6.06	0.69	3.46	1.90	2.08	3.81
FUN_005538	4.33	3.63	3.63	0.17	1.04	1.21	1.21	1.04
FUN_005543	5.54	0.00	5.02	0.00	1.21	0.00	0.00	0.00
FUN_005544	7.27	7.27	7.96	0.00	0.35	0.87	0.87	0.35
FUN_005699	3.46	2.94	2.94	0.00	0.17	0.00	0.00	0.17
FUN_005740	1.21	1.21	1.21	0.00	0.35	0.00	0.00	0.35
FUN_005758	6.75	4.33	4.33	0.17	1.90	4.15	0.17	4.15
FUN_005762	3.29	3.46	3.29	0.00	0.17	0.00	0.17	0.17
FUN_005785	4.50	4.50	4.33	0.00	0.35	0.00	0.00	0.35
FUN_005787	3.63	3.63	3.63	0.00	0.35	0.00	0.00	0.35
FUN_005834	3.11	3.11	3.11	0.00	0.69	0.00	0.00	0.69
FUN_005847	8.30	8.30	8.13	0.00	0.00	0.00	0.00	0.00
FUN_005850	4.15	4.84	3.46	0.00	0.52	0.00	0.00	0.52
FUN_005883	4.33	4.50	4.67	0.00	0.87	0.87	0.87	0.87
FUN_005907	4.33	4.15	4.33	0.00	0.52	0.00	0.00	0.52
FUN_005940	5.19	5.19	4.67	0.00	0.00	2.60	2.60	0.00
FUN_005952	4.84	3.98	4.33	0.00	0.00	0.69	0.69	0.00
FUN_005989	5.88	6.57	6.06	0.00	1.04	0.17	0.17	0.87
FUN_005998	6.06	6.23	5.88	0.00	0.35	0.17	0.00	0.35
FUN_006007	8.13	8.30	7.61	0.00	0.00	2.77	2.77	0.00
FUN_006010	4.15	4.33	3.81	0.00	0.17	0.35	0.35	0.17

FUN_006056	3.63	3.63	3.81	0.00	0.00	0.17	0.00	0.00
FUN_006163	3.98	1.90	4.15	0.00	0.17	1.90	1.90	0.17
FUN_006164	3.98	1.90	A	0.00	0.00	1.73	0.00	0.17
FUN_006190	5.36	5.88	5.71	0.00	6.06	0.69	6.23	0.00
FUN_006412	6.40	4.67	4.67	0.00	1.04	0.52	1.04	1.04
FUN_006481	3.29	2.08	3.29	0.00	0.17	0.52	0.52	0.17
FUN_006483	3.98	4.33	4.67	0.17	0.17	0.52	0.35	0.17
FUN_006775	8.65	8.65	8.65	0.00	0.87	0.35	0.35	0.87
FUN_006835	2.42	2.42	2.77	0.00	1.04	1.56	1.38	1.04
FUN_006841	5.36	4.84	5.36	0.00	0.52	0.87	0.87	0.52
FUN_006904	6.23	6.23	7.09	0.00	0.69	0.00	0.00	0.69
FUN_006905	4.67	4.50	6.06	0.00	0.00	0.17	0.00	0.00
FUN_007007	5.88	5.88	7.27	0.00	1.38	0.00	0.00	1.38
FUN_007011	2.42	2.60	1.73	0.00	0.17	0.00	0.00	0.17
FUN_007012	6.06	5.71	6.23	0.00	0.35	0.00	0.00	0.35
FUN_007129	4.84	5.36	5.36	0.00	0.52	0.00	0.00	0.52
FUN_007254	4.33	4.33	4.50	0.00	0.87	1.04	1.04	0.87
FUN_007288	8.13	7.27	8.13	0.00	1.38	0.87	0.87	1.38
FUN_007567	2.77	2.94	2.60	0.00	0.00	0.17	0.17	0.00
FUN_007581	7.44	7.27	6.92	0.00	0.35	0.52	0.52	0.35
FUN_007661	4.67	3.98	4.15	0.00	0.69	0.87	0.87	0.69
FUN_007684	6.75	7.27	6.57	0.00	0.00	1.38	1.38	0.17
FUN_007704	6.23	6.40	5.71	0.00	0.00	0.52	0.69	0.00
FUN_007825	2.42	2.42	2.42	0.00	0.00	1.56	1.56	0.00
FUN_007837	4.84	1.73	5.02	0.17	0.69	1.04	1.21	0.69
FUN_007838	1.21	1.04	1.21	0.00	0.00	0.35	0.17	0.00
FUN_007850	2.08	1.21	2.08	0.00	0.00	0.00	0.00	0.35
FUN_007851	3.63	2.08	3.63	0.00	0.52	0.17	0.17	0.52
FUN_007855	5.19	3.63	5.71	0.00	0.69	0.52	0.52	0.69
FUN_007860	6.40	5.19	6.40	0.00	2.25	1.73	1.56	2.25
FUN_007991	1.56	6.40	1.73	0.17	0.69	0.35	0.35	0.69
FUN_008329	2.60	2.60	2.60	0.00	1.38	0.00	0.00	1.38
FUN_008352	2.42	2.42	2.42	0.00	1.04	0.00	0.00	1.04
FUN_008369	6.40	6.23	6.40	0.00	0.69	0.00	0.00	0.69
FUN_008395	3.63	2.94	3.63	0.00	1.21	0.00	0.00	1.21
FUN_008445	2.25	2.60	2.60	0.00	0.35	0.00	0.00	0.35
FUN_008500	2.60	1.90	2.08	0.00	0.17	0.00	0.00	0.17
FUN_008562	2.77	3.11	2.25	0.17	0.00	0.17	0.00	0.00

FUN_008574	5.02	5.71	4.84	0.17	2.60	0.00	0.00	2.42
FUN_008666	5.02	5.71	5.54	0.00	0.35	0.00	0.17	0.35
FUN_008681	A	A	A	0.00	0.52	0.52	0.69	0.52
FUN_008714	6.57	3.98	3.98	0.00	1.04	1.04	1.04	1.04
FUN_008830	5.02	5.19	5.19	0.00	0.52	0.52	0.52	0.52
FUN_009063	6.57	6.57	6.57	0.00	2.42	0.00	0.17	2.42
FUN_009073	5.88	5.19	5.19	0.17	0.87	0.00	0.17	0.87
FUN_009124	4.33	4.33	4.33	0.00	1.21	0.00	0.00	1.21
FUN_009151	5.54	5.54	5.54	0.00	0.52	0.00	0.00	0.52
FUN_009222	6.57	5.02	6.57	0.00	0.52	0.35	0.35	0.52
FUN_009264	3.63	2.25	3.81	0.00	1.56	1.56	1.73	1.73
FUN_009294	2.25	2.25	2.42	0.00	0.00	1.04	1.04	0.00
FUN_009350	4.67	4.67	4.84	0.00	0.52	0.00	0.00	0.52
FUN_009516	1.38	1.38	1.38	0.00	0.00	0.00	0.00	0.00
FUN_009552	5.36	6.40	5.54	0.00	1.04	1.38	1.38	1.04
FUN_009576	4.67	4.33	4.84	0.00	2.77	2.60	2.60	2.94
FUN_009991	5.54	5.71	5.54	0.00	2.42	0.69	1.04	2.42
FUN_010039	3.29	3.29	3.11	0.00	1.21	1.38	1.21	1.21
FUN_010054	6.92	6.92	6.57	0.00	1.38	2.08	2.25	1.38
FUN_010164	A	A	A	0.00	1.21	0.00	0.17	1.21
FUN_010225	9.52	9.52	9.34	0.00	0.35	0.00	0.00	0.52
FUN_010331	2.08	1.73	1.90	0.00	0.52	0.52	0.52	0.52
FUN_010336	13.49	12.63	13.32	0.00	2.25	3.46	3.98	2.25
FUN_010366	4.50	4.67	4.15	0.00	0.17	0.00	0.17	0.17
FUN_010414	1.90	1.73	1.90	0.00	0.35	0.52	0.52	0.35
FUN_010496	3.63	3.63	3.63	0.00	0.35	0.35	0.52	0.35
FUN_010499	1.04	1.04	0.87	0.00	0.00	0.00	0.00	0.00
FUN_010529	4.15	7.09	5.36	2.42	4.15	3.46	4.15	3.11
FUN_010575	1.38	1.38	1.38	0.00	0.00	0.00	0.00	0.00
FUN_010594	3.98	3.98	3.81	0.00	0.35	0.00	0.35	0.35
FUN_010651	3.46	4.15	3.46	0.17	0.69	0.00	0.00	0.87
FUN_010656	4.15	4.15	4.15	A	0.69	0.00	0.00	0.69
FUN_010853	19.20	6.23	20.07	0.00	3.46	0.00	0.35	3.29
FUN_010873	7.61	6.92	7.44	0.00	2.08	0.00	0.00	2.08
FUN_010899	8.82	8.48	8.13	0.00	0.52	0.17	0.00	0.52
FUN_010928	5.54	5.54	5.54	0.00	1.04	1.56	0.17	0.87
FUN_011077	5.36	5.19	5.71	0.00	0.00	0.35	0.69	0.00
FUN_011081	1.56	1.90	1.90	0.00	0.52	0.17	0.17	0.52

FUN_011148	1.90	1.90	1.73	0.00	0.17	0.52	0.52	0.17
FUN_011352	3.81	3.63	4.33	0.00	0.17	0.35	0.52	0.17
FUN_011359	3.46	0.17	3.29	0.17	0.17	0.35	0.35	0.35
FUN_011399	2.94	2.77	2.77	0.35	0.35	0.00	0.00	0.00
FUN_011519	4.33	3.81	2.94	0.35	0.69	0.35	0.35	0.35
FUN_011522	26.12	25.95	25.95	0.00	3.81	0.87	0.35	0.52
FUN_011531	A	A	A	12.98	A	1.90	0.17	3.81
FUN_011546	4.84	4.84	4.67	0.00	0.87	1.21	1.21	0.87

* While grey boxes labelled with "A" indicate effector gene absence, numbers indicate the SNP ratio (%) in the homolog when compared with the effector gene in *R. necatrix* strain R18. Green cells indicate identical effector genes that lack SNPs when compared with the sequence in strain R18.

Supplemental Table 3. Annotated secondary metabolite clusters of *R. necatrix* strain R18.

Contig	From	To	Most similar known cluster	Type	Organism	Similarity	Known activity[a]
4	28,584	63,895	Swainsonine	Polyketide	*Alternaria oxytropis*	33%	Phytotoxic (Cook et al., 2017)
5	1,431,139	1,452,194	Copalyl diphosphate	Terpene	*Diaporthe amygdali*	42%	Super-elongation disease in plants (Kawaide, 2006; Rademacher and Graebe, 1979)
5	2,494,569	2,532,303	Cytochalasin E/K	NRP+Polyketide	*Aspergillus clavatus*	23%	Phytotoxic (Sawai et al., 1983; Thomas, 1978)
6	409,707	450,119	Wortmanamide A/B	NRP + Polyketide	*Talaromyces wortmannii*	83%	Unknow (Hai and Tang, 2018)
6	1,123,590	1,166,755	Pyriculol	Polyketide	*Neurospora crassa*	26%	Phytotoxic (Zhao et al., 2019)
6	3,495,713	3,545,733	Apicidin	NRP	*Fusarium incarnatum*	54%	Antiprotozoal activity (Darkin-Rattray et al., 1996)
6	3,953,658	3,994,676	Yanuthone D	Polyketide	*Aspergillus niger*	20%	Antibiotic (Holm et al., 2014)
6	4,187,217	4,235,557	Iso-A82775C	Other	*Pestalotiopsis fici*	41%	Antibacterial activity (Pan et al., 2018)
7	2,248,951	2,299,047	Enniatin	NRP	*Fusarium equiseti*	100%	Phytotoxic (Walton, 1990)
7	3,449,415	3,495,060	Naphthalene	Polyketide	*Daldinia eschscholzii*	33%	Phytotoxic (Xu et al., 2021)
8	3,062,127	3,105,143	Melanin	Polyketide	*Glarea lozoyensis*	100%	No involve in virulence in *R. necatrix* (Shimizu et al., 2014)
9	1,168,004	1,220,639	Cytochalasin E/K	NRP+Polyketide	*Aspergillus clavatus*	30%	Phytotoxic (Sawai et al., 1983; Thomas, 1978)
10	2,744,211	2,797,043	Fusaridione A	NRP + Polyketide	*Fusarium heterosporum*	12%	Unknow (Kalule et al., 2013)

4

[a]References:

Cook, D., Donzelli, B. G. G., Creamer, R., Baucom, D. L., Gardner, D. R., Pan, J., Moore, N., Krasnoff, S. B., Jaromczyk, J. W., and Schardl, C. L. (2017). Swainsonine biosynthesis genes in diverse symbiotic and pathogenic fungi. *Genes, Genomes, Genetics*, 7: 1791-1797.

Kawaide, H. (2006). Biochemical and molecular analyses of gibberellin biosynthesis in fungi. *Bioscience, Biotechnology, and Biochemistry*, 70: 583-590.

Rademacher, W., and Graebe, J. E. (1979). Gibberellin A4 produced by *Sphaceloma manihoticola*, the cause of the super elongation disease of cassava (*Manihot esculenta*). *Biochemical and Biophysical Research Communications*, 91: 35-40.

Sawai, K., Okuno, T., Fujioka, H., and Furuya, M. (1983). The relation between the phytotoxicity of Cythochalasin E and its molecular structure. *Annals of the Phytopathological Society of Japan*, 49: 262-265.

Thomas, D. D. (1978). Cytochalasin effects in plants and eukaryotic microbial systems. *Frontiers in Biology*, 46: 257-275.

Hai, Y., and Tang, Y. (2018). Biosynthesis of long-chain N-acyl amide by a truncated PKS-NRPS hybrid megasynthase in fungi. *Journal of the American Chemical Society*, 140: 1271-1274.

Zhao, Z., Ying, Y., Hung, Y., and Tang, Y. (2019). Genome mining reveals Neurospora crassa can produce the salicylaldehyde sordarial. *Journal of Natural Products*, 82: 1029-1033.

Darkin-Rattray, S. J., Gurnett, A. M., Myers, R. W., Dulski, P. M., Crumley, T. M., Allocco, J. J., Cannova, C., Mainke, P. T., Colletti, S. L., Bednarek, M. A., Singh, S. B., Goetz, M. A., Dombrowski, A. W., Polishook, J. D. and Schmatz, D. M. (1996). Apicidin: a novel antiprotozoal agent that inhibits parasite histone deacetylase. *Proceedings of the National Academy of Sciences*, 93: 13143–13147.

Holm, D. K., Petersen, L. M., Klitgaard, A., Knudsen, P. B., Jarczynska, Z. D., Nielsen, K. F., Gotfredsen, C. H., Larsen, T. O., and Mortensen, U. H. (2014). Molecular and chemical characterization of the biosynthesis of the 6-MSA-derived meroterpenoid yanuthone D in *Aspergillus niger*. *Chemistry and Biology*, 21: 519-529.

Pan, Y., Liu, L., Guan, F., Li, E., Jin, J., Li, J., Che, Y., and Liu, G. (2018). Characterization of a Prenyltransferase for Iso-A82775C biosynthesis and generation of new congeners of chloropestolides. *ACS Chemical Biology*, 13: 703-711.

Walton, J. D. (1990). Peptide phytotoxins from plant pathogenic fungi. In Biochemistry of peptide antibiotics. Kleinkauf, H., and von Dohren, H. (eds). Berlin, 179-203 pp.

Xu, D., Xue, M., Shen, Z., Jia, X., Hou, X., Lai, D., and Zhou, L. (2021). Phytotoxic secondary metabolites from fungi. *Toxins*, 13: 1-65.

Shimizu, T., Tsutae, I., and Kanematsu, S. (2014). Functional analysis of a melanin biosynthetic gene using RNAi-mediated gene silencing in *Rosellinia necatrix*. *Fungal Biology*, 118: 413-421.

Thomas, D. D. (1978). Cytochalasin effects in plants and eukaryotic microbial systems. *Frontiers in Biology*, 46: 257-275.

Kakule, T. B., Sardar, D., Lin, Z., and Schmidt, E. W. (2013). Two related pyrrolidinedione synthetase loci in *Fusarium heterosporum* ATCC 74349 produce divergent metabolites. *ACS Chemical Biology*, 8: 1549-1557.

4

Supplemental Table 4. Bacterial strains used in this study.

Strain	Species	Family	Order	Medium	Gram
R102	*Pseudomonas knackmussii*	Pseudomonadaceae	Pseudomonadales	R2A	Negative
R19	*Pseudomonas corrugata*	Pseudomonadaceae	Pseudomonadales	LBA	Negative
R103	*Bacillus drentensis*	Bacillaceae	Bacillales	R2A	Positive
S7	*Bacillus licheniformis*	Bacillaceae	Bacillales	TSA	Positive
R104	*Paenarthrobacter ureafaciens*	Micrococcaceae	Micrococcales	R2A	Positive
S39	*Arthrobacter enclensis*	Micrococcaceae	Micrococcales	R2A	Positive
R109	*Ochrobactrum intermedium*	Rhizobiaceae	Rhizobiales	R2A	Negative
S26	*Brucella ovis*	Rhizobiaceae	Rhizobiales	TSA	Negative
R30	*Serratia ureilytica*	Enterobacteriaceae	Enterobacterales	TSA	Negative
S27	*Enterobacter soli*	Enterobacteriaceae	Enterobacterales	TSA	Negative
R139	*Microbacterium foliorum*	Microbacteriaceae	Micrococcales	TSA	Positive
S23	*Microbacterium esteraromaticum*	Microbacteriaceae	Micrococcales	TSA	Positive
R121	*Chryseobacterium indoltheticum*	Weeksellaceae	Flavobacteriales	TSA	Negative
Ri8	*Chryseobacterium wanjuense*	Weeksellaceae	Flavobacteriales	TSA	Negative
R143	*Cellulomonas soli*	Cellulomonadaceae	Micrococcales	R2A	Positive
R151	*Paenibacillus lautus*	Paenibacillaceae	Paenibacillales	TSA	Positive
S6	*Paenibacillus illinoisensis*	Paenibacillaceae	Paenibacillales	TSA	Positive
R155	*Achromobacter denitrificans*	Alcaligenaceae	Burkholderiales	LBA	Negative
S72	*Candidimonas bauzanensis*	Alcaligenaceae	Burkholderiales	TSA	Negative
R42	*Solibacillus isronensis*	Planococcaceae	Bacillales	TSA	Positive
S15	*Solibacillus silvestris*	Planococcaceae	Bacillales	LBA	Positive
R93	*Streptomyces flavogriseus*	Streptomycetaceae	Streptomycetales	LBA	Positive
Ri17	*Rhodanobacter spathiphylli*	Rhodanobacteraceae	Xanthomonadales	TSA	Negative
Ri21	*Sphingobium mellinum*	Sphingomonadaceae	Sphingomonadales	TSA	Negative
Ri29	*Pedobacter steynii*	Sphingobacteriaceae	Sphingobacteriales	TSA	Negative
Ri32	*Pedobacter panaciterrae*	Sphingobacteriaceae	Sphingobacteriales	TSA	Negative
Ri55	*Flavobacterium hauense*	Flavobacteriaceae	Flavobacteriales	LBA	Negative
Ri56	*Nocardia coeliaca*	Nocardiaceae	Corynebacteriales	LBA	Positive
S13	*Xanthomonas campestris*	Xanthomonadaceae	Xanthomonadales	R2A	Negative
S37	*Pseudoxanthomonas suwonensis*	Xanthomonadaceae	Xanthomonadales	R2A	Negative
S19	*Brevibacterium sediminis*	Brevibacteriaceae	Micrococcales	LBA	Positive

S55	*Brevibacterium anseongense*	Brevibacteriaceae	Micrococcales	TSA	Positive
S25	*Devosia riboflavina*	Devosiaceae	Rhizobiales	TSA	Negative
S29	*Aeromonas hydrophila*	Aeromonadaceae	Enterobacterales	TSA	Negative
S52	*Kaistia adipata*	Kaistiaceae	Rhizobiales	R2A	Negative
S64	*Exiguobacterium artemiae*	Exiguobacteraceae	Exiguobacterales	TSA	Positive
S65	*Cellulosimicrobium cellulans*	Promicromonosporaceae	Micrococcales	TSA	Positive
S71	*Nocardioides zeae*	Nocardioidaceae	Propionibacteriales	TSA	Positive
Si1	*Herbaspirillum rhizosphaerae*	Oxalobacteraceae	Burkholderiales	TSA	Negative

Supplemental Table 5. Primers used in this study.

Primer name	Oligonucleotide sequence (5'→3')	Usage
RnGAPDH-F	TCAGCGACCAGGAGCTAGTCA	qPCR
RnGAPDH-R	TTGAAAAAATTTGGATTGAGCTCTAC	qPCR
coRUB-Fw	GAACAGTTTCTCACTGTTGAC	qPCR
coRUB-Rv	CGTGAGAACCATAAGTCACC	qPCR
RnITS-F	CTGTTCGAGCGTCATTTCAA	qPCR
RnITS-R	CCTACCTGATCCGAGGTCAA	qPCR
FUN_3304_NdeI_fw	ATCATATGATGATTTCCAACATCCTCCCTGTT	Protein production
FUN_3304_BamHI_rv	CCGGATCCTTAGCTGCTGCAGCCACCAAGC	Protein production
FUN_4580_NdeI_fw	ATCATATGATGAAGGCAACGATTTTGGACATCG	Protein production
FUN_4580_BamHI_rv	CCGGATCCTTATTCGCTGAAGGTGATGGTAACTG	Protein production
FUN_5751_NdeI_fw	ATCATATGATGCAGATCTTCACGACAGTCTTGGCCGT	Protein production
FUN_5751_BamHI_rv	AGCCGGATCCTCAGCTAGTCCCGGAGCAG	Protein production
FUN_9266_NdeI_fw	ATCATATGATGCGTGTCTCAGCTGCTCTCTTCG	Protein production
FUN_9266_BamHI_rv	CCGGATCCCTAAAGGGGGTCCGTCCGTC	Protein production
FUN_9480_NdeI_fw	ATCATATGATGAAGGCAACTCTGATCTCCGTCGCCGT	Protein production
FUN_9480_BamHI_rv	CCGGATCCTTACAGAAGAGCGGCGGCAGCCA	Protein production

Supplemental Table 6. Annotation of BLAST and HMMER hits to effector FUN_004580.

Accession ID[a]	Annotation[b]	Organism[c]	Query coverage	E value	Identity (%)d
BLAST					
XM_047979610.1	Hypothetical protein	*Xylaria bambusicola*	97%	0.0	71.68%
XM_049263194.1	Hypothetical protein	*Hypoxylon fragiforme*	96%	1E-151	57.95%
XM_051520408.1	Hypothetical protein	*Durotheca rogersii*	100%	1E-144	54.59%
XM_047931715.1	Hypothetical protein	*Daldinia caldariorum*	97%	2E-141	54.34%
XM_049244863.1	Hypothetical protein	*Daldinia decipiens*	97%	1E-138	53.94%
XM_033578433.1	Hypothetical protein	*Daldinia childiae*	97%	4E-137	53.06%
XM_049303926.1	Hypothetical protein	*Daldinia loculata*	97%	2E-135	53.57%
XM_047960472.1	Hypothetical protein	*Annulohypoxylon maeteangense*	96%	9E-135	51.28%
XM_048007749.1	Hypothetical protein	*Daldinia vernicosa*	97%	1E-134	53.55%
XM_047993846.1	Hypothetical protein	*Annulohypoxylon truncatum*	97%	4E-133	52.91%
XM_051460929.1	Hypothetical protein	*Hypoxylon trugodes*	96%	9E-132	51.79%
XM_049311849.1	Hypothetical protein	*Neoarthrinium moseri*	100%	7E-130	52.33%
XM_007830382.1	Hypothetical protein	*Pestalotiopsis fici*	100%	3E-122	49.40%
XM_040853841.1	Hypothetical protein	*Pseudomassariella vexata*	99%	4E-120	50.61%
XM_046099206.1	Hypothetical protein	*Truncatella angusta*	83%	2E-105	60.57%
XM_046156523.1	Hypothetical protein	*Microdochium trichocladiopsis*	95%	3E-105	46.56%
XM_018284675.1	Hypothetical protein	*Pochonia chlamydosporia*	95%	2E-102	47.31%
XM_024896116.1	Hypothetical protein	*Trichoderma citrinoviride*	69%	4E-100	56.54%
XM_006963277.1	Hypothetical protein	*Trichoderma reesei*	69%	1E-99	56.99%
XM_024900564.1	Hypothetical protein	*Trichoderma asperellum*	96%	7E-99	43.24%
XM_038885939.1	Hypothetical protein	*Colletotrichum karsti*	67%	4E-98	56.20%
XM_018296053.1	Hypothetical protein	*Colletotrichum higginsianum*	68%	1E-97	55.40%
XM_016786253.1	Hypothetical protein	*Scedosporium apiospermum*	94%	1E-97	45.83%
XM_036632953.1	Hypothetical protein	*Colletotrichum siamense*	61%	1E-96	58.23%
XM_045404242.1	Hypothetical protein	*Colletotrichum gloeosporioides*	61%	2E-96	58.23%
XM_037316359.1	Hypothetical protein	*Colletotrichum aenigma*	61%	2E-96	58.23%
XM_053175963.1	Hypothetical protein	*Colletotrichum chrysophilum*	61%	2E-96	58.23%
XM_032030074.1	Hypothetical protein	*Colletotrichum fructicola*	61%	2E-96	58.23%
XM_049274743.1	Hypothetical protein	*Colletotrichum spaethianum*	61%	4E-96	60.00%
XM_043142060.1	Hypothetical protein	*Ustilaginoidea virens*	68%	6E-96	55.20%
XM_046250215.1	Hypothetical protein	*Ilyonectria robusta*	67%	2E-94	54.21%
XM_018809009.1	Hypothetical protein	*Trichoderma gamsii*	69%	6E-94	52.63%

4

XM_044846055.1	Hypothetical protein	*Fusarium poae*	95%	4E-93	42.65%
XM_007818233.1	Hypothetical protein	*Metarhizium robertsii*	95%	7E-93	42.93%
XM_024922373.1	Hypothetical protein	*Trichoderma harzianum*	69%	2E-92	53.55%
XM_036723064.1	Hypothetical protein	*Colletotrichum truncatum*	61%	5E-92	57.43%
XM_035468007.1	Hypothetical protein	*Geosmithia morbida*	67%	1E-91	54.58%
XM_014688387.1	Hypothetical protein	*Metarhizium brunneum*	95%	1E-91	42.68%
XM_009264636.1	Hypothetical protein	*Fusarium pseudograminearum*	68%	2E-91	51.97%
XM_003651639.1	Hypothetical protein	*Thermothielavioides terrestris*	96%	4E-91	43.73%
XM_047979610.1	Hypothetical protein	*Xylaria bambusicola*	97%	0.0	71.68%
XM_049263194.1	Hypothetical protein	*Hypoxylon fragiforme*	96%	1E-151	57.95%
XM_051520408.1	Hypothetical protein	*Durotheca rogersii*	100%	1E-144	54.59%
XM_047931715.1	Hypothetical protein	*Daldinia caldariorum*	97%	2E-141	54.34%
XM_003651639.1	Hypothetical protein	*Thermothielavioides terrestris*	96%	4E-91	43.73%
XM_025729660.1	Hypothetical protein	*Fusarium venenatum*	68%	1E-90	51.25%
XM_008095090.1	Hypothetical protein	*Colletotrichum graminicola*	61%	3E-90	56.22%
XM_014092778.1	Hypothetical protein	*Trichoderma atroviride*	69%	3E-90	52.28%
XM_049285132.1	Hypothetical protein	*Colletotrichum lupini*	60%	4E-90	56.68%
CP077948.1	Hypothetical protein	*Colletotrichum gigasporum*	92%	1E-89	45.48%
XM_053195163.1	Hypothetical protein	*Colletotrichum fioriniae*	60%	6E-89	56.56%
OW971920.1	Hypothetical protein	*Trichoderma pseudokoningii*	67%	1E-88	56.57%
XM_031165144.1	Hypothetical protein	*Fusarium coffeatum*	68%	2E-88	51.25%
XM_006691392.1	Hypothetical protein	*Thermochaetoides thermophila*	94%	7E-88	41.45%
CP021290.1	Hypothetical protein	*Trichoderma reesei*	66%	1E-87	57.88%
CP040201.1	Hypothetical protein	*Trichoderma reesei*	66%	1E-87	57.88%
CP020724.1	Hypothetical protein	*Trichoderma reesei*	66%	1E-87	57.88%
CP020875.1	Hypothetical protein	*Trichoderma reesei*	66%	1E-87	57.88%
CP021304.1	Hypothetical protein	*Trichoderma reesei*	66%	1E-87	57.88%
CP021297.1	Hypothetical protein	*Trichoderma reesei*	66%	1E-87	57.88%
CP016232.1	Hypothetical protein	*Trichoderma reesei*	66%	1E-87	57.88%
CP021311.1	Hypothetical protein	*Trichoderma reesei*	66%	1E-87	57.88%
CP084946.1	Hypothetical protein	*Trichoderma asperellum*	94%	1E-87	43.11%
XM_022625650.1	Hypothetical protein	*Colletotrichum orchidophilum*	68%	3E-87	51.97%
XM_011318840.1	Hypothetical protein	*Fusarium graminearum*	68%	4E-87	51.97%
XM_046123457.1	Hypothetical protein	*Fusarium flagelliforme*	68%	4E-87	51.60%

CP072834.1	Hypothetical protein	*Trichoderma asperellum*	94%	7E-87	42.75%
XM_014095116.1	Hypothetical protein	*Trichoderma virens*	69%	1E-86	52.13%
XM_053146149.1	Hypothetical protein	*Fusarium falciforme*	68%	1E-86	50.18%
XM_028643441.1	Hypothetical protein	*Verticillium nonalfalfae*	61%	2E-86	54.66%
XM_003350974.1	Hypothetical protein	*Sordaria macrospora*	68%	3E-86	49.64%
XM_053050566.1	Hypothetical protein	*Fusarium keratoplasticum*	67%	1E-85	50.55%
XM_046270538.1	Hypothetical protein	*Fusarium solani*	67%	1E-85	50.55%
XM_035474047.1	Hypothetical protein	*Colletotrichum scovillei*	60%	1E-85	56.68%
CP083246.1	Hypothetical protein	*Epichloe scottii*	66%	1E-84	53.73%
CP101605.1	Hypothetical protein	*Ustilaginoidea virens*	65%	2E-84	55.43%
CP072756.1	Hypothetical protein	*Ustilaginoidea virens*	65%	2E-84	55.43%
CP049928.1	Hypothetical protein	*Ustilaginoidea virens*	65%	2E-84	55.43%
XM_018276255.1	Hypothetical protein	*Pseudogymnoascus verrucosus*	93%	4E-84	40.57%
CP079833.1	Hypothetical protein	*Fusarium graminearum*	68%	9E-84	51.97%
XM_003003371.1	Hypothetical protein	*Verticillium alfalfae*	61%	9E-84	54.66%
CP064806.1	Hypothetical protein	*Epichloe typhina subsp. clarkii*	67%	1E-83	51.25%
CP003010.1	Hypothetical protein	*Thermothielavioides terrestris*	95%	1E-83	43.65%
XM_008086879.1	Hypothetical protein	*Glarea lozoyensis*	68%	1E-83	49.47%
CP117785.1	Hypothetical protein	*Colletotrichum graminicola*	65%	2E-83	54.72%
CP019475.1	Hypothetical protein	*Colletotrichum lupini*	60%	4E-83	56.68%
XM_009858316.1	Hypothetical protein	*Neurospora tetrasperma*	68%	4E-83	49.28%
XM_046198521.1	Hypothetical protein	*Fusarium redolens*	69%	6E-83	51.42%
CP100344.1	Hypothetical protein	*Epichloe festucae*	66%	1E-82	53.36%
CP031387.1	Hypothetical protein	*Epichloe festucae*	66%	1E-82	53.36%
CP098298.1	Hypothetical protein	*Epichloe typhina subsp. poae*	67%	2E-82	51.61%
CP084938.1	Hypothetical protein	*Trichoderma atroviride*	67%	2E-82	52.71%
XM_047982779.1	Hypothetical protein	*Purpureocillium takamizusanense*	69%	2E-82	48.41%
XM_001907097.1	Hypothetical protein	*Podospora anserina*	97%	3E-82	37.78%
XM_040954205.1	Hypothetical protein	*Penicillium solitum*	68%	3E-82	49.82%
CP069151.1	Hypothetical protein	*Verticillium nonalfalfae*	65%	4E-82	53.61%
HMMER					
A0A5N6KR04_9ROSI	Hypothetical protein	*Carpinus fangiana*	59.2%	1.8E-66	41.1%

[a]Database accession ID where subject was deposited.
[b]Annotation of the best hit using BLAST (tblastn).
[c]Organism where the homolog was annotated.
[d]Percentage of identity of the query.

Supplemental Table 7. Annotation of BLAST and HMMER hits to effector FUN_011519.

Accession ID[a]	Annotation[b]	Organism[c]	Query coverage	E value	Identity (%)d
BLAST and HMMER					
XM_007838424.1	Hypothetical protein	*Pestalotiopsis fici*	100%	6E-10	68.57%
XM_014319017.1	Hypothetical protein	*Grosmannia clavigera*	100%	1E-09	71.43%
XM_006668457.1	Hypothetical protein	*Cordyceps militaris*	100%	1E-09	71.43%
XM_032032777.1	Hypothetical protein	*Colletotrichum fructicola*	100%	2E-09	65.71%
XM_024655518.1	Hypothetical protein	*Sordaria macrospora*	100%	1E-08	68.57%
XM_003659946.1	Hypothetical protein	*Thermothelomyces thermophilus*	100%	2E-08	71.43%
XM_048011148.1	Hypothetical protein	*Daldinia vernicosa*	100%	2E-08	62.86%
XM_046108154.1	Hypothetical protein	*Truncatella angusta*	100%	6E-08	60.00%
XM_051511661.1	Hypothetical protein	*Durotheca rogersii*	100%	6E-08	62.86%
XM_001907105.1	Hypothetical protein	*Podospora anserina*	100%	7E-08	65.71%
XM_046158086.1	Hypothetical protein	*Microdochium trichocladiopsis*	100%	9E-08	60.00%
XM_047937750.1	Hypothetical protein	*Daldinia caldariorum*	100%	1E-07	60.00%
XM_028614903.1	Hypothetical protein	*Sodiomyces alkalinus*	100%	2E-07	68.57%
XM_051457076.1	Hypothetical protein	*Hypoxylon trugodes*	100%	4E-07	65.71%
XM_049244688.1	Hypothetical protein	*Daldinia decipiens*	100%	4E-07	65.71%
XM_014686345.1	Hypothetical protein	*Metarhizium brunneum*	100%	5E-07	60.00%
XM_003007773.1	Hypothetical protein	*Verticillium alfalfae*	100%	2E-06	60.00%
XM_003651533.1	Hypothetical protein	*Thermothielavioides terrestris*	97%	3E-11	79.41%
XM_046265423.1	Hypothetical protein	*Emericellopsis atlantica*	97%	2E-09	73.53%
XM_008095371.1	Hypothetical protein	*Colletotrichum graminicola*	97%	5E-09	70.27%
XM_040863558.1	Hypothetical protein	*Pseudomassariella vexata*	97%	7E-09	67.65%
XM_960199.2	Hypothetical protein	*Neurospora crassa*	97%	2E-08	76.47%
XM_047972197.1	Hypothetical protein	*Xylaria bambusicola*	97%	4E-08	64.71%
XM_049302929.1	Hypothetical protein	*Daldinia loculata*	97%	2E-07	64.71%
XM_049293600.1	Hypothetical protein	*Colletotrichum lupini*	97%	2E-07	67.57%
XM_035467298.1	Hypothetical protein	*Geosmithia morbida*	97%	4E-07	61.76%
XM_022620490.1	Hypothetical protein	*Colletotrichum orchidophilum*	97%	4E-07	62.16%
XM_044863015.1	Hypothetical protein	*Hirsutella rhossiliensis*	97%	7E-07	67.65%
XM_047991640.1	Hypothetical protein	*Purpureocillium takamizusanense*	97%	1E-06	70.59%
XM_007808999.1	Hypothetical protein	*Metarhizium acridum*	97%	2E-06	61.76%
XM_009653120.1	Hypothetical protein	*Verticillium dahliae*	97%	2E-06	61.76%

XM_046253466.1	Hypothetical protein	*Ilyonectria robusta*	97%	3E-06	61.76%
XM_053054048.1	Hypothetical protein	*Fusarium keratoplasticum*	97%	5E-05	55.88%
XM_031161470.1	Hypothetical protein	*Fusarium coffeatum*	97%	6E-05	55.88%
XM_025733484.1	Hypothetical protein	*Fusarium venenatum*	97%	1E-04	55.88%
XM_023579291.1	Hypothetical protein	*Fusarium fujikuroi*	97%	2E-04	52.94%
XM_046198815.1	Hypothetical protein	*Fusarium redolens*	97%	2E-04	52.94%
XM_053149576.1	Hypothetical protein	*Fusarium falciforme*	97%	3E-04	55.88%
XM_046283930.1	Hypothetical protein	*Fusarium solani*	97%	4E-04	55.88%
XM_029896370.1	Hypothetical protein	*Pyricularia pennisetigena*	94%	2E-08	72.73%
XM_003720841.1	Hypothetical protein	*Pyricularia oryzae*	94%	9E-08	69.70%
XM_014087113.1	Hypothetical protein	*Trichoderma atroviride*	94%	4E-07	63.64%
XM_024898021.1	Hypothetical protein	*Trichoderma citrinoviride*	94%	5E-07	66.67%
XM_031130497.1	Hypothetical protein	*Pyricularia grisea*	94%	1E-06	69.70%
XM_024548995.1	Hypothetical protein	*Trichoderma gamsii*	94%	3E-06	60.61%
XM_024901739.1	Hypothetical protein	*Trichoderma asperellum*	94%	8E-06	60.61%
XM_024919849.1	Hypothetical protein	*Trichoderma harzianum*	94%	1E-05	66.67%
XM_043141820.1	Hypothetical protein	*Ustilaginoidea virens*	91%	6E-07	65.62%
XM_009229853.1	Hypothetical protein	*Gaeumannomyces tritici*	91%	5E-06	59.38%
CP023323.1	Hypothetical protein	*Cordyceps militaris*	88%	2E-07	74.19%
CP003010.1	Hypothetical protein	*Thermothielavioides terrestris*	88%	3E-07	77.42%
XM_040822091.1	Hypothetical protein	*Metarhizium album*	88%	2E-06	70.97%
XM_049264651.1	Hypothetical protein	*Hypoxylon fragiforme*	88%	3E-06	58.06%
XM_009857960.1	Hypothetical protein	*Neurospora tetrasperma*	88%	4E-06	74.19%
CP045886.1	Hypothetical protein	*Beauveria bassiana*	88%	4E-06	61.29%
CP098299.1	Hypothetical protein	*Epichloe typhina*	88%	4E-06	67.74%
CP098307.1	Hypothetical protein	*Epichloe typhina*	88%	4E-06	67.74%
CP064797.1	Hypothetical protein	*Epichloe typhina*	88%	5E-06	67.74%
CP003002.1	Hypothetical protein	*Thermothelomyces thermophilus*	88%	8E-06	70.97%
CP031390.1	Hypothetical protein	*Epichloe festucae*	88%	2E-05	67.74%
CP100347.1	Hypothetical protein	*Epichloe festucae*	88%	2E-05	67.74%
XM_031143259.1	Hypothetical protein	*Thyridium curvatum*	88%	2E-05	64.52%
CP098267.1	Hypothetical protein	*Epichloe bromicola*	88%	2E-05	67.74%
CP064805.1	Hypothetical protein	*Epichloe typhina*	88%	2E-05	67.74%
CP049927.1	Hypothetical protein	*Ustilaginoidea virens*	88%	2E-05	64.52%
CP072755.1	Hypothetical protein	*Ustilaginoidea virens*	88%	2E-05	64.52%
CP101604.1	Hypothetical protein	*Ustilaginoidea virens*	88%	2E-05	64.52%

4

CP099637.1	Hypothetical protein	*Epichloe amarillans*	88%	2E-05	67.74%
CP098274.1	Hypothetical protein	*Epichloe elymi*	88%	2E-05	67.74%
CP077954.1	Hypothetical protein	*Colletotrichum gigasporum*	88%	3E-05	64.52%
XM_007825388.2	Hypothetical protein	*Metarhizium robertsii*	88%	3E-05	61.29%
XM_035474232.1	Hypothetical protein	*Colletotrichum scovillei*	88%	4E-05	64.71%
CP086364.1	Hypothetical protein	*Purpureocillium takamizusanense*	88%	5E-05	70.97%
XM_040763701.1	Hypothetical protein	*Sporothrix brasiliensis*	88%	6E-05	67.74%
AB669186.1	Hypothetical protein	*Colletotrichum orbiculare*	88%	7E-05	61.29%
CP096782.1	Hypothetical protein	*Nigrospora oryzae*	88%	7E-05	64.52%
CP069148.1	Hypothetical protein	*Verticillium nonalfalfae*	88%	9E-05	58.06%
CP069139.1	Hypothetical protein	*Verticillium nonalfalfae*	88%	9E-05	58.06%
CP019480.1	Hypothetical protein	*Colletotrichum lupini*	88%	1E-04	64.71%
XM_018304892.1	Hypothetical protein	*Colletotrichum higginsianum*	88%	2E-04	58.82%
CP010982.1	Hypothetical protein	*Verticillium dahliae*	88%	3E-04	58.06%
CP009079.1	Hypothetical protein	*Verticillium dahliae*	88%	3E-04	58.06%
CP058936.1	Hypothetical protein	*Metarhizium brunneum*	88%	3E-04	61.29%
LR026964.1	Hypothetical protein	*Podospora comata*	88%	4E-04	64.52%
CP071116.1	Hypothetical protein	*Trichoderma virens*	85%	7E-06	66.67%
XM_014102688.1	Hypothetical protein	*Trichoderma virens*	85%	2E-05	66.67%
CP084938.1	Hypothetical protein	*Trichoderma atroviride*	85%	4E-05	63.33%
CP091464.1	Hypothetical protein	*Pyricularia oryzae*	85%	7E-05	66.67%
CP084944.1	Hypothetical protein	*Trichoderma asperellum*	85%	8E-05	60.00%
CP072831.1	Hypothetical protein	*Trichoderma asperellum*	85%	1E-04	60.00%
CP034210.1	Hypothetical protein	*Pyricularia oryzae*	85%	2E-04	66.67%
CP060336.1	Hypothetical protein	*Pyricularia oryzae*	85%	2E-04	66.67%
CP099702.1	Hypothetical protein	*Pyricularia oryzae*	85%	2E-04	66.67%
CP050926.1	Hypothetical protein	*Pyricularia oryzae*	85%	2E-04	66.67%
CP075865.1	Hypothetical protein	*Trichoderma simmonsii*	85%	2E-04	66.67%
CP071108.1	Hypothetical protein	*Trichoderma virens*	85%	2E-04	66.67%
OW971923.1	Hypothetical protein	*Trichoderma pseudokoningii*	85%	3E-04	66.67%
CP021293.1	Hypothetical protein	*Trichoderma reesei*	85%	3E-04	66.67%
CP016235.1	Hypothetical protein	*Trichoderma reesei*	85%	3E-04	66.67%
CP021307.1	Hypothetical protein	*Trichoderma reesei*	85%	3E-04	66.67%

[a]Database accession ID where subject was deposited.
[b]Annotation of the best hit using BLAST (tblastn).
[c]Organism where the homolog was annotated.
[d]Percentage of identity of the query.

4

Revealing antimicrobial activities through capturing synthetic community changes using Nanopore sequencing

Edgar A. Chavarro-Carrero, Ilaria Martino[$], Martina Cardoni[$], Anton Kraege, Ana López-Moral, Nick Snelders, Michael F. Seidl and Bart P.H.J. Thomma

[$]These authors contributed equally

ABSTRACT

Plant pathogens can modulate host microbiota compositions to facilitate host colonization. To this end, fungal pathogens secrete a range of effector proteins with selective antimicrobial activity during host ingress. In the present study, we aimed to develop a method to demonstrate antimicrobial activity of candidate effector proteins and to reveal their bacterial target ranges. To this end, we assembled two synthetic communities (SynComs) that contain all taxonomical families that were previously identified in a culture collection of tomato-associated bacteria, one with the faster growing taxa and one with the slower growing taxa. Besides testing the sensitivity of all 19 individual taxa to five fungal effector proteins, three of which were previously reported to display antimicrobial activity, we also tested the effect of adding the effector proteins to the SynComs. When the sensitivity of each bacterial taxon to either of the five effector proteins was tested individually, the effectors could inhibit the growth of a subset (between one and nine) of the 19 taxa. However, pronounced differences in sensitivity of several bacterial taxa to antimicrobials were observed when individually cultured bacteria were tested versus when treatments were performed on bacterial SynComs. This study provides a methodology that can demonstrate the antimicrobial activities of effector proteins through the use of SynComs, but also reveals that it may not be straightforward to reliably identify bacterial target ranges as we reveal differences when using single bacterial cultures versus SynComs. These observations highlight the importance of testing antimicrobial proteins in the niche in which they are naturally secreted, or close mimics thereof, to identify relevant bacterial target ranges.

INTRODUCTION

In nature, plants are continuously surrounded by a plethora of microbes with which they engage in interactions on a spectrum ranging from beneficial through commensal to parasitic (Cook et al., 2015). The molecular characterization of plant-pathogen interactions has shown that plant pathogens secrete dozens to hundreds of effector molecules into the apoplast or cytosol of their host plants to mediate host colonization (Rovenich et al., 2014; Wilson and McDowell, 2022). Recently, it has been shown that effector proteins not only fulfill functions in the direct manipulation of host immune responses, or more broadly in the manipulation of host physiology, but can also modulate plant-associated microbiota compositions inside as well as outside the host plant to support host colonization (Snelders et al., 2020; 2021; 2022; 2023; Chavarro-Carrero et al., 2023; Gómez-Pérez et al., 2023; Ökmen et al., 2023).

The plant-associated microbiota is of great importance for plant performance as it supports plant growth, development, and health (Trivedi et al., 2020; Mesny et al., 2023). Perhaps the best-known examples of beneficial microbiota members that positively impact plant performance are mycorrhiza that support plants in their uptake of water, phosphorus, and other limiting nutrients, and *Rhizobium* bacteria that fix atmospheric nitrogen in their symbiosis with legume plants (Mendes et al., 2013). Furthermore, the root-associated microbiota facilitates nutrient uptake by plants by weathering minerals and the degradation of recalcitrant organic matter. In return, the microbiota is provided with carbon through root exudates (van der Heijden et al., 2008).

In addition to supporting plant growth, the root microbiota plays an important role in promoting plant immunity (Rudrappa et al., 2008; Berendsen et al., 2018). Root exudates actively recruit soil bacteria that promote plant health and suppress disease development (Rudrappa et al., 2008; Berendsen et al., 2018; Goossens et al., 2023). For example, several members of the bacterial genera *Bacillus* and *Pseudomonas*, and of the fungal genus *Trichoderma*, are beneficial for plant health through several mechanisms, including direct antagonism, plant growth promotion, and the induction of systemic immune responses in their plant hosts (Dimkić et al., 2022). Recent studies demonstrate that, in return, pathogens modulate root microbiota compositions to facilitate plant host colonization. The fungal broad host-range vascular wilt pathogen *Verticillium dahliae* was shown to exploit a range of effector proteins with selective antimicrobial activity (Snelders et al., 2020; 2021; 2022, 2023). The *V. dahliae* effector Ave1 suppresses antagonistic bacteria that belong to the Spingomonadaceae during host colonization as well as during soil-dwelling stages (Snelders et al., 2020). Furthermore, through its selective antibacterial activity VdAMP2 contributes to *V. dahliae* survival in soil (Snelders et al., 2020), while VdAMP3 possesses antifungal activity and is expressed in decaying host tissue to promote resting structure formation (Snelders et

al., 2021). Finally, VdAve1L2 suppresses antagonistic Actinobacteria to promote host colonization (Snelders et al., 2022). Importantly, *V. dahliae* is not the only pathogen that was demonstrated to use effector proteins with antimicrobial activity to promote host colonization. Most recently, two *in planta*-expressed effectors of the broad host-range white root rot pathogen *Rosellinia necatrix*, FUN_004580 and FUN_011519, were shown to display selective antimicrobial activity towards several fungi and plant-associated bacteria (Chapter 2 of this thesis; Chavarro-Carrero et al., 2023). Additionally, the smut fungus *Ustilago hordei* was shown to secrete the ribonuclease effector protein UhRibo1 during early stages of plant colonization to inhibit the growth of plant-associated bacteria (Ökmen et al., 2023) in a similar fashion as has been proposed for the ribonuclease effector protein Zt6 secreted by the fungal wheat pathogen *Zymoseptoria tritici* (Kettles et al., 2018). Furthermore, the obligate plant parasite *Albugo candida* secretes various proteins with selective antimicrobial activity directed against plant-associated Gram-positive bacteria occurring on its *Arabidopsis thaliana* host (Gómez-Pérez et al., 2023).

AMPs from *V. dahliae* and *R. necatrix* have been identified by mining the predicted secretomes of both pathogens for structural homologues of known antimicrobial proteins (AMPs) (Snelders et al., 2020; Chavarro-Carrero et al., 2023). To assess antibacterial activity, the growth inhibition of selected bacterial species was assessed. Furthermore, modulation of synthetic bacterial communities and natural microbiome compositions has been assessed using Illumina 16S profiling. However, this sequencing technique produces only short reads (<600 bp) which restrains sequencing of the entire 16S rRNA gene in a single read (~1,500 bp) (Frank et al., 2008). Short-read sequencing might result in incomplete coverage of the 16S rRNA gene, missing variable regions that are critical for taxonomic identification, reducing the taxonomic resolution. Especially when working with closely related bacterial taxa, as small differences in the sequence can result in misclassification (Polz and Cavanaugh, 1998; Kanagawa, 2003; Pollock et al., 2018). Oxford Nanopore Technologies (ONT) sequencing is a rapid, portable, and low-cost solution for in-house sequencing (ONT, 2020) capable of long DNA fragment sequencing (Lei et al., 2022). High-throughput generation of reads is achieved in a pocket-sized portable device called a MinION (Lu et al., 2016), allowing real-time data analysis, drastically reducing sequencing turnaround times, and lowering the cost per sequenced base (Branton et al., 2008). In contrast to Sanger and Illumina sequencing, ONT sequencing allows the sequencing of entire 16S rRNA genes in samples with bacterial mixtures (Benítez-Páez et al., 2016). In the present study, we exploited ONT sequencing to capture shifts in the composition of synthetic communities that are induced by fungal pathogen effector proteins in an attempt to develop this method to demonstrate antimicrobial activities of novel candidate effector proteins and identify their specific bacterial target ranges.

RESULTS

Synthetic community assembly

To generate a synthetic community (SynCom) that represents the bacterial diversity found in a plant microbiota, we selected a single bacterial strain for each of the 19 taxonomical families that were previously identified in a collection of tomato-associated bacteria (Chavarro-Carrero et al., 2023) (Table 1). To extract the maximum of genetic information from the 19 bacterial strains, including the structure and sequence information of the 16S locus, we performed whole-genome sequencing with an Oxford Nanopore Technologies (ONT) MinION device and assembled the genome of each bacterial strain, resulting in assemblies of one to nine contigs per species (Table 1). From these assemblies, we extracted the 16S regions of the ribosomal DNA and composed a local database. Next, the growth of the 19 bacteria was individually assessed in lysogeny broth (LB), tryptone soy broth (TSB), and Reason's 2A broth (R2A). After 20 h of incubation, all bacteria grew in all cultivation media, although nine bacteria accumulated to lower densities (OD600 < 1) than the remaining ten (OD600 > 1) (Table 2).

To assemble a SynCom, each of the 19 bacteria was grown separately for 24 h in LB, TSB, or R2A, after which each of the cultures was adjusted to an OD600 of 0.05, and equal volumes were mixed (designated SynCom A) in six replicate samples. While three samples were immediately used for DNA isolation, the remaining three samples were incubated for 20 hours at 22°C, with constant shaking at 120 rpm, after which the bacterial cells were harvested, and DNA isolation was performed. Subsequently, 16S PCR was performed, followed by ONT sequencing, and the relative abundance of each SynCom A member was determined based on mapping the reads to the database of 16S sequences.

The 16S rRNA gene encompasses nine variable regions (V1-V9) that are crucial for identifying bacterial species (Bukin et al., 2019). To reliably map reads that belong to the correct bacterial species in the dataset we only retained sequences that encompass multiple variable regions. To this end, we kept reads longer than 1 kb that mapped with an identity >85% to the database of 16S sequences. Furthermore, only the best match was kept for reads with multiple matches above 85% identity to the database of 16S sequences, which concerned less than 1% of the total sequenced reads. Mapping rates ranged from 88.89% to 99% of the sequenced reads (Table 3).

After 20 h of incubation, rDNA sequences from several members of SynCom A could not be detected in LB and TSB (Figure 1A): eight out of 19 members were no longer detected in LB, while ten members were no longer detected in TSB (Figure 1A, 1D). Although in R2A all SynCom A members were detected after incubation, the composition was quite imbalanced, with *Chryseobacterium wanjuense* and

5

Rhodanobacter spathiphylli making up more than half of the SynCom A composition (Figure 1A).

To design SynComs in which all members would be able to establish themselves, we divided the set of 19 bacteria into two separate SynComs based on their differences in growth, with one SynCom containing the ten bacteria that accumulated to OD600 > 1.0 in separate cultures (SynCom B), and a second SynCom with the nine bacteria that accumulated to OD600 < 1.0 (SynCom C) (Table 2). Accordingly, we kept reads longer than 1 kb with identities >85%, and for reads with multiple matches above 85% identity only the best match was kept, obtaining high mapping rates from 80% to 97.78% with SynCom B and 76,92% to 99% with SynCom C (Table 3). Alike we observed for SynCom A, several members of SynCom B and C could not be detected after incubation in LB and TSB (Figure 1B-D). More specifically, for SynCom B, three out of ten members were no longer detected in either of the two cultivation media (Figure 1B, 1D), while for SynCom C, three members were no longer detected in LB, and four members were not detected in TSB (Figure 1C, 1D). In contrast, all members of SynCom B and C were detected in R2A (Figure 1B, 1C, 1D). Moreover, the relative abundance of the members was evenly distributed in each of the two SynComs. Thus, we pursued further experiments with SynComs B and C in R2A medium.

Table 1. Genome assembly statistics based on Nanopore sequencing of 19 bacterial strains isolated from a tomato microbiota and used for SynCom assembly.

Strain	Species	Family	Order	Data (Mb)	Assembly size (Mb)	No. of Contigs	Contig N50 (Mb)	GC content (%)
R19	*Pseudomonas corrugata*	Pseudomonadaceae	Pseudomonadales	300	6.2	1	6.2	60.5
R103	*Bacillus drentensis*	Bacillaceae	Bacillales	250	5.5	5	1.4	61.3
Ri53	*Arthrobacter rhombi*	Micrococcaceae	Micrococcales	650	4.9	1	4.9	61.2
S26	*Brucella ovis*	Rhizobiaceae	Rhizobiales	500	6.2	1	6.2	60.3
R139	*Microbacterium foliorum*	Microbacteriaceae	Micrococcales	600	8.8	9	4.9	64.4
Ri8	*Chryseobacterium wanjuense*	Weeksellaceae	Flavobacteriales	300	4.6	1	4.6	35.4
R143	*Cellulomonas soli*	Cellulomonadaceae	Micrococcales	850	3.5	1	3.4	73.1
S6	*Paenibacillus illinoisensis*	Paenibacillaceae	Paenibacillales	600	6.5	5	5.4	47.4
R155	*Achromobacter denitrificans*	Alcaligenaceae	Burkholderiales	700	3.8	2	3.7	36.5
R42	*Solibacillus isronensis*	Planococcaceae	Bacillales	400	4.4	3	4.0	38.3
Ri17	*Rhodanobacter spathiphylli*	Rhodanobacteraceae	Xanthomonadales	250	4.9	1	4.9	61.2
Ri21	*Sphingobium mellinum*	Sphingomonadaceae	Sphingomonadales	300	5.5	2	5.5	39.1
Ri32	*Pedobacter panaciterrae*	Sphingobacteriaceae	Sphingobacteriales	500	6.2	2	6.1	38.7
Ri55	*Flavobacterium hauense*	Flavobacteriaceae	Flavobacteriales	300	6.8	3	6.5	64.8
S13	*Xanthomonas campestris*	Xanthomonadaceae	Xanthomonadales	300	3.8	1	3.8	69.5
S25	*Devosia riboflavina*	Devosiaceae	Rhizobiales	350	4.9	4	2.5	61.2
S64	*Exiguobacterium artemiae*	Exiguobacteraceae	Exiguobacterales	400	3.2	2	3.0	47.5
S65	*Cellulosimicrobium cellulans*	Promicromonosporaceae	Micrococcales	300	4.3	2	4.2	74.6
Si1	*Herbaspirillum rhizosphaerae*	Oxalobacteraceae	Burkholderiales	400	6.2	1	6.2	38.7

5

Table 2. SynCom compositions based on bacterial densities after cultivation in different media.

Strain	Species	OD$_{600}$[a]			SynCom		
		LB	R2A	TSB	A	B	C
R19	*Pseudomonas corrugata*	1.734	1.034	1.111	X	X	
R103	*Bacillus drentensis*	1.834	1.234	1.659	X	X	
Ri53	*Arthrobacter rhombi*	0.654	0.599	0.732	X		X
S26	*Brucella ovis*	1.567	1.232	1.879	X	X	
R139	*Microbacterium foliorum*	0.856	0.546	0.893	X		X
Ri8	*Chryseobacterium wanjuense*	1.345	1.294	1.789	X	X	
R143	*Cellulomonas soli*	0.679	0.872	0.889	X		X
S6	*Paenibacillus illinoisensis*	1.231	1.289	1.673	X	X	
R155	*Achromobacter denitrificans*	1.943	1.101	1.549	X	X	
R42	*Solibacillus isronensis*	1.348	1.234	1.541	X	X	
Ri17	*Rhodanobacter spathiphylli*	0.449	0.674	0.798	X		X
Ri21	*Sphingobium mellinum*	0.620	0.549	0.728	X		X
Ri32	*Pedobacter panaciterrae*	1.563	1.098	1.692	X	X	
Ri55	*Flavobacterium hauense*	0.731	0.541	0.722	X		X
S13	*Xanthomonas campestris*	1.234	1.201	1.398	X	X	
S25	*Devosia riboflavina*	0.587	0.552	0.762	X		X
S64	*Exiguobacterium artemiae*	1.409	1.128	1.673	X	X	
S65	*Cellulosimicrobium cellulans*	0.804	0.716	0.945	X		X
Si1	*Herbaspirillum rhizosphaerae*	0.846	0.620	0.982	X		X

[a]OD$_{600}$ after 20 h of incubation at 22ºC (120 rpm) in lysogeny broth (LB), tryptone soy broth (TSB), or Reason's 2A broth (R2A).

Table 3. Nanopore sequencing data and amount of reads mapped to the 16S database.

SynCom	Incubation	Media used	Treatment	Amount of Nanopore reads[a]	N50 (Kb)[a]	N90 (Kb)[a]	Reads mapped[a]	% reads mapped[a]
A	0 h	LB	Untreated	$9x10^3$	1.6	1.5	$8x10^3$	88.89
A	24 h	LB	Untreated	$19x10^3$	1.6	1.5	$18x10^3$	94.74
A	0 h	R2A	Untreated	$7x10^3$	1.6	1.5	$6.5x10^3$	92.86
A	24 h	R2A	Untreated	$32x10^3$	1.6	1.5	$30x10^3$	93.75
A	0 h	TSB	Untreated	$7x10^3$	1.6	1.5	$7x10^3$	99.00
A	24 h	TSB	Untreated	$21x10^3$	1.6	1.5	$20x10^3$	95.24
B	0 h	LB	Untreated	$15x10^3$	1.6	1.5	$12x10^3$	80.00
B	24 h	LB	Untreated	$45x10^3$	1.6	1.5	$44x10^3$	97.78
B	0 h	R2A	Untreated	$19x10^3$	1.6	1.5	$18x10^3$	94.74
B	24 h	R2A	Untreated	$41x10^3$	1.6	1.5	$38x10^3$	92.68
B	0 h	TSB	Untreated	$10x10^3$	1.6	1.5	$9x10^3$	90.00
B	24 h	TSB	Untreated	$41x10^3$	1.6	1.5	$39x10^3$	95.12
C	0 h	LB	Untreated	$6x10^3$	1.6	1.5	$6x10^3$	99.00
C	24 h	LB	Untreated	$48x10^3$	1.6	1.5	$47x10^3$	97.92
C	0 h	R2A	Untreated	$13x10^3$	1.6	1.5	$10x10^3$	76.92
C	24 h	R2A	Untreated	$34x10^3$	1.6	1.5	$33x10^3$	97.06
C	0 h	TSB	Untreated	$12x10^3$	1.6	1.5	$10x10^3$	83.33
C	24 h	TSB	Untreated	$25x10^3$	1.6	1.5	$23x10^3$	92.00

[a]Average of three replicate runs.

5
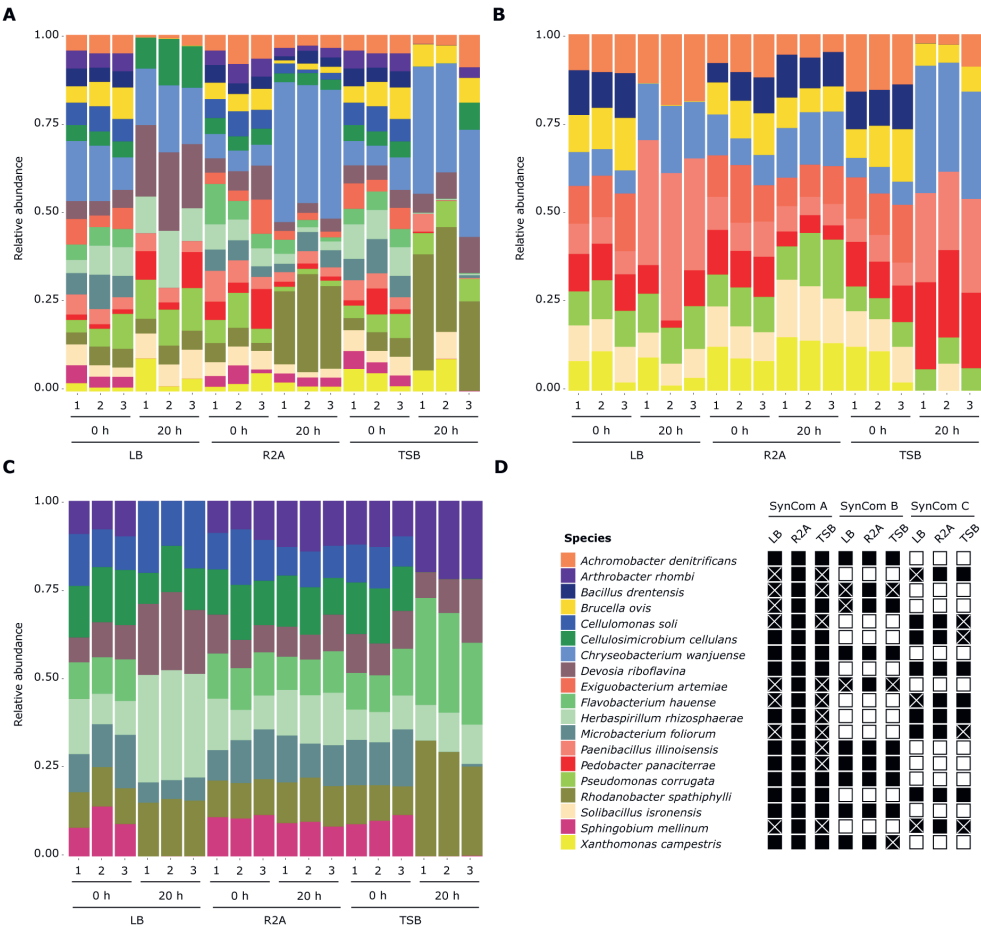
Figure 1. Relative abundance of bacterial members of three synthetic communities (SynCom) across different growth media. (A-C) Compositions of SynCom A (A), SynCom B (B), and SynCom C (C) in lysogeny broth (LB), tryptone soy broth (TSB), and Reason's 2A broth (R2A) in three replicates before (0 h) and after 20 h of incubation. (D) Schematic overview of the members that were included in each of the SynComs (black boxes), white crosses indicate members that are no longer detected after incubation.

Assessing the sensitivity of SynCom members to fungal effector proteins *in vitro*

To establish if any of the SynCom members are sensitive to AMPs, we tested the *in vitro* sensitivity of the 19 individual SynCom members to known antimicrobial effector proteins (AMPs) from plant pathogenic fungi in R2A medium. To this end, we selected the previously characterized antimicrobial effector proteins Ave1 from *V. dahliae* (Snelders et al., 2020), and proteins FUN_004580 and FUN_011519 from *R. necatrix* (Chavarro-Carrero et al., 2023; Chapter 4), while bovine serum albumin (BSA) was

included as negative control (Sun et al., 2015). Ave1 inhibited the growth of nine out of 19 bacteria, whereas inhibition of two bacteria was observed with FUN_004580 and three with FUN_011519, while BSA did not inhibit growth of any of the SynCom members (Figure 2A). To further test the sensitivity of the SynCom members we tested two effector proteins with unknown antimicrobial activity namely, the effector protein CP1 from *V. dahliae* (Zhang et al., 2017), and the LysM effector ELP2 from *Colletotrichum higginsianum* (Takahara et al., 2016). Intriguingly, five bacteria displayed sensitivity to CP1, while ELP2 inhibited the growth of one bacterium (Figure 2A). Some bacterial species were inhibited by multiple proteins. Specifically, *Xanthomonas campestris* was inhibited by Ave1 and CP1, *Achromobacter denitrificans* was inhibited by Ave1, FUN_011519, and CP1, *Bacillus drentensis* by all effectors except FUN_004580, *Sphingobium mellinum* by Ave1, FUN_011519, and CP1, and *Solibacillus isronensis* by Ave1 and CP1. Collectively, these results showed that some SynCom members are sensitive to the effector proteins tested. Based on these results we hypothesized that SynCom compositions can be modulated by the use of these antimicrobial effector proteins.

5
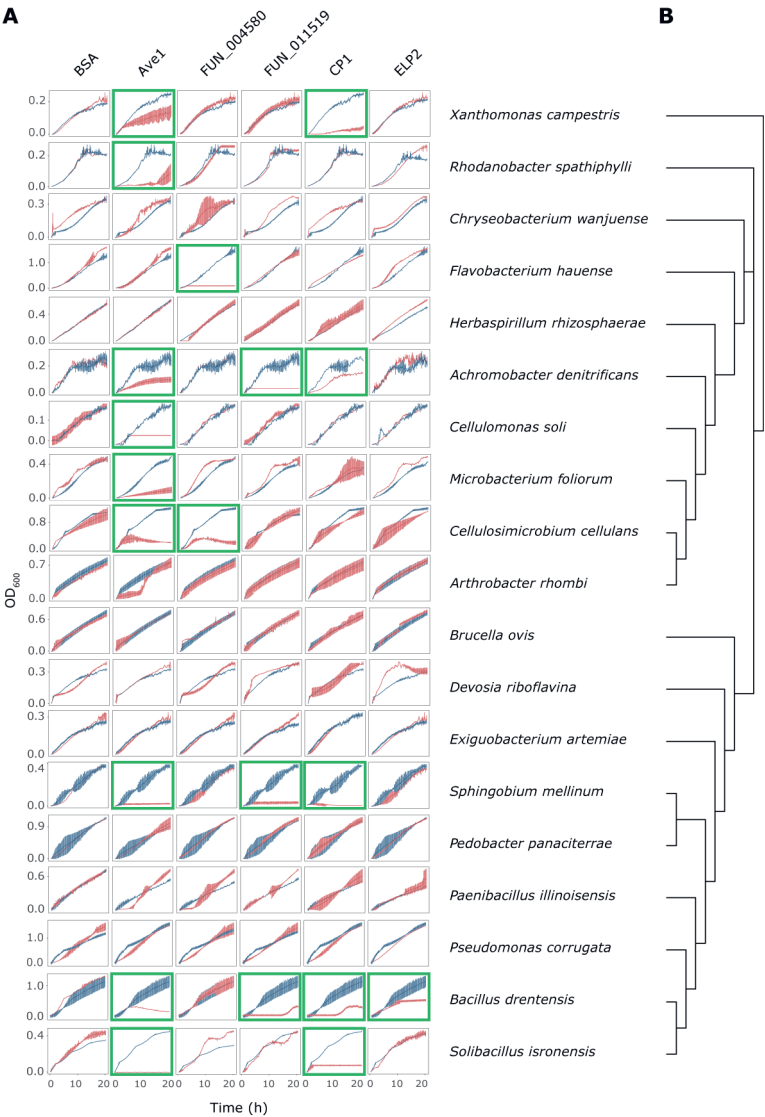
Figure 2. Sensitivity of plant-associated bacteria to antimicrobial proteins (AMPs). (A) Red lines show bacterial growth (OD600) in the presence of BSA (8 µM), Ave1 (8 µM), FUN_004580 (6 µM), FUN_011519 (10 µM), CP1 (8 µM) or ELP2 (8 µM), while blue lines show bacterial growth in R2A. Error bars display standard deviations (n=3). Green squares highlight bacterial species inhibited by the effector proteins (B) Phylogenetic tree based on whole-genome assemblies of the SynCom members inferred using Realphy (Langmead and Salzberg, 2012). Branch lengths represent sequence divergence.

Assessing antimicrobial activity of effector proteins in SynComs

To evaluate whether the effector proteins differentially modulate bacterial growth in the SynComs, we treated SynCom B and C with each of the previously tested proteins. To this end, 500 µL of each SynCom in R2A medium was mixed with 500 µL of protein solution (between 6 and 10 µM) or water as negative control in six replicate samples. Incubation, 16S profiling, and relative abundance analysis were performed as described before. Here we filtered and mapped the reads as previously described. The remaining reads account for 94% to 98.25% of the initial reads of SynCom B and from 93.75% to 99% of the initial reads of SynCom C (Table 4). While Ave1 inhibited nine bacteria when tested on individual cultures (Figure 2A), only four of these bacteria were depleted from the SynComs after incubation based on the absence of reads derived from the 16S sequences of these species, namely *Bacillus drentensis*, *Solibacillus isronensis*, *Cellulosimicrobium cellulans*, and *Sphingobium mellinum* (Figure 3). Interestingly, besides these four bacteria, also *Paenibacillus illinoisensis* (SynCom B) and *Devosia riboflavina* (SynCom C) were depleted from the SynComs treated with Ave1 (Figure 3), despite the observation that these species were insensitive to Ave1 when tested individually (Figure 2). CP1 inhibited five bacteria when tested on individual cultures (Figure 2), from which only one was depleted in SynCom B (Figure 3A, 3C). Conversely, *Cellulosimicrobium cellulans* was depleted from SynCom C when treated with CP1 (Figure 3B, 3D), while this species was not sensitive CP1 when tested individually (Figure 2). In cultures supplemented with FUN_004580, the two bacteria inhibited in individual cultures (*Cellulosimicrobium cellulans* and *Flavobacterium hauense*, Figure 2) were not depleted (Figure 3A-D), while five other bacteria were depleted from the SynComs after incubation (Figure 3A-D), despite appearing insensitive to FUN_004580 in individual cultures (Figure 2). For FUN_011519, two out of three bacteria that were sensitive to this protein (Figure 2) were depleted from the SynComs (Figure 3A-D). Furthermore, *Flavobacterium hauense* was depleted from SynCom C treated with FUN_011519 (Figure 3B, 3D), despite appearing insensitive to FUN_011519 in individual tests (Figure 2). *Bacillus drentensis* was depleted from the SynCom treated with ELP2, in agreement with its sensitivity in tests on individual cultures (Figure 2, 3A, 3C). However, also *Paenibacillus illinoisensis* and *Sphingobium mellinum* were depleted from the SynComs treated with ELP2, despite their apparent insensitivity to ELP2 in individual tests. Collectively, these results indicate that the bacterial sensitivity to AMPs differs when bacteria are cultured on their own or within a SynCom. Furthermore, even if the bacteria that were inhibited in the individual cultures were not depleted from the SynComs, the composition of SynComs shifted towards a reduction of members and a loss of diversity. To quantify the shifts in diversity of the SynComs, we calculated the Shannon diversity index (Shannon and Weaver, 1949). The SynComs treated with any

5

of the effector proteins displayed a lower Shannon diversity index than the index of the initial SynCom (0 h), and lower than the SynComs treated with water or BSA (P < 0.0001) (Figure 3E, 3F). These results imply that the SynComs treated with effector proteins carry fewer members and an uneven distribution of species abundances when compared with the initial SynCom or the water or BSA control.

Table 4. Nanopore sequencing data and amount of reads mapped to the 16S database.

SynCom	Incubation	Media used	Treatment	Amount of Nanopore reads[a]	N50 (Kb)[a]	N90 (Kb)[a]	Reads mapped[a]	% reads mapped[a]
B	0 h	R2A	Untreated	22×10^3	1.6	1.5	20×10^3	90.91
B	24 h	R2A	Water	57×10^3	1.6	1.5	56×10^3	98.25
B	24 h	R2A	BSA	52×10^3	1.6	1.5	50×10^3	96.15
B	24 h	R2A	CP1	44×10^3	1.6	1.5	43×10^3	97.73
B	24 h	R2A	FUN_004580	50×10^3	1.6	1.5	47×10^3	94.00
B	24 h	R2A	Ave1	40×10^3	1.6	1.5	38×10^3	95.00
B	24 h	R2A	ELP2	50×10^3	1.6	1.5	48×10^3	96.00
B	24 h	R2A	FUN_011519	48×10^3	1.6	1.5	47×10^3	97.92
C	0 h	R2A	Untreated	20×10^3	1.6	1.5	19×10^3	95.00
C	24 h	R2A	Water	52×10^3	1.6	1.5	51×10^3	98.08
C	24 h	R2A	BSA	33×10^3	1.6	1.5	31×10^3	93.94
C	24 h	R2A	CP1	32×10^3	1.6	1.5	32×10^3	99.00
C	24 h	R2A	FUN_004580	32×10^3	1.6	1.5	30×10^3	93.75
C	24 h	R2A	Ave1	42×10^3	1.6	1.5	41×10^3	97.62
C	24 h	R2A	ELP2	39×10^3	1.6	1.5	38×10^3	97.44
C	24 h	R2A	FUN_011519	40×10^3	1.6	1.5	38×10^3	95.00

[a]Average of three replicate runs.
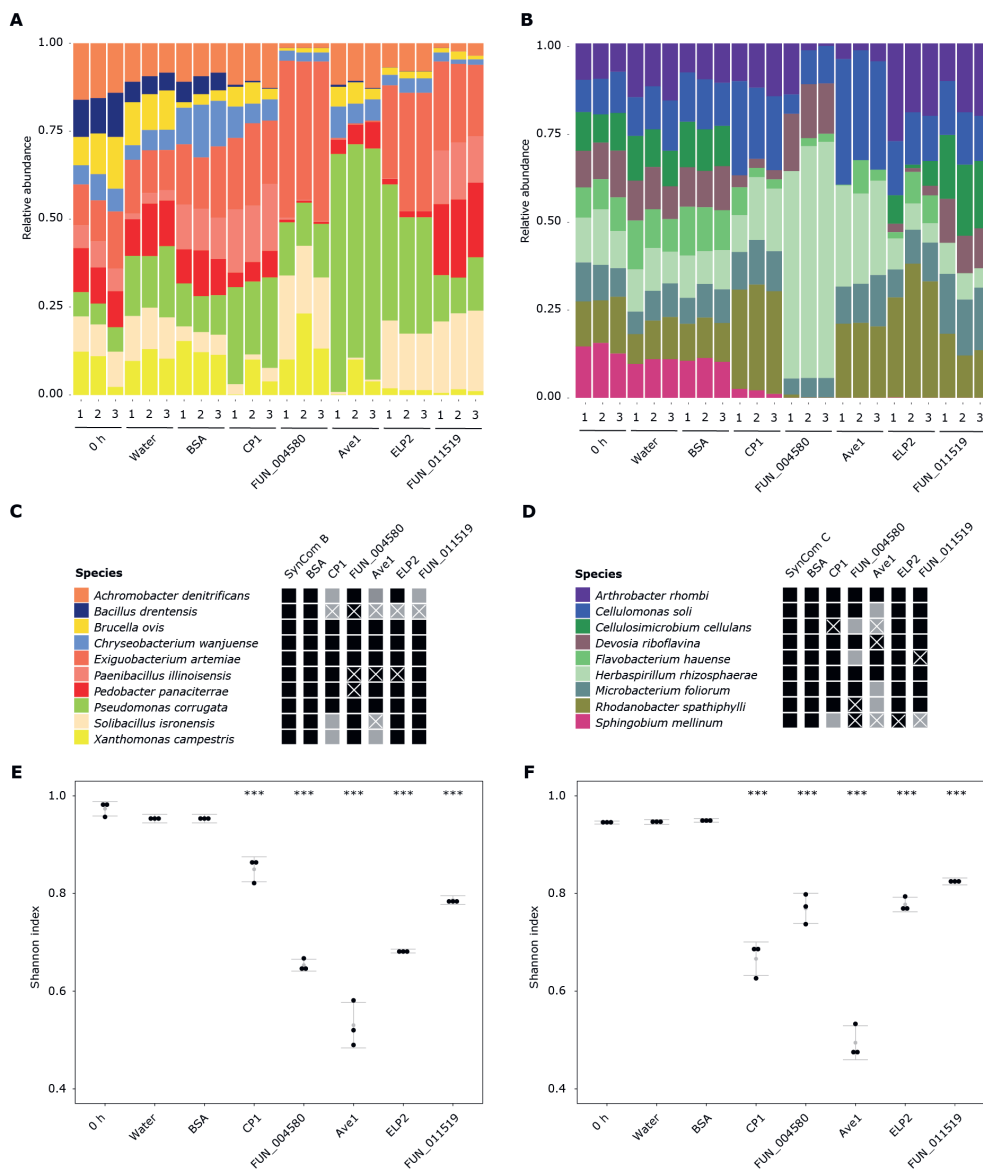
Figure 3. AMPs differentially affect the growth of members of the synthetic communities. Compositions of SynCom B (A), and SynCom C (B) in Reason's 2A broth (R2A) in three replicates before (0 h) and after 20 h of incubation in water or in the presence of BSA (8 μM), ELP2 (8 μM), Ave1 (8 μM), CP1 (8 μM), FUN_004580 (6 μM) or FUN_011519 (10 μM). (C and D) Schematic overview of the members that were included in each of the SynComs (black boxes). White crosses indicate which members were inhibited by the proteins after incubation, and gray boxes indicate the bacteria expected to be inhibited based on the individual growth assays (Figure 2). Shannon diversity index of SynCom B (E) and SynCom C (F). Asterisks indicate significant differences between protein-treated SynCom and water-treated SynCom as determined with an ANOVA followed by a Tukey test (P < 0.0001).

DISCUSSION

In this study, we aimed to identify antimicrobial activities of effector proteins by capturing synthetic community changes using ONT sequencing. To this end, we generated synthetic communities (SynComs) that represent the bacterial diversity found in plant microbiota by employing a collection of tomato-associated bacteria (Chavarro-Carrero et al., 2023) (Table 1). We show a disparity in bacterial responses to AMPs when cultured individually versus within SynComs, pointing towards a microbial interplay within complex microbial communities that affects their sensitivity towards particular antimicrobials. Several studies have highlighted the significant differences in bacterial responses when studied individually versus within complex microbial communities (Bottery et al., 2021). Such differences can be divided into three main mechanisms in which bacterial communities respond to exposure to antimicrobials due to interspecies interactions. Firstly, through collective resistance, where interactions within a community enhance the ability of its members to resist the action of an antimicrobial. For example, the enzymatic inactivation of β-lactam antibiotics via β-lactamase produced by *Escherichia coli* can protect the community member *Salmonella enterica* from concentrations of the antibiotic that would usually kill this bacterium in isolation (Perlin et al., 2009). Such collective resistance acknowledges that the benefit of antibiotic-inactivating enzyme production is not confined to the producer, rather it is shared across the community (Yurtsev et al., 2013; Bottery et al., 2016). Secondly, differences in bacterial responses between communities and individual species can be observed through collective tolerance, where interactions within a community alter cell state, slowing down the metabolism, and thus slowing down the rate of cell death during exposure to antimicrobials. It was reported, for example, that within an *in vitro* biofilm model of cystic fibrosis infection on lung epithelial cells, *Pseudomonas aeruginosa* could cause a metabolic shift in *Staphylococcus aureus*, reducing its growth and thereby providing *S. aureus* protection from the antibiotic vancomycin (Orazi and O'Toole, 2017). Reciprocally, *S. aureus* could enhance tobramycin tolerance of *P. aeruginosa* by increasing aggregation and altering the biofilm architecture of the bacterial community (Beaudoin et al., 2017). Lastly, differences in responses between communities and individual species can be caused by exposure protection, where interactions within a community protect its most sensitive members during antibiotic treatment. For example, it has been shown that antibiotic treatment of brewery bacteria communities, which were dominated by competitive interactions, resulted in reduced levels of competition due to the inhibition of highly competitive species within the population. This led to increased growth of species that were otherwise suppressed within the population (Parijs and Steenackers, 2018) and therefore elevated the antibiotic tolerance of these species, likely due to the density-dependent nature of collective tolerance mechanisms. Similar results were observed

within experimental bacterial communities (Cairns et al., 2018). Furthermore, indirect effects have been observed where the secretion of metabolites by one bacterium can induce a resistance mechanism to an antimicrobial compound in a different bacterium. For example, the secretion of indoles by *E. coli* activated the expression of an indole-dependent multi-drug efflux pump in *Pseudomonas putida*, which cannot produce the indole itself, leading to elevated levels of resistance to multiple antibiotics in *P. putida* (Molina-Santiago et al., 2014). In conclusion, our study shows that bacterial sensitivity to AMPs is different when the species are cultured individually versus within SynComs.

It has been established that fungal soil-borne plant pathogens secrete antimicrobial effector proteins to modulate root microbiota compositions to facilitate plant host colonization (Snelders et al., 2020; 2021; 2022; 2023; Chavarro-Carrero et al., 2023). In our study, we developed a methodology to demonstrate such antimicrobial activities of effector proteins using SynComs. We successfully showed shifts in SynCom composition caused by the known antimicrobial effector proteins Ave1, FUN_004580 and FUN_011519. Additionally, we revealed antimicrobial traits of two novel effector proteins that were not previously reported to possess such activity (CP1 and ELP2). We quantified these shifts in SynCom composition using the Shannon diversity index and showed that the SynComs treated with the effector proteins carry fewer members and lead to an uneven distribution of species abundances when compared with the initial SynCom or the water or BSA control. However, we also showed a discrepancy in bacterial sensitivity to AMPs when cultured individually versus within SynComs, suggesting the resilience of some bacterial species to AMPs or the emergence of previously undetected sensitive species within the context of the SynComs. Such differences have already been described for the antimicrobial effector protein Ave1. Studies with single bacterial cultures showed different sensitivity of certain bacterial species when compared to root microbiome and SynCom compositions (Snelders et al., 2020). Therefore, our findings show that SynComs can successfully be used to identify antimicrobial activities, but unraveling target ranges remains challenging. The use of plant-associated microbial communities that are relevant for the context of the plant-pathogen interaction will be more informative about true bacterial target ranges than studies with single bacterial cultures

The ability to precisely identify changes in SynCom compositions at the species level through Nanopore sequencing is fundamental to understanding the impact of antimicrobial activities within complex plant-associated microbial consortia. In the present study, we showed that Nanopore captures the complete composition of the initial SynComs (0 h) as well as the complete SynCom composition when all members are present after 24h incubation in R2A. We validated the alignment accuracy of Nanopore-generated reads against the 16S sequence database. Specifically, we retained reads

5

>1 kb, as they encompassed multiple essential variable regions crucial for accurate bacterial species identification (Bukin et al., 2019). Additionally, we maintained reads with high identity and excluded those mapping to multiple 16S sequences in the dataset, even though they constituted less than 1% of the reads generated in each experiment. Overall, we showed that on average 94% of the Nanopore reads aligned to a specific 16S sequence in the dataset. Furthermore, we showed how Nanopore sequencing captures shifts within SynComs based on the absence of particular 16S sequences although, admittedly, we have not validated the Nanopore sequencing-based quantification with an independent other method such as real-time PCR, for example. This methodology can further be exploited with diverse SynCom compositions, for example, with SynComs that carry closely related species that can be distinguished with full-length 16S rRNA sequencing, potentially overcoming the limitations of short-read sequencing technologies (Frank et al., 2008). Furthermore, it may be attractive to exploit Nanopore sequencing on *in planta* conditions to reveal plant microbiota composition shifts caused by AMPs. Currently, Nanopore sequencing of environmental DNA (eDNA) from water samples was shown to successfully capture the microbiota diversity from such environment, improving the taxonomical resolution as compared to short-read sequencing technologies (Egeter et al., 2022; Doorenspleet et al., 2023).

To generate SynComs that accurately represent the bacterial diversity found in the plant microbiota, we selected a single bacterial strain representing each of the 19 taxonomical families previously identified in a collection of tomato-associated bacteria (Table 1) and designed three different SynComs. Our approach involved testing the growth of the SynComs after 20 hours of incubation in different growth media, considering that food sources can impact bacterial growth (Großkopf and Soyer, 2014), we showed that not all SynComs members incubated in lysogeny broth (LB) or tryptone soya broth (TSB) were present after incubation; while in Reason's 2A broth (R2A) all SynCom members were present. Therefore, we selected R2A as the suitable medium for SynCom composition. The selection of R2A as the most suitable medium for our SynComs aligns with previous studies demonstrating its efficacy in promoting the growth of diverse bacterial species (Yoon et al., 2012; Mangrola et al., 2017). The low-nutrient composition of R2A broth allows for the cultivation of fastidious and slow-growing bacteria that may not thrive in more nutrient-rich media like LB or TSB (Wang et al., 2021). This characteristic of R2A makes it an ideal choice for fostering the growth of a diverse SynCom representing multiple taxonomical families (Wang et al., 2021). Besides medium selection, bacteria selection plays an important role when designing SynComs. The designing, assembling, and testing SynComs can be divided into two approaches (van Leeuwen et al., 2023). The top-down approach starts at the microbial composition profiling from the environmental niche to study, followed by the selection

of which bacteria are added into the SynCom, and subsequently profiling to confirm the presence of all initial bacteria to then either adjust the SynCom members or use the adapted SynCom (Atarashi et al., 2013). The top-down approach identifies the most abundant bacteria and assembles a subset that captures the diversity of the native microbiota (Vazquez-Castellanos et al., 2019). The bottom-up approach uses existing knowledge of the metagenome, abundances, and growth parameters of candidate microorganisms. Furthermore, when the SynCom is required to have a specific function, the candidate microorganisms can be adjusted accordingly (van der Lelie et al., 2021). In our study, we successfully use a top-down approach that allows us to capture the diversity of a plant-associated bacteria collection in two SynComs that were used to explore the antimicrobial activity of effector proteins.

In conclusion, our study provides a methodology to demonstrate the antimicrobial activities of effector proteins through the use of synthetic communities (SynComs) and highlights the importance of using relevant plant-associated microbial communities to reveal bacterial target ranges of specific antimicrobials. This contributes to our understanding of the dynamic interactions of plant pathogens with plant-associated microbial communities and highlights the tools and strategies necessary for comprehensive analysis of effector functions as antimicrobials.

5

MATERIALS AND METHODS

High Molecular Weight (HMW) DNA isolation and Nanopore sequencing

Bacterial cells were grown in R2A medium overnight at 22°C with constant shaking at 120 rpm. Next, bacterial cells were pelleted and DNA isolation was performed. For this, bacterial cells were incubated for 20 minutes at 37°C with 400 µL TEN buffer (10 mM Tris/HCl pH 8.0, 10 mM EDTA, 150 mM NaCl) and 20 µL lysozyme (20 mg/µL). After incubation, 3 µL of RNase A (20 mg/µL) was added and incubated for 5 minutes at 65°C. Subsequently, 40 µL of SDS (10% w/v), 2 µL of proteinase K (20 mg/µL), and 550 µL of TEN-reduced buffer (10 mM Tris/HCl pH 8.0, 1 mM EDTA, 50 mM NaCl) was added and incubated for 2 hours at 60°C. Next, 900 µL of phenol was added followed by centrifugation at 13,000 g for five minutes. After transferring the aqueous phase to a new tube, the phenol extraction was repeated. After transfer of the aqueous phase to a new tube, chloroform was added (1:1), shaken, and centrifuged at 16,000 g for 5 min at RT, after which the chloroform extraction was repeated. Next, the aqueous phase was mixed with 10 volumes of ice-cold 100% ethanol at RT, and the DNA was fished out using a glass hook, transferred to a new tube, and washed twice with 500 µL 70% ethanol. Finally, the DNA was air-dried, resuspended in nuclease-free water, and incubated at 4°C overnight. The DNA quality, size, and quantity were assessed by Nanodrop, gel electrophoresis, and Qubit analyses.

Library preparation was performed with the Ligation sequencing DNA V14 kit (SQK-LSK114; Oxford Nanopore Technologies, Oxford, UK) according to the manufacturer's instructions. An R10 flow cell (Oxford Nanopore Technologies, Oxford, UK) was loaded with 400 ng HMW DNA and run for 24 hours. Base calling was performed using Guppy (version 3.1.5; Oxford Nanopore Technologies, Oxford, UK) with the high-accuracy base-calling algorithm. Adapter sequences were removed using Porechop (version 0.2.4 with default settings; Wick, 2018). Finally, the reads were self-corrected, trimmed, and assembled using Canu (Version 1.8; Koren et al., 2017) (Table 1). From each genome assembly, the 16S rRNA gene was extracted by using BLAST searches based on the 16S sequences originally obtained for identification, and used to create a local database.

Antimicrobial activity assays employing SynComs

The SynComs were grown in 2 mL Eppendorf tubes (n=6) in 500 µL R2A medium treated with 500 µL of demineralized water or one of the effector proteins tested (Table 5) to a final concentration of OD600 = 0.025. To confirm initial SynCom composition, the treated SynComs were immediately used for DNA extraction (n=3), and also after incubation for 22 hours at 22°C with constant shaking at 120 rpm (n=3). Next, DNA was

used to prepare the 16S rRNA gene amplicon library.

Table 5. Effector proteins.

Protein	Species	Protein size (kDa)	Cys (%)	pI	Reference
Ave1	*Verticillium dahliae*	12.6	3.45	9.02	de Jonge et al., 2012
CP1	*Verticillium dahliae*	12.6	3.33	8.50	Zhang et al., 2017
FUN_004580	*Rosellinia necatrix*	42.55	2.48	4.86	Chavarro-Carrero et al., 2023
FUN_011519	*Rosellinia necatrix*	3.65	5.71	4.88	Chavarro-Carrero et al., 2023
ELP2	*Colletotrichum higginsianum*	16.1	3.98	4.64	Takahara et al., 2016

[a]Average of three replicate runs.

Nanopore 16S profiling

Library preparation with the rapid 16S barcoding sequencing kit (SQK-16S024) was performed according to the manufacturer's instructions (Oxford Nanopore Technologies, Oxford, UK) with 400 ng HMW DNA. An R10 flow cell (Oxford Nanopore Technologies, Oxford, UK) was loaded and run for two hours. Base calling was performed using Guppy (version 3.1.5; Oxford Nanopore Technologies, Oxford, UK) with the high-accuracy base-calling algorithm. Adapter sequences and barcodes were removed using Porechop (version 0.2.4 with default settings; Wick, 2018). Using the customized reference database for bacteria classification of each bacterial strain included within the SynComs. Read mapping of the 16S rRNA gene reads on the custom database was performed with VSEARCH (version 2.23.0; Rognes et al., 2016) using the *vsearch --usearch_global* command with the *--sizein --id 0.85 –sizeout* parameters. Briefly, *–sizeout* option was set to 1000 retaining only reads with a length exceeding 1,000 bp. Relative abundance of the reads was then calculated and plotted using the R package "ggplot2" (Wickham, 2016).

In vitro antimicrobial activity assays

Growth assays were performed as previously described (Snelders et al., 2020; Chavarro-Carrero et al., 2023). Briefly, bacterial strains were grown overnight on lysogeny broth agar (LBA), at 28°C. Subsequently, single colonies were selected and grown overnight at 28°C while shaking at 130 rpm in Reason´s 2A broth (R2A). Overnight cultures were resuspended to OD600 = 0.05 in 100 µL of R2A and treated with 100 µL of purified effector proteins or water reaching a final OD600 of 0.025 in clear 96 well flat-bottom

5

polystyrene tissue culture plates (Greiner CELLSTAR®, Sigma, Burlington, Kentucky, U.S.A) that were incubated in a CLARIOstar plate reader (BMG LABTECH, Ortenberg, Germany) at 25°C with double orbital shaking parameter every 15 minutes and OD600 measurement every 15 minutes.

5

5

Chapter | **6**

General discussion

In nature, microbes engage with plants in positive (beneficial), neutral (commensal), and negative (parasitic) interactions. Particularly microbial pathogens engage in negative interactions that typically result in plant disease. Worldwide, crop losses due to plant diseases are estimated to amount up to 25% during plant cultivation as well as afterwards during storage as post-harvest diseases, causing a total annual loss of ~$220 billion (Agrios, 2005).

Studying the molecular basis of plant-pathogen interactions has been of great interest to understand how plant pathogens cause plant diseases. It is presently appreciated that plant pathogens secrete dozens to hundreds of effector molecules into the apoplast or cytosol of their host plants to mediate host colonization (Rovenich et al., 2014). In the narrowest definition, these effectors can be defined as small, secreted proteins of ≤300 amino acids that are cysteine-rich and have tertiary structures that are stabilized by disulfide bridges (Duplessis et al., 2011; Gan et al., 2013; Stergiopoulos et al., 2013; Lo Presti et al., 2015). However, more relaxed definitions also consider other types of secreted proteins, as well as non-proteinaceous molecules that are secreted to support host colonization (Weiberg et al., 2014; Collemare et al., 2019). Although it was initially proposed that effectors act in the suppression of host immunity and manipulation of other host physiological processes, recent studies have revealed that effector proteins can also modulate plant-associated microbiota compositions inside as well as outside of the host plant to support host colonization (Snelders et al., 2020; 2021; 2022; 2023). Although the primary role of effectors is to act as virulence factors by facilitating disease establishment, some effectors can also be recognized by the plant immune system, leading to the triggering of immune responses. These recognized effectors are then termed avirulence effectors (Avrs).

In my thesis, I identified new fungal pathogen effectors and investigated their role in the interaction with plant hosts. I identified the *Verticillium dahliae* avirulence gene encoding the Av2 effector that is recognized in tomato plants carrying the *V2* resistance locus (Chapter 2). Although a virulence function of this effector could not be demonstrated in our assays, we still expect this effector to contribute to host colonization. However, it is possible that this effector is functionally redundant with other effectors, and consequently targeted deletion did not result in a noticeable phenotype. Alternatively, the virulence function is only relevant under specific conditions that were not captured in our analyses. Furthermore, I revealed the contribution of the *V. dahliae* effector catalogue to disease development in roses (Chapter 3). In this chapter, I demonstrated that various effectors contribute to Verticillium wilt disease in roses and showed that a particular effector is responsible for defoliation symptoms. Furthermore, I sequenced the genomes of a collection of *Rosellinia necatrix* strains and identified the effector catalogue of one of the strains. Excitingly, I characterized two of the

6

effectors that are secreted during host colonization and propose that they act in host microbiota manipulation (Chapter 4). In the last experimental chapter, I assessed how Nanopore sequencing can be used as a tool to demonstrate microbiota manipulation by fungal effector proteins (Chapter 5). Finally, in the current chapter, I discuss the results obtained in my thesis, and I provide perspectives for the identification of effectors and characterization of their role in microbiota manipulation in a broader context.

Effector identification and functional characterization in soil-borne fungal pathogens

Effectors are of great interest to understand the molecular basis of plant-pathogen interactions. Initially, effectors were identified based on their recognition by plant immune receptors as avirulence effectors (Flor, 1942). This led to the use of effectors to detect resistance (*R*) genes as well as to detect pattern recognition receptors (PRRs), by functionally screening plant germplasm for immune responses to effectors (Vleeshouwers and Oliver, 2014; Seidl and van den Ackerveken, 2019). Thus, effector identification and functional characterization remains an important strategy to identify candidates that can be used for resistance screenings.

Over the last decade, major advances in next-generation sequencing have led to an increase in the availability of fungal genomes. Initially, Illumina and Thermo Fisher offered short-read (100 to 400 bp) sequencing platforms, while more recently Pacific Biosciences and Oxford Nanopore Technologies (ONT) developed long-read (>500 bp) sequencing platforms (Shendure and Ji, 2008; Gu et al., 2019; Petersen et al., 2022). Nowadays, sequencing technologies have improved even further and third-generation sequencing technologies, such as Oxford Nanopore Technologies (ONT), provide rapid, portable, and low-cost alternatives for in-house sequencing (ONT, 2020). Consequently, high-throughput generation of long reads in a pocket-sized portable device called MinION has become available to any molecular biology laboratory (Lu et al., 2016). Although Nanopore sequencing can produce reads of up to 2 Mb in length (Payne et al., 2019), the major disadvantage to date has been the high error rate (~10%) with their flow cells until recently (Lu et al., 2016). However, the latest generation of flow cells (version 10) utilize a new type of nanopore, and it has been claimed that this flow cell can deliver up to 99.99% base-calling accuracy (ONT, 2022). Nevertheless, despite the lower accuracy in base calling with earlier versions of the MinION flow cells, the use of Nanopore sequencing has gained popularity. To compensate for the error rate, often parallel sequencing with Illumina has been employed to correct the long reads. In addition, long reads generated by ONT have been used to fill in gaps in genomes that were assembled based on short-read platforms (Wick et al., 2017; George et al., 2017; Judge et al., 2016; Tyson et al., 2018). Throughout my thesis research, I successfully

6

exploited Nanopore sequencing (Chapters 2, 3, and 4) to increase the contiguity of genome assemblies that before were more fragmented and achieved with short-read sequencing approaches, which allowed the generation of a chromosome-level genome assembly of *R. necatrix* (Chapter 4). Furthermore, I exploited Nanopore sequencing to identify effector catalogs in the soil-borne pathogens *R. necatrix* and *V. dahliae* (Chapters 2, 3, and 4). In conclusion, Nanopore is a rapid in-house alternative to obtained more contiguous genomes when compared with short-read sequencing technologies.

The increasing availability of genome assemblies has allowed the prediction of effectors in several microorganisms using a diversity of approaches. Many bacterial pathogens have been shown to directly inject effectors into the host cytoplasm via a specialized secretion machinery, namely the type III secretion (T3S) system (Cambronne and Roy, 2006). To this end, and N-terminal sequence signal directs these bacterial effectors to the T3S system, and therefore machine learning approaches have been developed to predict effectors from bacterial genome sequences (McDermott et al., 2011). For oomycete effectors, the RxLR (Arg-x-Leu-Arg) and LxLFLAK amino acid motifs in the N-termini of effector proteins have been proposed to mediate host cell translocation (Whisson et al., 2007; Schornack et al., 2010). Accordingly, these consensus motifs can be used to query for so-called RxLR and Crinkler (CRN) effectors encoded in oomycete genomes (Tyler et al., 2006; Haas et al., 2009).

Prediction of effectors of fungal pathogens is less intuitive, as fungal effectors lack significant sequence similarity and consensus motifs (Sperschneider et al., 2015). Most characterized fungal effectors are small, secreted proteins (≤300 amino acids), cysteine-rich, and contain tertiary structures that are stabilized by disulfide bridges (Duplessis et al., 2011; Gan et al., 2013; Stergiopoulos et al., 2013; Lo Presti et al., 2015). However, larger secreted proteins have also been found to act as effectors, such as several LysM effectors (Djamei et al., 2011; Kombrink and Thomma, 2013). For fungal effector prediction, a machine-learning tool called EffectorP is generally used, which is trained to predict effector proteins from secretomes based on sequence properties, such as sequence length, molecular weight, protein charge, and cysteine, serine, and tryptophan content (Sperschneider et all., 2016). Together with *in planta* expression data, EffectorP has been used successfully to prioritize putative effector candidates (Sperschneider et al., 2016). These effector candidates can be then further functionally characterized to unravel their involvement in plant disease establishment.

More and more effectors have been studied regarding their role in plant disease establishment, which has revealed a wide diversity of functions in a wide range of cellular compartments (Göhre and Robatzek, 2008; Pritchard and Birch, 2011; de Jonge et al., 2011; Lo Presti et al., 2015; Kanja and Hammond-Kosack, 2020). Among the diverse functions described for effectors, pathogens have been shown to secrete

particular effectors to degrade cell wall polysaccharides to break down the cell wall during infection. Disruption of the sucrose *nonfermenting 1* (*SNF1*) gene in *Fusarium oxysporum* and *V. dahliae*, which encodes part of a kinase complex regulating the expression of CWDEs, compromises virulence (Ospina-Giraldo et al., 2003; Tzima et al., 2011). Studies in *F. oxysporum* f. sp. *lycopersici*, *V. dahliae*, *Ralstonia solanacearum*, *Phytophthora parasitica*, and *Phytophthora sojae* have shown that individual CWDEs can contribute to virulence (Novo et al., 2006; Wu et al., 2008; Poueymiro and Geran, 2009; Maruthachalam et al., 2011; Ma et al., 2015; Bravo-Ruiz et al., 2016). Other types of effectors were shown to prevent cell wall hydrolysis by plant chitinases and interfere with host immune responses. Lysin motif (LysM) effectors, such as Avr4, Ecp6 from *Cladosporium fulvum*, and Vd2LysM from *V. dahliae*, typically bind chitin and play roles in virulence through suppression of chitin-triggered immunity or shielding hyphae against host-derived chitinases (de Jonge et al., 2010; Kombrink and Thomma, 2013; Tian et al., 2021; 2022).

A different type of effectors is involved in the inhibition of plant proteases that are induced in the presence of pathogens as essential components of plant immunity. Two serine proteases, the extracellular proteinase inhibitor 1 and 10 (EPI1 and EPI10) from *Phytophthora infestans* were found to inhibit the tomato serine protease P69B (Tian et al., 2004; 2005). Furthermore, the effector EPIC1 and EPIC2B from *P. infestans* (Song et al., 2009), Avr2 from *Cladosporium fulvum* (Rooney et al., 2005), and Gr-VAP1 from the nematode *Globodera rostochiensis* (Lozano-Torres et al., 2012) inhibit the tomato PLCP (papain-like cysteine protease) Rcr3 (Required for *Cladosporium* resistance-3).

Another type of effectors is also associated with necrotic activity in dicotyledonous plants through plasma membrane permeabilization and cytolysis of plant cells (Ottmann et al., 2009). The necrosis and ethylene-inducing peptide 1 (NEP1) was originally identified in *F. oxysporum* (Bailey, 1995), and NEP1 homologues are named as NLPs (NEP1-like proteins). NLPs are widely distributed in microorganisms and are found in bacteria, fungi, and oomycetes (Gijzen and Nürnberger, 2006; Oome and van den Ackerveken, 2014; Seidl and van den Ackerveken, 2019). Most identified NLPs not only trigger cell death but also elicit strong immune responses in dicots (Gijzen and Nürnberger, 2006). NLP effectors show functional diversification in various pathogens (Dong et al., 2012; Zhou et al., 2012; Santhanam et al., 2013; Oome and van den Ackerveken, 2014). In *V. dahliae* the expanded NLP family displays functional diversification, with differential cytotoxicity and host-dependent virulence (Zhou et al., 2012; Santhanam et al., 2013). In chapter 3, I showed that various *V. dahliae* effectors contribute to Verticillium wilt disease in roses. Furthermore, I also observed functional diversification of NEP1 and NEP2, as NEP2 was not expressed during rose colonization while NEP1 contributes to disease establishment. Additionally, two distinct disease symptoms were observed,

6

stunting and defoliation. While most effectors contribute to stunting in roses, the D effector was shown to be responsible for the defoliation symptom in roses. This effector was previously identified based on comparative genomics between *V. dahliae* isolates belonging to the defoliating and the non-defoliating pathotype, and its role in defoliation was described in cotton and olive plants (Li, 2019).

Although different functions executed by pathogen effector proteins during plant colonization have been elucidated, the contribution to disease establishment and the functions of most candidate effectors remain unknown today. Mainly due to the sequence uniqueness of most effectors (i.e., many are strain- or species-specific) and the lack of known protein domains, functional characterization based on homology is complicated. Consequently, determination of effector functions and contribution to disease establishment typically depends on dedicated functional characterization studies based on experimental approaches trying to identify direct interactions of effectors with the plant. Interestingly, recent studies have shown that effector proteins also modulate the plant-associated microbiota to support host colonization (Snelders et al., 2020; 2021; 2022; 2022b). For instance, it was demonstrated that the effector protein Ave1 from the soil-borne pathogen *V. dahliae* displays selective antimicrobial activity against antagonistic members of the *Sphingomonadaceae*, facilitating the colonization of tomato and cotton plants (Snelders et al., 2020). Additionally, ten potentially antimicrobial effector protein candidates were predicted by mining the *V. dahliae* secretome for structural homologues of known antimicrobial proteins (AMPs) (Snelders et al., 2020). From these candidates, VdAMP2 was subsequently found to contribute to *V. dahliae* survival in soil through its efficacy in microbial competition (Snelders et al., 2020), while VdAMP3 was shown to have antifungal activity to promote microsclerotia formation in decaying host tissue (Snelders et al., 2021). Most recently, a multiallelic gene homologous to VdAve1 was identified as VdAve1-like (VdAve1L) of which the VdAve1L2 variant suppresses antagonistic Actinobacteria in the host microbiota to promote tomato colonization (Snelders et al., 2022). Until that moment, *V. dahliae* was the only fungal pathogen that was shown to exploit effector proteins for microbiota manipulation to support host colonization (Snelders et al., 2022). Interestingly, in my thesis, I identified two effectors (FUN_004580 and FUN_011519) that are secreted by the soil-borne pathogen *R. necatrix* that, during host colonization, possess selective antimicrobial activity against fungi and antagonistic plant-associated bacteria that reduce Rosellinia root rot disease in cotton (Chapter 4). These results support the hypothesis that also other pathogenic fungi, like demonstrated for *V. dahliae*, exploit effector proteins with antimicrobial activity during host colonization, although it needs to be acknowledged that genetic evidence implicating the *R. necatrix* effectors in disease development is still lacking.

Effectors have been extensively studied in binary contexts in plant-pathogen interactions. Nevertheless, plants coexist with a plethora of microorganisms and are engaged in more complex interactions than merely in one-to-one interactions. Plants actively employ exudates to recruit mutualists and beneficial endophytes to assemble an associated microbiota (Bais et al., 2006; Rudrappa et al., 2008; Mendes et al., 2011; Berendsen et al., 2012; van der Heijden et al., 2015; Huang et al., 2019; Koprivova et al., 2019). Such beneficial microbes can contribute to plant health, for instance by promoting nutrient acquisition, enhancing abiotic stress tolerance, or suppressing pathogen attack (Dimkpa et al., 2009; Innerebner et al., 2011; Vorholt, 2012; Almario et al., 2017; Durán et al., 2018; Lu et al., 2018; Stringlis et al., 2018; Carrión et al., 2019; Fitzpatrick et al., 2019; Sarkar et al., 2019; Chen et al., 2020; Pfeilmeier et al., 2021; Yu et al., 2021). The complex dynamics of the microbiota with the plant, together with the functions performed for the plant, makes the plant-associated microbiota an essential contributor to plant health. Plants can therefore be considered as "meta-organisms" or so-called "holobionts", composed of the plant and its associated microbiota. Accordingly, effectors should not only be studied regarding their direct interaction with the plant but rather study in the context of the holobiont. Moreover, fungal effectors that target host physiology may also impact the host microbiota composition indirectly. Recent studies showed that *Zymoseptoria tritici* induces local and systemic modulation of wheat leaf microbiota compositions during plant colonization that are probably the result of effector-mediated immune suppression (Seybold et al., 2020). Therefore, fungal pathogens may employ effectors to indirectly manipulate the host microbiome to ultimately colonize distal tissues.

To date, effector involvement in plant-associated bacterial microbiota manipulation by fungal plant pathogens has been initially investigated by performing experiments with single bacterial strains, synthetic communities, and natural microbiota compositions *in planta* for each effector protein candidate (Snelders et al., 2020; Snelders et al., 2022). Particularly experiments with individual bacterial strains typically requires screening of relatively large quantities of taxonomically diverse bacterial species to find inhibition of specific bacteria that ultimately shed light on the activity spectrum of each potential effector candidate, especially if the effector displays selective antimicrobial activity, which is time-consuming and requires large amounts of protein that can be challenging to obtain. To date, microbiota profiling is typically been performed based on 16S sequencing using the Illumina sequencing technology (Heikema et al., 2020; Celikkol-Aydin et al., 2016; Salipante et a., 2014; Ong et al., 2013). However, Illumina sequencing is limited to short (<600 bp) fragments, prohibiting sequencing of the entire 16S rRNA gene (~1,500 bp) (Fan et al., 2006). Therefore, relative abundances of individual taxa are determined by analyzing subregions of the 16S rRNA gene, and the

6

obtained results are biased by the selected subregion due to distinct primer binding affinities to each template (Polz and Cavanaugh, 1998; Kanagawa, 2003; Pollock et al., 2018). Nowadays, third-generation sequencing technologies, such as Oxford Nanopore Technologies (ONT), represent an alternative for Illumina sequencing as it allows sequencing of the complete 16S region in samples with bacterial mixtures. In my thesis research, I successfully exploited ONT sequencing to assess microbiota manipulation by fungal effector proteins (Chapter 5). More specifically, I developed stable synthetic communities (SynComs) of taxonomically diverse bacterial species from a plant-associated microbiota and demonstrated the selective antimicrobial activities of diverse fungal effector proteins on these SynComs with 16S profiling based on ONT sequencing.

Antimicrobial activity as new tool in the effector toolbox to develop innovative plant disease control strategies

The notion that some effector proteins can modulate plant-associated microbiota compositions to support host colonization can help to develop new plant disease management strategies. Biocontrol agents (BCAs) have been used as a strategy for plant disease control for many years, albeit with variable success. Biocontrol species from the bacterial genera *Bacillus* and *Pseudomonas*, and the fungal genus *Trichoderma*, are widely used as BCAs that are beneficial for plant health that may act through several mechanisms, including direct antagonism, plant growth promotion, and the induction of systemic immune responses in their plant hosts (Dimkić et al., 2022).

Bacillus is a phenotypically and genotypically heterogeneous group of Gram-positive bacteria commonly found in diverse environments (Abriouel et al., 2011). They are important members of the plant microbiota and play a significant role in plant disease management (Albayrak, 2019). Potential for biocontrol activity for several *Bacillus* species and strains has been demonstrated through direct antagonism, induction of plant immune responses, and competition for nutrients and space (Nakkeeran et al., 2019; Andrić et al., 2020). Interestingly, different compounds with antimicrobial activity (lipopeptides, antibiotics, and enzymes) have been characterized in *Bacillus*. *Bacillus thuringiensis* and *Bacillus cereus* have been shown to produce Zwittermicin A, which is an antibiotic with antagonistic activity against oomycetes, fungi, and bacteria (Nakkeeran et al., 2019). In the same manner, *Bacillus subtilis* has been shown to produce several antibiotics, such as bacitracin, bacilysin, rhizocticin, petrobactin, and bacillibactin with antibacterial and antifungal properties (Özcengiz and Öğülür, 2015). In chapter 4, I showed that the soil-borne fungal pathogen *R. necatrix* utilizes AMPs to inhibit particular plant-associated antagonistic bacteria. Among other plant-associated bacterial species, the effector FUN_011519 inhibits *Bacillus drentensis* that has the capacity to reduce Rosellinia rot root disease in cotton plants. Although this finding

might suggest that *B. dentrensis* could act as biocontrol agent to reduce Rosellinia rot root disease, I showed that *R. necatrix* also exploits effectors to target *B. dentrensis* during host colonization. To overcome this, effective BCAs need to be mutagenized to become tolerant to the pathogen AMPs. Such bacterial mutants that are tolerant to a specific effector AMP could be obtained through evolution experiments. As a proof of principle, the Ave1-sensitive bacterium *B. subtilis* was exposed to the *V. dahliae* effector protein Ave1 throughout repetitive transfers of the bacterium to a medium with a gradual concentration increase of the effector protein Ave1 until a tolerant *B. subtilis* mutant was obtained (Snelders, 2020). Nevertheless, the mutagenized bacteria need to be tested for use in crop soils. In the case of *R. necatrix*, mutagenized *B. dentrensis* should be able to establish itself in the soil microbiota community and successfully colonize the plant host to ultimately be able to be use as BCA.

Plant disease management strategies include disease forecasting, physical and chemical techniques, biocontrol strategies, plant resistance breeding, and cultural modifications. Knowledge of effector functions can help to develop more reliable combinations of plant disease management strategies. For example, a *V. dahliae* effector that is secreted during host colonization and that is recognized by tomato carrying the Ve1 resistance gene was identified as Ave1 (de Jonge et al., 2012). Ave1 acts as a virulence factor on tomato plants that lack the *Ve1* gene and that, consequently, cannot recognize Ave1 (de Jonge et al., 2012). Ave1 also displays selective antimicrobial activity against antagonistic members of the *Sphingomonadaceae* (Snelders et al., 2020). To avoid plant recognition, *V. dahliae* strains analyzed to date are characterized by complete loss of the *Ave1* locus (de Jonge et al., 2012; Faino et al., 2016). Therefore, one possible plant disease management strategy is to combine the soil enrichment of tomato plantations using antagonistic *Sphingomonadaceae* members with the use of tomato cultivars that carry the *Ve1* resistance gene. This combination can increase resistance durability because the pathogen will need to retain the effector to inhibit antagonistic bacteria, which will lead to recognition by the plant in turn, followed by the activation of appropriate immune responses. Thus, correct use and combinations of different disease management strategies can enhance plant disease control.

Perspectives on plant cultivation to overcome diseases caused by soil-borne pathogens

Plant cultivation is threatened by fungal soil-borne plant pathogens and new strategies to control plant disease are therefore required. In the context of the plant as a holobiont, the plant-associated microbiota has become of great interest as a major contributor to plant health. The selection of specific genomic plant traits such as plant yield, fruit size, flavor, or color has negatively influenced the interactions between

6

plants and beneficial microorganisms (Chen et al., 2015; Perez-Jaramillo et al., 2016). Recent studies have shown that root exudates of elite cultivars assemble different microbiota compositions when compared with those of wild relatives (Wang et al., 2012; Perez-Jaramillo et al., 2016; Zhalnina et al., 2018; Chai and Schachtman, 2022). For example, plants roots of commercial cultivars recruit less beneficial microbiota and more detrimental microbiota when compared to the wild progenitors (Martín-Robles et al., 2020). A recent study of diverse hybrid populations of wild and domesticated tomatoes has identified quantitative trait loci for the differential recruitment of various rhizobacterial lineages, including a Streptomyces-associated region encoding, among others, the iron regulator FIT and the water channel aquaporin SlTIP2.3 (Oyserman et al., 2022). Another study showed that plants can recruit specific beneficial microbes to suppress soil-borne pathogens (Liu et al., 2021). Clear enrichment of *Stenotrophomonas rhizophila* was observed in the rhizosphere and root endosphere of wheat plants infected with *Fusarium pseudograminearum* (Liu et al., 2021). When the soil was pre-treated with *S. rhizophila*, plant growth was enhanced and plant defense was promoted during *F. pseudograminearum* infection (Liu et al., 2021). Findings like these suggests that holobiont-driven approaches can support plant resistance breeding programs.

The plant-associated microbiota is tightly interlinked with the soil and the pool of microbes present in it. Current agricultural practices are based on intensive cropping systems, continuous mono-cropping, and limited crop rotations, resulting in soil degradation with increasing soil acidification/salinization and low soil nutrient concentration that ultimately hamper ecological services and functions of the soil (Sanaullah et al. 2020). The soil is a complex and dynamic environment that holds the microbiome, including microbial genes, transcripts, metabolites, or proteins (Schlatter et al., 2017). The microbiome acts in the suppression of a broad spectrum of soil-borne pathogens (Schlatter et al., 2017; Jayaraman et al., 2021), and soils that suppress soil-borne pathogens are usually termed disease suppressive soils (DSS) (Jayaraman et al., 2021), which have the ability to suppress the various plant pathogens by improving the plant health, induce plant defense responses, produce antibiotics, compete against pathogens for essential nutrients, or hyperparasite the pathogen (Liu et al. 2021; Schlatter et al. 2017; Mousa and Raizada, 2016). To date, several microbial species have been isolated and proposed as key contributors in disease suppression and therefore use as BCAs (Niu et al., 2021; Umesha et al., 2018; Busby et al., 2017; Álvarez and Biosca, 2017; Cazorla and Mercado-Blanco, 2016). The use of DSS and/or BCAs in combination with plants that recruit beneficial microbes will represent a novel strategy to control fungal soil-borne pathogens.

Many intensive cropping systems worldwide are based on soil-based crop systems. Soilless crop systems, also known as hydroponic systems, have evolved as

alternative to control soil-borne pathogens (Uyeda et al. 2011; Maucieri et al., 2019a). In these systems, soil is exchanged with substrates that can be of organic, inorganic, and/or synthetic origin. Substrates provide plant support, while the supply of water and minerals is ensured via nutrient solutions mainly of inorganic origin (Maucieri et al., 2019b). Organic nutrient solutions have also been exploited in hydroponic systems (Shinohara, 2006; Shinohara et al. 2011; Chinta et al., 2015). These organic nutrient solutions can promote the growth of beneficial microbial communities in the substrate (Shinohara 2006; Shinohara et al. 2011; Fujiwara et al. 2012; Chinta et al. 2014; Chinta et al., 2015) that are able to colonize the rhizosphere of the cultivated plants (Valance et al. 2010), and ultimately are able to control bacterial (Fujiwara et al. 2012) and fungal soil-borne pathogens (Chinta et al. 2014). Different studies have shown that antagonistic microorganisms identified in the organic nutrient solution can reduce root rot disease in lettuce caused by *Fusarium oxysporum* f.sp. *lactuca* (Fujiwara et al., 2013; Chinta et al. 2014). Therefore, the use of organic nutrients in hydroponic systems combined with the usage of BCAs and plants that recruit beneficial microbes could be used as a strategy to control plant diseases caused by soil-borne pathogens.

In conclusion, in my thesis research, I identified effectors of the soil-borne fungal pathogens *V. dahliae* and *R. necatrix* and provided novel information regarding their role in disease establishment. Importantly, I showed that *R. necatrix*, similar to *V. dahliae*, likely exploits effectors for microbiota manipulation to promote disease development. This information could help to develop new strategies to control plant diseases. Given that both *V. dahliae* and *R. necatrix* are soil-borne pathogens, future research will have to reveal whether microbiota-manipulating effector proteins are also employed by other types of pathogens that do not reside in the soil for part of their life cycle. Considering the extreme microbe-richness in soils and the fierce inter-microbial competition for limited nutrients in soils, it is conceivable that microbiota manipulation is a trait that is particularly relevant for soil-borne pathogens.

6

References

Abriouel, H., Franz, C. M., Ben Omar, N., and Gálvez, A. (2011). Diversity and applications of *Bacillus bacteriocins*. *FEMS Microbiology Reviews*, 35(1):201-32.

Agrios, G. N. (2009). Plant pathogens and disease: general introduction. Elsevier Inc, University of Florida; Gainesville, FL USA: 2009.

Albayrak, C. B. (2020). *Bacillus* Species as Biocontrol Agents for Fungal Plant Pathogens. In: Bacilli and Agrobiotechnology: Phytostimulation and Biocontrol, Springer. 239–265 pp.

Alexander, L. J. (1962). Susceptibility of certain Verticillium-resistant tomato varieties to an Ohio isolate of the pathogen. *Phytopathology*, 52:998–1000.

Almagro, J. J. A., Tsirigos, K. D., Sønderby, C. K., Petersen, T. N., Winther, O., Brunak, S., von Heijne, G., and Nielsen, H. (2019). SignalP 5.0 improves signal peptide predictions using deep neural networks. *Nature Biotechnology*, 37:420-423.

Almario, J., Jeena, G., Wunder, J., Langen, G., Zuccaro, A., Coupland, G., and Bucher, M. (2017). Root-associated fungal microbiota of nonmycorrhizal *Arabis alpina* and its contribution to plant phosphorus nutrition. *Proceedings of the National Academy of Sciences*, 114 (44) E9403-E9412.

Álvarez, B., and Biosca, E. G. (2017). Bacteriophage-Based Bacterial Wilt Biocontrol for an Environmentally Sustainable Agriculture. *Frontiers in Plant Science*, 8:1218.

Andrić, S., Meyer, T., and Ongena, M. (2020). *Bacillus* Responses to Plant-Associated Fungal and Bacterial Communities. *Frontiers in Microbiology*, 11:1350.

Anh, V. L., Inoue, Y., Asuke, S., Vy, T. T. P., Anh, N. T., Wang, S., Chuma, I., and Tosa, Y. (2018). *Rmg8* and *Rmg7*, wheat genes for resistance to the wheat blast fungus, recognize the same avirulence gene AVR-Rmg8. *Molecular Plant Pathology*, 19:1252–1256.

Atarashi, K., Tanoue, T., Oshima, K., Suda, W., Nagano, Y., Nishikawa, H., Fukuda, S., Saito, T., Narushima, S., Hase, K., Kim, S., Fritz, J. V., Wilmes, P., Ueha, S., Matsushima, K., Ohno, H., Sakaguchi, S., Taniguchi, T., Morita, H., Hattori, M., and Honda, K. (2013). Treg induction by a rationally selected mixture of Clostridia strains from the human microbiota. *Nature*, 500: 232–236.

Badri, D. V., and Vivanco, J. M. (2009). Regulation and function of root exudates. *Plant Cell and Environment*, 32:666-681.

Baergen, K. D., Hewitt, J. D., and St. Clair, D. A. (1993). Resistance of tomato genotypes to four isolates of *Verticillium dahliae* race 2. *HortScience*, 28:833–836.

Beaudoin, T., Yau, Y. C. W., Stapleton, P. J., Gong, Y., Wang, P. W., Guttman, D. S., and Waters, V. (2017). *Staphylococcus aureus* interaction with *Pseudomonas aeruginosa* biofilm enhances tobramycin resistance. *Npj Biofilms and Microbiomes*, 3: 25.

Bailey, B. A. (1995). Purification of a Protein from Culture Filtrates of *Fusarium oxysporum* that Induces Ethylene and Necrosis in Leaves of *Erythroxylum coca*. *Biochemistry and Cell Biology*, 85:10.

Bailly-Bechet, M., Haudry, A., and Lerat, E. (2014). "One code to find them all": a perl tool to conveniently parse RepeatMasker output files. *Mobile DNA*, 5:1-15.

Bais, H. P., Weir, T. L., Perry, L. G., Gilroy, S., Vivanco, J. M. (2006). The role of root exudates in rhizosphere interactions with plants and other organisms. *Annual Review of Plant Biology*, 57:233-66.

Barguil, B. M., Viana, F. M. P., Anjos, R. M., and Cardoso, J. E. (2009). First report of dry

rot caused by *Fusarium oxysporum* on rose (*Rosa* spp.) in Brazil. *Plant Disease*, 93:766–766.

Beilsmith, K., Thoen, M. P. M., Brachi, B., Gloss, A. D., Khan, M. H., and Bergelson, J. (2019). Genome-wide association studies on the phyllosphere microbiome: Embracing complexity in host–microbe interactions. *The Plant Journal*, 97:164-181.

Benítez-Páez, A., Portune, K. J., and Sanz, Y. (2016). Species-level resolution of 16S rRNA gene amplicons sequenced through the MinION™ portable nanopore sequencer. *GigaScience*, 5: 1-9.

Berendsen, R. L., Pieterse, C. M. J., and Bakker, P. A. H. M. (2012). The rhizosphere microbiome and plant health. *Trends in Plant Science*, 17:478-486.

Berendsen, R. L., Vismans, G., Yu, K., Song, Y., de Jonge, R., Burgman, W. P., Burmølle, M., Herschend, J., Bakker, P. A. H. M., and Pieterse, C. M. J. (2018). Disease-induced assemblage of a plant-beneficial bacterial consortium. *The ISME Journal*, 12:1496–1507.

Bertels, F., Silander, O. K., Pachkov, M., Rainey, P. B., and van Nimwegen, E. (2014). Automated reconstruction of whole-genome phylogenies from short-sequence reads. *Molecular Biology and Evolution*, 31:1077-1088.

Bhat, R. G., and Subbarao, K. V. (1999). Genetics and resistance host range specificity in *Verticillium dahliae*. *Phytopathology*, 89:1218-1225.

Blin, K., Shaw, S., Steinke, K., Villebro, R., Ziemert, N., Lee, S. Y., Medema, M. H., and Weber, T. (2019). AntiSMASH 5.0: updates to the secondary metabolite genome mining pipeline. *Nucleic Acids Research*, 47:81–87.

Bolton, A. T. (1982). Reduction in yield of greenhouse roses caused by root infection with *Pythium aphanidermatum* and *Rhizoctonia solani*. *Canadian Journal of Plant Pathology*, 4:281–284.

Bormann, C., Baier, D., Hörr, I., Raps, C., Berger, J., Jung, G., and Schwarz, H. (1999). Characterization of a novel, antifungal, chitin-binding protein from *Streptomyces tendae* Tü901 that interferes with growth polarity. *Journal of Bacteriology*, 181:7421-7429.

Bos, J. I., Armstrong, M. R., Gilroy, E. M., Boevink, P. C., Hein, I., Taylor, R. M., Zhendong, T., Engelhardt, S., Vetukuri, R. R., Harrower, B., Dixelius, C., Bryan, G., Sadanandom, A., Whisson, S. C., Kamoun, S., and Birch, P. R. (2010). *Phytophthora infestans* effector AVR3a is essential for virulence and manipulates plant immunity by stabilizing host E3 ligase CMPG1. *Proceedings of the National Academy of Sciences*, 107(21):9909-14.

Boshoven, J. (2017). Virulence contribution and recognition of homologs of the *Verticillium dahliae* effector Ave1. Wageningen University, Wageningen, The Netherlands.

Boskabady, M. H., Shafei, M. N., Saberi, Z., and Amini, S. (2011). Pharmacological effects of *Rosa damascena*. *Iranian Journal of Basic Medical Sciences*, 14:295–307.

Bottery, M. J., Pitchford, J. W., and Friman, V. (2021). Ecology and evolution of antimicrobial resistance in bacterial communities. *The ISME Journal*, 15: 939-948.

Bottery, M. J., Wood, A. J., and Brockhurst, M. A. (2016). Selective conditions for a multidrug resistance plasmid depend on the sociality of antibiotic resistance. *Antimicrobial Agents and Chemotherapy*, 60: 2524-2527.

Bourras, S., Kunz, L., Xue, M., Praz, C. R., Müller, M.C., Kälin, C., Schläfli, M., Ackermann, P., Flückiger, S., Parlange, F., Menardo, F., Schaefer, L. K., Ben-David, R., Roffler, S., Oberhaensli, S., Widrig, V., Lindner, S., Isaksson, J., Wicker, T., Yu, D., and Keller, B. (2019). The AvrPm3-Pm3 effector-NLR interactions control both race-specific resistance and hostspecificity of cereal mildews on wheat. *Nature Communications*, 10:1–16.

Bourras, S., McNally, K. E., Ben-David, R., Parlange, F., Roffler, S., Praz, C. R., Oberhaensli, S., Menardo, F., Stirnweis, D., Frenkel, Z., Schaefer, L. K., Flückiger, S., Treier, G., Herren, G., Korol, A.B., Wicker, T., and Keller, B. (2015). Multiple avirulence loci and allele-specific effector recognition control the *Pm3* race-specific resistance of wheat to powdery mildew. *Plant Cell*, 27:2991–3012.

Branton, D., Deamer, D. W., Marziali, A., Bayley, H., Benner, S. A., Butler, T., Di Ventra, M., Garaj, S., Hibbs, A., Huang, X., Jovanovich, S. B., Krstic, P. S., Lindsay, S., Ling, X. S., Mastrangelo, C. H., Meller, A., Oliver, J. S., Pershin, Y. V., Ramsey, J. M., Riehn, R., Soni, G. V., Tabard-Cossa, V., Wanunu, M., Wiggin, M., and Schloss, J. A. (2008). The potential and challenges of nanopore sequencing. *Nature Biotechnology*, 26: 1146-1153.

Bravo-Ruiz, G., Di Pietro, A., and Roncero, M. I. (2016). Combined action of the major secreted exo- and endopolygalacturonases is required for full virulence of *Fusarium oxysporum*. *Molecular Plant Pathology*, 17(3):339-53.

Bray, N. L., Pimentel, H., Melsted, P., and Pachter, L. (2016). Near-optimal probabilistic RNA-seq quantification. *Nature Biotechnology*, 34:525-527.

Bressan, M., Roncato, M., Bellvert, F., Comte, G., Haichar, F., Achouak, W., and Berge, O. (2009). Exogenous glucosinolate produced by *Arabidopsis thaliana* has an impact on microbes in the rhizosphere and plant roots. *Multidisciplinary Journal of Microbial Ecology*, 3:1243–1257.

Broekaert, W. F., Marien, W., Terras, F. R. G., De Bolle, M. F. C., Proost, P., Van Damme, J., Dillen, L., Claeys, M., Rees, A. B., Vanderleyden, J., and Cammue, B. P. A. (1992). Antimicrobial peptides from *Amaranthus caudatus* seeds with sequence homology to the cysteine/glycine-rich domain of chitin-binding proteins. *Biochemistry*, 31:4308-4314.

Brown, J. K. M. (2015). Durable resistance of crops to disease: a Darwinian perspective. *Annual Review of Phytopathology*, 53:513–539.

Bukin, Y. S., Galachyants, Y. P., Morozov, I. V., Bukin, S. V., Zakharenko, A. S., and Zemsakaya, T. I. (2019). The effect of 16S rRNA region choice on bacterial community metabarcoding results. *Scientific Data*, 6: 190007.

Burton, J. N., Adey, A., Patwardhan, R. P., Qiu, R., Kitzman, J. O., and Shendure, J. (2013). Chromosome-scale scaffolding of *de novo* genome assemblies based on chromatin interactions. *Nature Biotechnology*, 31:1119–1125.

Busby, P. E., Soman, C., Wagner, M. R., Friesen, M. L., Kremer, J., Bennett, A., Morsy, M., Eisen, J. A., Leach, J. E., and Dangl, J. L. (2017). Research priorities for harnessing plant microbiomes in sustainable agriculture. *PLoS Biology*, 15(3):e2001793.

Cabrera, R. I., Solís-Pérez A. R., and Sloan, J. J. (2009). Greenhouse rose yield and ion accumulation responses to salt stress as modulated by rootstock selection. *HortScience*, 44(7):2000–2008.

Cairns, J., Ruokolainen, L., Hultman, J., Tamminem, M., Virta, M., and Hiltunen, T. (2018). Ecology determines how low antibiotic concentration impacts community composition and horizontal transfer of resistance genes. *Communications Biology*, 1: 35.

Callaham, B. J., Wong, J., Heiner, C., Oh, S., Theriot, C. M., Gulati, A. S., McGill, S. K., and Dougherty, M. K. (2019). High-throughput amplicon sequencing of the full-length 16S rRNA gene with single-nucleotide resolution. *Nucleic Acids Research*, 47:1-12.

Cambronne, E. D., and Roy, C. R. (2006). Recognition and Delivery of Effector Proteins into Eukaryotic Cells by Bacterial Secretion Systems. *Traffic*, 7:929–939.

Campos-Olivas, R., Hörr, I., Bormann, C., Jung, G., and Gronenborn, A. M. (2001). Solution structure, backbone dynamics and chitin binding of the anti-fungal protein from *Streptomyces tendae* TÜ901. *Journal of Molecular Biology*, 308:765-782.

Carresi, L., Pantera, B., Zoppi, C., Cappugi, G., Oliveira, A. L., Pertinhez, T. A., Spisni, A., Scala, A., and Pazzagli, L. (2006). Cerato-platanin, a phytotoxic protein from *Ceratocystis fimbriata*: expression in *Pichia pastoris*, purification and characterization. *Protein Expression and Purification*, 49:159-167.

Carrión, V. J., Perez-Jaramillo, J., Cordovez, V., Tracanna, V., de Hollander, M., Ruiz-Buck, D., Mendes, L. W., van Ijcken, W. F. J., Gomez-Exposito, R., Elsayed, S. S., Mohanraju, P., Arifah, A., van der Oost, J., Paulson, J. N., Mendes, R., van Wezel, G. P., Medema, M. H., and Raaijmakers, J. M. (2019). Pathogen-induced activation of disease-suppressive functions in the endophytic root microbiome. *Science*, 366(6465):606-612.

Cazorla, F., and Mercado-Blanco, J. (2016). Biological control of tree and woody plant diseases: an impossible task? *BioControl*, 61:233–242.

Cazorla, F. M., Duckett, S. B., Bergström, E. T., Noreen, S., Odijk, R., Lugtenberg, B. J. J., Thomas-Oates, J. E., and Bloemberg, G. V. (2006). Biocontrol of avocado dematophora root rot by antagonistic *Pseudomonas fluorescens* PCL1606 correlates with the production of 2-hexyl 5-propyl resorcinol. *Molecular Plant-Microbe Interactions*, 19:418–428.

Celikkol-Aydin, S., Gaylarde, C. C., Lee, T., Melchers, R. E., Witt, D. L., and Beech, I. B. (2016). 16S rRNA gene profiling of planktonic and biofilm microbial populations in the Gulf of Guinea using Illumina NGS. *Marine Environmental Research*, 122:105-112.

Chai, Y. N., and Schachtman, D. P. (2022). Root exudates impact plant performance under abiotic stress. *Trends in Plant Science*, 27(1):80-91.

Chaloner, T. M., Gurr S. J., and Bebber D. P. (2021). Plant pathogen infection risk tracks global crop yields under climate change. *Nature Climate Change*, 11:710–715.

Chavarro-Carrero, E. A., Snelders, N., Torres, D. E., Kraege, A., Lopez-Moral, A., Petti, G., Punt, W., Wieneke, J., Garcia-Velasco, R., Lopez-Herrera, C., Seidl, M. F., and Thomma, B. P. H. J. (2023). The soil-borne white root rot pathogen *Rosellinia necatrix* expresses antimicrobial proteins during host colonization. *PLOS Pathogens*, 20(1): e1011866.

Chavarro-Carrero, E. A., Vermeulen, J. P., E. Torres, D., Usami, T., Schouten, H. J., Bai, Y., Seidl, M. F., and Thomma, B. P. H. J. (2021). Comparative genomics reveals the *in planta*-secreted *Verticillium dahliae* Av2 effector protein recognized in tomato

plants that carry the *V2* resistance locus. *Environmental Microbiology*, 23:1941–1958.

Chen, J., Upadhyaya, N. M., Ortiz, D., Sperschneider, J., Li, F., Bouton, C., Chen, J., Upadhyaya, N. M., Ortiz, D., Sperschneider, J., Li, F., Bouton, C., Breen, S., Dong, C., Xu, B., Zhang, X., Mago, R., Newell, K., Xia, X., Bernoux, M., Taylor, J. M., Steffenson, B., Jin, Y., Zhang, P., Kanyuka, K., Figueroa, M., Ellis, J. G., Park, R. F., and Peter, N. D. (2017). Loss of *AvrSr50* by somatic exchange in stem rust leads to virulence for *Sr50* resistance in wheat. *Science*, 358:1607–1610.

Chen, T., Nomura, K., Wang, X., Sohrabi, R., Xu, J., Yao, L., Paasch, B. C., Ma, L., Kremer, J., Cheng, Y., Zhang, L., Wang, N., Wang, E., Xin, X. F., and He, S. Y. (2020). A plant genetic network for preventing dysbiosis in the phyllosphere. *Nature*, 580(7805):653-657.

Chen, Y. H., Gols, R., and Benrey, B. (2014). Crop domestication and its impact on naturally selected trophic interactions. *Annual Review of Entomology*, 60:35-58.

Chen, Z., Shen, Z., Zhao, D., Xu, L., Zhang, L., and Zou, Q. (2020). Genome-Wide Analysis of LysM-Containing Gene Family in Wheat: Structural and Phylogenetic Analysis during Development and Defense. *Genes*, 29;12(1):31.

Chinta, Y. D., Eguchi, Y., Widiastuti, A., Shinohara, M., and Sato, T., (2015). Organic hydroponics induces systemic resistance against the air-borne pathogen, *Botrytis cinerea* (gray mould). *Journal of Plant Interactions*, 10:243-251.

Chinta, Y. D., Kano, K., Widiastuti, A., Fukahori, M., Kawasaki, S., Eguchi, Y., Misu, H., Odani, H., Zhou, S., Narisawa, K., Fujiwara, K., Shinohara, M., and Sato, T. (2014). Effect of corn steep liquor on lettuce root rot (*Fusarium oxysporum* f.sp. *lactucae*) in hydroponic cultures. *Journal of the Science of Food and Agriculture*, 94(11):2317-23.

Christie, T. (1966). Studies on the nitrogen metabolism of species of *Verticillium*. *New Zealand Journal of Agricultural Research*, 9:995–998.

Cirulli, M. (1969). Un isolato di *Verticillium dahliae* Kleb. virulento verso varietà resistenti di Pomodoro. *Phytopathologia Mediterranea*, 8:132–136.

Collemare, J., and Lebrun, M.-H. (2011). Fungal Secondary Metabolites: Ancient Toxins and Novel Effectors in Plant–Microbe Interactions. In: Effectors in Plant–Microbe Interactions. John Wiley & Sons, Inc., United Kingdom. 377-400 pp.

Collemare, J., O'Connell, R., and Lebrun, M.-H. (2019). Nonproteinaceous effectors: theterra incognitaof plant–fungal interactions. *New Phytologist*, 223:590–596.

Cook, D. E., Kramer, M., Seidl, M. F., and Thomma, B. P. H. J. (2020). Chromatin features define adaptive genomic regions in a fungal plant pathogen. *BioRxiv*, https://dx.doi.org/10.1101/2020.01.27.921486.

Cook, D. E., Mesarich, C. H., and Thomma, B. P. H. J. (2015). Understanding plant immunity as a surveillance system to detect invasion. *Annual Review of Phytopathology*, 53:541–563.

Cook, D., Donzelli, B. G. G., Creamer, R., Baucom, D. L., Gardner, D. R., Pan, J., Moore, N., Krasnoff, S. B., Jaromczyk, J. W., and Schardl, C. L. (2017). Swainsonine biosynthesis genes in diverse symbiotic and pathogenic fungi. *G3: Genes, Genomes, Genetics*, 7:1791-1797.

Cordovez, V., Rotoni, C., Dini-Andreote, F., Oyserman, B., Carrión, V. J., and Raaijmakers, J. M. (2021). Successive plant growth amplifies genotype-specific assembly of the

tomato rhizosphere microbiome. *Science of the Total Environment*, 772:144825.

Danecek, P., Bonfield, J. K., Liddle, J., Marshall, J., Ohan, V., Pollard, M. O., Whitwham, A., Keane, T., McCarthy, S. A., Davies, R. M., and Li, H. (2021). Twelve years of SAMtools and BCFtools. *Gigascience*, 10:1-4.

Dangl, J. L., and Jones, J. D. G. (2001). Plant pathogens and integrated defence responses to infection. *Nature*, 411:826–833.

Dangl, J. L., Horvath, D. M., and Staskawicz, B. J. (2013). Pivoting the plant immune system. *Science*, 341:745–751.

Darkin-Rattray, S. J., Gurnett, A. M., Myers, R. W., Dulski, P. M., Crumley, T. M., Allocco, J. J., Cannova, C., Mainke, P. T., Colletti, S. L., Bednarek, M. A., Singh, S. B., Goetz, M. A., Dombrowski, A. W., Polishook, J. D., and Schmatz, D. M. (1996). Apicidin: a novel antiprotozoal agent that inhibits parasite histone deacetylase. *Proceedings of the National Academy of Sciences*, 93:13143–13147.

Darvill, A. G., and Albersheim, P. (1984). Phytoalexins and their elicitors-a defense against microbial infection in plants. *Annual Review of Plant Physiology*, 35:243–275.

Davey, J. W., Davis, S. J., Mottram, J. C., and Ashton, P. D. (2020). Tapestry: validate and edit small eukaryotic genome assemblies with long reads. *BioRxiv*, https://doi.org/10.1101/2020.04.24.059402.

de Guillen, K., Ortiz-Vallejo, D., Gracy, J., Fournier, E., Kroj, T., and Padilla, A. (2015). Structure analysis uncovers a highly diverse but structurally conserved effector family in phytopathogenic fungi. *PLoS Pathogens*, 11:1-27.

de Hoog, J., Jr. (2001). Handbook for modern greenhouse rose cultivation. Applied Plant Research, Aalsmeer, The Netherlands. 220 p.

de Jonge, R., and Thomma, B. P. H. J. (2009). Fungal LysM effectors: extinguishers of host immunity? *Trends in Microbiology*, 17:151–157.

de Jonge, R., Bolton, M. D., Kombrink, A., van den Berg, G. C. M., Yadeta, Koste, A., and Thomma, B. P. H. J. (2013). Extensive chromosomal reshuffling drives evolution of virulence in an asexual pathogen. *Genome Research*, 23:1271–1282.

de Jonge, R., van Esse, H. P., Kombrink, A., Shinya, T., Desaki, Y., Bours, R., van der Krol, S., Shibuya, N., Joosten, M. H. A. J., and Thomma, B. P. H. J. (2010). Conserved fungal LysM effector Ecp6 prevents chitin-triggered immunity in plants. *Science*, 329:953-955.

de Jonge, R., van Esse, H. P., Maruthachalam, K., Bolton, M. D., Santhanam, P., Saber, M. K., Zhang, Z., Usami, T., Lievens, B., Subbarao, K. V., and Thomma, B. P. H. J. (2012). Tomato immune receptor Ve1 recognizes effector of multiple fungal pathogens uncovered by genome and RNA sequencing. *Proceedings of the National Academy of Science*, 109:5110–5115.

de Vries, D. P. 2003. Clonal rootstocks. In: Roberst, A.V., T. Debener, and S. Gudin (eds.). Encyclopedia of rose science. Elsevier Academic Press, Oxford, UK. 651–656 pp.

Debener, T., and Byrne D. H. (2014). Disease resistance breeding in rose: current status and potential of biotechnological tools. *Plant Science*, 228:107–117.

Delgado-Baquerizo, M., Guerra, C. A., Cano-Díaz, C., Egidi, E., Wang J., Eisenhauer, N., Singh B. K., and Maestre F. T. (2020). The proportion of soil-borne pathogens increases with warming at the global scale. *Nature Climate Change*, 10:550–554.

Depotter, J. R. L., Shi-Kunne, X., Missonnier, H., Liu, T., Faino, L., van den Berg, G. C. M., Wood, T. A., Zhang, B., Jacques, A., Seidl, M. F., and Thomma, B. P. H. J. (2019). Dynamic virulence-related regions of the plant pathogenic fungus *Verticillium dahliae* display enhanced sequence conservation. *Molecular Ecology*, 28:3482–3495.

Deseret News and Telegram. (1955). From Jungles Of Peru. Deseret News and Telegram.

Dimkić, I., Janakiev, T., Petrović, M., Degrassi, G., and Fira, D. (2022). Plant-associated *Bacillus* and *Pseudomonas* antimicrobial activities in plant disease suppression via biological control mechanisms - A review. *Physiological and Molecular Plant Pathology*, 117.

Dimkpa, C., Weinand, T., and Asch, F. (2009). Plant-rhizobacteria interactions alleviate abiotic stress conditions. *Plant, Cell & Environment*, 32(12):1682-94.

Diwan, N., Fluhr, R., Eshed, Y., Zamir, D., and Tanksley, S. D. (1999). Mapping of *Ve* in tomato: a gene conferring resistance to the broad-spectrum pathogen *Verticillium dahliae* race 1. *Theoretical and Applied Genetics*, 98:315–319.

Djamei, A., Schipper, K., Rabe, F., Ghosh, A., Vincon, V., Kahnt, J., Osorio, S., Toghe, T., Fernie, A. R., Feussner, K., Meinicke, P., Stierhof; Y., Schwarz, H., Macek, B., Mann, M., and Kahmann, R. (2011). Metabolic priming by a secreted fungal effector. *Nature*, 478:395-398.

Dobhal, S., Olson, J. D., Arif, M., Garcia Suarez, J. A., and Ochoa-Corona, F. M. (2016). A simplified strategy for sensitive detection of rose rosette virus compatible with three RT-PCR chemistries. *Journal of Virological Methods*, 232:47–56.

Dobinson, K. F., Tenuta, G. K., and Lazarovits, G. (1996). Occurrence of race 2 of *Verticillium dahliae* in processing tomato fields in southwestern Ontario. *Canadian Journal of Plant Pathology*, 18:55–58.

Dodds, P. N., and Rathjen, J. P. (2010). Plant immunity: towards an integrated view of plant-pathogen interactions. *Nature Reviews Genetics*, 11:539–548.

Dong, S., Kong, G., Qutob, D., Yu, X., Tang, J., Kang, J., Dai, T., Wang, H., Gijzen, M., and Wang, Y. (2012). The NLP toxin family in *Phytophthora sojae* includes rapidly evolving groups that lack necrosis-inducing activity. *Molecular Plant-Microbe Interactions*, 25(7):896-909.

Dong, S., Raffaele, S., and Kamoun, S. (2015). The two-speed genomes of filamentous pathogens: waltz with plants. *Current Opinion in Genetics and Development*, 35:57-65.

Doorenspleet, K., Jansen, L., Oosterbroek, S., Kamermans, P., Bos, O., Wurz, E., Murk, A., and Nijland, R. (2023). The long and the short of it: Nanopore based eDNA metabarcoding of marine vertebrates works; sensitivity and specificity depend on amplicon lengths. *BioRxiv*, doi: https://doi.org/10.1101/2021.11.26.470087.

Du, J., Verzaux, E., Chaparro-Garcia, A., Bijsterbosch, G., Keizer, L. C. P., Zhou, J., Liebrand, T. W. H., Xie, C., Govers, F., Robatzek, S., van der Vossen, E. A. G., Jacobsen, E., Visser, R. G. V., Kamoun, S., and Vleeshouwers, V. G. A. A. (2015). Elicitin recognition confers enhanced resistance to *Phytophthora infestans* in potato. *Nature Plants*, 1:1–5.

Dudchenko, O., Batra, S. S., Omer, A. D., Nyquist, S. K., Hoeger, M., Durand, N. C., Shamin, M. S., Machol, I., Lander, E. S., Aiden, A. P., and Aiden, E. L. (2017). *De*

novo assembly of the *Aedes aegypti* genome using Hi-C yields chromosome-length scaffolds. *Science*, 356:92–95.

Dudchenko, O., Shamim, M. S., Batra, S. S., Durand, N. C., Musial, N. T., Mostofa, R., Pham, M., St Hilaire, B. G., Yao, W., Stamenova, E., Hoeger, M., Nyquist, S., Korchina, V., Pletch, K., Flanagan, J. P., Tomaszewicz, A., McAloose, D., Perez-Estrada, C., Novak, B. J., Omer, R. D., and Aiden, E. L. (2018). The juicebox assembly tools module facilitates *de novo* assembly of mammalian genomes with chromosome-length scaffolds for under \$1000. *BioRxiv*, https://doi.org/10.1101/254797.

Duplessis, S., Cuomo, C. A., Lin, Y., Aerts, A., Tisserant, E., Veneault-Fourrey, C., Joly, D., Hacquard, S., Amselem, J., Cantarel, B. L. Chiu, R., Coutinho, P. M., Feau, N., Field, M., Frey, P., Gelhaye, E., Goldberg, J., Grabherr, M. G., Kodira, C. D., Kohler, A., Kües, U., Lindquist, E. A., Lucas, S. M., Mago, R., Mauceli, E., Morin, E., Murat, C., Pangilinan, J. L., Park, R., Pearson, M., Quesneville, H., Rouhier, N., Sakthikumar, S., Salamov, A., Schmutz, J., Selles, B., Shapiro, H., Tanguay, P., Tuskan, G. A., Henrissat, B., van de Peer, Y., Rouzé, P., Ellis, J. G., Dodds, P. N., Schein, J. E., Zhong, S., Hamelin, R. C., Grigoriev, I. V., Szabo, L. J., and Martin, F. (2011). Obligate biotrophy features unraveled by the genomic analysis of rust fungi. *Proceedings of the National Academy of Sciences*, 108:9166-9171.

Durán, P., Thiergart, T., Garrido-Oter, R., Agler, M., Kemen, E., Schulze-Lefert, P., and Hacquard, S. (2018). Microbial Interkingdom Interactions in Roots Promote *Arabidopsis* Survival. *Cell*, 175(4):973-983.e14.

Durand, N. C., Shamim, M. S., Machol, I., Rao, S. S. P., Huntley, M. H., Lander, E. S., and Aiden, E. L. (2016). Juicer Provides a One-Click System for Analyzing Loop-Resolution Hi-C Experiments. *Cell Systems*, 3:95–98.

Egeter, B., Veríssimo, J., Lopes-Lima, M., Chaves, C., Pinto, J., Riccardi, N., Beja, P., and Fonseca, N. A. (2022). Speeding up the detection of invasive bivalve species using environmental DNA: A Nanopore and Illumina sequencing comparison. *Molecular Ecology Resources*, 2022;00:1–16..

Eguchi, N., Kondo, K., and Yamagishi, N. (2009). Bait twig method for soil detection of *Rosellinia necatrix*, causal agent of white root rot of Japanese pear and apple, at an early stage of tree infection. *Journal of General Plant Pathology*, 75:325–330.

Faino, L., Seidl, M. F., Datema, E., van den Berg, G. C. M., Janssen, A., Wittenberg, A. H. J., and Thomma, B. P. H. J. (2015). Single-molecule real-time sequencing combined with optical mapping yields completely finished fungal genome. *MBio*, 6:1–11.

Faino, L., Seidl, M. F., Shi-Kunne, X., Pauper, M., van den Berg, G. C., Wittenberg, A. H., and Thomma, B. P. H. J. (2016). Transposons passively and actively contribute to evolution of the two-speed genome of a fungal pathogen. *Genome Research*, 26:1091–1100.

Fan, J. B., Gunderson, K. L., Bibikova, M., Yeakley, J. M., Chen, J., Wickham Garcia, E., Lebruska, L. L., Laurent, M., Shen, R., and Barker, D. (2006). Illumina universal bead arrays. *Methods in Enzymology*, 410:57-73.

Fan, R., Cockerton, H. M., Armitage, A. D., Bates, H., Cascant-Lopez, E., Antanaviciute, L., Xu, X., Hu, X., and Harrison, R. J. (2018). Vegetative compatibility groups partition variation in the virulence of *Verticillium dahliae* on strawberry. *PLoS One*, 13:1–21.

Farr, D. F., and Rossman A. Y. (2021). Fungal Databases, U.S. National Fungus Collections,

ARS, USDA. https://nt.ars-grin.gov/fungaldatabases/ (Accessed April, 2022).

Fisher, M. C., Henk, D. A., Briggs, C. J., Brownstein, J. S., Madoff, L. C., McCraw, S. L., and Gurr, S. J. (2012). Emerging fungal threats to animal, plant and ecosystem health. *Nature*, 484:186–194.

Fitzpatrick, C. R., Mustafa, Z., and Viliunas, J. (2019). Soil microbes alter plant fitness under competition and drought. *Journal of Evolutionary Biology*, 32(5):438-450.

Flor, H. H. (1942). Inheritance of pathogenicity in *Melampsora lini*. *Phytopathology*, 32:653–669.

Food and Agriculture Organization of the United Nations (FAO). (2019). New standards to curb the global spread of plant pests and diseases. Retrieved from https://www.fao.org/news/story/en/item/1187738/icode/.

Fouché, S., Badet, T., Oggenfuss, U., Plissonneau, C., Francisco, C. S., and Croll, D. (2020). Stress-driven transposable element de-repression dynamics and virulence evolution in a fungal pathogen. *Molecular Biology and Evolution*, 37:221-239.

Fradin, E. F., and Thomma, B. P. H. J. (2006). Physiology and molecular aspects of Verticillium wilt diseases caused by *V. dahliae* and *V. albo-atrum*. *Molecular Plant Pathology*, 7:71–86.

Fradin, E. F., Zhang, Z., Juarez Ayala, J. C., Castroverde, C. D. M., Nazar, R. N., Robb, J., Liu, C.-M., and Thomma, B. P. H. J. (2009). Genetic dissection of Verticillium wilt resistance mediated by tomato Ve1. *Plant Physiology*, 150:320–332.

Frank, J. A., Reich, C. I., Sharma, S, Weisbaum, J. S., Wilson, B. A, and Olsen, G., J. (2008). Critical evaluation of two primers commonly used for amplification of bacterial 16S rRNA genes. *Applied and Environmental Microbiology*, 74: 2461 - 2470.

Frantzeskakis, L., Di Pietro, A., Rep, M., Schirawski, J., Wu, C., and Panstruga, R. (2020). Rapid evolution in plant–microbe interactions – a molecular genomics perspective. *Plant Phytologist*, 225:1134-1142.

Frantzeskakis, L., Kracher, B., Kusch, S., Yoshikawa-Maekawa, M., Bauer, S., Pedersen, C., Spanu, P. D., Maekawa, T., Schulze-Lefert, P., and Panstruga, R. (2018). Signatures of host specialization and a recent transposable element burst in the dynamic one-speed genome of the fungal barley powdery mildew pathogen. *BMC Genomics*, 19:381.

Freitas, D. A., Leclerc, S., Miyoshi, A., Oliveira, S. C., Sommer, P. S. M., Rodrigues, L., Correa-Junior, A., Gautier, M., Langella, P., Azevedo, V. A., and Le Loir, Y. (2005). Secretion of *Streptomyces tendae* antifungal protein 1 by *Lactococcus lactis*. *Brazilian Journal of Medical and Biological Research*, 38:1585-1592.

Fuchs, H. (1994). Scion-rootstock relationships and root behaviour in glasshouse roses. PhD thesis, Wageningen University, Wageningen, The Netherlands.

Fujiwara, K., Aoyama, C., Takano, M., and Shinohara, M. (2012). Suppression of *Ralstonia solanacearum* bacterial wilt disease by an organic hydroponic system. *Journal of General Plant Pathology*, 78:217–220.

Fujiwara, K., Iida, Y., Iwai, T., Aoyama, C., Inukai, R., Ando, A., Ogawa, J., Ohnishi, J., Terami, F., Takano, M., and Shinohara, M. (2013). The rhizosphere microbial community in a multiple parallel mineralization system suppresses the pathogenic fungus *Fusarium oxysporum*. *Microbiologyopen*, 2(6):997-1009.

Gahlaut, V., Kumari, P., Jaiswal V., and Kumar S. (2021). Genetics, genomics and breeding

in *Rosa* species. *The Journal of Horticultural Science and Biotechnology*, 96(5):545–559.

Gan, P., Ikeda, K., Irieda, H., Narusaka, M., O'Connell, R. J., Narusaka, Y., Takano, Y., Kubo, Y., and Shirasu, K. (2013). Comparative genomic and transcriptomic analyses reveal the hemibiotrophic stage shift of *Colletotrichum* fungi. *New Phytologist*, 197:1236–1249.

Gao, F., Zhang, B.-S., Zhao, J.-H., Huang, J.-F., Jia, P.-S., Wang, S., Zhang, J., Zhou, J.-M., and Guo, H. S. (2019). Deacetylation of chitin oligomers increases virulence in soil-borne fungal pathogens. *Nature Plants*, 5(11):1167-1176.

García-Velasco, R., González-Díaz, J. G., Domínguez-Arizmendi, G., Ayala-Escobar, V., and Aguilar-Medel, S. (2012). *Rosellinia necatrix* in *Rosa* sp., and an evaluation of its sensitivity to fungicides. *Revista Chapingo Serie Horticultura*, 18(1):39–54.

Gel, B., Díez-Villanueva, A., Serra, E., Buschbeck, M., Peinado, M. A., and Malinverni, R. (2016). regioneR: an R/Bioconductor package for the association analysis of genomic regions based on permutation tests. *Bioinformatics*, 32:289–291.

George, S., Pankhurst, L., Hubbard, A., Votintseva, A., Stoesser, N., Sheppard, A. E., Mathers, A., Norris, R., Navickaite, I., Eaton, C., Iqbal, Z., Crook, D. W., and Phan, H. T. T. (2017). Resolving plasmid structures in *Enterobacteriaceae* using the MinION nanopore sequencer: assessment of MinION and MinION/Illumina hybrid data assembly approaches. *Microbial Genomics*, 3(8):e000118.

Gibriel, H. A. Y., Thomma, B. P. H. J., and Seidl, M. F. (2016). The age of effectors: genome-based discovery and applications. *Phytopathology*, 106:1206–1212.

Gibriel, H., Li, J., Zhu, L., Seidl, M., and Thomma, B. P. H. J. (2019). *Verticillium dahliae* strains that infect the same host plant display highly divergent effector catalogs. *BioRxiv*, https://doi.org/10.1101/528729.

Gijzen, M., and Nürnberger, T. (2006). Nep1-like proteins from plant pathogens: recruitment and diversification of the NPP1 domain across taxa. *Phytochemistry*, 67(16):1800-7.

Göhre, V., and Robatzek, S. (2008). Breaking the barriers: microbial effector molecules subvert plant immunity. *Annual Review of Phytopathology*, 46:189-215.

Gómez-Pérez, D., Schmid, M., Chaudhry, V., Hu, Y., Velic, A., Maček, B., Ruhe, J., Kemen, A., and Kemen E. (2023). Proteins released into the plant apoplast by the obligate parasitic protist *Albugo* selectively repress phyllosphere-associated bacteria. *New Phytologist*, 239: 2320-2334.

Goossens, P., Spooren, J., Baremans, K. C. M., Andel, A., Lapin, D., Echobardo, N., Pieterse, C. M. J., Van den Ackerveken, G., and Berendsen, R. L. (2023). Obligate biotroph downy mildew consistently induces near-identical protective microbiomes in *Arabidopsis thaliana*. *Nature Microbiology*, 8, 2349–2364.

Gout, L., Kuhn, M. L., Vincenot, L., Bernard-Samain, S., Cattolico, L., Barbetti, M., Moreno-Rico, O., Balesdent, M.-H., and Rouxel, T. (2007). Genome structure impacts molecular evolution at the AvrLm1 avirulence locus of the plant pathogen *Leptosphaeria maculans*. *Science*, 113:207–208.

Green, R. J. (1951). Studies on the host range of the Verticillium that causes wilt of *Mentha piperita* L. *Science*, 113:207–208.

Großkopf, T., and Soyer, O. S. (2014). Synthetic microbial communities. *Current Opinion*

in Microbiology, 18, 72-77.

Gu, W., Miller, S., and Chiu, C. Y. Clinical Metagenomic Next-Generation Sequencing for Pathogen Detection. *Annual Review of Pathology*, 14:319-338.

Guillaumin, J., Mercier, S., and Dubos, B. (1982). Les pourridiés à Armillariella et Rosellinia en France sur vigne, arbres fruitiers et cultures florales I. Etiologie et symptomatologie. *Agronomie*, 2:71–80.

Haas, B. J., Kamoun, S., Zody, M. C., Jiang, R. H., Handsaker, R. E., Cano, L. M., Grabherr, M., Kodira, C. D., Raffaele, S., Torto-Alalibo, T., Bozkurt, T. O., Ah-Fong, A. M., Alvarado, L., Anderson, V. L., Armstrong, M. R., Avrova, A., Baxter, L., Beynon, J., Boevink, P. C., Bollmann, S. R., Bos, J. I., Bulone, V., Cai, G., Cakir, C., Carrington, J. C., Chawner, M., Conti, L., Costanzo, S., Ewan, R., Fahlgren, N., Fischbach, M. A., Fugelstad, J., Gilroy, E. M., Gnerre, S., Green, P. J., Grenville-Briggs, L. J., Griffith, J., Grünwald, N. J., Horn, K., Horner, N. R., Hu, C. H., Huitema, E., Jeong, D. H., Jones, A. M., Jones, J. D., Jones, R. W., Karlsson, E. K., Kunjeti, S. G, Lamour, K., Liu ,Z,. Ma, L., Maclean, D., Chibucos, M. C., McDonald, H., McWalters, J., Meijer, H. J., Morgan, W., Morris, P. F., Munro, C. A., O'Neill, K., Ospina-Giraldo, M., Pinzón, A., Pritchard, L., Ramsahoye, B., Ren, Q., Restrepo, S., Roy, S., Sadanandom, A., Savidor, A., Schornack, S., Schwartz, D. C., Schumann, U. D., Schwessinger, B., Seyer, L., Sharpe, T., Silvar, C., Song, J., Studholme, D. J., Sykes, S., Thines, M., van de Vondervoort, P. J., Phuntumart, V., Wawra, S., Weide, R., Win, J., Young, C., Zhou, S., Fry, W., Meyers, B. C., van West, P., Ristaino, J., Govers, F., Birch, P. R., Whisson, S. C., Judelson, H. S., and Nusbaum, C. (2009). Genome sequence and analysis of the Irish potato famine pathogen *Phytophthora infestans*. *Nature*, 461(7262):393-8.

Hahne, F., and Ivanek, R. (2016). Visualizing genomic data using Gviz and Bioconductor. *Methods in Molecular Biology*, 1418:335–351.

Hai, Y., and Tang, Y. (2018). Biosynthesis of long-chain N-acyl amide by a truncated PKS-NRPS hybrid megasynthase in fungi. *Journal of the American Chemical Society*, 140:1271-1274.

Hammett, K. R. W. (1971). Symptom differences between rose wilt virus and Verticillium wilt of roses. *Plant Disease Reporter*, 55:916–920.

Heikema, A. P., Horst-Kreft, D., Boers, S. A., Jansen, R., Hiltemann, S. D., de Koning, W., Kraaij, R., de Ridder, M. A. J., van Houten, C. B., Bont, L. J., Stubbs, A. P., and Hays, J. P. (2020). Comparison of Illumina versus Nanopore 16S rRNA Gene Sequencing of the Human Nasal Microbiota. *Genes*, 11(9):1105.

Holm, D. K., Petersen, L. M., Klitgaard, A., Knudsen, P. B., Jarczynska, Z. D., Nielsen, K. F., Gotfredsen, C. H., Larsen, T. O., and Mortensen, U. H. (2014). Molecular and chemical characterization of the biosynthesis of the 6-MSA-derived meroterpenoid yanuthone D in *Aspergillus niger*. *Chemistry and Biology*, 21:519-529.

Horiuchi, S., Hagiwara, H., and Takeuchi, S. (1990). Host specificity of isolates of *Verticillium dahliae* towards cruciferous and solanaceous plants. *CAB International*, 285–298.

Horst R. K., and Cloyd R. A. (2007). Compendium of Rose Diseases and Pests. Second Edition. The American Phytopathological Society, St. Paul, Minnesota, USA. 83 pp.

Huang, A. C., Jiang, T., Liu, Y. X., Bai, Y. C., Reed, J., Qu, B., Goossens, A., Nützmann, H. W., Bai, Y., and Osbourn, A. (2019). A specialized metabolic network selectively

modulates *Arabidopsis* root microbiota. *Science*, 364(6440):eaau6389.

Huisman, O.C. (1982). Interrelations of root growth dynamics to epidemiology of root-invading fungi. *Annual Review of Phytopathology*, 20:303 –327.

Inami, K., Yoshioka-Akiyama, C., Morita, Y., Yamasaki, M., Teraoka, T., and Arie, T. (2012). A genetic mechanism for emergence of races in *Fusarium oxysporum* f. sp. *lycopersici*: inactivation of avirulence gene *AVR1* by transposon insertion. *PLoS One*, 7:1–10.

Ingham, A. B., and Moore, R. J. (2007). Recombinant production of antimicrobial peptides in heterologous microbial systems. *Biotechnology and Applied Biochemistry*, 47:1-9.

Innerebner, G., Knief, C., and Vorholt, J. A. (2011). Protection of *Arabidopsis thaliana* against leaf-pathogenic *Pseudomonas syringae* by *Sphingomonas* strains in a controlled model system. *Applied and Environmental Microbiology*, 77(10):3202-10.

Inoue, Y., Vy, T. T. P., Yoshida, K., Asano, H., Mitsuoka, C., Asuke, S., Anh, V. L., Cumagun, C. J. R, Chuma, I., Terauchi, R., Kato, K., Mitchell, T., Valent, B., Farman, M., and Tosa, Y. (2017). Evolution of the wheat blast fungus through functional losses in a host specificity determinant. *Science*, 357:80–83.

Ismail, I. A., and Able, A. (2016). Secretome analysis of virulent *Pyrenophora teres* f. *teres* isolates. *Proteomics*, 16:2625-2636.

Jayaraman, S., Naorem, A., Lal, R., Dalal, R. C., Sinha, N.K., Patra, A.K., and Chaudhari, S.K. (2021). Disease-Suppressive Soils—Beyond Food Production: a Critical Review. *Journal of Soil Science and Plant Nutrition*, 21:1437–1465.

Jeffares, D. C., Jolly, C., Hoti, M., Speed, D., Shaw, L., Rallis, C., Balloux, F., Dessimoz, C., Bähler, J., and Sedlazeck, F. J. (2017). Transient structural variations have strong effects on quantitative traits and reproductive isolation in fission yeast. *Nature Communications*, 8:1-11.

Jeong, J., Yun, K., Mun, S., Chung, W., Choi, S., Nam, Y., Lim, M. Y., Hong, C. P., Park, C. H., Ahn, Y. J., and Han, K. (2021). The effect of taxonomic classification by full-length 16S rRNA sequencing with a synthetic long-read technology. *Scientific Reports*, 11:1-12.

Jimenez-Diaz, R. M., Cirulli, M., Bubici, G., del Mar Jimenez-Gasco, M., Antoniou, P. P., and Tjamos, E. C. (2012). Verticillium wilt, a major threat to olive production: Current status and feature prospects for its management. *Plant Disease*, 96:304–329.

Jones, J. D. G., and Dangl, J. L. (2006). The plant immune system. Nature, 444:323–329.

Joosten, M. H. A. J., Cozijnsen, T. J., and de Wit, P. J. G. M. (1994). Host resistance to a fungal tomato pathogen lost by a single base-pair change in an avirulence gene. *Trends in Genetics*, 10:117.

Judge, K., Hunt, M., Reuter, S., Tracey, A., Quail, M. A., Parkhill, J., and Peacock, S. J. (2016). Comparison of bacterial genome assembly software for MinION data and their applicability to medical microbiology. *Microbial Genomics*, 2(9):e000085.

Jumper, J., Evans, R., Pritzel, A., Green, T., Figurnov, M., Ronneberger, O., Tunyasuvunakool, K., Bates, R., Žídek, A., Potapenko, A., Bridgland, A., Meyer, C., Kohl, S. A. A., Ballard, A. J., Cowie, A., Romera-Paredes, B., Nikolov, S., Jain, R., Adler, J., Back, T., Petersen,

S., Reiman, D., Clancy, E., Zielinski, M., Steinegger, M., Pacholska, M., Berghammer, T., Bodenstein, S., Silver, D., Vinyals, O., Senior, A. W., Kavukcuoglu, K., Kohli, P., and Hassabis, D. (2021). Highly accurate protein structure prediction with AlphaFold. *Nature*, 596:583–589.

Kakule, T. B., Sardar, D., Lin, Z., and Schmidt, E. W. (2013). Two related pyrrolidinedione synthetase loci in *Fusarium heterosporum* ATCC 74349 produce divergent metabolites. *ACS Chemical Biology*, 8:1549-1557.

Kanagawa, T. (2003). Bias and artifacts in multitemplate polymerase chain reactions (PCR). *Bioscience and Bioengineering*, 96(4):317-23.

Kanja, C., and Hammond-Kosack, K. E. (2020). Proteinaceous effector discovery and characterization in filamentous plant pathogens. *Molecular Plant Pathology*, 21(10):1353-1376.

Katoh, K., and Standley, D. M. (2013). MAFFT multiple sequence alignment software version 7:Improvements in performance and usability. *Molecular Biology and Evolution*, 30:772–780.

Kawaide, H. (2006). Biochemical and molecular analyses of gibberellin biosynthesis in fungi. *Bioscience, Biotechnology, and Biochemistry*, 70:583-590.

Kelley, L. A., Mezulis, S., Yates, C. M., Wass, M. N., and Sternberg, M. J. E. (2015). The Phyre2 web portal for protein modeling, prediction and analysis. *Nature Protocols*, 10:845-858.

Kema, G. H. J., Mirzadi Gohari, A., Aouini, L., Gibriel, H. A. Y., Ware, S. B., Van Den Bosch, F., Manning-Smith, R., Alonso-Chavez, V., Helps, J., Ben M'Barek, S., Mehrabi, R., Diaz-Trujillo, C., Zamani, E., Schouten, H. J., van der Lee, T. A. J., Waalwijk, C., de Waard, M. A., de Wit, P. J. G. M., Verstappen, E. C. P., Thomma, B. P. H. J., Meijer, H. J. G., and Seidl, M. F. (2018). Stress and sexual reproduction affect the dynamics of the wheat pathogen effector *AvrStb6* and strobilurin resistance. *Nature Genetics*, 50:375–380.

Kettles, G. J., Bayon, C., Sparks, C. A., Canning, G., Kanyuka, K., and Rudd, J. J. (2018). Characterization of an antimicrobial and phytotoxic ribonuclease secreted by the fungal wheat pathogen *Zymoseptoria tritici*. *New Phytologist*, 217: 320-331.

Khang, C. H., Berruyer, R., Giraldo, M. C., Kankanala, P., Park, S.-Y., Czymmek, K., Kang, S., and Valent, B. (2010). Translocation of *Magnaporthe oryzae* effectors into rice cells and their subsequent cell-to-cell movement. *Plant Cell*, 22(4):1388-403.

King, S. R., McLellan, H., Boevink, P. C., Armstrong, M. R., Bukharova, T., Sukarta, O., Win, J., Kamoun, S., Birch, P.R., and Banfield, M.J. (2014). *Phytophthora infestans* RXLR effector PexRD2 interacts with host MAPKKK ε to suppress plant immune signaling. *Plant Cell*, 26(3):1345-59.

Klosterman, S. J., Atallah, Z. K., Vallad, G. E., and Subbarao, K. V. (2009). Diversity, pathogenicity, and management of *Verticillium* species. *Annual Review of Phytopathology*, 47:39–62.

Klosterman, S. J., Subbarao, K. V., Kang, S., Veronese, P., Gold, S. E., Thomma, B. P. H. J., Chen, Z., Henrissat, B., Lee, Y. H., Park, J., Garcia-Pedrajas, M. D., Barbara, D. J., Anchieta, A., de Jonge, R., Santhanam, P., Maruthachalam, K., Atallah, Z., Amyotte, S. G., Paz, Z., Inderbitzin, P., Hayes, R. J., Heiman, D. I., Young, S., Zeng, Q., Engels, R., Galagan, J., Cuomo, C. A., Dobinson, K. F., and Ma, L. J. (2011). Comparative

genomics yields insights into niche adaptation of plant vascular wilt pathogens. *PLoS Pathogens*, 7:1-19.

Kombrink, A., and Thomma, B. P. H. J. (2013). LysM effectors: secreted proteins supporting fungal life. *PLoS Pathogens*, 9:1–4.

Kombrink, A., Rovenich, H., Shi-Kunne, X., Rojas-Padilla, E., van den Berg, G. C. M., Domazakis, E., de Jonge, R., Valkenburg, D. J., Sánchez-Vallet, A., Seidl, M. F., and Thomma, B. P. H. J. (2017). *Verticillium dahliae* LysM effectors differentially contribute to virulence on plant hosts. *Molecular Plant Pathology*, 18:596–608.

Kombrink, A., Sanchez-Vallet, A., and Thomma, B. P. H. J. (2011). The role of chitin detection in plant–pathogen interactions. *Microbes and Infection*, 13, 1168–1176.

Koprivova, A., Schuck, S., Jacoby, R. P., Klinkhammer, I., Welter, B., Leson, L., Martyn, A., Nauen, J., Grabenhorst, N., Mandelkow, J. F., Zuccaro, A., Zeier, J., and Kopriva, S. (2019). Root-specific camalexin biosynthesis controls the plant growth-promoting effects of multiple bacterial strains. *Proceedings of the National Academy of Sciences*, 116(31):15735-15744.

Koren, S., Walenz, B. P., Berlin, K., Miller, J. R., Bergman, N. H., and Phillippy, A. M. (2017). Canu: scalable and accurate long-read assembly via adaptive k-mer weighting and repeat separation. *Genome Research*, 27:722–736.

Langmead, B., and Salzberg, S. L. (2012). Fast gapped-read alignment with Bowtie 2. *Nature Methods*, 9:357–359.

Lauge, R., Joosten, M. H. A. J., Haanstra, J. P. W., Goodwin, P. H., Lindhout, P., and de Wit, P. J. G. M. (1998). Successful search for a resistance gene in tomato targeted against a virulence factor of a fungal pathogen. *Proceedings of the National Academy of Sciences*, 95:9014–9018.

Lei, Y., Xu, L., Cao, H., and Wang, X. (2022). A method of large DNA fragment enrichment for nanopore sequencing in region 22q11.2. *Frontiers in Genetics*, 13: 959883.

Lenarčič, T., Albert, I., Böhm, H., Hodnik, V., Pirc, K., Zavec, A. B., Podobnik, M., Pahovnik, D., Žagar, E., Pruitt, R., Greimel, P., Yamaji-Hasegawa, A., Kobayashi, T., Zienkiewicz, A., Gömann, J., Mortimer, J. C., Fang, L., Mamode-Cassim, A., Deleu, M., Lins, L., Oecking, C., Feussner, I. Mongrand, S., Anderluh, G., and Nürnberger, T. (2017). Eudicot plant-specific sphingolipids determine host selectivity of microbial NLP cytolysins. *Science*, 358:1431-1434.

Li, H. (2013). Aligning sequence reads, clone sequences and assembly contigs with BWA-MEM. *ArXiv*, https://doi.org/10.48550/arXiv.1303.3997.

Li, H. (2018). Minimap2: pairwise alignment for nucleotide sequences. *Bioinformatics*, 34:3094–3100.

Li, H., and Durbin, R. (2009). Fast and accurate short read alignment with burrows-wheeler transform. *Bioinformatics*, 25:1754–1760.

Li, H., Handsaker, B., Wysoker, A., Fennell, T., Ruan, J., Homer, N., Marth, G., Abecasis, G., Durbin, R., and 1000 Genome Project Data Processing Subgroup (2009). The sequence alignment/map format and SAMtools. *Bioinformatics*, 25:2078–2079.

Li, J. (2019). Identification of host-specific effectors mediating pathogenicity of the vascular wilt pathogen. Wageningen University, Wageningen, The Netherlands.

Liu, H., Li, J., Carvalhais, L. C., Percy, C. D., Prakash Verma, J., Schenk, P. M., and Singh, B. K. (2021). Evidence for the plant recruitment of beneficial microbes to suppress

soil-borne pathogens. *New Phytologist*, 229(5):2873-2885.

Liu, T., Song, T., Zhang, X., Yuan, H., Su, L., Li, W., Xu, J., Liu, S., Chen, L., Chen, T., Zhang, M., Gu, L., Zhang, B., and Dou, D. (2014). Unconventionally secreted effectors of two filamentous pathogens target plant salicylate biosynthesis. *Nature Communications*, 5:1-10.

Lo Presti, L., Lanver, D., Schweizer, G., Tanaka, S., Liang, L., Tollot, M., Zuccaro, A., Reissmann, S., and Kahmann, R. (2015). Fungal effectors and plant susceptibility. *Annual Review of Plant Biology*, 66:513-545.

Lorang, J., Kidarsa, T., Bradford, C. S., Gilbert, B., Curtis, M., Tzeng, S.-C., Maier, C. S., and Wolpert, T. J. (2012). Tricking the guard: exploiting plant defense for disease susceptibility. *Science*, 338(6107):659-62.

Lozano-Torres, J. L., Wilbers, R. H., Gawronski, P., Boshoven, J. C., Finkers-Tomczak, A., Cordewener, J. H., America, A. H., Overmars, H. A., Van 't Klooster, J. W., Baranowski, L., Sobczak, M., Ilyas, M., van der Hoorn, R. A., Schots, A., de Wit, P. J., Bakker, J., Goverse, A., and Smant, G. (2012). Dual disease resistance mediated by the immune receptor Cf-2 in tomato requires a common virulence target of a fungus and a nematode. *Proceedings of the National Academy of Sciences*, 19;109(25):10119-24.

Lu, H., Giordano, F., and Ning, Z. (2016). Oxford Nanopore MinION Sequencing and Genome Assembly. *Genomics Proteomics Bioinformatics*, 14(5):265-279.

Lu, T., Ke, M., Lavoie, M., Jin, Y., Fan, X., Zhang, Z., Fu, Z., Sun, L., Gillings, M., Peñuelas, J., Qian, H., and Zhu, Y.-G. (2018). Rhizosphere microorganisms can influence the timing of plant flowering. *Microbiome*, 6:231.

Lu, X., Kracher, B., Saur, I. M. L., Bauer, S., Ellwood, S. R., Wise, R., Yaeno, T., Maekawa, T., and Schulze-Lefert, P. (2016). Allelic barley MLA immune receptors recognize sequence-unrelated avirulence effectors of the powdery mildew pathogen. *Proceedings of the National Academy of Sciences*, 113:E6486–E6495.

Lu, Y., Xue, Q., Eisele, M. R., Sulistijo, E. S., Brower, K., Han, L., Amir, E. D., Pe'er, D., Miller-Jensen, K., and Fan, R. (2015). Highly multiplexed profiling of single-cell effector functions reveals deep functional heterogeneity in response to pathogenic ligands. *Proceedings of the National Academy of Sciences*, 112:E607-E615.

Luciano-Rosario, D., Eagan, J. L., Aryal, N., Dominguez, E. G., Hull, C. M., and Keller, N. P. (2022). The hydrophobin gene family confers a fitness trade-off between spore dispersal and host colonization in *Penicillium expansum*. *mBio*, e02754-22.

Luderer, R., Takken, F. L. W., de Wit, P. J. G. M., and Joosten, M. H. A. J. (2002). *Cladosporium fulvum* overcomes Cf-2-mediated resistance by producing truncated AVR2 elicitor proteins. *Molecular Microbiology*, 45:875–884.

Ma, Z., Song, T., Zhu, L., Ye, W., Wang, Y., Shao, Y., Dong, S., Zhang, Z., Dou, D., Zheng, X., Tyler, B. M., and Wang, Y. (2015). A *Phytophthora sojae* Glycoside Hydrolase 12 Protein Is a Major Virulence Factor during Soybean Infection and Is Recognized as a PAMP. *The Plant Cell*, 27:2057–2072.

Madden, L. (1931). Verticillium wilt of roses. *Rivista di Patologia Vegetale*, 22:7–8.

Malinovsky, F. G., Fangel, J. U., and Willats, W. G. T. (2014). The role of the cell wall in plant immunity. *Frontiers in Plant Science*, 5:1-12.

Mangrola, A. V., et al. (2017). Evaluation of media for culture-dependent enumeration

of bacteria from diverse aquatic samples. *Microbiological Research*, 204, 26-34.

Manikas, I., Malindretos, G., and Abeliotis, K. (2020). Sustainable Cities through Alternative Urban Farming: The Case of Floriculture. *Journal of International Food and Agribusiness Marketing*, 32:295–311.

Mapuranga, J., Chang, J., Zhang, L., Zhang, N., and Yang, W. (2022). Fungal Secondary Metabolites and Small RNAs Enhance Pathogenicity during Plant-Fungal Pathogen Interactions. *Journal of Fungi,* 20;9(1):4.

Marshall, R., Kombrink, A., Motteram, J., Loza-Reyes, E., Lucas, J., Hammond-Kosack, K. E., Thomma, B. P. H. J., and Rudd, J.J. (2011). Analysis of two i*n planta* expressed LysM effector homologs from the fungus *Mycosphaerella graminicola* reveals novel functional properties and varying contributions to virulence on wheat. *Plant Physiology*, 156(2):756-69.

Martín-Robles, N., García-Palacios, P., Rodríguez, M., Rico, D., Vigo, R., Sánchez-Moreno, S., De Deyn, G. B., and Milla, R. (2020). Crops and their wild progenitors recruit beneficial and detrimental soil biota in opposing ways. *Plant Soil*, 456, 159–173.

Martins, J. C., Maes, D., Loris, R., Pepermans, H. A. M., Wyns, L., Willen, R., and Verheyden, P. (1996). 1H NMR study of the solution structure of Ac-AMP2, a sugar binding antimicrobial protein isolated from *Amaranthus caudatus*. *Journal of Molecular Biology*, 258:322-333.

Maruthachalam, K., Klosterman, S. J., Kang, S., Hayes, R. J., and Subbarao, K. V. (2011). Identification of pathogenicity-related genes in the vascular wilt fungus *Verticillium dahliae* by *Agrobacterium tumefaciens*-mediated T-DNA insertional mutagenesis. *Molecular Biotechnology*, 49(3):209-21.

Maucieri, C., Nicoletto, C., van Os, E., Anseeuw, D., Van Havermaet, R., and Junge, R. (2019b). Hydroponic Technology. In: Aquaponics Food Production Systems, Springer, Switzerland. 77–110 pp.

Maucieri, C., Nicoletto, C., Zanin, G., Birolo, M., Trocino, A., Sambo, P., Borin, M., and Xiccato, G. (2016a). Effect of stocking density of fish on water quality and growth performance of European Carp and leafy vegetables in a low-tech aquaponic system. *PLoS One*, 14(5):e0217561.

McDermott, J. E., Corrigan, A., Peterson, E., Oehmen, C., Niemann, G., Cambronne, E. D., Sharp, D., Adkins, J. N., Samudrala, R., and Heffron, F. (2011). Computational prediction of type III and IV secreted effectors in gram-negative bacteria. *Infection and Immunity*, 79(1):23-32.

Meile, L., Croll, D., Brunner, P. C., Plissonneau, C., Hartmann, F. E., McDonald, B. A., and Sánchez-Vallet, A. (2018). A fungal avirulence factor encoded in a highly plastic genomic region triggers partial resistance to septoria tritici blotch. *New Phytologist*, 219:1048–1061.

Mendes, R., Garbeva, P., and Raaijmakers, J. M. (2013). The rhizosphere microbiome: significance of plant beneficial, plant pathogenic, and human pathogenic microorganisms. *FEMS Microbiology Reviews*, 37: 634-663.

Mendes, R., Kruijt, M., de Bruijn, I., Dekkers, E., van der Voort, M., Schneider, J. H., Piceno, Y. M., DeSantis, T. Z., Andersen, G. L., Bakker, P. A., and Raaijmakers, J. M. (2011). Deciphering the rhizosphere microbiome for disease-suppressive bacteria. *Science*, 332(6033):1097-100.

Mentlak, T. A., Kombrink, A., Shinya, T., Ryder, L.S., Otomo, I., Saitoh, H., Terauchi, R., Nishizawa, Y., Shibuya, N., Thomma. B. P. H. J., and Talbot, N. J. (2012). Effector-mediated suppression of chitin-triggered immunity by *Magnaporthe oryzae* is necessary for rice blast disease. *Plant Cell*, 24(1):322-35.

Mesarich, C. H., Griffiths, S. A., van der Burgt, A., Ökmen, B., Beenen, H. G., Etalo, D. W., Joosten, M. H. A. J., de Wit, P. J. G. M. (2014). Transcriptome sequencing uncovers the *Avr5* avirulence gene of the tomato leaf mold pathogen *Cladosporium fulvum*. *Molecular Plant-Microbe Interactions Journal*, 27:846–857.

Mesny, F., Hacquard, S., and Thomma, B. P. H. J. (2023). Co-evolution within the plant holobiont drives host performance. *EMBO reports*, 24: e57455.

Mol, L., Scholte, K., and Vos, J.(1995). Effects of crop rotation and removal of crop debris on the soil population of two isolates of *Verticillium dahliae*. *Plant Pathology*, 44, 1070 –1074.

Molina-Santiago, C., Daddaoua, A., Fillet, S., Duque, E. and Ramos, J. L. (2014). Interspecies signalling: *Pseudomonas putida* efflux pump TtgGHI is activated by indole to increase antibiotic resistance. *Environmental Microbiology*, 16: 1267-1281.

Mousa, W. K., and Raizada, M. N. (2016). Natural Disease Control in Cereal Grains. In: Encyclopedia of Food Grains, Academic Press. 257-263 pp.

Na, R., and Gijzen, M. (2016). Escaping host immunity: new tricks for plant pathogens. *PLoS Pathogens*, 12:1–6.

Nakkeeran, S., Surya, T., and Vinodkumar, S. (2019). Antifungal Potential of Plant Growth Promoting *Bacillus* Species Against Blossom Blight of Rose. *Journal of Plant Growth Regulation*, 39:99–111.

Ngou, B. P. M, Ahn, H. K., Ding, P., and Jones, J. D. G. (2021). Mutual potentiation of plant immunity by cell-surface and intracellular receptors. *Nature*, 592(7852):110-115.

Niu, B., Wang, W., Yuan, Z., Sederoff, R. R., Sederoff, H., Chiang, V. L., and Borriss, R. (2020). Microbial Interactions Within Multiple-Strain Biological Control Agents Impact Soil-Borne Plant Disease. *Frontiers in Microbiology*, 11:585404.

Niu, X., Zhao, X., Ling, K. S., Levi, A., Sun, Y., and Fan, M. (2016). The *FonSIX6* gene acts as an avirulence effector in the *Fusarium oxysporum* f. sp. *niveum* – watermelon pathosystem. *Scientific Reports*, 6:1–7.

Novo, M., Pomar, F., Gayoso, C., and Merino, F. (2006). Cellulase Activity in Isolates of *Verticillium dahliae* Differing in Aggressiveness. *Plant Disease*, 90(2):155-160.

Oggenfuss, U., Badet, T., Wicker, T., Hartmann, F. E., Singh, N. K., Abraham, L., Karisto, P., Vonlanthen, T., Mundt, C., McDonald, B. A., and Croll, D. (2021). A population-level invasion by transposable elements triggers genome expansion in a fungal pathogen. *eLife*, 10:e69249.

Ökmen, B., Etalo, D. W., Joosten, M. H. A. J., Bouwmeester, H. J., de Vos, R. C. H., Collemare, J., and de Wit, P. J. G. M. (2013). Detoxification of α-tomatine by *Cladosporium fulvum* is required for full virulence on tomato. *New Phytologist*, 198:1203–1214.

Ökmen, B., Katzy, P., Huang, L., Wenhöner, R., and Doehlemann, G. (2023). A conserved extracellular Ribo1 with broad-spectrum cytotoxic activity enables smut fungi to compete with host-associated bacteria. *New Phytologist*, 240: 1976-1989.

Olsson, S., and Nordbring-Hertz, B.(1985). Microsclerotial germination of *Verticillium dahliae* as affected by rape rhizosphere. *FEMS Microbiology Ecology*, 31, 293 –299.

Ong, S. H., Kukkillaya, V. U., Wilm, A., Lay, C., Ho, E. X., Low, L., Hibberd, M. L., and Nagarajan, N. (2013). Species identification and profiling of complex microbial communities using shotgun Illumina sequencing of 16S rRNA amplicon sequences. *PLoS One*, 8(4):e60811.

Oome, S., and Van den Ackerveken, G. (2014). Comparative and functional analysis of the widely occurring family of Nep1-like proteins. *Molecular Plant-Microbe Interactions*, 27(10):1081-94.

Orazi, G., and O'Toole, G. A. (2017). *Pseudomonas aeruginosa* alters *Staphylococcus aureus* sensitivity to vancomycin in a biofilm model of cystic fibrosis infection. *mBio*, 8: e00873–17.

Ospina-Giraldo, M. D., Mullins, E., and Kang, S. (2003). Loss of function of the *Fusarium oxysporum SNF1* gene reduces virulence on cabbage and *Arabidopsis*. *Current Genetics*, 44(1):49-57.

Ottmann, C., Luberacki, B., Küfner, I., Koch, W., Brunner, F., Weyand, M., Mattinen, L., Pirhonen, M., Anderluh, G., Seitz, H. U., Nürnberger, T., and Oecking, C. (2009). A common toxin fold mediates microbial attack and plant defense. *Proceedings of the National Academy of Sciences*, 106(25):10359-64.

Ou, S., Su, W., Liao, Y., Chougule, K., Agda, J. R. A., Hellinga, A. J., Blanco-Lugo, C. S., Elliot, T. A., Waren, D., Peterson, T., Jiang, N., Hirsch, C. N., and Hufford, M. B. (2019). Benchmarking transposable element annotation methods for creation of a streamlined, comprehensive pipeline. *Genome Biology*, 20:275.

Oyserman, B. O., Flores, S. S., Griffioen, T., Pan, X., van der Wijk, E., Pronk, L., Lokhorst, W., Nurfikari, A., Paulson, J. N., Movassagh, M., Stopnisek, N., Kupczok, A., Cordovez, V., Carrión, V. J., Ligterink, W., Snoek, B. L., Medema, M. H., and Raaijmakers, J. M. (2022). Disentangling the genetic basis of rhizosphere microbiome assembly in tomato. *Nature Communications*, 13(1):3228.

Özcengiz, G., and Öğülür, İ. (2015). Biochemistry, genetics and regulation of bacilysin biosynthesis and its significance more than an antibiotic. *New Biotechnology*, 32(6):612-9.

Pallaghy, P. K., Norton, R. S., Nielsen, K. J., and Craik, D. J. (1994). A common structural motif incorporating a cystine knot and a triple-stranded β-sheet in toxic and inhibitory polypeptides. *Protein Science*, 3:1833–1839.

Palmer, J., and Stajich, J. E. (2017). Funannotate: Eukaryotic genome annotation pipeline. Retrieved from https://funannotate.readthedocs.io/en/latest/

Pan, Y., Liu, L., Guan, F., Li, E., Jin, J., Li, J., Che, Y., and Liu, G. (2018). Characterization of a Prenyltransferase for Iso-A82775C biosynthesis and generation of new congeners of chloropestolides. *ACS Chemical Biology*, 13:703-711.

Parijs, I., and Steenackers, H. P. (2018). Competitive inter-species interactions underlie the increased antimicrobial tolerance in multispecies brewery biofilms. *The ISME Journal*, 12: 2061-2075.

Parlange, F., Daverdin, G., Fudal, I., Kuhn, M.L., Balesdent, M. H., Blaise, F., Grezes-Besset, B., and Rouxel, T. (2009). *Leptosphaeria maculans* avirulence gene *AvrLm4-7* confers a dual recognition specificity by the *Rlm4* and *Rlm7* resistance genes of

oilseed rape, and circumvents *Rlm4*-mediated recognition through a single amino acid change. *Molecular Microbiology*, 71:851–863.

Payne, A., Holmes, N., Rakyan, V., and Loose, M. (2019). BulkVis: a graphical viewer for Oxford nanopore bulk FAST5 files. *Bioinformatics*, 35(13):2193-2198.

Pegg, G. F., and Dixon, G. R. (1969). The reactions of susceptible and resistant tomato cultivars to strains of *Verticillium albo-atrum*. *Annals of Applied Biology*, 63:389–400.

Pérez-Jaramillo, J. E., Mendes, R., and Raaijmakers, J. M. (2016). Impact of plant domestication on rhizosphere microbiome assembly and functions. *Plant Molecular Biology*, 90:635-644.

Pérez-Jiménez, R. M. (2006). A review of the biology and pathogenicity of *Rosellinia necatrix* – the cause of white root rot disease of fruit trees and other plants. *Journal of Phytopathology*, 154:257–266.

Pérez-Jiménez, R. M., Jiménez-Díaz, R. M., and López-Herrera, C. J. (2002). Somatic incompatibility of *Rosellinia necatrix* on avocado plants in southern Spain. *Mycological Research*, 106:239–244.

Pérez-Jiménez, R. M., Zea-Bonilla, T., and López-Herrera, C. J. (2003). Studies of *Rosellinia necatrix perithecia* found in nature on avocado roots. *Journal of Phytopathology*, 151:660–664.

Perlin, M. H., Clark, D. R., McKenzie, C., Patel, H., Jackson, N., Kormanick, C., Powell, C., Bajorek, A., Myers, D. A., Dugatkin, L. A., and Atlas, R. M. (2009). Protection of *Salmonella* by ampicillin-resistant *Escherichia coli* in the presence of otherwise lethal drug concentrations. *Proceedings: Biological Sciences*, 276: 3759-3768.

Petersen, C., Sørensen, T., Westphal, K. R., Fechete, L. I., Sondergaard, T. E., Sørensen, J. L., and Nielsen, K. L. (2022). High molecular weight DNA extraction methods lead to high quality filamentous ascomycete fungal genome assemblies using Oxford Nanopore sequencing. *Microbial Genomics*, 8(4):000816.

Petersen, T.N., Brunak, S., Von Heijne, G., and Nielsen, H. (2011). SignalP 4.0: discriminating signal peptides from transmembrane regions. *Nature Methods*, 8:785–786.

Petit-Houdenot, Y., Degrave, A., Meyer, M., Blaise, F., Ollivier, B., Marais, C. L., Jauneau, A., Audran, C., Rivas, S., Veneault-Fourrey, C., Brun, H., Rouxel, T., Fudal, I., and Balesdent, M.-H. (2019). A two genes – for – one gene interaction between *Leptosphaeria maculans* and *Brassica napus*. *New Phytologist*, 223:397–411.

Pfeilmeier, S., Petti, G. C., Bortfeld-Miller, M., Daniel, B., Field, C. M., Sunagawa, S., and Vorholt, J. A. (2021). The plant NADPH oxidase RBOHD is required for microbiota homeostasis in leaves. *Nature Microbiology*, 6(7):852-864.

Pliego, C., Kanematsu, S., Ruano-Rosa, D., de Vicente, A., López-Herrera, C., Cazorla, F. M., and Ramos, C. (2009). GFP sheds light on the infection process of avocado roots by *Rosellinia necatrix*. *Fungal Genetics and Biology*, 46:137–145.

Plissonneau, C., Daverdin, G., Ollivier, B., Blaise, F., Degrave, A., Fudal, I., Rouxel, T., and Balesdent, M.-H. (2016). A game of hide and seek between avirulence genes *AvrLm4-7* and *AvrLm3* in *Leptosphaeria maculans*. *New Phytologist*, 209:1613–1624.

Pollock, J., Glendinning, L., Wisedchanwet, T., and Watson, M. (2018). The Madness of

Microbiome: Attempting To Find Consensus "Best Practice" for 16S Microbiome Studies. *Applied and Environmental Microbiology,* 84(7):e02627-17.

Polz, M. F., and Cavanaugh, C. M. (1998). Bias in template-to-product ratios in multitemplate PCR. *Applied and Environmental Microbiology*, 64(10):3724-30.

Poueymiro, M., and Genin, S. (2009). Secreted proteins from *Ralstonia solanacearum*: a hundred tricks to kill a plant. *Current Opinion in Microbiology*, 12(1):44-52.

Praz, C.R., Bourras, S., Zeng, F., Sánchez-Martín, J., Menardo, F., Xue, M., Yang, L., Roffler, S., Böni, R., Herren, G., McNally, K. E., Ben-David, R., Parlange, F., Oberhaensli, S., Flückiger, S., Schäfer, L. K., Wicker, T., Yu, D., and Keller, B. (2016). *AvrPm2* encodes an RNase-like avirulence effector which is conserved in the two different specialized forms of wheat and rye powdery mildew fungus. *New Phytologist*, 213:1301–1314.

Pritchard, L., and Birch, P. (2010). A systems biology perspective on plant-microbe interactions: biochemical and structural targets of pathogen effectors. *Plant Science*, 180(4):584-603.

Pruitt, R. N., Locci, F., Wanke, F., Zhang, L., Saile, S. C., Joe, A., Karelina, D., Hua, C., Fröhlich, K., Wan, W.-L., Hu, M., Rao, S., Stolze, S. C., Harzen, A., Gust, A. A., Harter, K., Joosten, M. H. A. J., Thomma, B. P. H. J., Zhou, J.-M., Dangl, J. L., Weigel, D., Nakagami, H., Oecking, C., Kasmi, F. E., Parker, J. E., and Nürnberger, T. (2021). The EDS1-PAD4-ADR1 node mediates *Arabidopsis* pattern-triggered immunity. *Nature*, 598(7881):495-499.

Qin, J., Wang, K., Sun, L., Xing, H., Wang, S., Li, L., Chen, S., Guo, H. S., and Zhang, J. (2018). The plant-specific transcription factors CBP60g and SARD1 are targeted by a *Verticillium* secretory protein VdSCP41 to modulate immunity. *eLife*, 7:e34902.

Quinlan, A. R., and Hall, I. M. (2010). BEDTools: a flexible suite of utilities for comparing genomic features. *Bioinformatics*, 26:841-842.

Rademacher, W., and Graebe, J. E. (1979). Gibberellin A4 produced by *Sphaceloma manihoticola*, the cause of the super elongation disease of cassava (*Manihot esculenta*). *Biochemical and Biophysical Research Communications*, 91:35-40.

Rafaelle, S., Farrer, R. A., Cano, L. M., Studholme, D. J., Maclean, D., Thines, M., Jiang, R. H. Y., Zody, M. C., Kunjeti, S. G., Donofrio, N. M., Meyers, B. C., Nusbaum, C., and Kamoun, S. (2010). Genome evolution following host jumps in the irish potato famine pathogen lineage. *Science*, 330:1540-1543.

Raffaele, S., and Kamoun, S. (2012). Genome evolution in filamentous plant pathogens: why bigger can be better. *Nature Reviews Microbiology*, 10:417-430.

Raymond, O., Gouzy, J., Just, J., Badouin, H., Verdenaud, M., Lemainque, A., Vergne, P., Moja, S., Choisne, N., Pont, C., Carrère, S., Caissard, J., Couloux, A., Cottret, L., Aury, J., Szécsi, J., Latrasse, D., Madoui, M., François, L., Fu, X., Yang, S., Dubois, A., Piola, F., Larrieu, A., Perez, M., Labadie, K., Perrier, L., Govetto, B., Labrousse, Y., Villand, P., Bardoux, C., Boltz, V., Lopez-Roques, C., Heitzler, P., Vernoux, T., Vandenbussche, M., Quesneville, H., Boualem, A., Bendahmane, A., Liu, C., Le Bris, M., Salse, J., Baudino, S., Benhamed, M., Wincker P., and Bendahmane, M. (2018). The *Rosa* genome provides new insights into the domestication of modern roses. *Nature Genetics*, 50:772–777.

Resende, M. L. V., Flood, J., and Cooper, R. M. (1994). Host specialization of *Verticillium dahliae*, with emphasis on isolates from cocoa (*Theobroma cacao*). *Plant Pathology,*

43:104-111.

Ritter, G., Hojo, E. T. D., Villa, F., and da Silva, D. F. (2018). Rooting of Tineke and Natal Briar rose stem cuttings in different substrates. *Ciencia Rural*, 48(8):1–5.

Robert, X., and Gouet, P. (2014). Deciphering key features in protein structures with the new ENDscript server. *Nucleic Acids Research*, 42:320–324.

Robinson, D. B. (1957). Verticillium Wilt of Potato in Relation to Symptoms, Epidemiology and Variability of the Pathogen, Madison, WI: University of Wisconsin Agricultural Experiment Station Results Bulletin, p. 49.

Robinson, J. T., Thorvaldsdóttir, H., Winckler, W., Guttman, M., Lander, E. S., Getz, G., and Mesirov, J. P. (2011). Integrative Genome Viewer. *Nature Biotechnology*, 29:24–26.

Rocafort, M., Bowen, J. K., Hassing, B., Cox, M. P., McGreal, B., de la Rosa, S., Plummer, K. M., Bradshaw, R. E., and Mesarich, C. H. (2022). The *Venturia inaequalis* effector repertoire is dominated by expanded families with predicted structural similarity, but unrelated sequence, to avirulence proteins from other plant-pathogenic fungi. *BMC Biology*, 20:1-24.

Rodriguez-Jurado, D., Lopez, M. A. B., Rapoport, H. F., and Jimenez Diaz, R. M. (1993). Present status of Verticillium wilt of olive in Andalucia (southern Spaiin). *EPPO Bulletin*, 23:513-516.

Rooney, H. C. E., Van't Klooster, J. W., van der Hoorn, R. A. L., Joosten, M. H. A. J., Jones, J. D. G., and de Wit, P. J. G. M. (2005). Cladosporium Avr2 inhibits tomato Rcr3 protease required for *Cf-2*-dependent disease resistance. *Science*, 308(5729):1783-6.

Rovenich, H., Boshoven, J. C., and Thomma, B. P. H. J. (2014). Filamentous pathogen effector functions: of pathogens, hosts and microbiomes. *Current Opinion in Plant Biology*, 20:96-103.

Rudrappa, T., Czymmek, K. J., Paré, P. W., and Bais, H. P. (2008). Root-secreted malic acid recruits beneficial soil bacteria. *Plant Physiology*, 148(3):1547-56.

Sadat, S. S., Khani, S., Goudarzi, M., Zare-Zardini, H., Shams-Ghahfarokhi, M., Jamzivar, F., and Razzaghi-Abyaneh, M. (2021). Characterization, biological activity, and mechanism of action of a plant-based novel antifungal peptide, Cc-AFP1, isolated from *Carum carvi*. *Frontiers in Cellular and Infection Microbiology*, 11: 1-12.

Safi, M. I., (2005). Flower production related to reblooming time of three *Rosa hybrida* L. cultivars in response to rootstock type. *Science Asia*, 31:179–181.

Saint-Oyant, L. H., Ruttink, T., Hamama, L., Kirov, I., Lakhwani, D., Zhou, N. N., Bourke, P. M., Daccord, N., Leus, L., Schulz, D., Van de Geest, H., Hesselink, T., Van Laere, K., Debray, K., Balzergue, S., Thouroude, T., Chastellier, A., Jeauffre, J., Voisine, L., Gaillard, S., Borm, T. J. A., Arens, P., Voorrips, R. E., Maliepaard, C., Neu, E., Linde, M., Le Paslier, M. C., Bérard, A., Bounon, R., Clotault, J., Choisne, N., Quesneville, H., Kawamura, K., Aubourg, S. Sakr, S., Smulders, M. J. M., Schijlen, E., Bucher, E., Debener, T., De Riek, J., and Foucher, F. (2018). A high-quality genome sequence of *Rosa chinensis* to elucidate ornamental traits. *Nature Plants*, 4:473–484.

Salcedo, A., Rutter, W., Wang, S., Akhunova, A., Bolus, S., Chao, S., Anderson, N., Fernandez De Soto, M., Rouse, M., Szabo, L., Bowden, R. L., Dubcovsky, J., and Akhunov, E. (2017). Variation in the *AvrSr35* gene determines *Sr35* resistance against wheat stem rust race Ug99. *Science*, 358:1604–1606.

Salipante, S. J., Kawashima, T., Rosenthal, C., Hoogestraat, D. R., Cummings, L. A., Sengupta, D. J., Harkins, T. T., Cookson, B. T., and Hoffman, N. G. (2014). Performance comparison of Illumina and ion torrent next-generation sequencing platforms for 16S rRNA-based bacterial community profiling. *Applied and Environmental Microbiology*, 80(24):7583-91.

Sanaullah, M., Usman, M., Wakeel, A., Cheema, S. A., Ashraf, I., and Farooq, M. (2020). Terrestrial ecosystem functioning affected by agricultural management systems: A review. *Soil and Tillage Research*, 196:104464.

Santhanam, P., and Thomma, B. P. H. J. (2013). *Verticillium dahliae Sge1* differentially regulates expression of candidate effector genes. *Molecular Plant-Microbe Interactions*, 26:249–256.

Santhanam, P., Boshoven, J. C., Salas, O., Bowler, K., Islam, M. T., Saber, M. K., van den Berg, G. C. M., Bar-Peled, M., and Thomma, B. P. H. J. (2017). Rhamnose synthase activity is required for pathogenicity of the vascular wilt fungus *Verticillium dahliae*. *Molecular Plant Pathology*, 18:347–362.

Santhanam, P., van Esse, H. P., Albert, I., Faino, L., Nürnberger, T., and Thomma, B. P. H. J. (2013). Evidence for functional diversification within a fungal Nep1-like protein family. *Molecular Plant-Microbe Interactions*, 26:278–286.

Sarkar, D., Rovenich, H., Jeena, G., Nizam, S., Tissier, A., Balcke, G. U., Mahdi, L. K., Bonkowski, M., Langen, G., and Zuccaro, A. (2019). The inconspicuous gatekeeper: endophytic *Serendipita vermifera* acts as extended plant protection barrier in the rhizosphere. *New Phytologist*, 224(2):886-901.

Saur, I. M. L., Bauer, S., Kracher, B., Lu, X., Franzeskakis, L., Müller, M. C., Sabelleck, B., Kümmel, F., Panstruga, R., Maekawa, T., and Schulze-Lefert, P. (2019). Multiple pairs of allelic MLA immune receptor-powdery mildew AVRa effectors argue for a direct recognition mechanism. *eLife*, 8:1–31.

Sawai, K., Okuno, T., Fujioka, H., and Furuya, M. (1983). The relation between the phytotoxicity of Cythochalasin E and its molecular structure. *Annals of the Phytopathological Society of Japan*, 49:262-265.

Schaible, L., Cannon, O.S., and Waddoups, V. (1951). Inheritance of resistance to Verticillium wilt in a tomato cross. *Phytopathology*, 41:986–990.

Schlatter, D., Kinkel, L., Thomashow, L., Weller, D., and Paulitz, T. (2017). Disease Suppressive Soils: New Insights from the Soil Microbiome. *Phytopathology*, 107(11):1284-1297.

Schmidt, S. M., Lukasiewicz, J., Farrer, R., van Dam, P., Bertoldo, C., and Rep, M. (2016). Comparative genomics of *Fusarium oxysporum* f. sp. *melonis* reveals the secreted protein recognized by the *Fom-2* resistance gene in melon. *New Phytologist*, 209:307–318.

Schnathorst, W. C. (1969). A severe form of *Verticillium alboatrum* in *Gossypium barbadense* in Peru. *Plant Disease Reporter*, 53:149–150.

Schnathorst, W. C., and Mathre, D. E. (1966). Host range and differentiation of a severe form of *Verticillium albo-atrum* in cotton. *Phytopathology*, 56:1155–1161.

Schnathorst, W. C., and Sibbett, G. S. (1971). The relation of strains of *Verticillium albo-atrum* to severity of Verticillium wilt in *Gossypium hirsutum* and *Olea europaea* in California. *Plant Disease Reporter*, 55:780–782.

Schornack, S., van Damme, M., Bozkurt, T. O., and Huitema, E. (2010). Ancient class of translocated oomycete effectors targets the host nucleus. *Proceedings of the National Academy of Sciences*, 107(40):17421-6.

Schreiber, L.R., and Green, R.J. (1963). Effect of root exudates on germination of conidia and microsclerotia of *Verticillium albo-atrum* inhibited by the soil fungistatic principle. *Phytopathology*, 53,260 –264.

Schwessinger, B., Sperschneider, J., Cuddy, W. S., Garnica, D. P., Miller, M. E., Taylor, J. M., Dodds, P. N., Figueroa, M., Park, R. F., and Rathjen, J. P. (2018). A near-complete haplotype-phased genome of the dikaryotic wheat stripe rust fungus *Puccinia striiformis* f. sp. *tritici* reveals high interhaplotype diversity. *mBio*, 9:e02275-17.

Seidl, M. F., and Thomma, B. P. H. J. (2014). Sex or no sex: evolutionary adaptation occurs regardless. *Bioessays*, 36:335-345.

Seidl, M. F., and Thomma, B. P. H. J. (2017). Transposable elements direct the coevolution between plants and microbes. *Trends in Genetics*, 33:842–851.

Seidl, M. F., and van den Ackerveken, G. (2019). Activity and phylogenetics of the broadly occurring family of microbial nep1-like proteins. *Annual Review of Phytopathology*, 57:367–386.

Seidl, M. F., Kramer, H. M., Cook, D. E., Fiorin, G. L., van den Berg, G. C. M., Faino, L., and Thomma, B. P. H. J. (2020). Repetitive elements contribute to the diversity and evolution of centromeres in the fungal genus *Verticillium*. *mBio*, 11:1–22.

Seybold, H., Demetrowitsch, T. J., Hassani, M. A., Szymczak, S., Reim, E., Haueisen, J., Lübbers, L., Rühlemann, M., Franke, A., Schwarz, K., and Stukenbrock, E. H. (2020). A fungal pathogen induces systemic susceptibility and systemic shifts in wheat metabolome and microbiome composition. *Nature Communications*, 11(1):1910.

Shan, W., Cao, M., Leung, D., and Tyler, B. M. (2004). The *Avr1b* locus of *Phytophthora sojae* encodes an elicitor and a regulator required for avirulence on soybean plants carrying resistance gene *Rps1b*. *Molecular Plant Microbe Interactions*, 17:394–403.

Shendure, J., and Ji, H. (2008). Next-generation DNA sequencing. *Nature Biotechnology*, 26(10):1135-45.

Shi-Kunne, X., Faino, L., van den Berg G. C. M., Thomma, B. P. H. J., and Seidl, M. F. (2018). Evolution within the fungal genus *Verticillium* is characterized by chromosomal rearrangement and gene loss. *Environmental Microbiology*, 20:1362-1373.

Shimizu, T., Kanematsu, S., and Yaegashi, H. (2018). Draft genome sequence and transcriptional analysis of *Rosellinia necatrix* infected with a virulent mycovirus. *Phytopathology*, 108:1206–1211.

Shimizu, T., Tsutae, I., and Kanematsu, S. (2014). Functional analysis of a melanin biosynthetic gene using RNAi-mediated gene silencing in *Rosellinia necatrix*. *Fungal Biology*, 118:413-421.

Shinohara, M. (2006). Hydroponics with organic fertilizers – a method for building an ecological system of microorganisms in culture liquid by a parallel mineralization method. *Biological Agriculture & Horticulture*, 81, 753–764.

Shinohara, M., Aoyama, C., Fujiwara, K., Watanabe, A., Ohmori, H., Uehara, Y., and Takano, M. (2011). Microbial mineralization of organic nitrogen into nitrate to allow the use of organic fertilizer in hydroponics. *Soil Science and Plant Nutrition*, 57, 190—203.

Simão, F. A., Waterhouse, R. M., Ioannidis, P., Kriventseva, E. V., and Zdobnov, E. M. (2015). BUSCO: Assessing genome assembly and annotation completeness with single-copy orthologs. *Bioinformatics*, 31:3210–3212.

Sivanesan, A., and Holliday, P. (1972). *Rosellinia necatrix*. In Description of Pathogenic Fungi and Bacteria, p. 352.

Smercina, D. N., Bailey, V. L., and Hofmockel, K. S. (2021). Micro on a macroscale: relating microbial-scale soil processes to global ecosystem function. *FEMS Microbiology Ecology*, 97:1-11.

Snelders, N. C., Boshoven, J. C., Song, Y., Schmitz, N., Fiorin, G. L., Rovenich, H., van den Berg, G. C. M., Torres, D. E., Petti, G. C., Prockl, Z., Faino, L., Seidl, M. F., and Thomma, B. P. H. J. (2023). A highly polymorphic effector protein promotes fungal virulence through suppression of plant-associated Actinobacteria. *New Phytologist*, 237(3):944-958.

Snelders, N. C., Kettles, G. J., Rudd, J. J., and Thomma, B. P. H. J. (2018). Plant pathogen effector proteins as manipulators of host microbiomes? *Molecular Plant Pathology*, 19:257-259.

Snelders, N. C., Petti, G. C., van den Berg, G. C. M., Seidl, M. F., and Thomma, B. P. H. J. (2021). An ancient antimicrobial protein co-opted by a fungal plant pathogen for *in planta* mycobiome manipulation. *Proceedings of the National Academy of Sciences*, 118:e2110968118.

Snelders, N. C., Rovenich, H., and Thomma, B. P. H. J. (2022). Microbiota manipulation through the secretion of effector proteins is fundamental to the wealth of lifestyles in the fungal kingdom. *FEMS Microbiology Reviews*, 46:1-16.

Snelders, N. C., Rovenich, H., Petti, G. C., Rocafort, M., van den Berg, G. C. M., Vorholt, J. A., Mesters, J. R., Seidl, M., Nijland, R., and Thomma, B. P. H. J. (2020). Microbiome manipulation by a soil-borne fungal plant pathogen using effector proteins. *Nature Plants*, 6:1365-1374.

Song, J., Win, J., Tian, M., Schornack, S., Kaschani, F., Ilyas, M., van der Hoorn, R. A., and Kamoun, S. (2009). Apoplastic effectors secreted by two unrelated eukaryotic plant pathogens target the tomato defense protease Rcr3. *Proceedings of the National Academy of Sciences*, 106(5):1654-9.

Song, Y., Zhang, Z., Seidl, M. F., Majer, A., Jakse, J., Javornik, B., and Thomma, B. P. H. J. (2017). Broad taxonomic characterization of Verticillium wilt resistance genes reveals an ancient origin of the tomato *Ve1* immune receptor. *Molecular Plant Pathology*, 18:195–209.

Spanu, P. D. (2017). Cereal immunity against powdery mildews targets RNase-Like Proteins associated with Haustoria (RALPH) effectors evolved from a common ancestral gene. *New Phytologist*, 213:1301-1314.

Sperschneider, J., Dodds, P. N., Gardiner, D. M., Manners, J. M., Singh, K. B., and Taylor, J. M. (2015). Advances and challenges in computational prediction of effectors from plant pathogenic fungi. *PLoS Pathogens*, 11(5):e1004806.

Sperschneider, J., Dodds, P. N., Gardiner, D. M., Singh, K. B., and Taylor, J. M. (2018). Improved prediction of fungal effector proteins from secretomes with EffectorP 2.0. *Molecular Plant Pathology*, 19:2094-2110.

Sperschneider, J., Gardiner, D. M., Dodds, P. N., Tini, F., Covarelli, L., Singh, K. B., Manners,

J. M., and Taylor, J. M. (2016). EffectorP: predicting fungal effector proteins from secretomes using machine learning. *New Phytologist*, 210(2):743-61.

Stamatakis, A. (2014). RAxML version 8: a tool for phylogenetic analysis and post-analysis of large phylogenies. *Bioinformatics*, 30:1312–1313.

Stam, R., Münsterkötter, M., Pophaly, S. D., Fokkens, L., Sghyer, H., Güldener, U., Hückelhoven, R., and Hess, M. (2018). A new reference genome shows the one-speed genome structure of the barley pathogen *Ramularia collo-cygni*. *Genome Biology and Evolution*, 10: 3243–3249.

Stamatakis, A. (2014). RAxML version 8: A tool for phylogenetic analysis and post-analysis of large phylogenies. *Bioinformatics*, 30: 1312–1313.

Stancu, M. C., Van Roosmalen, M. J., Renkens, I., Nieboer, M. M., Middelkamp, S., de Ligt, J., Pregno, G., Giachino, D., Mandrile, G., Espejo, J. V., Korzelius, J., de Bruijn, E., Cuppen, E., Talkowski, M. E., Marschall, T., de Ridder, J., and Kloosterman, W. P. (2017). Mapping and phasing of structural variation in patient genomes using nanopore sequencing. *Nature Communications*, 8:1–13.

Stanke, M., Tzvetkova, A., and Morgenstern, B. (2006). AUGUSTUS at EGASP: using EST, protein and genomic alignments for improved gene prediction in the human genome. *Genome Biology*, 7:1–8.

Staskawicz, B.J., Dahlbeck, D., and Keen, N.T. (1984). Cloned avirulence gene of *Pseudomonas syringae* pv. *glycinea* determines race-specific incompatibility on *Glycine max* (L.) Merr. *Proceedings of the National Academy of Sciences*, 81:6024–6028.

Stergiopoulos, I., Collemare, J., Mehrabi, R., and de Wit, P. J. G. M. (2013). Phytotoxic secondary metabolites and peptides produced by plant pathogenic *Dothideomycete* fungi. *FEMS Microbiology Review*, 37:67-93.

Stergiopoulos, I., De Kock, M. J. D., Lindhout, P., and de Wit, P. J. G. M. (2007). Allelic variation in the effector genes of the tomato pathogen *Cladosporium fulvum* reveals different modes of adaptive evolution. *Molecular Plant Microbe Interactions*, 20:1271–1283.

Stringlis, I. A., Yu, K., Feussner, K., de Jonge, R., Van Bentum, S., Van Verk, M. C., Berendsen, R. L., Bakker, P. A. H. M., Feussner, I., and Pieterse, C. M. J. (2018). MYB72-dependent coumarin exudation shapes root microbiome assembly to promote plant health. *Proceedings of the National Academy of Sciences*, 115(22):E5213-E5222.

Stukenbrock, E. H., and McDonald, B. A. (2008). The origins of plant pathogens in agro-ecosystems. *Annual Review of Phytopathology*, 46:75–100.

Sztejnberg, A., and Madar, Z. (1980). Host range of *Dematophora necatrix*, the cause of white root rot disease in fruit trees. *Plant Disease*, 64:662–664.

Takahara, H., Hacquard, S., Kombrink, A., Hughes, H. B., Halder, V., Robin, G. P., Hiruma, K., Neumann, U., Shinya, T., Kombrink, E., Shibuya, N., Thomma, B. P. H. J., and O'Connell, R.J. (2016). *Colletotrichum higginsianum* extracellular LysM proteins play dual roles in appressorial function and suppression of chitin-triggered plant immunity. *New Phytologist*, 211(4):1323-37.

Takai, S. (1974). Pathogenicity and cerato-ulmin production in *Ceratocystis ulmi*. *Nature*, 252:124-126.

Takken, F. L. W., Luderer, R., Gabriëls, S. H. E. J., Westerink, N., Lu, R., de Wit, P. J. G. M.,

and Joosten, M. H. A. J. (2000). A functional cloning strategy, based on a binary PVX-expression vector, to isolate HR-inducing cDNAs of plant pathogens. *The Plant Journal*, 24:275–283.

Takken, F. L. W., Thomas, C. M., Joosten, M. H. A. J., Golstein, C., Westerink, N., Hille, J., Nijkamp, H. J., de Wit P. J. G. M., and Jones, J. D. (1999). A second gene at the tomato Cf-4 locus confers resistance to *Cladosporium fulvum* through recognition of a novel avirulence determinant. *The Plant Journal*, 279–288.

Talbot, N. J., Kershaw, M. J., Wakley, G. E., de Vries, O. M. H., Wessels, J. G. H., and Hamer, J. E. (1996). *MPG1* encodes a fungal hydrophobin involved in surface interaction during infection-related development of *Magnaporthe grisea*. *The Plant Cell*, 8:985-999.

Thomas, D. D. (1978). Cytochalasin effects in plants and eukaryotic microbial systems. *Frontiers in Biology*, 46:257-275.

Thomma, B. P. H. J., Nürnberger, T., and Joosten, M. H. A. J. (2011). Of PAMPs and effectors: the blurred PTI-ETI dichotomy. *The Plant Cell*, 23:4–15.

Thomma, B. P. H. J., Seidl, M. F., Shi-Kunne, X., Cook, D. E., Bolton, M. D., van Kan, J. A. L., and Faino, L. (2016). Mind the gap; seven reasons to close fragmented genome assemblies. *Fungal Genetics and Biology*, 90:24–30.

Tian, H., Fiorin, G. L., Kombrink, A., Mesters, J. R., and Thomma, B. P. H. J. (2022). Fungal dual-domain LysM effectors undergo chitin-induced intermolecular, and not intramolecular, dimerization. *Plant Physiology*, 190:2033-2044.

Tian, H., MacKenzie, C. I., Rodriguez-Moreno, L., van den Berg, G. C. M., Chen, H., Rudd, J. J., Mesters, J. R., and Thomma, B. P. H. J. (2021). Three LysM effectors of Zymoseptoria tritici collectively disarm chitin-triggered plant immunity. *Molecular Plant Pathology*, 22:683-693.

Tian, M., Benedetti, B., and Kamoun, S. (2005). A Second Kazal-like protease inhibitor from *Phytophthora infestans* inhibits and interacts with the apoplastic pathogenesis-related protease P69B of tomato. *Plant Physiology*, 138(3):1785-93.

Tian, M., Huitema, E., da Cunha, L., Torto-Alalibo, T., and Kamoun, S. (2004). A Kazal-like Extracellular Serine Protease Inhibitor from *Phytophthora infestans* Targets the Tomato Pathogenesis-related Protease P69B*. *Enzyme Catalysis and Regulation*, 279(25):26370-26377.

Törönen, P., and Holm, L. (2022). PANNZER-A practical tool for protein function prediction. *Protein Science*, 31:118-128.

Torres, D. E., Oggenfuss, U., Croll, D., and Seidl, M. (2020). Genome evolution in fungal plant pathogens: looking beyond the two-speed genome model. *Fungal Biology Reviews*, 34:136-143.

Tubbs, F. R., (1973). Research fields in interaction of rootstocks and scions in woody perennials part 1. *Horticultural abstracts*, 43:247–253.

Trivedi, P., Leach, J. E., Tringe, S. G., Sa, T., and Singh, B. K. (2020). Plant–microbiome interactions: from community assembly to plant health. *Nature Reviews Microbiology*, 18: 607-621.

Tyler, B. M., Tripathy, S., Zhang, X., Dehal, P., Jiang, R. H., Aerts, A., Arredondo, F. D., Baxter, L., Bensasson, D., Beynon, J. L., Chapman, J., Damasceno, C. M., Dorrance, A. E., Dou, D., Dickerman, A. W., Dubchak, I. L., Garbelotto, M., Gijzen, M., Gordon,

S. G., Govers, F., Grunwald, N. J., Huang, W., Ivors, K. L., Jones, R. W., Kamoun, S., Krampis, K., Lamour, K. H., Lee, M. K., McDonald, W. H., Medina, M., Meijer, H. J., Nordberg, E. K., Maclean, D. J., Ospina-Giraldo, M. D., Morris, P. F., Phuntumart, V., Putnam, N. H., Rash, S., Rose, J. K., Sakihama, Y., Salamov, A. A., Savidor, A., Scheuring, C. F., Smith, B. M., Sobral, B. W., Terry, A., Torto-Alalibo, T. A., Win, J., Xu, Z., Zhang, H., Grigoriev, I. V., Rokhsar, D. S., and Boore, J. L. (2006). Phytophthora genome sequences uncover evolutionary origins and mechanisms of pathogenesis. *Science*, 313(5791):1261-6.

Tyson, J. R., O'Neil, N. J., Jain, M., Olsen, H. E., Hieter, P., and Snutch, T.P. (2018). MinION-based long-read sequencing and assembly extends the *Caenorhabditis elegans* reference genome. *Genome Research*, 28(2):266-274.

Tzima, A. K., Paplomatas, E. J., Rauyaree, P., Ospina-Giraldo, M. D., and Kang, S. (2011). *VdSNF1*, the sucrose nonfermenting protein kinase gene of *Verticillium dahliae*, is required for virulence and expression of genes involved in cell-wall degradation. *Molecular Plant-Microbe Interactions*, 24(1):129-42.

Umesha, S., Singh, P. K., and Singh, R. P. (2018). Microbial Biotechnology and Sustainable Agriculture. In: Biotechnology for Sustainable Agriculture – Emerging Approaches and Strategies. Woodhead Publishing , Duxford, United Kingdom. 185-205 pp.

Underwood, W. (2012). The plant cell wall: a dynamic barrier against pathogen invasion. *Frontiers in Plant Science*, 3:1-6.

Usami, T., Momma, N., Kikuchi, S., Watanabe, H., Hayashi, A., Mizukawa, M., Yoshino, K., and Ohmori, Y. (2017). Race 2 of *Verticillium dahliae* infecting tomato in Japan can be split into two races with differential pathogenicity on resistant rootstocks. *Plant Pathology*, 66:230–238.

Uyeda, J., Cox, L. J., and Radovich, T. J. (2011). An economic comparison of commercially available organic and inorganic fertilizers for hydroponic lettuce production. *College of Tropical Agriculture and Human Resources*, SA-5:1–4.

Valance, J., Deniel, F., Le Floch, G., Guerin-Dubrana, L., Blancard, D., and Rey, P. (2010). Pathogenic and beneficial microorganisms in soilless cultures. *Agronomy for Sustainable Development*, 191–203.

van der Heijden, M. G. A., Bardgett, R. D., and van Straalen, N. M. (2008). The unseen majority: soil microbes as drivers of plant diversity and productivity in terrestrial ecosystems. *Ecology Letters*, 11: 269-310.

van der Heijden, M. G. A., Martin, F. M., Selosse, M. A., and Sanders, I. R. (2015). Mycorrhizal ecology and evolution: the past, the present, and the future. *New Phytologist*, 205(4):1406-1423.

van der Lelie, D., Oka, A., Taghavi, S., Umeno, J., Fan, T., Merrell, K. E., Watson, S. D., Ouellette, L., Liu, B., Awoniyi, M., Lai, Y., Chi, L., Lu, K., Henry, C. S., and Sartor, R. B. (2021). Rationally designed bacterial consortia to treat chronic immune-mediated colitis and restore intestinal homeostasis. *Nature Communications*, 12: 1-17.

van Leeuwen, P. T., Brul, S., Zhang, J., and Wortel, M. K. (2023). Synthetic microbial communities (SynComs) of the human gut: design, assembly, and applications. *FEMS Microbiology Reviews*, 47: 1-14.

van Kan, J.A., van den Ackerveken, G.F., and de Wit, P.J. (1991). Cloning and characterization of cDNA of avirulence gene *avr9* of the fungal pathogen

Cladosporium fulvum, causal agent of tomato leaf mold. *Molecular Plant Microbe Interactions*, 4:52–59.

Varoquaux, N., Liachko, I., Ay, F., Burton, J. N., Shendure, J., Dunham, M. J., Vert, J. P., and Noble, W. S. (2015). Accurate identification of centromere locations in yeast genomes using Hi-C. *Nucleic Acids Research*, 43:5331–5339.

Vázquez-Castellanos, J. F., Biclot, A., Vrancken, G., Huys, G. R. B., and Raes, J. (2019). Design of synthetic microbial consortia for gut microbiota modulation. *Current Opinion in Pharmacology*, 49: 52–59.

Vazquez-Iglesias, I., Adams, I. P., Hodgetts, J., Fowkes, A., Forde, S., Ward, R., Buxton-Kirk, A., Kelly, M., Santin-Azcona, J., Skelton, A., Harju, V., Boonham, N., Robinson, R., Clover, G., and Fox, A. (2019). High throughput sequencing and RT-qPCR assay reveal the presence of rose cryptic virus-1 in the United Kingdom. *Journal of Plant Pathology*, 101:1171–1175.

Virtanen, P., Gommers, R., Oliphant, T. E., Haberland, M., Reddy, T., Cournapeau, D., Burovski, E., Peterson, P., Weckesser, W., Bright, J., van der Walt, S. J., Brett, M., Wilson, J., Millman, K. J., Mayorov, N., Nelson, A. R. J., Jones, E., Kern, R., Larson, E., Carey, C. J., Polat, İ., Feng, Y., Moore, E. W., VanderPlas, J., Laxalde, D., Perktold, J., Cimrman, R., Henriksen, I., Quintero, E. A., Harris, C. R., Archibald, A. M., Ribeiro, A., Pedregosa, F., van Mulbregt, P., and SciPy 1.0 Contributors (2020). SciPy 1.0: fundamental algorithms for scientific computing in Python. *Nature Methods,* 17:261–272.

Vleeshouwers, V. G. A. A., and Oliver, R. P. (2014). Effectors as tools in disease resistance breeding against biotrophic, hemibiotrophic and necrotrophic plant pathogens. *Molecular Plant Microbe Interactions*, 27:196–206.

Vorholt, J. A. (2012). Microbial life in the phyllosphere. *Nature Reviews Microbiology*, 10(12):828-40.

Walton, J. D. (1990). Peptide phytotoxins from plant pathogenic fungi. In Biochemistry of peptide antibiotics. Kleinkauf, H., and von Dohren, H. (eds). Berlin, 179-203 pp.

Wang, E., Schornack, S., Marsh, J. F., Gobbato, E., Schwessinger, B., Eastmond, P., Schultze, M., Kamoun, S., and Oldroyd, G. E. D. (2012). A common signaling process that promotes Mycorrhizal and Oomycete colonization of plants. *Current Biology*, 22:2242-2246.

Wang, J., Carper, D. L., Burdick, L. H., Shrestha, H. K., Appidi, M. R., Abraham, P. E., Timm, C. M., Hettich, R. B., Pelletier, D. A., and Doktycz, M. J. (2021). Formation, characterization and modeling of emergent synthetic microbial communities. *Computational and Structural Biotechnology Journal*, 19: 1917-1927.

Wang, J. R., Holt, J., McMillan, L., and Jones, C. D. (2018). FMLRC: Hybrid long read error correction using an FM-index. *BMC Bioinformatics*, 19:1–11.

Wawra, S., Fesel, P., Widmer, H., Neumann, U., Lahrmann, U., Becker, S., Hehemann, J., Langen, G., and Zuccaro, A. (2019). FGB1 and WSC3 are *in planta*-induced *β*-glucan-binding fungal lectins with different functions. *New Phytologist*, 222:1493-1506.

Weiberg, A., Wang, M., Bellinger, M., and Jin, H. (2014). Small RNAs: a new paradigm in plant-microbe interactions. *Annual Review of Phytopathology*, 52:495-516.

Weinert, N. Piceno, Y., Ding, G., Meincke, R., Heuer, H., Berg, G., Schloter, M., Andersen, G., and Smalla, K. (2011). PhyloChip hybridization uncovered an enormous bacterial

diversity in the rhizosphere of different potato cultivars: many common and few cultivar-dependent taxa. *FEMS Microbiology Ecology*, 75:497-506.

Whisson, S. C., Boevink, P. C., Moleleki, L., Avrova, A. O., Morales, J.G., Gilroy, E. M., Armstrong, M. R., Grouffaud, S., van West, P., Chapman, S., Hein, I., Toth, I. K., Pritchard, L., and Birch, P. R. (2007). A translocation signal for delivery of oomycete effector proteins into host plant cells. *Nature*, 450(7166):115-8.

Wick, R. (2018). Porechop. Retrieved from https://github.com/rrwick/Porechop

Wick, R. R., Judd, L.M., Gorrie, C. L., and Holt, K. E. (2017). Unicycler: Resolving bacterial genome assemblies from short and long sequencing reads. *PLoS Computational Biology*, 13(6):e1005595.

Wilson, R. A., and McDowell, J. M. (2022). Recent advances in understanding of fungal and oomycete effectors. *Current Opinion in Plant Biology*, 68:102228.

Wingfield, B. D., Berger, D. K., Coetzee, M. P. A., Duong, T. A., Martin, A., Pham, N. Q., van den Berg, N., Wilken, P. M., Arun-Chinnappa, K. S., Barnes, I., Buthelezi, S., Dahanayaka, B. A., Durán, A., Engelbrecht, J., Feurtey, A., Fourie, A., Fourie, G., Hartley, J., Kabwe, E. N. K., Maphosa, M., Mensah, D. L. N., Nsibo, D. L., Potgieter, L., Poudel, B., Stukenbrock, E. H., Thomas, C., Vaghefi, N., Welgemoed, T., and Wingfield, M. J. (2022). IMA genome-F17: Draft genome sequences of an *Armillaria* species from Zimbabwe, *Ceratocystis colombiana*, *Elsinoë necatrix*, *Rosellinia necatrix*, two genomes of *Sclerotinia minor*, short-read genome assemblies and annotations of four *Pyrenophora teres* isolates from barley grass, and a long-read genome assembly of *Cercospora zeina. IMA Fungus*, 13:1-22.

Wu, H. J., Wang, A. H., and Jennings, M. P. (2008). Discovery of virulence factors of pathogenic bacteria. *Current Opinion in Chemical Biology*, 12(1):93-101.

Xu, D., Xue, M., Shen, Z., Jia, X., Hou, X., Lai, D., and Zhou, L. (2021). Phytotoxic secondary metabolites from fungi. *Toxins*, 13:1-65.

Yoon, S. H., et al. (2012). Introducing EzBioCloud: A taxonomically united database of 16S rRNA gene sequences and whole-genome assemblies. *International Journal of Systematic and Evolutionary Microbiology*, 67: 1613-1617.

Yu, P., He, X., Baer, M., Beirinckx, .S, Tian, T., Moya, Y. A. T., Zhang, X., Deichmann, M., Frey, F. P., Bresgen, V., Li, C., Razavi, B. S., Schaaf, G., von Wirén, N., Su, Z., Bucher, M., Tsuda, K., Goormachtig, S., Chen, X., and Hochholdinger, F. (2021). Plant flavones enrich rhizosphere Oxalobacteraceae to improve maize performance under nitrogen deprivation. *Nature Plants*, 7(4):481-499.

Yuan, M., Ngou, B. P. M., Ding, P., and Xin, X.F. (2021). PTI-ETI crosstalk: an integrative view of plant immunity. *Current Opinion in Plant Biology*, 62:102030.

Yurtsev, E. A., Chao, H. X., Datta, M. S., Artemova, T., and Gore, J. (2013). Bacterial cheating drives the population dynamics of cooperative antibiotic resistance plasmids. *Molecular Systems Biology*, 9: 683.

Zhalnina, K., Louie, K. B., Hao, Z., Mansoori, N., da Rocha, U. N., Shi, S., Cho, H., Karaoz, U., Loqué, D., Bowen, B. P., Firestone, M. K., Northern, T. R., and Brodie, E. L. (2018). Dynamic root exudate chemistry and microbial substrate preferences drive patterns in rhizosphere microbial community assembly. *Nature Microbiology*, 3(4):470-480.

Zhang, Y., and Skolnick J. (2005). TM-align: a protein structure alignment algorithm based on the TM-score. Nucleid Acids Research, 33:2302–2309.

Zhao, Z., Ying, Y., Hung, Y., and Tang, Y. (2019). Genome mining reveals Neurospora crassa can produce the salicylaldehyde sordarial. Journal of Natural Products, 82:1029-1033.

Zhong, Z., Marcel, T.C., Hartmann, F.E., Ma, X., Plissonneau, C., Zala, M., Ducasse, A., Confais, J., Compain, J., Lapalu, N., Amselem, J., McDonald, B. A., Croll, D., and Palma-Guerrero, J. (2017). A small secreted protein in *Zymoseptoria tritici* is responsible for avirulence on wheat cultivars carrying the *Stb6* resistance gene. *New Phytologist*, 214:619–631.

Zhou, B. J., Jia, P. S., Gao, F., and Guo, H. S. (2012). Molecular characterization and functional analysis of a necrosis- and ethylene-inducing, protein-encoding gene family from *Verticillium dahliae*. *Molecular Plant-Microbe Interactions*, 25(7):964-75.

Zhou, E., Jia, Y., Singh, P., Correll, J.C., and Lee, F.N. (2007). Instability of the *Magnaporthe oryzae* avirulence gene *AVR-Pita* alters virulence. *Fungal Genetics and Biology*, 44:1024–1034.

Summary
Acknowledgments
About the author
List of publications

SUMMARY

Crop production is constantly threatened by plant diseases caused by a wide diversity of pathogens and pests. To understand such plant diseases, the molecular basis of plant-pathogen interactions has received much attention over the last decades. To establish disease, during host ingress plant pathogenic microbes secrete effector molecules that promote host colonization. Typically, effectors are defined as small, secreted proteins that are cysteine-rich and have tertiary structures that are stabilized by disulfide bridges. Collectively, effectors function through a multitude of mechanisms by targeting crucial components of host physiology, including immune responses, that typically have been revealed in the context of the binary interactions between the pathogen and the host. However, more recently it has been shown that some effectors can modulate root microbiota compositions to facilitate host colonization. **Chapter 1** introduces the impact of fungal plant pathogens on crop production, including the impact of the fungal soil-borne pathogens *Rosellinia necatrix* and *Verticillium dahliae* on rose cultivation. Furthermore, the molecular biology of plant-pathogen interactions as well as effectors and their role in disease establishment are described.

Although plant pathogens secrete effector molecules to promote host colonization, some effectors have become recognized by host immune receptors, encoded by so-called resistance genes, triggering immune responses. In **Chapter 2** we identified and functionally characterized the effector protein that is recognized by tomato plants carrying the *V2* resistance locus. To this end, we performed comparative genomics between race 2 strains that are contained by the *V2* locus, and resistance-breaking race 3 strains, to identify the avirulence effector that activates *V2* resistance, termed Av2. We identified 277 kb of race 2-specific sequence comprising only two genes that encode predicted secreted proteins, both of which are expressed by *V. dahliae* during tomato colonization. Subsequent functional analysis based on genetic complementation into race 3, and deletion from race 2 isolates, confirmed that one of the two candidates encodes the avirulence effector Av2 that is recognized in *V2* tomato plants.

In **Chapter 3,** we describe the ability of *V. dahliae* strains to infect rose plants. We show that, besides strains isolated from roses, also a phylogenetically diverse panel of *V. dahliae* strains isolated from other host species is capable to cause disease on rose plants, suggesting that pathogenicity on roses is widely distributed throughout the *V. dahliae* population. We furthermore show that various previously described *V. dahliae* effectors contribute to disease development on rose. Accordingly, we demonstrate that defoliation, which is caused by some *V. dahliae* strains that belong to the so-called defoliating pathotype, is caused by a recently identified defoliation (D) effector. Finally, we argue that individual *V. dahliae* strains cause disease on rose based on divergent

effector catalogues.

Recently, it has been shown that effectors not only interact directly with the host plant to cause disease, but also modulate root microbiota compositions to facilitate host colonization. More specifically, *V. dahliae* was shown to exploit a range of effector proteins with selective antimicrobial activity during host ingress. In **Chapter 4,** we investigated whether the soil-borne pathogen *R. necatrix* similarly encodes antimicrobials that are expressed during host colonization. To this end, we generated a gapless genome assembly of a *R. necatrix* strain into ten chromosomes, and identified 26 putative antimicrobial effector protein candidates in its secretome, nine of which are expressed during plant colonization. Subsequent functional analysis revealed that two of the candidates possess selective antimicrobial activity. Moreover, we show that some of the inhibited bacteria are antagonists of *R. necatrix* growth *in vitro* and can alleviate *R. necatrix* infection on cotton plants.

Understanding the antimicrobial activity of effector proteins is of great interest. Nevertheless, the identification of antimicrobial activity of among effector candidates has proven to be time-consuming and labor-intensive. Thus, a tool to test multiple effector candidates at once against a panel of potential target microorganisms could help to more efficiently discover antimicrobial activities. In **Chapter 5**, we developed a Nanopore sequencing-based screen to reveal antimicrobial activity among effector proteins based on the use of synthetic communities (SynComs). We compare the treatment of individual bacterial taxa with the effector proteins with the treatment of SynComs with these members, and use Nanopore sequencing to detect changes in relative abundances of the individual bacterial taxa.

Finally, in **Chapter 6**, the results described in this thesis are summarized and placed into a broader context, highlighting the importance of effector identification and functional characterization to reveal their role in disease establishment in order to develop novel plant disease control strategies.

ACKNOWLEDGMENTS

I would like to dedicate a few words to everyone who in one way or another helped me during my PhD journey.

First, to Bart, thank you for the opportunity to pursue a PhD in your group and for all the help and knowledge you have shared with me during these six years.

Michael, thank you for all the guidance and tremendous help during my time in Wageningen with you I got to learn so much about Nanopore sequencing and genomics, clearly new skills I only acquired thanks to you.

Gert and Jan, thank you for all your support in the last stretch of my PhD I wouldn't be able to finish without all your support and guidance.

To my beautiful wife, Katharina! danke für all die Unterstützung und Liebe in all den Jahren! I am glad our paths crossed during our PhD. I saw your struggles to finish your PhD and at the end of my PhD journey, you were there to support me and give me energy to continue and don't give up. I have no words to thank you enough for everything you have done for me. This thesis is as yours as is mine. I know our future is full of happiness as now we wait for our beautiful son to arrive. It´s been a journey that I couldn't have done without you! I love you!

To all my PhD peers in Cologne, Gabriella, Anton, Wilko, Chen-Yu, Gerlind, Tanya, Ciaran, Andrea, Danielle, Ilaria, and Martina, thank you for all your support and the memories we had together. I enjoyed sharing my office with Gabbo and Chen-Yu even if we had to tolerate Wilko. Anton thank you for all the nice work discussions and hugs. Ilaria and Martina, it was a pleasure to work with you during your internships, you were of great help in building up my last chapter.

To team Thomma in Cologne, Vittorio, Hanna, Hui, Yuki, Fantin, Jinyi, Ana, Jan, Eva, Heidrun, Jana, Zoe, Conny, Miriam, Paula, Thea, Natalie, and Ane, thank you for all your support. You made the lab a family and you made me feel part of that family since day 1. Vittorio thank you for all your suggestions I learned a lot from you and of course, I appreciate the tension between us only a few can understand such a unique connection.

A toda la comunidad Latina en Colonia, Cristy, Cristina, Ana, David, Luis, Lean, Ale, Maca, Steve, Siba y Saul, ¡gracias por hacer de mi estancia en Colonia una fiesta latina! Cristy gracias por todo tu apoyo y todas las fiestas, sin ti nada hubiera sido lo mismo!

Thank you to all the members of Phytopathology at WUR, Gert, Jan, Francine, Mathieu, Sander, Ali, Grardy, Laurens, Xioqian, Sergio, Gabriel, and Jasper. Grardy thank you for all the lab techniques I learned with you, you helped me from day 1.

To all my Colombian community at WUR, Amalia, Lorena Jose, and Carolina,

thank you for all the lunch breaks and endless chats. Amalia and Lorena thank you for always being there for me and for all the support all these years.

To my Waterhouse and Wageningen friends, Nuran, Lissane, Guy, Dimitri, Khalid, Ymke, Carlo, Mauricio, Sabine, Antonio, Nayara, Esteri, Samara, Junior, Dandara, Jaap, Bruno, Melania and many others, thank you all for the corona nights together and all the fun.

Finalmente, quiero agradecer a mis padres, Pedro y Omaira, ustedes me apoyaron durante toda mi carrera. ¡Gracias por todo y les prometo que esta es mi última tesis!

ABOUT THE AUTHOR

Edgar Andres Chavarro Carrero was born on April 3, 1990, in Grecia, Alajuela, Costa Rica, and spent his formative years in Colombia, where his parents worked as agronomists. Growing up in a household deeply connected to agriculture, he developed an early fascination with the field that would profoundly influence his academic journey. He earned his Bachelor's degree from the Universidad Autonoma del Estado de Mexico at the Centro Universitario UAEM Tenancingo, followed by a Master's degree from the Colegio de Postgraduados. During his time in Mexico, Edgar developed a strong foundation in statistics and specialized in the integrated management of pests and diseases, areas that would shape his future research in phytopathology. He later transitioned into a role as a lecturer at the Centro Universitario UAEM Tenancingo, where he shared his expertise with students. In 2017, Edgar made the decision to pursue a PhD, leading him to move to the Netherlands to join the Lab of Phytopathology at Wageningen University & Research under the supervision of prof. dr. Bart Thomma and dr. Michael Seidl. From 2021 to 2023, he also spent time as a visiting PhD candidate at the Institute for Plant Sciences at the University of Cologne, Germany.

Outside of academia, Edgar is a passionate basketball player and enjoys (long distance) cycling. Known for his outgoing nature, he effortlessly forges connections with others, nurturing a broad network of friendships around the globe. In 2022, he tied the knot with Katharina, marking a significant milestone in his personal life.

LIST OF PUBLICATIONS

Chavarro-Carrero, E. A., Snelders, N., Torres, D. E., Kraege, A., Lopez-Moral, A., Petti, G., Punt, W., Wieneke, J., Garcia-Velasco, R., Lopez-Herrera, C., Seidl, M. F., and Thomma, B. P. H. J. (2024). The soil-borne white root rot pathogen *Rosellinia necatrix* expresses antimicrobial proteins during host colonization. *PLoS Pathogens*, 20(1): e1011866.

van Westerhoven, A., Aguilera-Galvez, C., Nakasato-Tagami, G., Shi-kunne, X., Martinez de la Parte, E., **Chavarro-Carrero, E. A.**, Meijer, H., Feurtey, A., Maryani, N., Ordonez, N., Schneiders, H., Nijbroek, K., Wittenberg, A., Hofstede, R., Garcia-Bastidas, F., Sørensen, A., Swennen, R., Drenth, A., Stukenbrock, E., Kema, G., and Seidl, M. (2024). Segmental duplications drive the evolution of accessory regions in a major crop pathogen. Accepted in *New Phytologist*.

You, Y., Suraj, H. M., Matz, L., Herrera-Valderrama, A. L., Ruigrok, P., Shi-Kunne, X., Pieterse, P. J., Beenen, H. G., **Chavarro-Carrero, E. A.**, Qin, S., Verstappen, F. W. A., Kappers, I. F., Fleißner, A., van Kan, J. A. L. (2023). The grey mould *Botrytis cinerea* employs multiple mechanisms to protect itself from antifungal plant metabolites. *Nature Communications* (under review).

Kraege, A., **Chavarro-Carrero, E. A.**, Guiglielmoni, N., Schnell, E., Kirangwa, J., Heilmann-Heimbach, S. Becker, K., Köhrer, K., WGGC Team, DerGA Community, Schiffer, P., Thomma, P. H. J. T., and Rovenich, H. (2023). High quality genome assembly and annotation (v1) of the eukaryotic terrestrial microalga *Coccomyxa viridis* SAG 216-4. *bioRxiv*, 2023.07.11.548521.

Depotter, J.R.L., van Beveren, F., Rodriguez-Moreno, L., Kramer, H. M., **Chavarro-Carrero, E. A.**, Fiorin, G. L., van der Berg, G. C. M., Wood, T. A., Thomma, B. P. H. J. and Seidl, M. F. (2021). The interspecific fungal hybrid *Verticillium longisporum* displays sub-genome-specific gene expression. *mBio*, 12(4): e01496-21.

Chavarro-Carrero, E. A., Vermeulen, J. P., E. Torres, D., Usami, T., Schouten, H. J., Bai, Y., Seidl, M. F. and Thomma, B. P. H. J. (2021). Comparative genomics reveals the *in planta*-secreted V*erticillium dahliae* Av2 effector protein recognized in tomato plants that carry the V2 resistance locus. *Environmental Microbiology*, 23(4), 1941–1958.

Garcia-Velasco, R. and **Chavarro-Carrero, E. A.** (2020). *Purpureocillium lilacinum* (Hypocreales: Ophiocordycipitaceae) as a biocontrol agent of *Nacobbus aberrans* (Tylenchida: Pratylenchidae) and *Meloidogyne incognita* (Tylenchida: Meloidogynidae) in tomato cv. Río Grande. *Acta Agricola y Pecuaria*, 6:1-10.